| 1. Report No.<br>FHWA/TX-92/1249-1F | 2. Government Accession No. | 3. Recipient's Catalog No. | |
|---|---|---|---|
| 4. Title and Subtitle<br><br>Design and Use of Superior Asphalt Binders | | 5. Report Date<br>November, 1991<br>August, 1992/Revised | |
| | | 6. Performing Organization Code | |
| 7. Author(s)<br><br>R.R. Davison, J.A. Bullin, C.J. Glover, H.B. Jemison, C.K. Lau, K.M. Lunsford, and Penny L. Bartnicki | | 8. Performing Organization Report No.<br>Research Report 1249-1F | |
| 9. Performing Organization Name and Address<br><br>Texas Transportation Institute and<br>Chemical Engineering Department<br>The Texas A & M University System<br>College Station, Texas 77843 | | 10. Work Unit No. | |
| | | 11. Contract or Grant No.<br>Study No. 2-9-90-1249 | |
| 12. Sponsoring Agency Name and Address<br><br>Texas Department of Transportation:<br>Texas Transportation Planning Division<br>P. O. Box 5051<br>Austin, Texas 78763 | | 13. Type of Report and Period Covered<br>September 1, 1990<br>Final -<br>August 31, 1991 | |
| | | 14. Sponsoring Agency Code | |

15. Supplementary Notes
Research performed in cooperation with TxDOT, FHWA
Research Study Title: Design and Use of Superior Asphalt Binders

16. Abstract

This study is a continuation of Study 1155 whose major objective was to use supercritical fractionation of asphalt to study the effect of asphalt composition changes on properties and to use this knowledge to reblend fractions to make superior asphalts. In this study both supercritical cyclohexane and supercritical pentane have been used to fractionate three reduced crudes and the corresponding AC-20 asphalts into a range of fractions.

Because it is not possible to evaluate an asphalt without its long-term road aging characteristics, and because no satisfactory road aging simulation existed, a major effort in this study became the development of a satisfactory aging procedure. It is shown that no aging test run at a single elevated temperature can predict performance at road temperature. Methods are given for predicting low temperature aging from values measured at several higher temperatures. It is shown that the aging characteristics of asphalt can be broken into two parts: the rate of oxidation as measured by carbonyl formation and the susceptibility of the viscosity to increase due to this carbonyl formation. Data indicate that the latter may be primarily a function of compatibility. The relation between viscosity change and carbonyl growth is highly correlated for each asphalt.

| 17. Key Words<br><br>Asphalt binders, asphalt reblending, supercritical fractionation, asphalt fractionation, asphalt aging | | 18. Distribution Statement<br>No restrictions. This document is available to the public through the<br>National Technical Information Service<br>5285 Port Royal Road<br>Springfield, Virginia 22161 | |
|---|---|---|---|
| 19. Security Classif. (of this report)<br>Unclassified | 20. Security Classif. (of this page)<br>Unclassified | 21. No. of Pages<br>201 | 22. Price |

Form DOT F 1700.7 (8-69)

# DESIGN AND USE OF SUPERIOR ASPHALT BINDERS

by

Richard R. Davison
Jerry A. Bullin
Charles J. Glover
Howard B. Jemison
Chee K. Lau
Kevin M. Lunsford
Penny L. Bartnicki

Chemical Engineering Department
and
Texas Transportation Institute
Texas A & M University
College Station, Texas 77843
November, 1991
August, 1992/Revised

# METRIC (SI*) CONVERSION FACTORS

## APPROXIMATE CONVERSIONS TO SI UNITS

| Symbol | When You Know | Multiply By | To Find | Symbol |
|--------|---------------|-------------|---------|--------|

### LENGTH

| Symbol | When You Know | Multiply By | To Find | Symbol |
|--------|---------------|-------------|---------|--------|
| in | inches | 2.54 | centimetres | cm |
| ft | feet | 0.3048 | metres | m |
| yd | yards | 0.914 | metres | m |
| mi | miles | 1.61 | kilometres | km |

### AREA

| Symbol | When You Know | Multiply By | To Find | Symbol |
|--------|---------------|-------------|---------|--------|
| in² | square inches | 645.2 | centimetres squared | cm² |
| ft² | square feet | 0.0929 | metres squared | m² |
| yd² | square yards | 0.836 | metres squared | m² |
| mi² | square miles | 2.59 | kilometres squared | km² |
| ac | acres | 0.395 | hectares | ha |

### MASS (weight)

| Symbol | When You Know | Multiply By | To Find | Symbol |
|--------|---------------|-------------|---------|--------|
| oz | ounces | 28.35 | grams | g |
| lb | pounds | 0.454 | kilograms | kg |
| T | short tons (2000 lb) | 0.907 | megagrams | Mg |

### VOLUME

| Symbol | When You Know | Multiply By | To Find | Symbol |
|--------|---------------|-------------|---------|--------|
| fl oz | fluid ounces | 29.57 | millilitres | mL |
| gal | gallons | 3.785 | litres | L |
| ft³ | cubic feet | 0.0328 | metres cubed | m³ |
| yd³ | cubic yards | 0.0765 | metres cubed | m³ |

NOTE: Volumes greater than 1000 L shall be shown in m³.

### TEMPERATURE (exact)

| Symbol | When You Know | Multiply By | To Find | Symbol |
|--------|---------------|-------------|---------|--------|
| °F | Fahrenheit temperature | 5/9 (after subtracting 32) | Celsius temperature | °C |

* SI is the symbol for the International System of Measurements

## APPROXIMATE CONVERSIONS TO SI UNITS

### LENGTH

| Symbol | When You Know | Multiply By | To Find | Symbol |
|--------|---------------|-------------|---------|--------|
| mm | millimetres | 0.039 | inches | in |
| m | metres | 3.28 | feet | ft |
| m | metres | 1.09 | yards | yd |
| km | kilometres | 0.621 | miles | mi |

### AREA

| Symbol | When You Know | Multiply By | To Find | Symbol |
|--------|---------------|-------------|---------|--------|
| mm² | millimetres squared | 0.0016 | square inches | in² |
| m² | metres squared | 10.764 | square feet | ft² |
| km² | kilometres squared | 0.39 | square miles | mi² |
| ha | hectores (10 000 m²) | 2.53 | acres | ac |

### MASS (weight)

| Symbol | When You Know | Multiply By | To Find | Symbol |
|--------|---------------|-------------|---------|--------|
| g | grams | 0.0353 | ounces | oz |
| kg | kilograms | 2.205 | pounds | lb |
| Mg | megagrams (1 000 kg) | 1.103 | short tons | T |

### VOLUME

| Symbol | When You Know | Multiply By | To Find | Symbol |
|--------|---------------|-------------|---------|--------|
| mL | millilitres | 0.034 | fluid ounces | fl oz |
| L | litres | 0.264 | gallons | gal |
| m³ | metres cubed | 35.315 | cubic feet | ft³ |
| m³ | metres cubed | 1.308 | cubic yards | yd³ |

### TEMPERATURE (exact)

| Symbol | When You Know | Multiply By | To Find | Symbol |
|--------|---------------|-------------|---------|--------|
| °C | Celsius temperature | 9/5 (then add 32) | Fahrenheit temperature | °F |

```
°F
          32        98.6              °F
-40   0   40   80   120   160   200  212
 |----|----|----|----|----|----|----|
-40  -20   0   20   40   60   80  100
°C                    37              °C
```
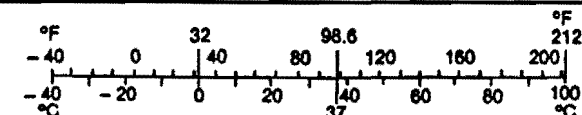
These factors conform to the requirement of FHWA Order 5190.1A.

**SUMMARY**

This study is a continuation of the work begun in Study 1155. In the previous study it was demonstrated that the aging index, measured by the Rolling Thin Film Oven Test, could be considerably improved by formulating asphalts from the more compatible fractions. There were a number of limitations to this study, however: 1) only three asphalts were studied, 2) the number of blends was limited, and 3) the rheometric properties were evaluated over limited conditions.

More important than these limitations, however, is that standard oven tests themselves are inadequate for evaluating asphalts. The most important characteristic of an asphalt, assuming that it meets specifications, is its long-term aging characteristics on the road, and no satisfactory method existed for measuring this. Therefore, attempts to design superior asphalts will be frustrated until a satisfactory test is developed. Development of such a test was a consideration in Study 1155 but it was a major effort in this study with very successful results.

In section one, the development of a preliminary form of the aging test is presented. It is shown that asphalt aging can be divided into two factors. The first is the sensitivity of viscosity hardening to oxidation. This is independent of temperature, and it is shown that for any asphalt, the log of the viscosity varies linearly with carbonyl formation and this phenomena has been named "hardening susceptibility". It is also shown that for any asphalt, the log of the rate of carbonyl formation varies linearly with the reciprocal of the absolute temperature, so that the rate can be extrapolated to road conditions and this phenomena has been named "aging rate". These data clearly show that no test at a single elevated temperature is valid because among a group of asphalts there may be reversals in relative reaction rates in going from high to low temperature.

Section two describes the supercritical fractionation, the properties of the fractions, their blending to make new asphalts, and the properties of these materials. Reduced crudes were fractionated first with cyclohexane and then the lightest fractions were fractionated with pentane to yield a total of seven fractions. For

asphalts this was repeated with pentane to yield a total of ten fractions. All fractions and blends obeyed the linear relation between carbonyl formation and the log of the viscosity. For most of the blends extremely low values of the hardening susceptibility were obtained. The aging rates were also very low at 160°F and 180°F but very limited data at 200°F prevented reliable extrapolation to road temperatures.

One unanswered question from Study 1155 was the effect of reblending on low temperature properties, as the temperature susceptibility results were ambiguous. In this work, complete rheometric data were obtained using mechanical spectrometers. This has been invaluable in expanding the correlation that we have found between infrared-measured carbonyl content and viscosity to a wide range of temperatures, which is a fundamental property used in the aging test development. It was found that all the rheometric data obeyed a simple linear relation between log viscosity and reciprocal absolute temperature from 0°C to 95°C. In general the blends were very similar to the whole asphalts in this respect, and the temperature susceptibility measured in this manner was virtually unchanged by aging.

# ACKNOWLEDGEMENT

# IMPLEMENTATION

The aging procedures developed in this study show excellent potential for development of a practical specification for estimating the resistance of asphalt to oxidative hardening at road conditions. The potential to completely fractionate asphalt supercritically for reblending has been demonstrated, but it is still too early in this work to recommend implementation.

## DISCLAIMER

The contents of this report reflect the views of the authors who are responsible for the facts and the accuracy of the data presented herein. The contents do not necessarily reflect the official views or policies of the Federal Highway Administration or the Texas Department of Transportation. This report does not constitute a standard, specification, or regulation. This report is not intended for construction, bidding, or permit purposes.

# TABLE OF CONTENTS

# LIST OF FIGURES

xiii

# LIST OF TABLES

# SECTION I

## Asphalt Aging and Aging Test Development

# CHAPTER I-1

## INTRODUCTION

From the standpoint of understanding and predicting asphalt performance, the properties of aged asphalt are more important in many respects than the properties of the original material. Years after placement, when a roadway is deteriorating, the asphalt properties may be greatly different from the original properties, and, as a result, if failure is due to the asphalt cement, it will be the properties of this aged material rather than those of the original which are causing the problem. This has been recognized for many years, and many test procedures have been devised to predict aging.

Aging really occurs in two modes: first, there is the very rapid aging that occurs in the hot-mix plant at high temperature on the aggregate surface and this is followed by the much slower, low temperature aging in the road. It is likely that the mechanisms in these modes of aging are quite different. This is borne out by the persistent failure of tests developed to predict hot-mix aging to prove useful in predicting road aging.

There are now two widely recognized hot-mix aging procedures: the Thin Film Oven Test, TFOT, ASTM D1754-83, and the Rolling Thin Film Oven Test, RTFOT, ASTM D2872-80. Numerous variations have been made on the TFOT and RTFOT methods with many intended to simulate road aging as well. Vallerga et al., (1957) proposed tilting the oven used for the TFOT and provided an effect similar to that of the RTFOT.

The recognition that thinner films may be desired to simulate hot mix aging led to the development of microfilm tests (Fink, 1958; Traxler, 1967). Thinner films correspond better to actual pavement mixtures, harden faster, and lessen any diffusion effects that may be present in thicker films. The Microfilm Durability Test of Griffin et al. (1955) was designed to simulate road aging, but has been correlated with hot-mix as well as road aging (Heithaus et al., 1958; Simpson et al., 1959).

Schmidt and Santucci (1969) developed a rolling microfilm test in which

2

benzene-dissolved asphalt was cast in bottles and aged in a manner similar to that used in the RTFOT. The modification of adding a circulating fan, as suggested by Schmidt (1973a), has been maintained and is called the RMFC (rolling microfilm circulating) test. Schmidt (1973b) has also used several modifications to the rolling microfilm test at various temperatures and rates of air circulation as well as in the presence of aggregate in an effort to simulate hot mix and road aging.

Kemp (1973) studied several durability tests and their relationship to field hardening. Kemp stated that no laboratory process seemed to predict performance satisfactorily. The void content of the mix is the only parameter that seems to give any prediction of the aging process for pavements with over 50 months of service. This leads to the conclusion that voids must be constant before an aging test can predict actual field hardening. The best correlation with the field data came from the RMFC test for 48 hour exposures. The RMFC test was modified by Petersen (1989). The test is run at 235°F using a larger sample and is purported to represent about ten years of field aging.

Evidence exists that aggregate can catalyze aging (Jennings, 1982; Petersen et al., 1974a; Petersen et al., 1974b; Plancher et al., 1977; Ensley et al., 1984; Barbour et al., 1974). Jennings (1982) studied the aging process using Gel Permeation Chromatography (GPC). Jennings stated that the molecular size distribution of an asphalt is a function of aggregate, additives, exposure, and time.

The most realistic road aging procedures would seem to be the low temperature (compared to the hot-mix temperatures) Pressure Oxygen Vessel (POV) tests in which lower temperatures can be partly compensated for with respect to required test duration by higher oxygen pressure and there are several reports using this kind of device. Lee (1968) simulated the hot-mix step first by TFOT aging. This material, still in the TFOT dish, was placed in a pressure vessel and aged at 150°F at various pressures. A standard procedure was proposed by Lee (1973) in which TFOT residues were aged at 150°F and 20 atm. for 1000 hours. They used a variety of criteria to correlate aging including viscosity, penetration, softening point, microductility and percent asphaltenes. Though the results are promising, the

3

rankings of the POV-aged asphalts by each criterion were not very consistent with the rankings of the field-aged asphalts, indicating that actual road aging was not being duplicated. They also found an overwhelming effect of voids that complicated relating properties to age. Jamieson and Hattingh (1970) report that POV results using 7mm films at 65°C and 300 psi did not agree with road performance.

Edler et al. (1985) reported results in which 30 $\mu$m asphalt films were contacted with oxygen at 300 psi at 149°F for 96 hours, but the results were not compared to field data. Kim et al., (1987) aged compacted cores at 100 psi and 60°C up to 5 days. Comparison to field cores was on the basis of the resilient modulus and Corbett analysis of extracted material. There was generally fair agreement between the lab and field cores for two of three sets of cores but they reported some problems with diffusion into cores of low air voids. It is likely that much of this work is complicated by diffusion into cores and problems with extraction and recovery (Burr et al., 1990) of the lab and field cores.

As indicated above, most road aging tests are lower temperature variations of the oven tests designed to simulate the hot-mix process and do not appear to correlate to road aging. One likely reason is that the tests are still conducted much above field temperatures. Another difficulty with correlation is that enough asphalt properties and their changes which result from aging have not been evaluated to establish that the aging test reproduces, or even approximates, field aging.

The primary objective of this work was to determine the significance of aging temperature with respect to oxidation rate and mechanism. By so doing, a rationale would exist for designing a laboratory test which would be optimal with respect to the ease and time to conduct the test and to the ability of the test to indicate or predict road aging.

This section contains data that demonstrate the feasibility of estimating aging rates at low temperatures from several measurements at higher temperatures. These data are then used to develop a preliminary aging test. In Chapter I-3 of this section, some interesting data are given demonstrating the extremely high rates of photo-oxidation that occur in sunlight.

4

# CHAPTER I-2
## POV AGING RATES AND HARDENING OF ASPHALTS

The POV aging apparatus was developed in Study 458. Some work was done in Study 1155 but the bulk of what is reported here was done in Study 1249. This equipment was designed to allow aging of many samples simultaneously and to essentially eliminate diffusion effects on the reaction rates.

### Apparatus and Procedures

The pressure oxygen vessel (POV) and sample holder are shown in Figures I-2-1 and I-2-2. The vessel is made of four inch standard stainless steel pipe. It is two feet long and flanged at each end. The top flange is equipped with a 1½ inch 400 psig rupture disk. The pressure vessel is wrapped with heating tape which, with a variable transformer, is used to control the temperature. A thermocouple is inserted through the bottom flange to detect the temperature which is read from a digital indicator. A control panel houses the temperature indicator as well as vacuum and pressure gauges. The pressure vessel is located behind a metal shield. All control valves are specially cleaned and teflon coated for oxygen service. Valves and tubing as shown in Figure I-2-1 are stainless steel. The sample holder is also stainless steel. It fits inside the pressure vessel and can support 88 asphalt samples.

Asphalt samples for the POV oxidation test are prepared by depositing about 20 grams of molten asphalt between two plastic sheets. The asphalt is then pressed between two glass plates until the asphalt between the plastic sheets formed a 6 inch circular disk to obtain a film thickness of about 1000 $\mu$m. If the asphalt cools down to the point that the pressing process becomes difficult, the whole setup is heated in an oven at a temperature of about 90 to 100°C until the asphalt becomes soft again. A thinner film can be obtained by pressing the asphalt into a bigger disk if desired. The composite sheet is then cooled to room temperature and is cut into rectangular pieces of 1.5 inches by 2.5 inches. The plastic sheets are removed from the asphalt film after cooling the composite film in a freezer. The asphalt films are then

5
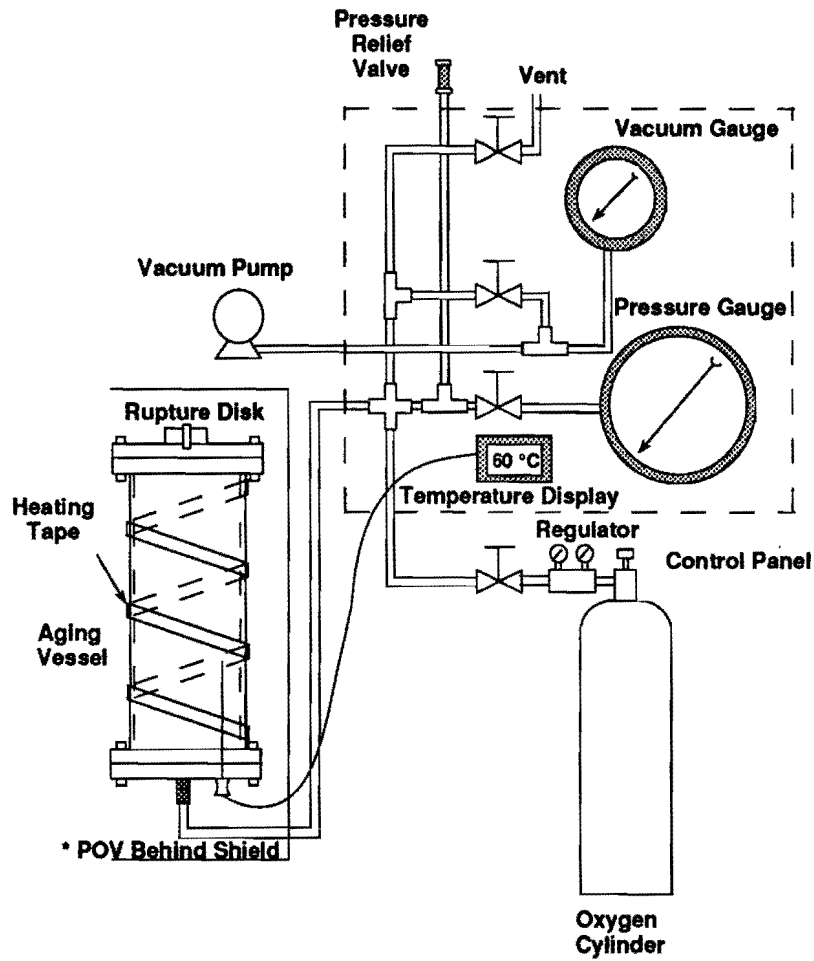
Figure I-2-1. Schematic of the
Pressure Oxygen Vessel
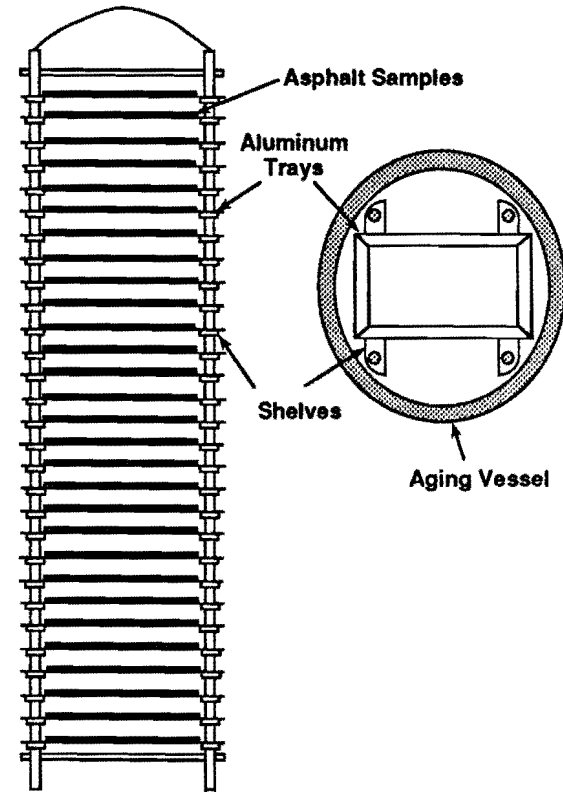


Figure I-2-2. Detail of the POV
Asphalt Sample Trays

deposited in 1.5 in. by 2.5 in. aluminum trays and are ready for the POV experiment.

Asphalt samples are placed in the stainless steel sample holder. The sample holder is placed inside the aging vessel and the flange is bolted down securely. With the venting valve, oxygen feed valve, and high pressure gauge valve closed and the vacuum valve opened, a vacuum is applied to the aging vessel to remove the air inside. The vacuum valve is then closed. The vessel is slowly pressurized to 300 psia oxygen from an oxygen cylinder with the oxygen feed valve and high pressure gauge valve open. When the desired oxygen pressure is reached, the oxygen feed valve is closed. Power to the heating tape is then turned on to heat the pressure vessel to the desired aging temperature. During the heating process, pressure in excess of the aging pressure can be vented off by opening the venting valve momentarily. When the desired period of oxidation time is attained, oxygen in the vessel is slowly vented to the atmosphere. Asphalt samples are taken from the vessel for further analysis at specified time intervals. The short time required to depressurize, remove the samples and return to operating pressure and temperature is small compared to the total aging time.

Infrared analyses were made of all samples with a Nicolet 60 SXB Fourier Transform Infrared Spectrometer (FT-IR) using an Attenuated Total Reflectance (ATR) procedure described by Jemison et al. (1992). The viscosities were measured at several temperatures using a dynamic spectrometer RMS-800 RDS11 from Rheometrics Inc. Measurements were made with 25 mm parallel plates operating in a dynamic mode with a 1 mm gap. Operation and data acquisition are monitored by an IBM PS-2 Model 30 computer with a REC CAPIII computer analysis package, also from Rheometrics Inc. The reported viscosities are low frequency values.

**Results and Discussion**

It was expected that the failure of aging procedures to represent road aging resulted primarily from using temperatures far above those experienced by the asphalts in road service, but the question remained how high a temperature could be used while still being representative of road aging. Experiments in the POV at 25°C

7

showed extremely low aging rates, and it was obvious that some compromise must be made with higher temperatures.

To study this effect, five asphalts were aged in the POV at 300 psia oxygen pressure at temperatures of 140°, 160°, and 180°F, and one asphalt, Fina, was aged at 200°F. Samples were withdrawn periodically for viscosity measurements and infrared analysis. A typical infrared spectrum is shown in Figure I-2-3. Figure I-2-4 shows the limiting complex dynamic viscosity, $\eta_0^*$, measured at 60°C (140°F) versus aging time for Fina at all temperatures. The limiting complex dynamic viscosity, $\eta_0^*$, is defined as the limiting, essentially frequency independent value which is reached at sufficiently low frequencies. The range of shear rate defining $\eta_0^*$ is material dependent. The linear relation of log $\eta_0^*$ versus aging time is characteristic of all asphalts studied, though with different slopes and intercepts. Figure I-2-5 shows a plot for the same asphalt of carbonyl growth (the area increase above the neat asphalt between 1820 to 1650 cm$^{-1}$) versus time exhibiting a constant rate of carbonyl growth.

As would be expected, a cross plot of log $\eta_0^*$ versus carbonyl is linear (Figure I-2-6). It can be seen that all temperatures combine to give a single line, strongly indicating that while the rate of oxidation changes with temperature, the mechanisms of oxidation do not. All five asphalts gave similar results as shown in Figure I-2-7.

The linear relation between log viscosity and carbonyl formation was reported previously by Martin et al. (1990) for road-aged asphalt. Jemison et al. (1992) showed that it also applied to TFOT and RTFOT aging, but the function was not the same as that resulting from hot-mix plant aging. The POV data further confirm that this is a universal characteristic of asphalt oxidation for each asphalt as long as the aging mechanism is unchanged.

This relation also appears to hold for viscosity measurements over a wide range of temperatures. Figure I-2-8 shows log viscosity at other temperatures versus carbonyl area. At lower temperatures, especially at 25°C, the samples are so hard that $\eta_0^*$ (the low shear rate limiting value) is attainable only at a very low shear rate. The same relation over a range of temperatures of course means that changes in

8
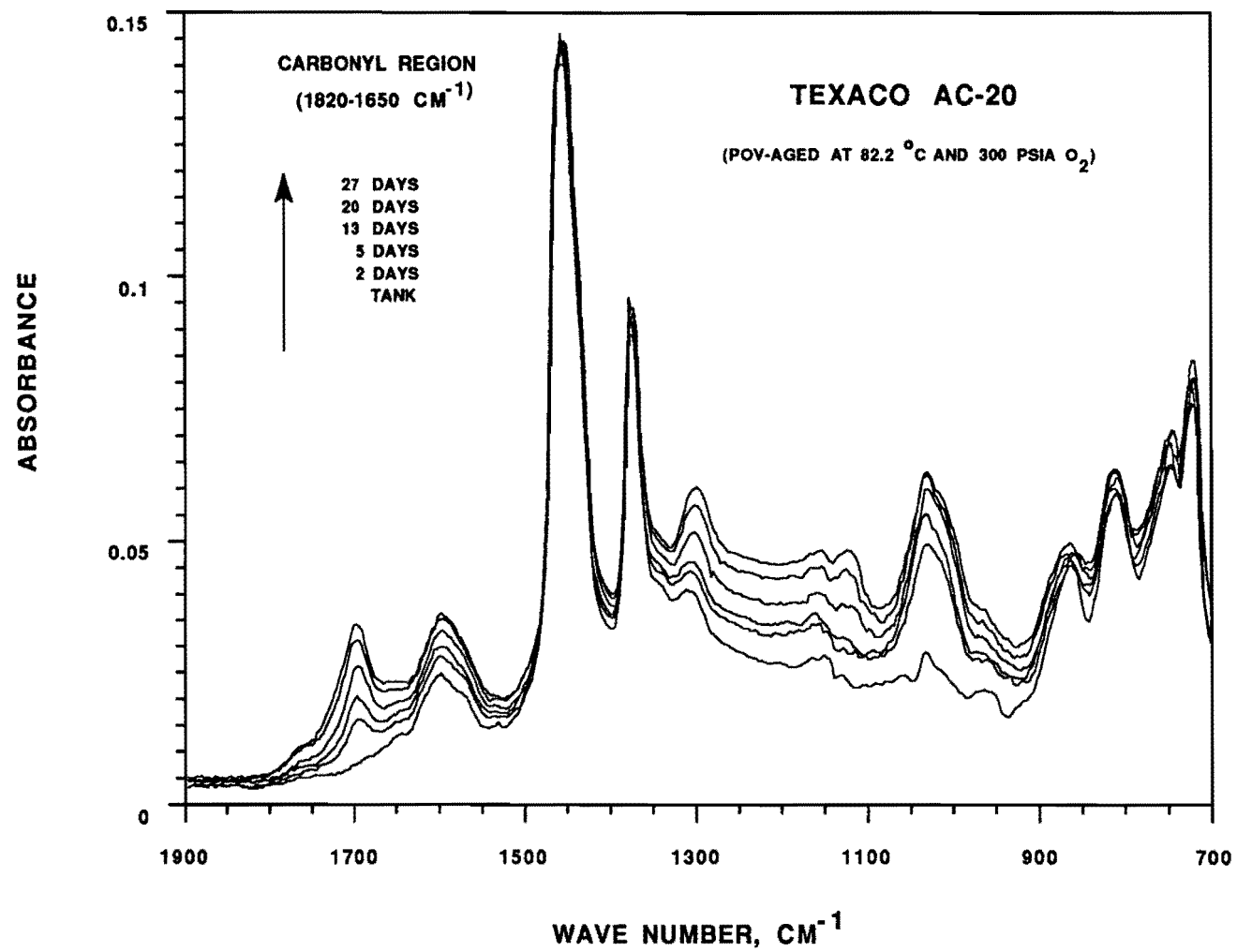
**Figure I-2-3. Typical FT-IR Spectra Using the ATR Method for Asphalts Aged in the POV**
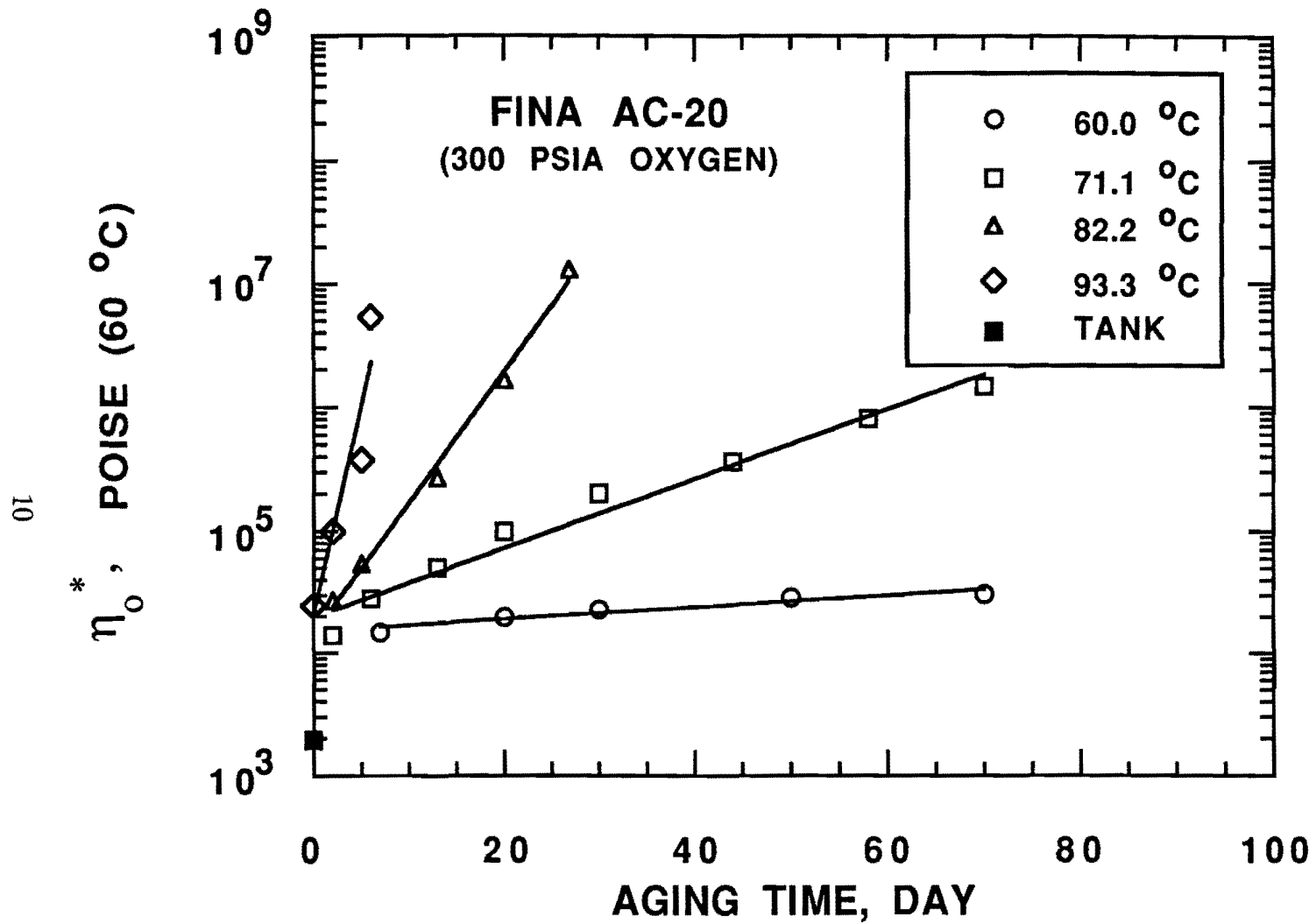
Figure I-2-4. Dynamic Viscosity Hardening with Time of an Fina AC-20 Asphalt Aged at Three Temperatures
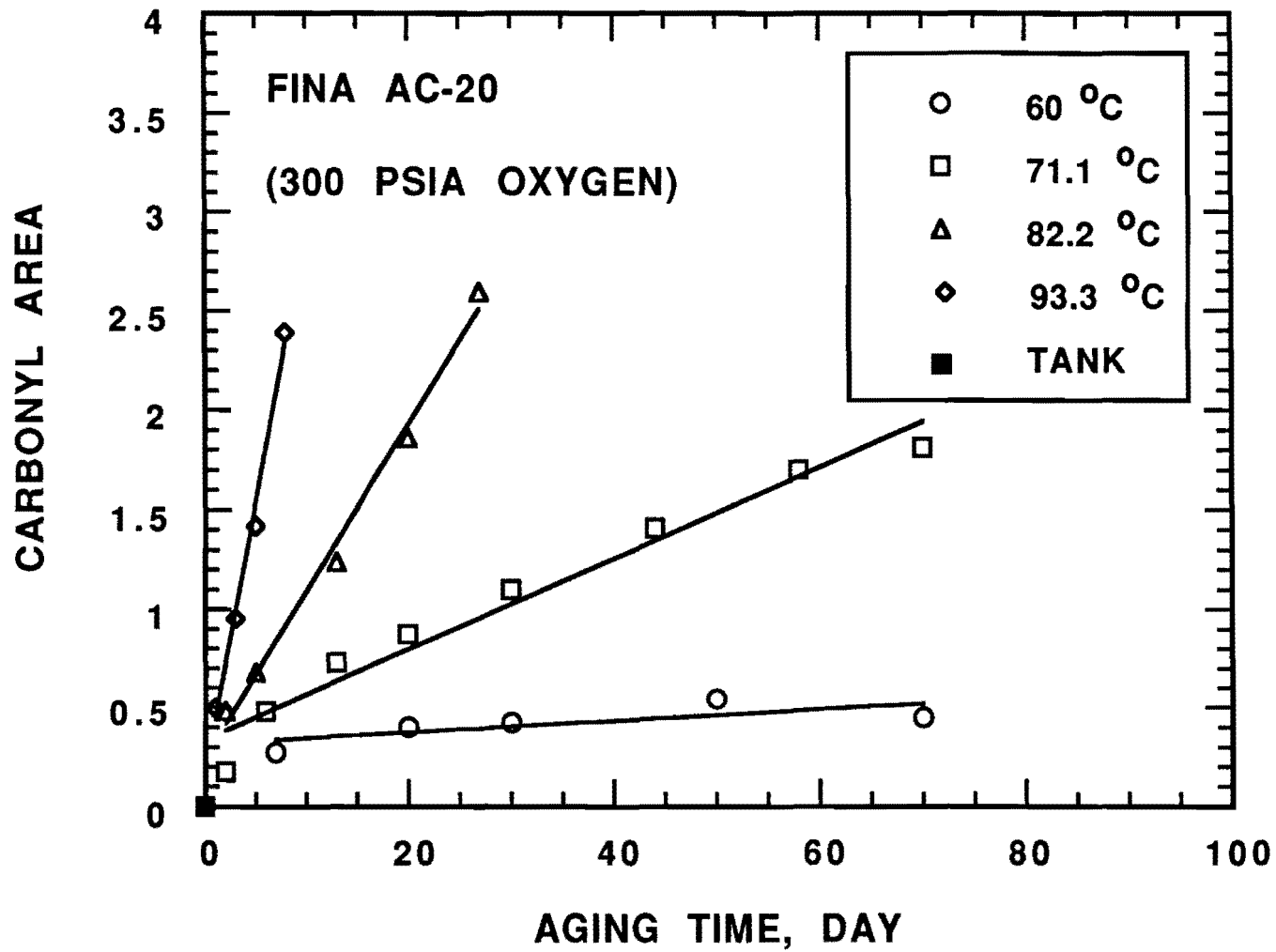
Figure I-2-5. Growth of the Infrared Carbonyl Band with Time for an Asphalt Aged at Four Different Temperatures
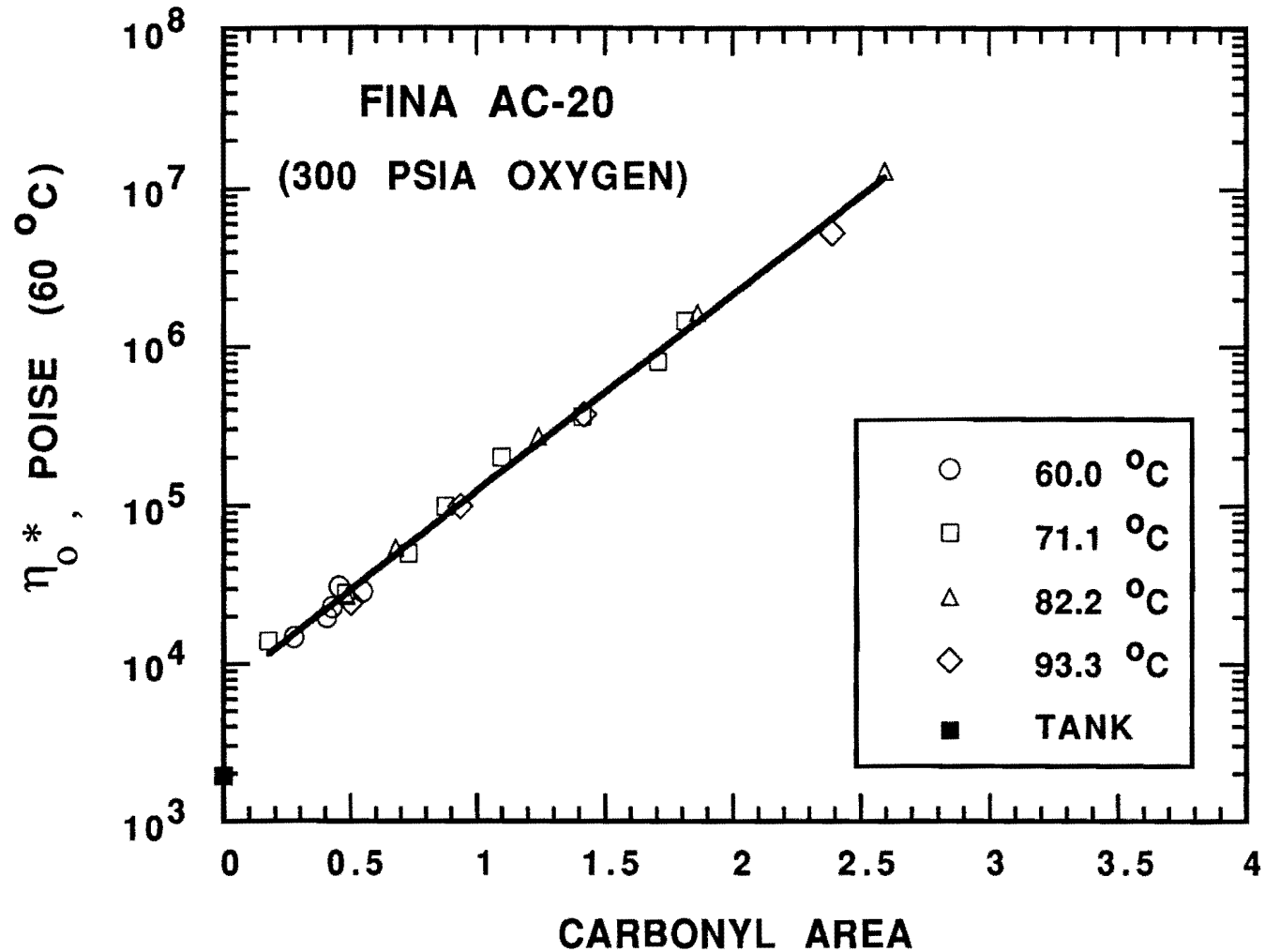
Figure I-2-6. Hardening of the Dynamic Viscosity with Growth of the
Carbonyl Peak Area for an Asphalt Aged at Three Temperatures
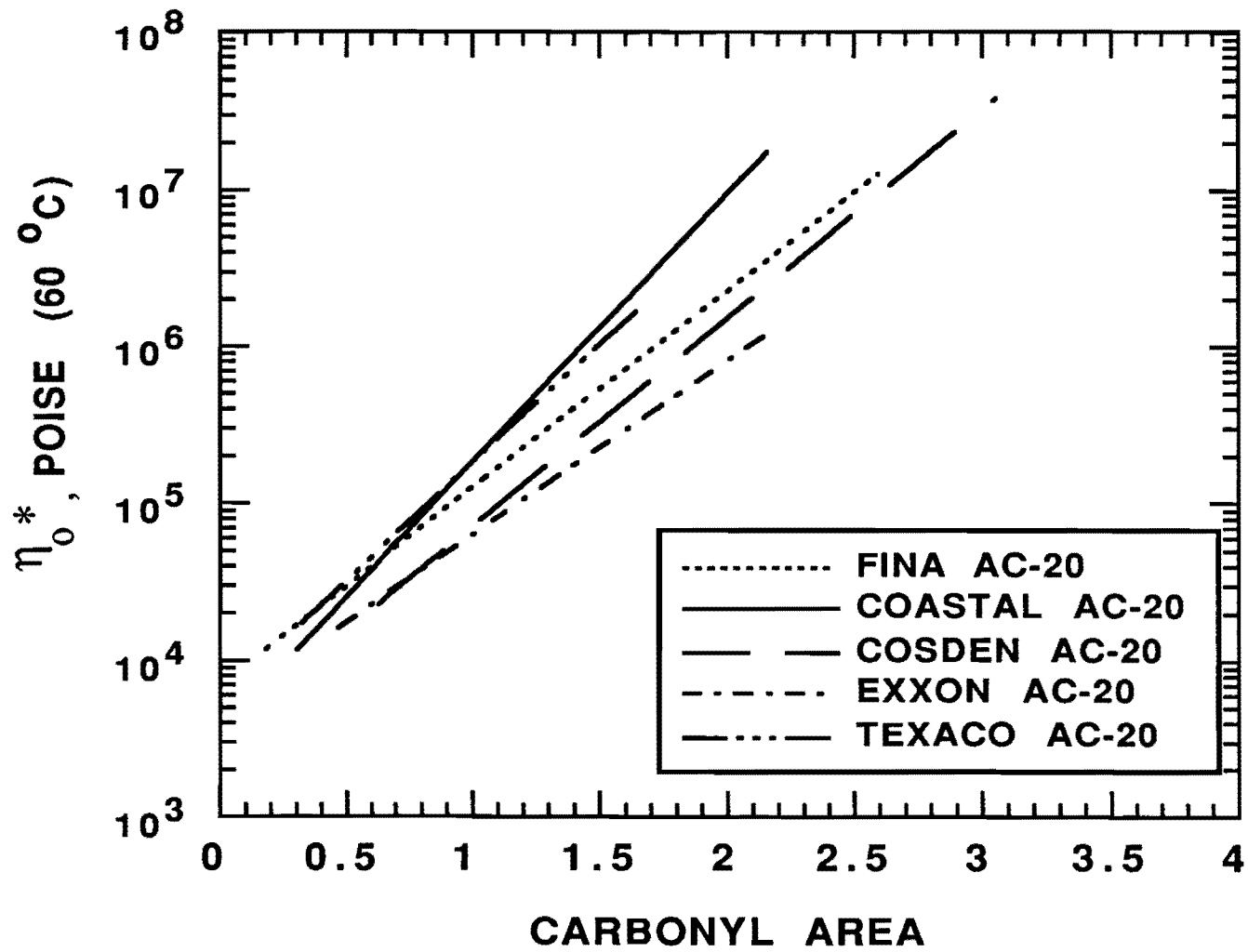
Figure I-2-7. Comparison of the Hardening Susceptibilities of Five Asphalts
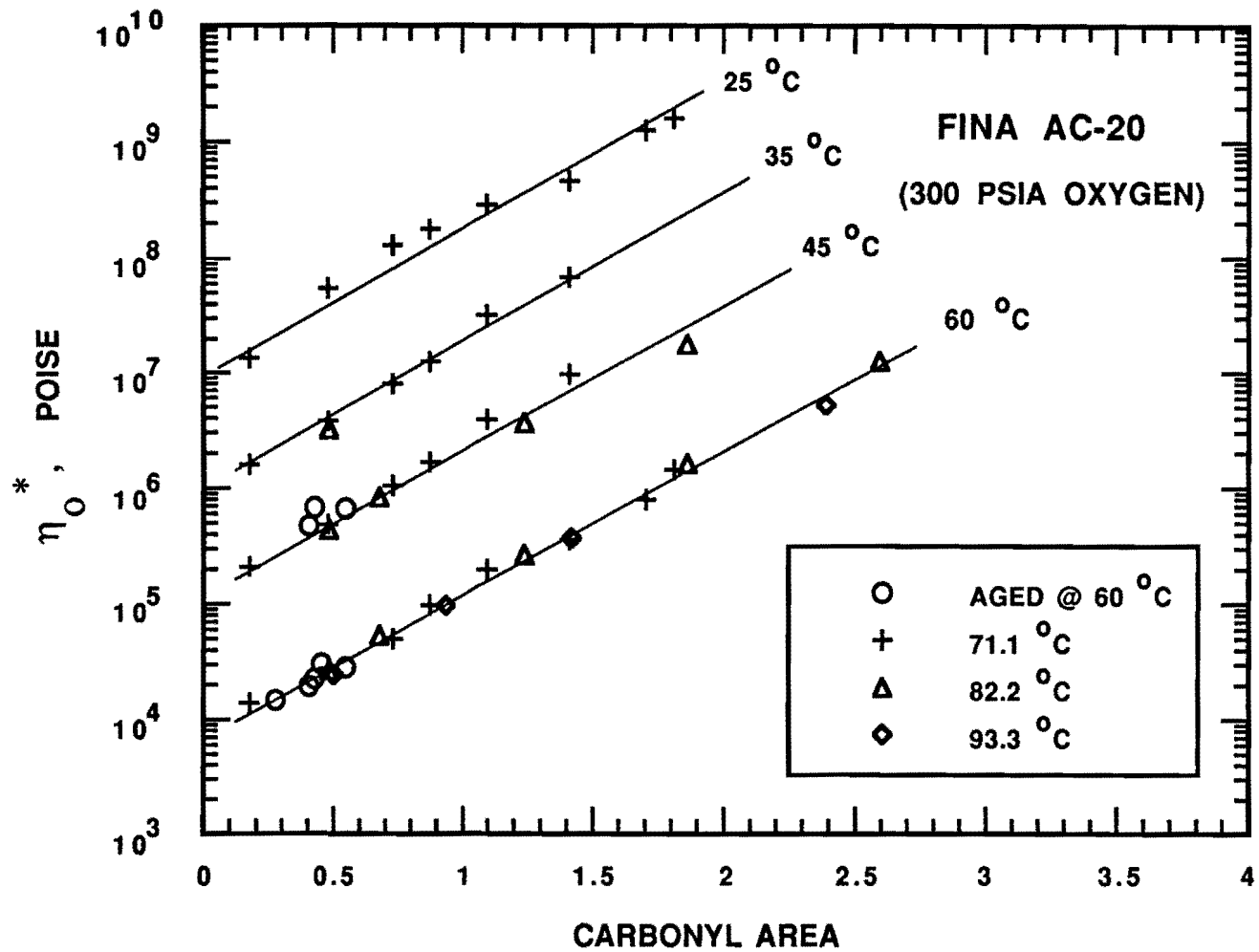
Figure I-2-8. Dynamic Viscosity Measured at Four Temperatures Versus Carbonyl Area for a Single Asphalt

14

viscosity temperature susceptibility are independent of the aging temperature within this range, giving additional confirmation of a constant aging mechanism.

We feel that the aging mechanism is the same as that on the road. However, this has not been verified. The results of Jemison et al. (in press) indicate that, at least in the hot-mix plant, the aggregate may play some role. Tables I-2-1 and I-2-2 show results obtained with two of the core asphalts used in the Strategic Highway Research Program (SHRP). These asphalts were aged in the presence of aggregate (either SHRP RL or RB) in two ways and under different conditions of temperature and oxygen concentration. Laboratory hot mixes either were compacted into cores which were subsequently aged in a pressurized oxygen vessel (POV) or were aged as loose mixes in a forced-draft oven. The aging times and temperatures are shown in the table. These aged mixes were then compacted and used in core physical property tests (not part of this work) and subsequently subjected to asphalt extraction and recovery using a recently-developed procedure designed to minimize solvent-aging of the asphalt and to maximize asphalt extraction and subsequent solvent removal (Burr et al. 1990, Burr et al., in press; Cipione et al., 1991). The recovered asphalt was compared to neat samples of the same asphalts after aging in the POV at 200°F and 300 psig (Figures I-2-9 and I-2-10). As can be seen, the differences, if any, are small indicating little difference between POV aging of neat asphalt and core aging at temperatures below about 200°F.

The SHRP AAG-1 asphalt is remarkable in that though it oxidizes like the others, the viscosity does not increase nearly as much. This shows that hardening as the asphalt ages involves two important and independent factors: the first, the slope of the log viscosity versus carbonyl area plot, as in Figures I-2-6 and I-2-7, is a measure of the sensitivity of the asphalt viscosity to carbonyl formation. We call this slope the *hardening susceptibility*. The second, the slope of the carbonyl area versus time, relation is the rate of oxidation which, as seen in Figure I-2-5, is a strong function of temperature. As a result of these two effects, an asphalt may oxidize relatively rapidly but not harden a great deal, compared to other asphalts, or it may harden considerably while oxidizing at a slower rate. Which situation holds can be

15

**Table I-2-1**
**Limiting Complex Dynamic Viscosity and Carbonyl Area for**
**SHRP Asphalt AAK-1 for Different Aging Conditions**

| Sample[a] | | Pre-Aging[b] | | Aging | | | Properties | | |
|---|---|---|---|---|---|---|---|---|---|
| Aggregate | Air Voids (%) | Time (days) | Temp. (°C) | Time (days) | Temp. (°C) | Oven[c] | $\eta^*_0$ (25°C,0.01s⁻¹) (10⁶ poise) | $\eta^*_0$ (60°C,0.1s⁻¹) (10³ poise) | Carbonyl Area |
| Neat | --- | 0 | --- | 0 | --- | --- | 1.987 | 3.992 | 0.000 |
| RL | 9.20 | 2 | 40 | 0 | --- | --- | 11.98 | 20.00 | 0.209 |
| RL | 9.10 | 2 | 40 | 7 | 107 | --- | 270.2 | 1976. | 1.350 |
| RB | 8.00 | 2 | 40 | 0 | --- | --- | 11.16 | 17.36 | 0.229 |
| RB | 8.90 | 2 | 40 | 7 | 107 | --- | 183.4 | 868.0 | 1.318 |
| RB | 6.57 | 2 | 60 | 0 | --- | --- | 11.19 | 17.92 | 0.271 |
| RB | 6.42 | 2 | 60 | 7 | 107 | --- | 150.9 | 560.9 | 1.071 |
| RL | --- | 0 | --- | 2 | 60 | 300 | 30.47 | 46.86 | 0.378 |
| RL | --- | 0 | --- | 7 | 25 | 300 | 15.45 | 34.43 | 0.291 |
| RB | --- | 0 | --- | 7 | 60 | 100 | 40.46 | 62.34 | 0.537 |
| Neat | --- | 0 | --- | 0.5 | 92.2 | 300 | 60.00 | 88.00 | 0.568 |
| Neat | --- | 0 | --- | 1.0 | 92.2 | 300 | 170.0 | 300.0 | 0.933 |
| Neat | --- | 0 | --- | 2.0 | 92.2 | 300 | --- | 40,000 | 2.736 |

[a] Asphalts are SHRP AAK-1 or AAG-1. Aggregates are SHRP RB or RL.

b The FDO-aged cores were aged as loose mix.

c The numbers indicate $O_2$ pressure in the POV. Where no number is given, the aging was done in the FDO.

Table I-2-2
Limiting Complex Dynamic Viscosity and Carbonyl Area for
SHRP Asphalt AAG-1 for Different Aging Conditions

| Sample[a] | | Pre-Aging[b] | | Aging | | | Properties | | |
| --- | --- | --- | --- | --- | --- | --- | --- | --- | --- |
| Aggregate | Air Voids (%) | Time (days) | Temp. (°C) | Time (days) | Temp. (°C) | Oven[c] | $\eta_0^*$ (25°C,0.01s$^{-1}$) (10$^6$ poise) | $\eta_0^*$ (60°C,0.1s$^{-1}$) (10$^3$ poise) | Carbonyl Area |
| Neat | --- | 0 | --- | 0 | --- | --- | 2.448 | 2.500 | 0.000 |
| RL | 7.91 | 2 | 60 | 0 | --- | --- | 13.80 | 8.334 | 0.490 |
| RL | 7.54 | 2 | 60 | 7 | 107 | --- | 165.0 | 83.95 | 2.071 |
| RB | --- | 0 | --- | 2 | 60 | 300 | 22.43 | 12.00 | 1.165 |
| RB | --- | 0 | --- | 7 | 25 | 300 | 11.78 | 8.132 | 0.940 |
| RL | --- | 0 | --- | 7 | 60 | 100 | 28.00 | 13.77 | 1.278 |
| Neat | --- | 0 | --- | 0.5 | 92.2 | 300 | 35.00 | 16.00 | 1.369 |
| Neat | --- | 0 | --- | 1.0 | 92.2 | 300 | 54.00 | 19.00 | 1.682 |
| Neat | --- | 0 | --- | 3.0 | 92.2 | 300 | 130.0 | 45.00 | 2.527 |
| Neat | --- | 0 | --- | 5.0 | 92.2 | 300 | 164.0 | 64.00 | 2.831 |
| Neat | --- | 0 | --- | 8.0 | 92.2 | 300 | 250.0 | 106.0 | 3.228 |

[a] Asphalts are SHRP AAK-1 or AAG-1. Aggregates are SHRP RB or RL.

[b] The FDO-aged cores were aged as loose mix.

[c] The numbers indicate $O_2$ pressure in the POV. Where no number is given, the aging was done in the FDO.
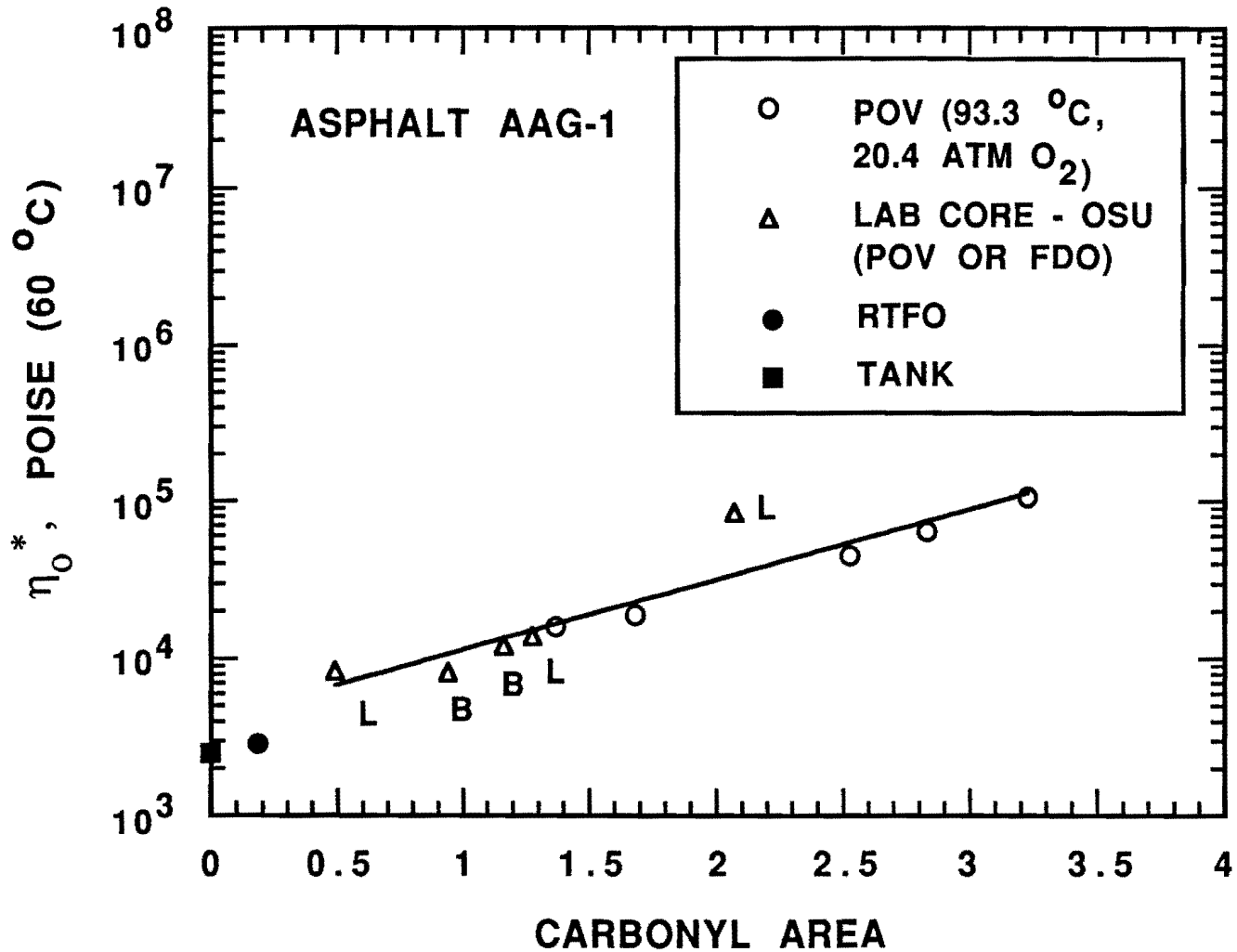
Figure I-2-9. Hardening Susceptibility for SHRP Asphalt AAG-1 as Determined by Both POV Aging of Neat Asphalt and Either POV or Forced Draft Oven Aging of Laboratory-Prepared Cores. The L and B Symbols Refer to SHRP Aggregates RL and RB
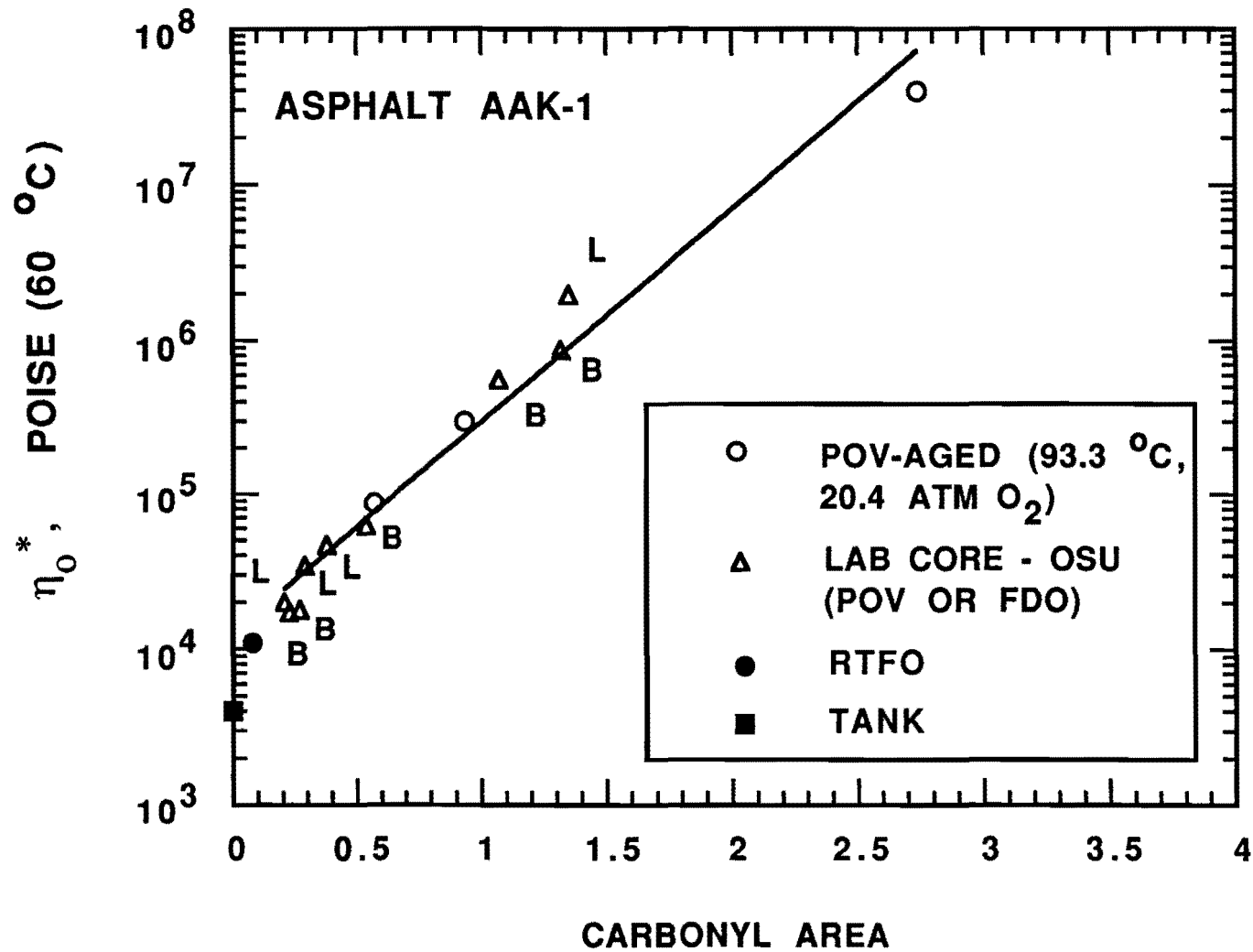
Figure I-2-10. Hardening Susceptibility for SHRP Asphalt AAK-1 as Determined by Both POV Aging of Neat Asphalt and Either POV or Forced Draft Oven Aging of Laboratory-Prepared Cores. The L and B Symbols Refer to SHRP Aggregates RL and RB

an important consideration in assessing an asphalt's durability.

There is considerable evidence that the hardening susceptibility is primarily a function of compatibility. Asphalt AAG-1, for instance, is exceptionally low in both saturates and asphaltene content which are mutually insoluble. Work by Stegeman et al. (1992) has shown that the hardening ratio before and after RTFOT aging can be significantly reduced by separating asphalt into fractions on the basis of solubility and then formulating asphalts from the more mutually soluble fractions. Chemical reaction rate constants generally vary as the exponent of the reciprocal absolute temperature. The rate of reaction is then given by this constant times a function of reactant concentrations. At the conditions in the POV, oxygen pressure is constant, and the actual oxygen uptake by the asphalt is so small compared to the number of available reaction sites that effectively the reactant concentrations are constant. Therefore, if the rate of oxidation can be considered proportional to the growth in carbonyl area, then

$$\frac{dA}{d\theta} = k = C \exp(-E/RT)$$

where $A$ is the carbonyl area, $k$ the rate constant, $\theta$ is time, and $E$ a constant energy of activation unique to the reaction taking place. $C$ is a constant. From this equation

$$\ln k = -\frac{E}{R}\left(\frac{1}{T}\right) + \ln C$$

and hence, one would expect a plot of $\ln k$ versus $(1/T)$ to be linear.

Figure I-2-11 shows this expected linear relationship for the Fina asphalt and Figure I-2-12 shows it for all five asphalts. The striking thing is not that the rates are different for each asphalt but that the slopes are different. As can be seen, some asphalts that show higher rates of oxidation at elevated temperatures actually have

20
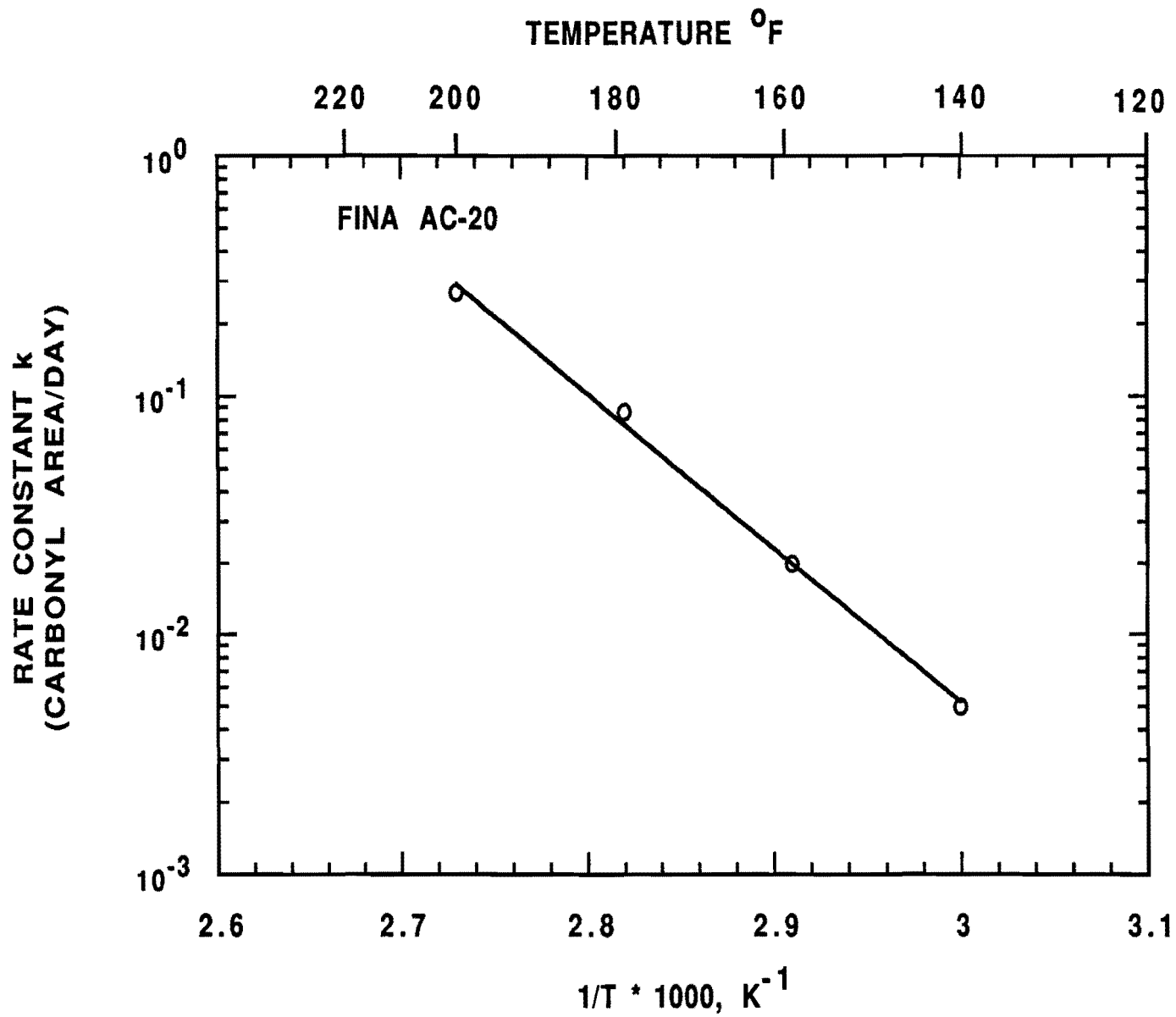
**TEMPERATURE °F**



Figure I-2-11. Arrhenius Plot for the Fina AC-20 Asphalt
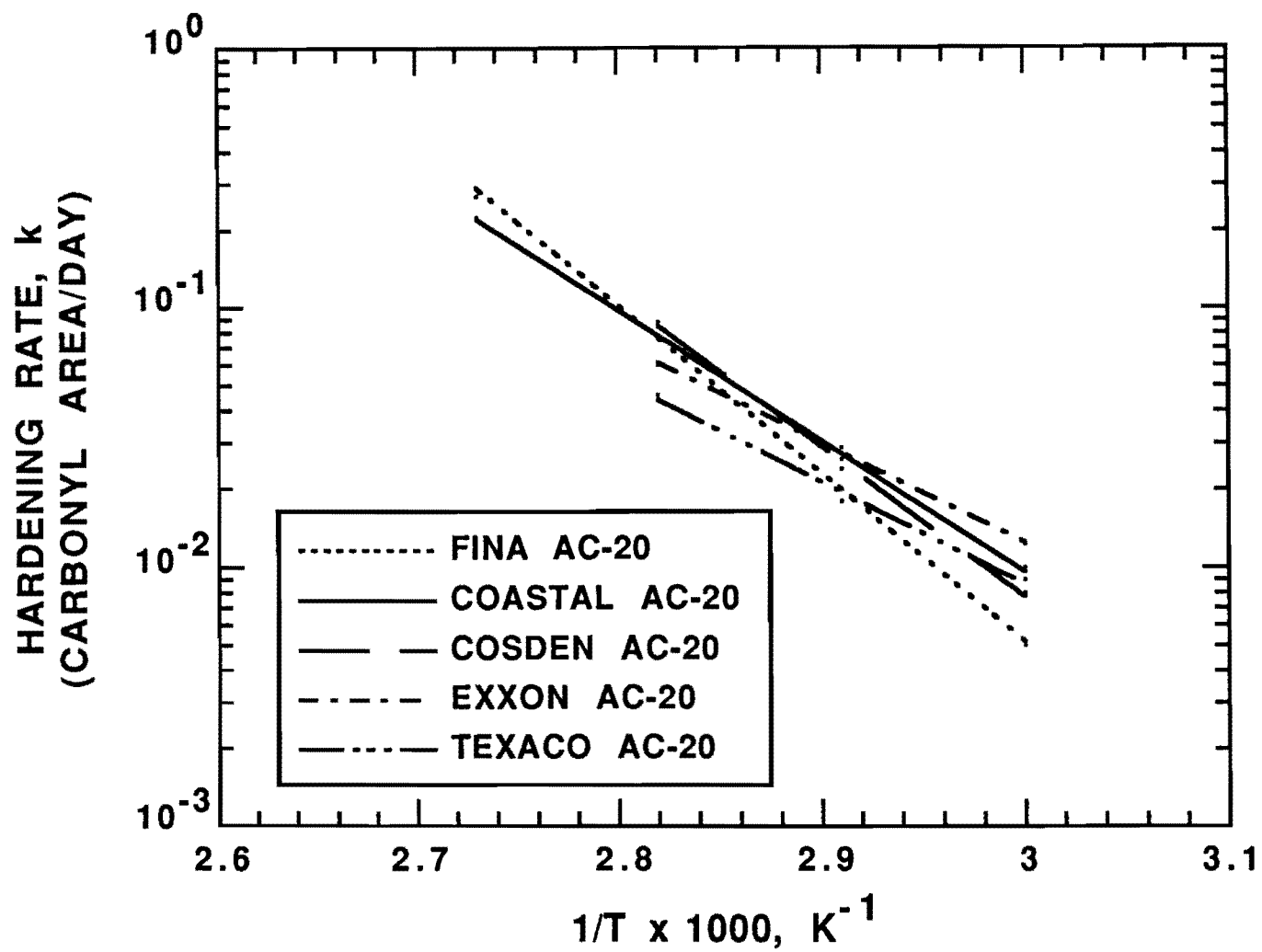
Figure I-2-12. A Comparison of the Arrhenius Plots for the Five Asphalts Studied

lower oxidation rates at temperatures expected during life on the road. This reversal can carry over to physical properties as well, as shown in Figure I-2-13 which shows the oxidative hardening of the Fina and Texaco asphalts at 60°C and 80°C. At the lower temperature, the Fina asphalt hardens more slowly, whereas at the higher temperature, the Texaco hardens more slowly. Thus no test run at a single elevated temperature is valid as a measure of expected road performance.

On the other hand, by running the POV at several temperatures, the resulting linear relations can be extrapolated to a realistic average road temperature or integrated over a typical road temperature history. To convert the rate data into a hardening (or other physical property) prediction, extrapolated rates, as could be obtained from Figure I-2-12, can be combined with hardening susceptibilities (or analogous physical-chemical property relation), such as those in Figure I-2-7. In this way the relative expected hardening rates could be calculated from the expected road temperature profile.

## Conclusions

POV-aging (300 psia $O_2$) of asphalt films (1000 $\mu$m thick) and subsequently measured FT-IR (ATR) spectra and complex dynamic viscosities has led to the following conclusions:

1) The degree of oxidation, as measured by the increase in the carbonyl peak area, relative to the unaged neat asphalt, increases linearly with oxidation time at a given temperature, over a range from 140 to 180°F (at least). The slope of this relation is indicative of the chemical reaction rate.

2) The degree of hardening due to oxidation increases essentially linearly with time, and hence is linearly related to the carbonyl peak area. The hardening susceptibility is a key measure of the effect of oxidative aging on a physical property. This effect is likely related to the compatibility of the asphalt.

3) Different asphalts exhibit different reaction rates at the same temperature and, just as importantly, exhibit different activation energies (different
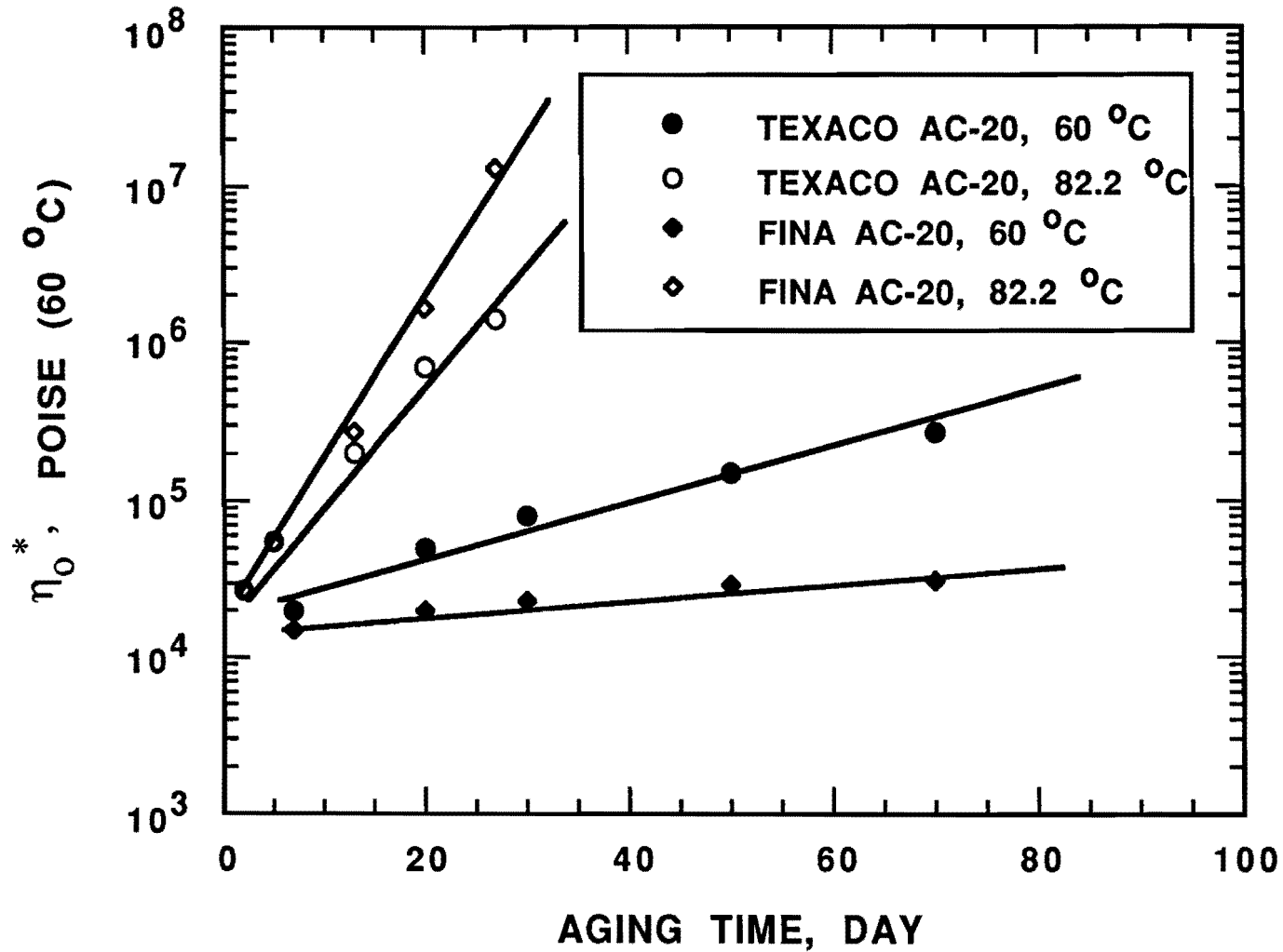
Figure I-2-13. A Comparison of the Hardening with Time of the Texaco and Fina Asphalts
Aged at Two Different POV Temperatures

slope of ln $k$ vs $1/T$). As a result, one asphalt may age faster than another at one temperature, while it may age slower at a different temperature. This crossover in aging rate is of profound significance in designing an asphalt road aging test. Such a test must be conducted at more than one temperature in order to accurately predict pavement aging.

4) Asphalts aged in contact with two different aggregates suggest that the reaction mechanisms are not significantly changed by the aggregate up to even 225°F.

# CHAPTER I-3
## AGING TEST DEVELOPMENT

**Introduction**

Many attempts have been made to simulate the different modes of asphalt aging with laboratory tests. The Thin Film Oven Test, TFOT, ASTM D1754-83 and the Rolling Thin Film Oven Test, RTFOT, ASTM D2872-80 are the two most recognized procedures to simulate the hot-mix aging. The TFOT procedure calls for the aging of asphalt in a ⅛ inch thick film in a shallow pan which is placed on a rotating shelf in an oven maintained at 325°F for 5 hours. The RTFOT is designed to age asphalt uniformly in thin films to account for the effect of oxygen diffusion. To simulate the hot-mix process, the procedure calls for the aging of about 35 grams of asphalt in a special rotating glass bottle maintained at 325°F for 75 minutes in an oven. The rotating bottle can constantly produce renewed films 5 to 10 $\mu$m thick.

Many variations of these original tests are reported in the literature over the years. As pointed out by Welborn (1984), all these test procedures tend to simulate the short-term aging due to the hot-mix process rather than the long-term aging in pavement which may involve different reaction mechanisms.

Recognizing the limitation of the TFOT, RTFOT, and their variations in simulating the long-term aging in a pavement, various researchers propose different aging procedures to simulate the long-term pavement aging at low temperatures.

In one study, residual asphalt from the TFOT was subjected to 20 atm oxygen pressure at 65.5°C for up to 1000 hours (Lee and Huang, 1973). Correlations of the viscosity with aging time and carbonyl absorption peak were made. It was also reported that 46 hours of aging was equivalent to 60 months of pavement service based on the asphaltene content.

Kim (1987) subjected asphalt samples of 0.5 mm thick to 100 psi oxygen pressure at 60°C for up to 5 days. Fraass breaking temperature, a measure of brittleness, of the aged samples was measured and correlated with aging time. It was reported that 5 days of aging was equivalent to 5-10 years of pavement service.

In more recent work, Petersen (1989) proposed a thin film accelerated aging test (TFAAT) which was a modification of the original RTFOT. The test procedure called for the aging of an asphalt in the RTFO bottle at 113°C and atmospheric pressure for up to 9 days. A capillary was placed in the RTFO bottle to reduce volatile losses which was considered a major problem that plagued all high-temperature aging procedures. Dynamic viscosity measured at 60°C and ketone content determined by reduction reaction of the aged samples (Dorrence et al., 1974) were compared to those obtained from the pavement core.

The work described in Chapter I-2 of this study is extremely important due to its implications on asphalt binder aging tests. Differences from one asphalt to the next in aging rates, rate dependence on temperature, and in hardening as the result of chemical aging were found to be significant in naturally occurring asphalts, thereby lending support for the notion that asphalts can be designed which have superior aging characteristics. Furthermore, evaluations of aging made at a single elevated temperature were found to be potentially very misleading with respect to predicted performance at the lower pavement temperatures.

Due to the significance of this aging work with respect to asphalt design and performance prediction, we devote this chapter to a brief summary of the results of Chapter I-2 and the presentation of a way in which these results might be used to make comparisons of predicted roadway performance.

**Summary of Aging Results**

Our studies of oxidative aging in Study 1249 reported in Chapter I-2 were conducted in a pressure oxygen vessel (POV). In this device, thin films of asphalt can be exposed to pressurized oxygen for given times and temperatures. The objective of using oxygen under pressure is to saturate the film with oxygen to eliminate diffusion as a variable.

In this work, there were several key questions which we wanted to answer. First, and perhaps foremost, was whether or not there was a change in the oxidation mechanism as the aging temperature was changed. That is, did the change in the

27

temperature simply change the rate or did it change the actual chemistry of the reaction. The second question was what were the oxidation rates and how did these vary with temperature?

Key to our success in unraveling oxidative aging has been the use of the infrared technique combined with dynamic viscosity measurements. Figure I-2-3 shows IR spectra for Texaco AC-20 which has been aged in the POV for various times at 180°F. The growth in the spectra with time is indicative of the oxidative aging. The rapid and highly accurate ATR technique developed as a part of this work has been instrumental in achieving results which can be quantitatively compared.

We found that there is a linear relationship between log viscosity and carbonyl formation as illustrated in Figures I-2-6 through I-2-10. Some results for lab compacted and oven-aged cores using two different aggregates are included in Figures I-2-9 and I-2-10. Based on the work, thus far, this relationship appears to hold regardless of the conditions including the aggregate. A plot of log viscosity vs carbonyl formation for all of the asphalts examined so far are shown in Figure I-3-1. The data points were omitted for clarity. Figures I-2-4 through I-2-10 show that the straight lines through the data do not intercept the original asphalt. There is an initial rapid oxidation and increase in viscosity before the linear functions are reached. As the time is short and the degree of hardening small, we have assumed it to be roughly the same for all asphalts and shifted the origin in Figure I-3-1 to the beginning of the linear range in which most of the hardening occurs. This assumption appears doubtful with some of the supercritical fractions, but this will be discussed later.

The results in Figures I-2-6 through I-2-10 and I-3-1 are most impressive in that they cover viscosity changes of three orders of magnitude and include the entire range of interest in asphalt work.

One additional very interesting result shown in Figure I-3-1 is that the various asphalts have distinctly different relationships between viscosity increase and the amount of aging as measured by carbonyl formation. For a given carbonyl increase,

28
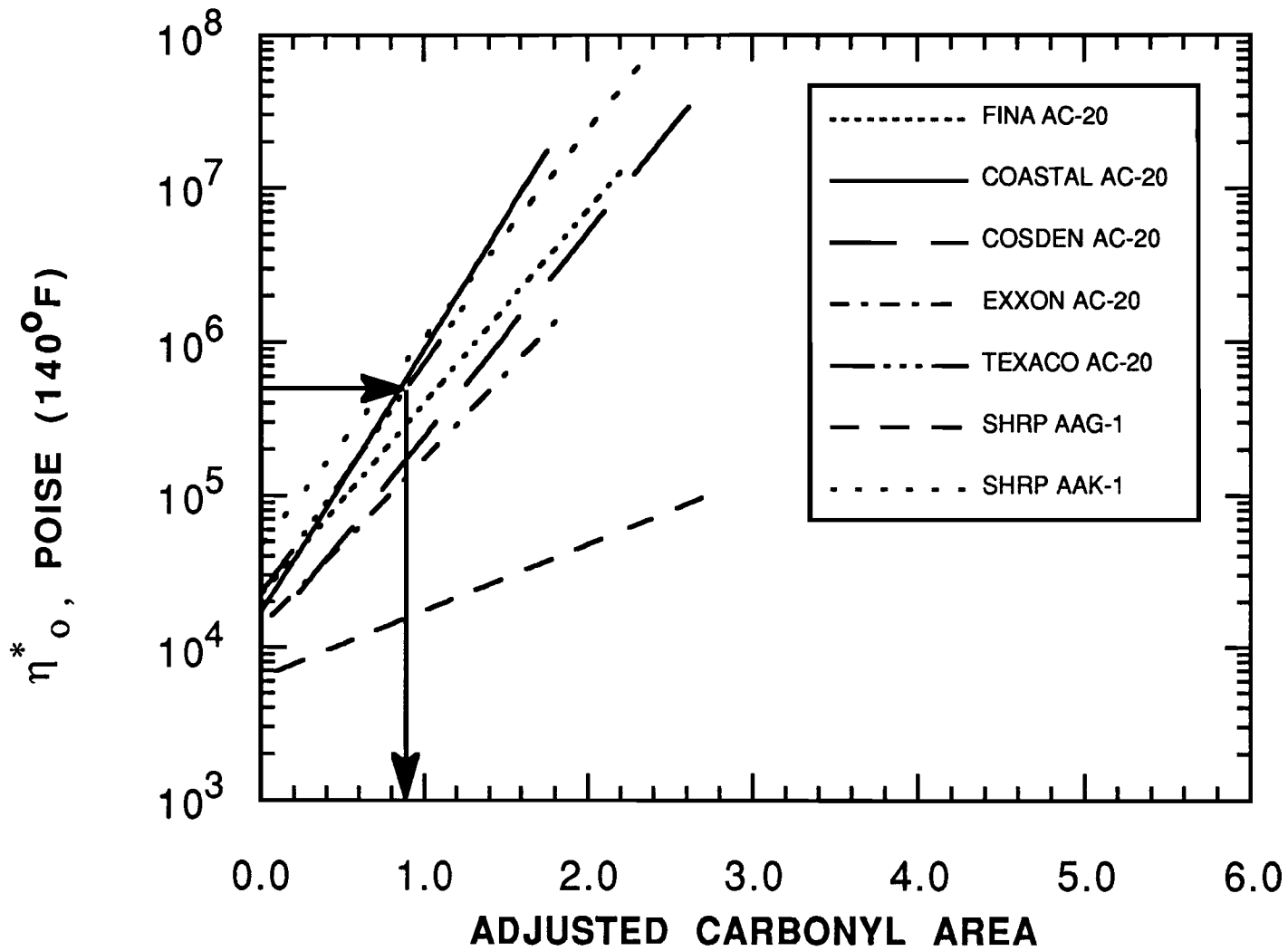
Figure I-3-1. 140°F Viscosity Versus Adjusted Carbonyl Area for Seven Asphalts

some asphalts will show a great deal of hardening whereas another asphalt will show much less hardening. This tendency of an asphalt to harden as a result of oxidation represents its "tolerance to aging." Based on the work thus far, this tolerance to aging is a critically important parameter for characterizing the nature of asphalt materials and to asphalt design. The fact that native asphalts can be considerably different in this respect suggest that asphalts can be designed which will show a relatively small amount of hardening with aging as exhibited by SHRP asphalt AAG-1 in Figure I-3-1.

The results from the aging tests were also used to determine the rate of oxidation for each asphalt. As was shown in Figure I-2-5, we found that the carbonyl area grows linearly with time over some extended period. Thus, an oxidation rate can be calculated for each temperature. When those oxidation rates are plotted in the usual manner for chemical reactions, a straight line is found as was shown in Figure I-2-11.

This same plotting technique was used for all of the asphalts as was shown in Figure I-2-12. The data points were omitted for clarity. This plot shows some surprising facts in that some asphalts oxidize much faster than the others at lower temperatures and slower than the others at higher temperatures. For example, the Fina and Texaco lines intersect at about 160°F. Above 160°F, Fina ages more rapidly and Texaco looks better while, below 160°F, the reverse is true. Thus, an aging test run at a single high temperature could give a totally incorrect conclusion about low temperature aging.

**Proposed Aging Test**

Because the "tolerance to aging" results in Figure I-3-1 show straight line relationships between log viscosity and carbonyl formation (i.e. the amount of oxidation or aging) and the "rate of oxidation" results in Figure I-2-12 show straight line relationships between rate of oxidation (or aging) and temperature, a simple performance related aging test can be formulated.

As an example, consider the Texaco AC-20 asphalt. The test time for this asphalt to reach a viscosity of 500,000 poise is as follows.

$$\frac{\text{Test Time to Reach}}{500,000 \text{ Poise}} = \frac{\text{Carbonyl Formation for 500,000 Poise}}{\text{Rate of Oxidation}}$$

As shown in Figure I-3-1, the amount of carbonyl formation required to give a viscosity of 500,000 poise for this asphalt is 0.88. From Figure I-3-2 using an average road temperature of 122°F, the rate of carbonyl formation is 0.0036. Thus for Texaco AC-20

$$\frac{\text{Test Time to Reach}}{500,000 \text{ Poise}} = \frac{0.88}{0.0036} = 244 \text{ days}$$

The test results for the asphalts tested thus far are shown in Table I-3-1. This table includes results for average road temperatures of 95°F and 122°F. As can be seen from this table, Fina takes 3.37 times as long as Texaco to reach 500,000 poise at 122°F and 8.59 times at 95°F. Analogous calculations made at 180°F show a different ranking from that determined at a lower temperature and show the error that can come from predicting aging relative rates based on a single high temperature measurement. These results are quite dramatic and offer great promise of developing a meaningful aging test.

**Future Work**

There really are three areas that still need investigation. One already alluded to is the need to better model the reaction rate during early aging. It is our belief that in actual practice much of this occurs in the hot-mix plant and if so will have little effect on the aging test. Secondly, the pressure effect on relative rates, if any, should be investigated.

The last step in completing the development of the aging test is verification with roadway samples. We have a large number of test sections for which we have the original tank asphalts. These test sections need to be cored and compared with the aging test results for verification.
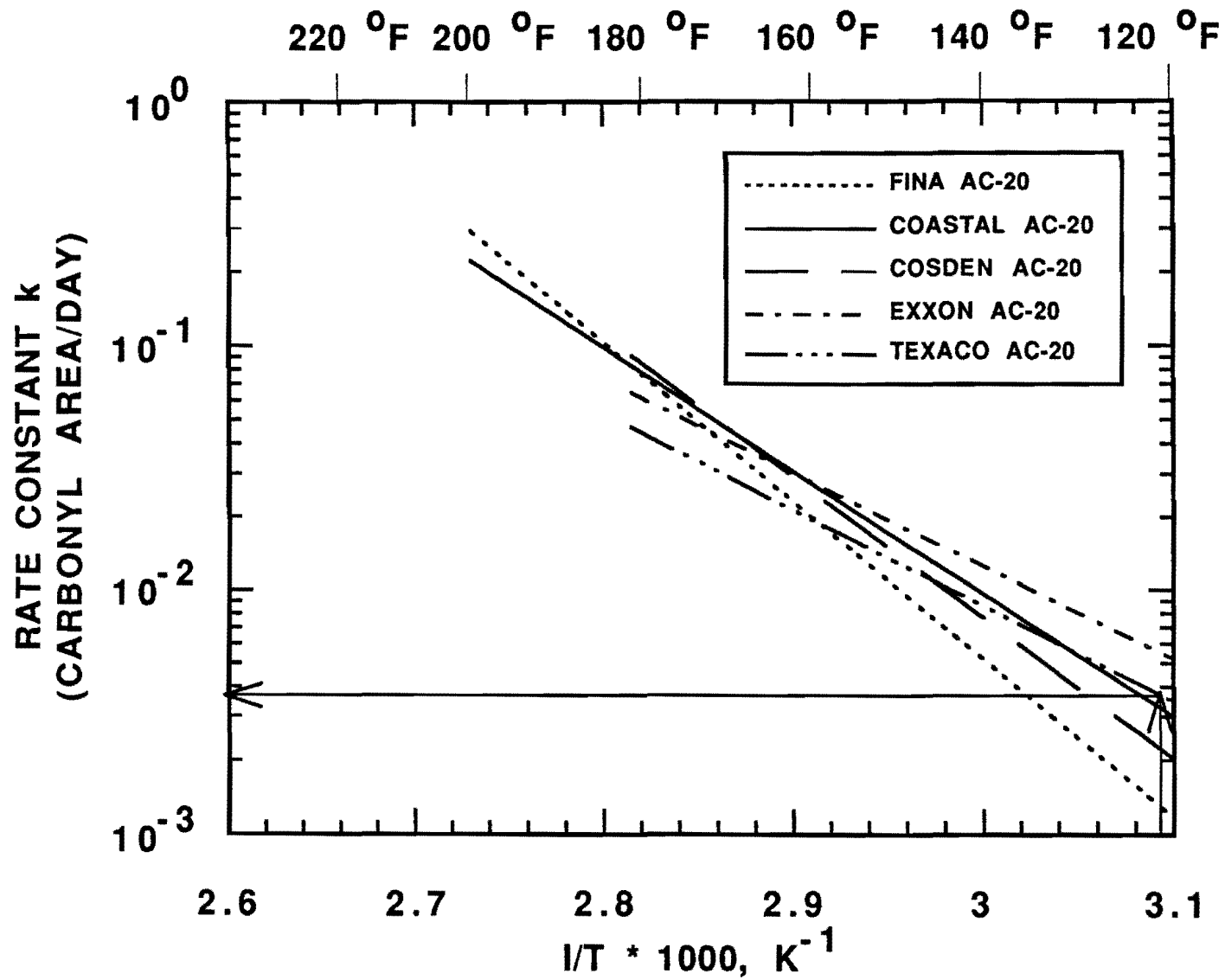
Figure I-3-2. The Rate of Carbonyl Formation as a Function of the Reciprocal Absolute Temperature for Five Asphalts

## Table I-3-1
## Aging Results for Five Asphalts

| AC-20 Asphalt | Test Time in Days to Reach 500,000 Poise | | | Relative Hardening Time | | |
|---|---|---|---|---|---|---|
| | 95°F | 122°F | 180°F | 95°F | 122°F | 180°F |
| Exxon | 1,000 | 259 | 22.20 | 1.04 | 1.06 | 2.20 |
| Texaco | 960 | 244 | 18.30 | 1.00 | 1.00 | 1.81 |
| Fina | 8,230 | 823 | 14.60 | 8.59 | 3.37 | 1.45 |
| Cosden | 4,310 | 568 | 13.20 | 4.50 | 2.33 | 1.31 |
| Coastal | 1,550 | 266 | 10.10 | 1.62 | 1.09 | 1.00 |

33

# CHAPTER I-4
## SUNLIGHT AGING OF ASPHALTS

**Introduction**

It is well established that light can promote oxidation reactions in an asphalt. Streiter and Snoke (1936), in his pioneer work on photo-oxidation of asphalt, observed that when asphaltic bitumen was exposed to light, water-soluble products were formed. The author attributed the weathering phenomenon to rain water leaching out these photo-oxidation products.

Kleinschmidt and Snoke (1959) exposed asphalt films of different thickness to carbon arc radiant energy and water treatment. Analysis was done by a chromatographic technique they had previously developed to separate asphalt into four fractions. Asphaltene was first precipitated from the asphalt with pentane and the maltene fraction was eluted with the solvents pentane, methylene chloride, and methyl ethyl ketone to obtain the remaining fractions designated as white oils, dark oils, and resins, respectively. These authors concluded that dark and white oils were selectively degraded during the photo-oxidation process.

Suspecting that photo-oxidation might be the cause for the rapid deterioration of some pavement surfaces in England, Oliver and Gibson (1972) conducted an elaborate experimental study to determine the major source of the water-soluble products formed during photo-oxidation in the various fractions of an asphalt. An asphalt was fractionated into asphaltenes, resins, dark oils and white oils by Kleinschmidt's procedure (1959). Samples of each fraction were isotopically labeled by exchanging hydrogen for tritium. Each labeled fraction was recombined with other unlabeled fractions to reconstitute the original asphalt. The reconstituted asphalts were repeatedly exposed to radiant energy of a carbon arc and extracted with water. Water-soluble products were analyzed for tritium. These authors concluded that the dark oils fraction accounted for most of the water-soluble products.

Beitchman (1959) described a method to prepare unsupported thin films of air-blown asphalts of about 25 $\mu$m thick for infrared analysis. The asphalt films were

34

prepared by pressing an asphalt sample between two sheets of cellophane in a heated hydraulic press to the desirable thickness. The cellophane sheets were separated from the asphalt film by soaking the composite sheet in cold water. The asphalt film was then mounted on a holder and subjected to radiation. The sample was then subjected to transmittance infrared analysis. The method was the first successful effort to produce infrared spectra of a neat asphalt film without resorting to solvents, mulls, pellets or salt-crystal supports. By exposing the unsupported films of asphalt to the radiant energy of a carbon arc, Beitchman observed increases in absorbance at 3435 $cm^{-1}$, 1700 $cm^{-1}$, and 1030 $cm^{-1}$ which were assigned as the infrared absorption frequencies of the hydroxyl (O-H), the carbonyl (C=O), and the sulfoxide (S=O) functional groups, respectively.

Employing Beitchman's technique in a series of studies on the photo-degradation of roofing asphalt, Campbell and Wright (1962, 1964a, 1964b, 1966) exposed unsupported Kuwait asphalt films of 25 $\mu$m thick to xenon-arc radiant energy for different exposure times. Oxidative change was measured by the increase in softening point and by infrared spectroscopy. They concluded that the principal oxygenated hydrocarbon products formed during the photo-oxidation process as assigned by infrared absorbance peak at 1700 $cm^{-1}$ was the carbonyl compounds. By using model carbonyl compounds and several colorimetric methods, they further concluded that the carbonyl compounds included acids, aldehydes, ketones, and peroxides.

**Sample Preparation and IR Analysis**

In the work of this study, multiple samples of each asphalt were simultaneously exposed to direct sunlight. Representative samples of each asphalt with the desired exposure time were then removed and stored in the dark for future analysis. The remaining samples were subjected to further exposure. This procedure ensured that the history and rate of solar aging for each asphalt could be obtained and compared even though the solar flux changed from time to time.

The ATR-IR technique allowed accurate analysis of the sunlight-aged surface.

However, because the photo-aged layer was only about 5 to 10 $\mu$m thick, any heating might cause the photo-aged layer to mix with or migrate to the layer below rendering the IR scan inaccurate. A sample of the size of the reflective surface of the prism was cut and the sample was pressed onto the prism surface by a special clamp to ensure good physical contact.

**Results**

When the surface of an asphalt film is first exposed to sunlight, the surface becomes hard and gradually loses adhesiveness. Subsequent exposure causes the surface to become dull and dry due to fine grooves resulting from surface microcracks. Prolonged exposure causes the fine grooves to widen.

In the past, infrared analysis of the chemical changes due to photo-oxidation was studied exclusively by the Beitchman's technique (1959) (Campbell and Wright, 1962, 1964a, 1964b, 1966) of exposing a thin film about 25 $\mu$m thick to radiation. Infrared analysis was then carried out by mounting the photo-aged sample in the path of the infrared light. Unfortunately, the technique was limited to short exposure time as the thin film tends to crack during longer exposure time, rendering it unsuitable for his unsupported-film transmittance IR technique. Attenuated Total Reflectance IR provides an excellent alternative to study the surface oxidation reaction of asphalt film subjected to long exposure time.

Figure I-4-1 shows the infrared spectra of the surfaces of the Texaco AC-20 asphalt films exposed to sunlight for various exposure times. Spectral changes due to photo-oxidation appear to be significantly different in both degree and chemistry from those resulting from aging in the dark. The absorbance peak in the carbonyl region (1700 cm$^{-1}$) increased more rapidly and to a much higher level than those aged in the dark. The rate of carbonyl increase could be a hundred times faster than the rate of thermal aging. For example, the carbonyl peak level obtained by aging in the POV at 300 psia oxygen and 71.1°C for 70 days could be achieved by exposing to sunlight for 3-4 hours.

Other spectral changes included a broad band in the 3400 cm$^{-1}$ region. This

36
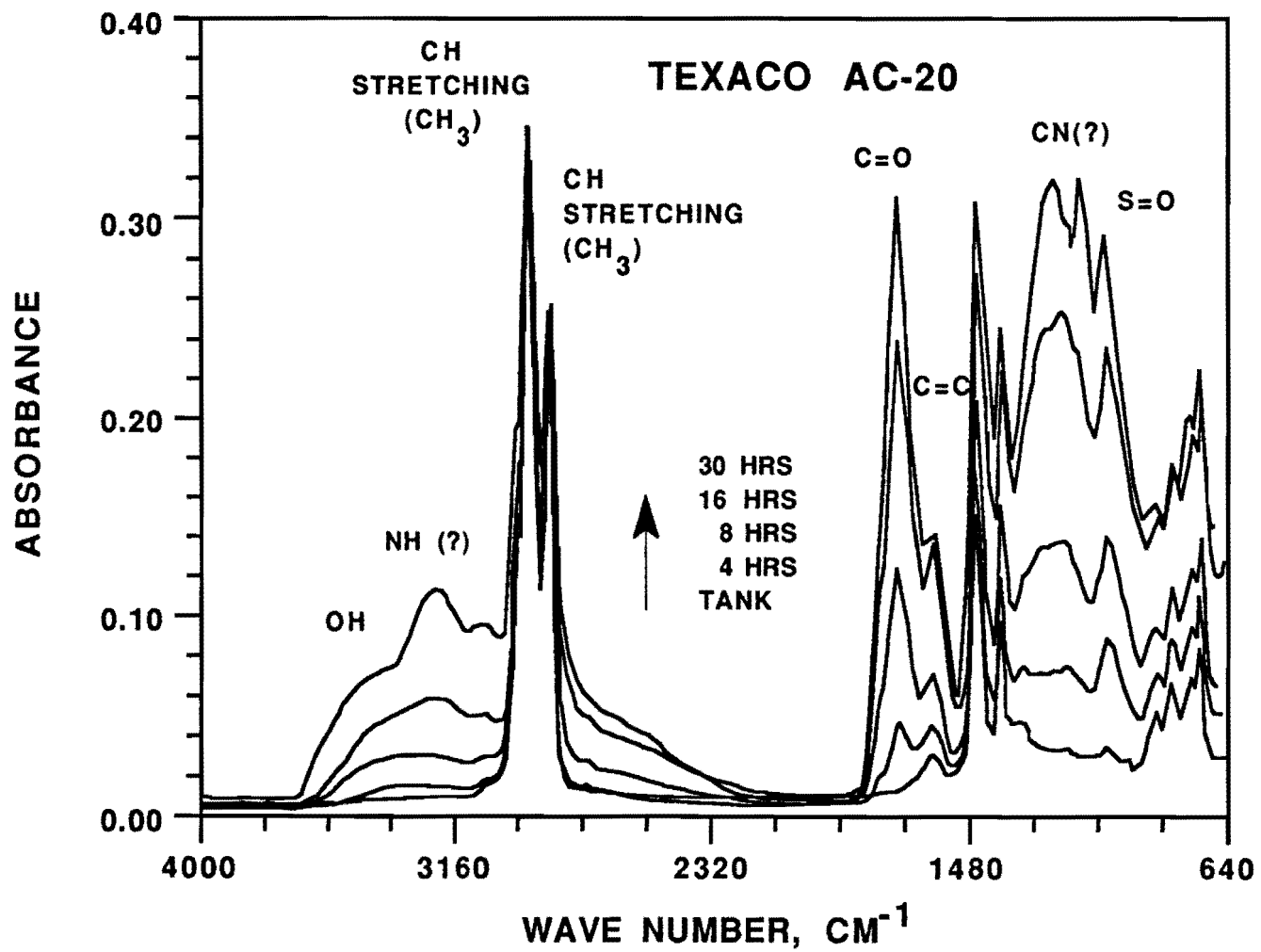
Figure I-4-1. ATR-IR Spectra for the Texaco AC-20 Asphalt with Various Exposure Times in Sunlight

band was due to O-H functional groups. Furthermore, the growth of a new peak at 3230 cm$^{-1}$ was observed after 16 hours of exposure time. The peak was fully developed after 30 hours of exposure time. The band was most likely attributed to N-H bond.

Another major spectral change was the broad absorbance band between 1100 to 1300 cm$^{-1}$. The band intensity increased with exposure time and finally developed into two distinct bands centered at 1170 and 1270 cm$^{-1}$, respectively, after 30 hours of exposure time. These two bands could be attributed to the formation of amine compounds as the C-N stretching of aromatic amines also show two characteristic peaks between 1180 and 1360 cm$^{-1}$.

**Carbonyl Region**

A comparison of the carbonyl absorbance peak of the photo-oxidation and the thermal oxidation in the dark revealed a subtle difference as shown in Figure I-4-2. As can be seen, the carbonyl absorption peak due to photo-oxidation of the unaged asphalt sample is centered at 1715 cm$^{-1}$ while the carbonyl peak due to thermal oxidation in the dark is centered at 1698 cm$^{-1}$. The shift was observed in all five AC-20 asphalts tested in this study.

The implications of this shift are not clear at this time. One possibility is that photo-oxidation may involve a different reaction site in a molecule from that of the thermal oxidation resulting in a shift in absorbance peak; it is well known that the relative position of the carbonyl group to an aromatic ring in a molecule can cause the carbonyl absorbance peak to shift. The shift may also be due to the preferential selection of particular groups of components by photo-oxidation which were not involved in thermal oxidation.

When the POV-aged samples (13 days, 300 psia oxygen, 71.1°C) were exposed to sunlight, the subsequent carbonyl peak increase remained centered at 1698 cm$^{-1}$ rather than shifting to 1715 cm$^{-1}$ as shown in Figure I-4-3. The results further confirm that the carbonyl shift due to sunlight exposure on the unaged asphalt is real. The implication of this phenomenon is not clear. It is hypothesized that pre-aging in the

38
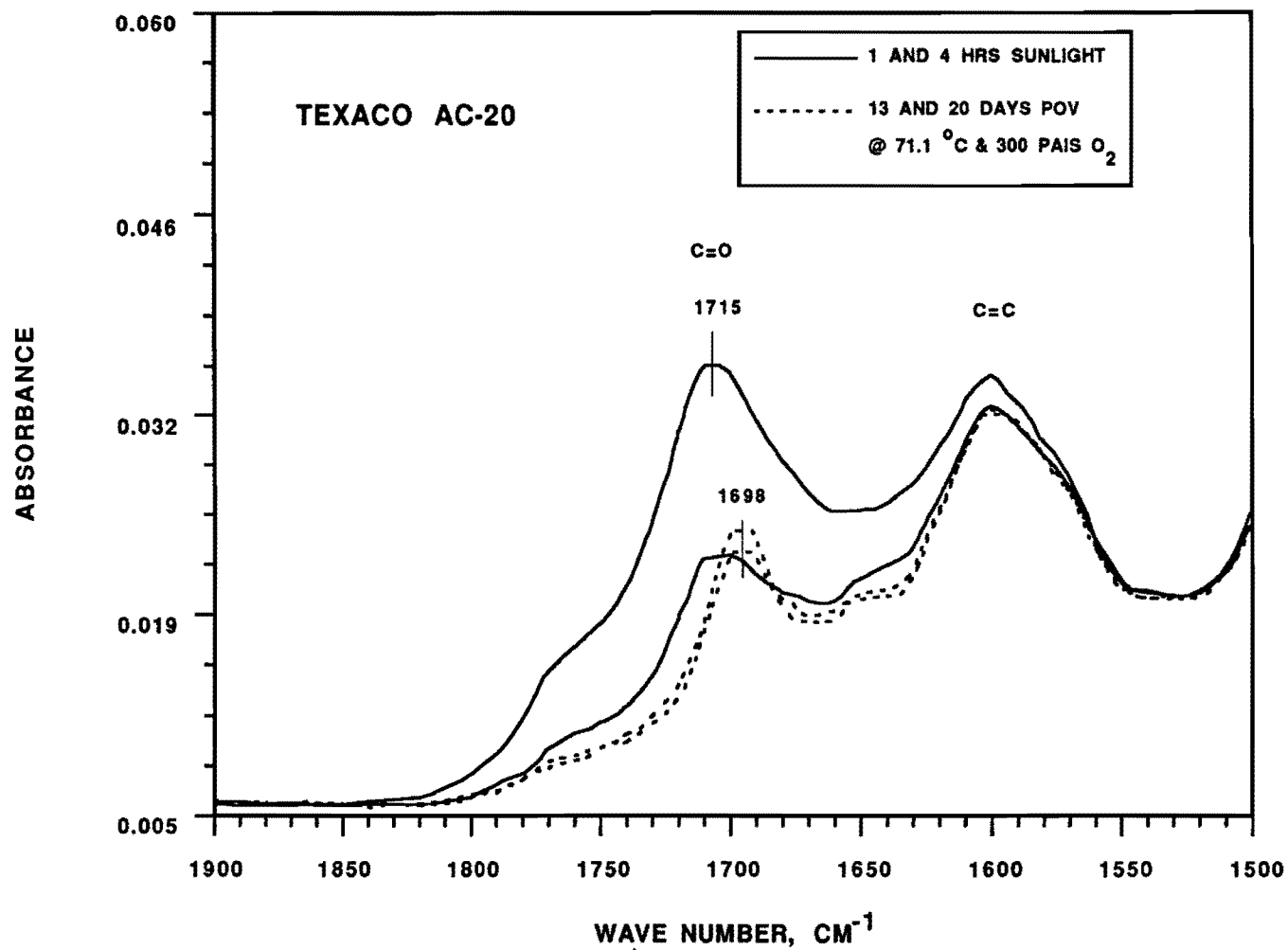
Figure I-4-2. Comparison of the ATR-IR Carbonyl Band for the POV- and Photo-aged Texaco AC-20 Asphalt
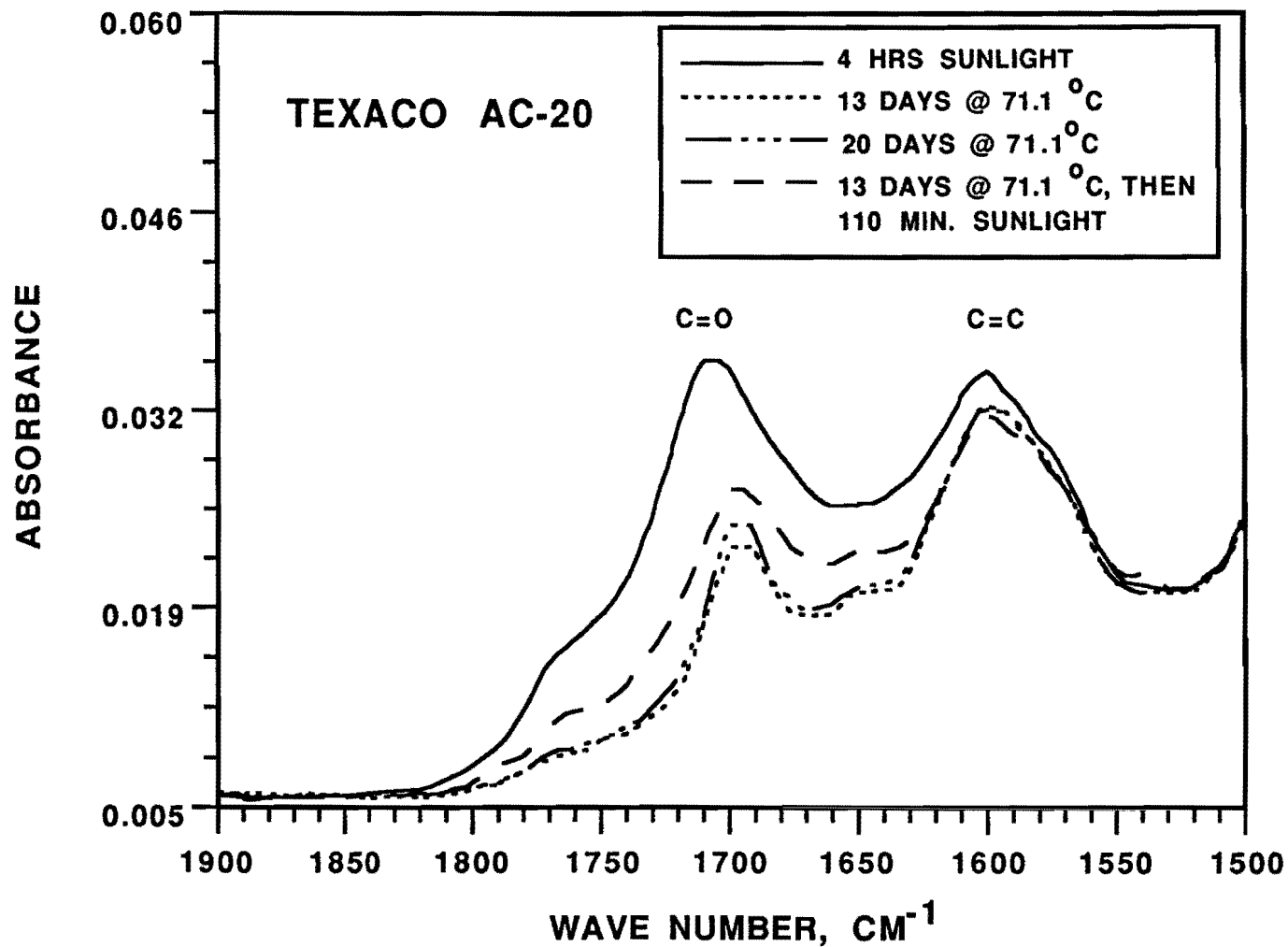
Figure I-4-3. Comparison of the ATR-IR Carbonyl Band for the
Texaco AC-20 Asphalt Samples Exposed to Sunlight with and without POV Pre-aging

40

POV caused the previously photo-favorable reaction site to become unfavorable through chemical reaction.

**Water Soluble Materials**

Formation of water soluble materials during the photo-oxidation of asphalt has been reported in the literature by several investigators (Kleinschmidt and Snoke, 1959; Oliver and Gibson, 1972; Streiter and Snoke, 1936) and has also been investigated in this study using the ATR-IR technique. Asphalt films exposed to 4 and 30 hours of sunlight were soaked in distilled water and IR spectra were taken before and after the soaking. For the Texaco AC-20 asphalt with 4 hours of sunlight exposure time, IR spectra showed no significant difference before and after soaking in distilled water for 30 minutes.

However, for the sample exposed to sunlight for 30 hours, IR spectra showed dramatic spectral changes before and after the soaking process as illustrated in Figure I-4-4. After leaching with distilled water for 15 minutes, the peaks at 3200, 1270, and 1170 cm$^{-1}$ had disappeared together with a significant reduction in absorbance intensity in the carbonyl region. Additional leaching caused further absorbance reduction in the carbonyl region and the band between 1100 and 1300 cm$^{-1}$. The spectral changes were attributed to the water soluble materials being leached away. The result demonstrated that the natural weather cycle could have an erosive effect on the top layer of asphalt binder which was exposed to direct sunlight.
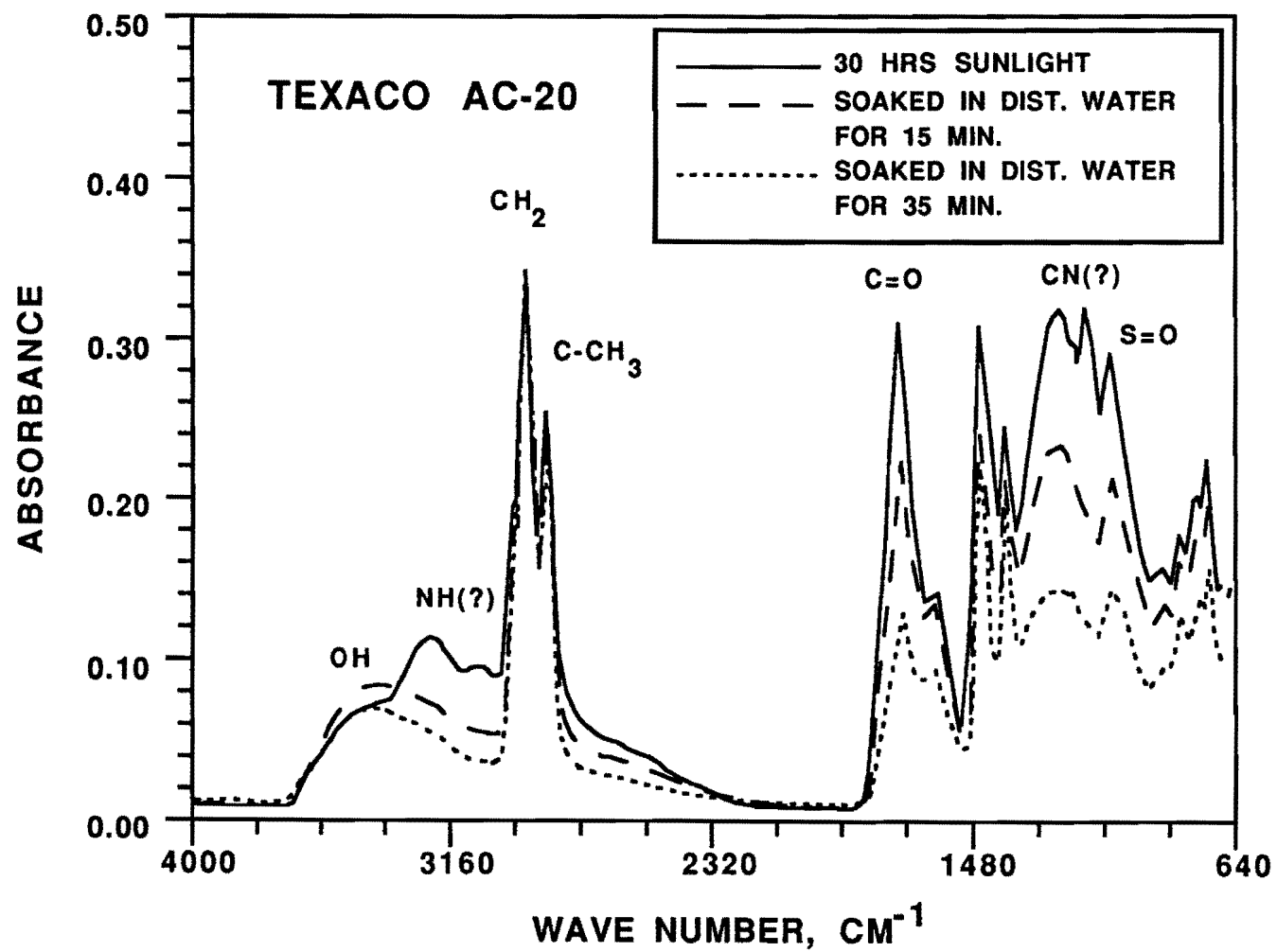
Figure I-4-4. Comparison of the ATR-IR Spectra for the Photo-aged Texaco AC-20 Asphalt Leached with Distilled Water for Various Times

# SECTION II

## Supercritical Fractionation and Fraction Blending

# CHAPTER II-1
## INTRODUCTION

In Study 1155 three asphalts were fractionated using supercritical pentane to separate the lightest 60% and then mixtures of pentane and cyclohexane to fractionate the heavier material. This was necessary because the harder material would not flow. The unit was modified so that solid material could be collected, and cyclohexane was used so that cuts could be made to any depth in the material. Because of its better selectivity, pentane was still used to fractionate the lighter material.

In this study three reduced crudes and three asphalts were used. The idea of running reduced crude was to consider the practicality of eliminating the vacuum tower. In practice, this had considerable effect on the operating temperatures which, for cyclohexane, were already high. All of the blends were actually made from the asphalt fractions.

The operation of the supercritical unit was described in the Study 1155 report, but it will be reviewed here with emphasis on the modifications. This description of the process is followed by description of the analytical methods and then by operating conditions and fraction properties for both the reduced crude and asphalt fractions. Chapter II-5 contains some interesting correlations relating physical and chemical properties of fractions and whole asphalt. Chapter II-6 discusses asphalt blends and blend properties.

# CHAPTER II-2
## PREVIOUS WORK

**Supercritical Fluids**

A supercritical fluid (SCF) is defined as a fluid maintained at a state above its critical temperature. Above the critical temperature of a substance, increasing the pressure cannot produce more than one phase; therefore, the fluid will remain in a dense gas state. Comparing the typical properties of gases, liquids, and SCFs in Table II-2-1 shows that SCFs may be useful for separations and reactions (Ely and Baker, 1983; Klesper, 1980; McHugh and Krukonis, 1986; Stahl et al., 1988; Williams, 1981; Yilgor and McGrath, 1984).

### Table II-2-1
### Typical Properties of Gases, Liquids, and SCFs

| property | units | gas | liquid | SCF |
|---|---|---|---|---|
| density | $g/cm^3$ | $10^{-3}$ | 1 | 0.3 |
| viscosity | poise | $10^{-4}$ | $10^{-2}$ | $10^{-4}$ |
| diffusivity | $cm^2/s$ | $10^{-1}$ | $5 \cdot 10^{-6}$ | $10^{-3}$ |

SCFs separate multicomponent mixtures by differences in component volatilities and interactions between components and the solvent. Thus, supercritical (SC) separations contain characteristics of both distillation and liquid extraction (Irani and Funk, 1977; McHugh and Krukonis, 1986; Zosel, 1980). As with conventional processes, product purity may be enhanced by adding reflux lines, trays, or mixers to SC separators. The low viscosities and high diffusivities of SCFs allow for rapid phase separation and mass transfer between phases (Stahl et al., 1988; Williams, 1981; Yilgor and McGrath, 1984).

The solvent power of a SCF is related to its density, which is easily controlled

by adjusting the temperature and/or pressure (Ely and Baker, 1983; McHugh and Krukonis, 1986; Randall, 1983; Stahl et al., 1988; Streett, 1983). More accurately, the free volume, the molecular geometry, and specific interactions of the solvent and substrate affect the SCF solvent power (Klesper, 1980). Only slight changes in temperature or pressure of a SCF produce remarkably large changes in solvent power. The chemical nature of the solvent also affects the selectivity of the separation (Ely and Baker, 1983). SC processes allow easy and efficient solvent recovery by isothermal decompression or isobaric heating (Ely and Baker, 1983; King and Bott, 1982; McHugh and Krukonis, 1986; Randall, 1982; Randall, 1983; Stahl et al., 1988; Zosel, 1980).

SC separation processes have many advantages over conventional methods. SC processes dissolve involatile substances. The high diffusivity and low viscosity of SCFs allow more efficient extraction of materials from solid structures. Thermally sensitive substances separate more easily with SCFs due to lower operating temperatures than conventional distillation. The higher pressures enable processing of easily oxidized materials. SC processes allow the use of a wide range of solvents. Present separations may use safer and more environmentally friendly solvents such as carbon dioxide by implementing SC methods. SC processes are equally suited for selective extraction and refining of crude extracts (Stahl et al., 1988). SCFs are particularly effective for separating substances of medium molecular weight, relatively low volatility, and low polarity.

Excellent separation of solvent and solute may be realized with lower energy consumption than normal liquid extraction. This efficient solvent regeneration and low contamination in the products provides the major economic driving force for supporting SC separations (Bakshi and Lutz, 1986; Ely and Baker, 1983; Gearhart and Garwin, 1976a; Gearhart and Garwin, 1976b; Irani and Funk, 1977; King and Bott, 1982; Peter and Brunner, 1980; Randall, 1982; Randall, 1983; Stahl et al., 1988; Williams, 1981; Yilgor and McGrath, 1984; Zosel, 1980). Obviously, SCFs merit consideration for polymer and petroleum product separation.

Considerable industrial research has been done for various substances, but

public access is limited. Patents on SC processes describe hydrocarbon and residuum separation and refining (Katz and Whaley, 1945; Roach, 1981; Zarchy, 1985), liquified coal deashing (Conaway et al., 1978; Ely and Baker, 1983), and various separations of other natural substances, such as coffee decaffeination (McHugh and Krukonis, 1986; Randall, 1982).

The behavior of natural substances with wide ranges of chemical components and properties, such as asphalt, are especially difficult to predict (Monge and Prausnitz, 1983). Products from different sources may exhibit substantially different behavior in SC processes due to the varying properties of constituents (Ely and Baker, 1983). Phase equilibria and process design can be based on effective properties of fractions or pseudocomponents of the material, but require empirical models dependent upon origin (Ely and Baker, 1983; Randall, 1983; Stahl et al., 1988).

SC separation divides components roughly according to molecular weight, but chemical properties also affect separation (McHugh and Krukonis, 1986; Stegeman et al., 1992; Yilgor and McGrath, 1984). Differences in molecular weight and polarity more strongly influence miscibility in SCFs than aromaticity and unsaturation (Ely and Baker, 1983). The solubility of a substance in the SCF controls the separation, so the class of compounds often overlaps component volatility (Zosel, 1980). Entrainers, components having volatility between that of the solvent and substance to be extracted, provide changes in the selectivity and capacity of the solvent while still allowing easy solvent regeneration (Ely and Baker, 1983; Stahl et al., 1988). Thus, SC separation provides another valuable tool for the processing of an assortment of synthetic and natural products.

## Resid Upgrading

Most refineries further process residues from atmospheric distillation by vacuum distillation (Holbrook, 1984; Speight, 1981). This process, separating strictly on component volatilities, usually operates at temperatures of 400-413°C (750-775°F) and under a slight vacuum (Hydrocarbon Processing, 1990; McHugh and Krukonis,

1986; Zosel, 1980). Substantial thermal decomposition occurs at temperatures above 350°C (660°F), so some degradation occurs at these operating temperatures (Speight, 1981). Vacuum distillation also produces low value asphalt or vacuum residue. The consistency of asphalts produced by vacuum distillation depends largely on the crude source (Corbett, 1984; Holbrook, 1984; Speight, 1981). Refiners use vacuum distillation to produce gas oils suitable for feed to catalytic cracking units.

Liquid extraction techniques called deasphalting have long been used to remove the more valuable heavy gas oils from asphalt. These smaller oil molecules remain in asphalt after vacuum distillation due to their low volatilities, but separate from the asphaltic components using liquid extraction due to their solubility in light hydrocarbon solvents. Deasphalting produces deasphalted oil (DAO) stripped of most of the metals and asphaltenes. The metals are rejected more thoroughly than the sulfur and nitrogen compounds. DAO reduces coke formation in further processing such as catalytic cracking and may also produce lube stocks. Components of lowest molecular weight and greatest paraffinicity are preferentially extracted using various light hydrocarbons. Propane deasphalting is the most common, but some operations use butane or pentane. Foster Wheeler's Low-Energy Deasphalting Process (LEDA) uses light hydrocarbon solvents at temperatures of 50-230°C (120-450°F) and pressures of 20-35 bar (300-500 psig).

As with vacuum distillation, the process economics and the product yields depend on the crude source. For most crudes, deasphalting is more flexible than coking and more economical than direct hydrotreating. Therefore, solvent deasphalting can help increase cash flow. The main drawback of solvent deasphalting and other processes used to increase gas oil yields is the production of large amounts of a low-value by-product -- asphalt (Bakshi and Lutz, 1986; Billon et al., 1977; Bousquet and Laboural, 1987; Ditman, 1973; Eisenbach et al., 1983; Ely and Baker, 1983; Gearhart, 1980; Gearhart and Garwin, 1976b; Hydrocarbon Processing, 1990; McHugh and Krukonis, 1986; Pilat and Godlewicz, 1940; Speight, 1981; Stahl et al., 1988; Vermillion and Gearhart, 1983; Williams, 1981; Zosel, 1980).

Some industrial solvent deasphalting processes use the advantages of SCF

properties to recover the light hydrocarbon solvent under SC conditions. SC processes recycle solvent much more efficiently than conventional evaporation and condensation steps (Bakshi and Lutz, 1986; Gearhart and Garwin, 1976b). Increasing the temperature reduces the solubility of the oil in the hydrocarbon solvent allowing the oil to precipitate and the clean solvent to pass overhead. This efficiency insures minimal solvent loss, low product contamination, and utility savings (Bakshi and Lutz, 1986; Ely and Baker, 1983; Gearhart and Garwin, 1976a; Gearhart and Garwin, 1976b; Williams, 1981). The high pressures and relatively low temperatures minimize thermal decomposition during processing (Ely and Baker, 1983). The resulting DAO contains less asphaltenes and fewer metals than vacuum flashed oils (Audeh and Yan, 1982; Gearhart and Garwin, 1976a; Gearhart and Garwin, 1976b; McHugh and Krukonis, 1986; Roach, 1981; Wilson et al., 1936; Zarchy, 1985).

Supercritical processes can also deasphalt waxy crudes that cannot be vacuum distilled (Gearhart and Garwin, 1976a). Higher DAO yields and quality combined with more efficient solvent recovery provide sufficient economic incentive to upgrade residua by SC deasphalting (Eisenbach et al., 1983). Many SC deasphalting processes have been patented. These include Messmore's 1947 patent using SC natural gas and Audeh and Yan's (1982) process using SC catalytic cracker gasoline. However, most processes use SC propane and propylene, such as UOP's Demex process (Hydrocarbon Processing, 1984; McHugh and Krukonis, 1986; Williams, 1981; Wilson et al., 1936; Zhuze, 1960).

Propane deasphalting was the first industrial application of SC extraction (Stahl et al., 1988). Propane is more selective than heavier solvents such as butane and pentane but extracts more slowly and produces lower yields of DAO. Butane and pentane are more suitable for the separation of resins and asphalts and reduce metal contents to acceptable levels, but their DAO often requires hydrotreating before being fed to a cracker (Bousquet and Laboural, 1987; Gearhart, 1980; Gearhart and Garwin, 1976a; Gearhart and Garwin, 1976b). As with other resid upgrading processes, the nature of the feed determines the operating conditions and yields (Gearhart and Garwin, 1976a).

Processes such as Kerr-McGee's Residuum Oil Supercritical Extraction (ROSE) and France's Solvahl process use primarily SC butane and pentane solvents to deasphalt atmospheric and vacuum residues (Bakshi and Lutz, 1986; Gearhart and Garwin, 1976a; Gearhart and Garwin, 1976b; Hydrocarbon Processing, 1990; Vermillion and Gearhart, 1983; Williams, 1981). The high versatility of these processes allows production of DAO, lube stocks, catalytic cracker and hydrocracker feeds, and specification asphalts from many types of crudes (Gearhart, 1980; Gearhart and Garwin, 1976a; Gearhart and Garwin, 1976b). The pentane operating conditions of the ROSE process enable high enough temperatures to maintain the asphaltene fraction in a fluid state to avoid plugging problems (Gearhart and Garwin, 1976a; Gearhart and Garwin, 1976b). The asphaltene fraction can be blended into fuel oil or coal, burned directly as fuel, blended with coker feed, or charged to a partial oxidation unit to produce hydrogen (Ditman, 1973; Gearhart, 1980). SC processes also allow fractionation of the extract to produce intermediate resin fractions and specification asphalt blends from crudes that were unable to produce asphalt using vacuum flashing or conventional solvent deasphalting (Bousquet and Laboural, 1987; Gearhart, 1980; Gearhart and Garwin, 1976a; Gearhart and Garwin, 1976b; Stahl et al., 1988; Vermillion and Gearhart, 1983). The physical properties of the SC solvent enable higher solvent-to-feed ratios than conventional solvent deasphalting to improve selectivity while maintaining lower utility costs (Gearhart, 1980; Vermillion and Gearhart, 1983).

**Asphalt Fractionation**

The complexity of petroleum derived asphalts makes a complete chemical understanding impossible. However, by fractionating asphalts, a divide and conquer strategy can be used to understand asphalt composition and predict behavior using the fractions or pseudocomponents. Many fractionation methods previously used to dissect asphalts include distillation, liquid chromatography, solvent methods, and SC separation.

Since asphalts are generally distillation residues of crude oil, distillation

50

produces inadequate fractions for analysis. Distillation separates only according to component volatilities and provides insufficient chemical subdivisions. The high temperatures required in the distillation of asphalts guarantees thermal decomposition of the less volatile components (Rostler, 1979).

Liquid chromatographic methods separate asphalt according to the polarity of the components. Rostler discusses many similar methods in his 1979 review. Corbett developed the primary chromatographic method used today (ASTM-D4124) (Corbett, 1970; Petersen, 1984; Thenoux et al., 1988). Early solvent fractionation methods, such as that described in Traxler and Schweyer's 1953 paper, used various solvents to separate asphalts (Petersen, 1984). Traxler precipitated asphaltenes with n-pentane while the n-butanol and acetone precipitated the asphaltics and paraffinic oils, respectively, leaving only the cyclic oils in solution. Rostler and White (1970) used chemical reactivity as the basis for solvent fractionation (Petersen, 1984; Rostler, 1979; Simpson et al., 1961).

SC extraction allows very flexible fractionation of asphalts with neutral hydrocarbon solvents. The solubility of the SC solvent is adjusted by varying the temperature and pressure to control the solvent density. SC separation techniques use characteristics of both solvent methods and distillation to fraction asphalts, but operate at lower temperatures than distillation and provide easier solvent removal than solvent methods. Stegeman et al. (1991) showed that SC methods separate roughly according to molecular weight and chemical functionality, and produce highly compatible fractions. SC separation, the only fractionation method economically applicable for the industrial production of specification asphalts, is the logical choice.

## Asphalt Blending

The modification and blending of asphalts with various additives is intended to enhance the performance and durability of asphalt pavements. Polymer and rubber additives attempt to improve the elasticity and strength of asphalt without chemical reactions (Rostler and White, 1970). However, the addition of these large molecules to the asphalt does not contribute to compatibility and tends to increase

the viscosity. Even small percentages of polymer additives in asphalt can be very expensive, and the ultimate contribution to pavement performance has yet to be determined.

The contributions of the various fractions has been studied to modify asphalt composition in order to optimize performance. Rostler claims that the saturates fraction is beneficial up to a certain amount in asphalt due to its resistance to oxidation (Rostler, 1979). Saturates would be much more useful and practical as cracker feed and are usually retained in the asphalt in order to meet viscosity specifications. The presence of waxy saturates in asphalts would decrease compatibility and increase the viscosity temperature susceptibility (VTS). The aromatic compounds provide the ductility of an asphalt, but are the most reactive of the maltene fractions and may be converted to asphaltenes during aging (Que et al., 1991).

Asphaltenes influence the asphalt rheological properties and durability more than the other fractions (Hattingh, 1984; Rostler, 1979). The amount, composition, and influence of the asphaltenes fraction is strongly dependent on the crude source (Corbett, 1984; Simpson et al., 1961). Asphaltenes have a relatively high carbon-to-hydrogen ratio indicating high aromaticity and contain most of the metals in the asphalt as well as high concentrations of sulfur, nitrogen, and oxygen (Rostler, 1979). The asphaltenes of waxy crudes may also contain hard waxes. A high percentage of asphaltenes may cause cracking and low ductility after aging, while a low percentage may cause setting problems and bleeding. Although asphaltenes are formed during aging, they appear to contribute differently to asphalt properties and have lower molecular weights (Rostler, 1979).

Researchers have blended various fractions to determine their influence on pavement performance and durability (Petersen, 1984; Rostler, 1979; Simpson et al., 1961). Studies indicate that higher concentrations of the heavy aromatics fractions improves durability (Rostler, 1979; Stegeman, 1991). Petersen (1984) suggests that the blending of asphalts and asphalt fractions can lead to an understanding of the influences of chemical composition on compatibility, physical properties and

durability. Simpson et al. (1961) state that the blending of asphalt components to preferred composition is the most promising approach to the manufacture of products of the desired quality. Stegeman et al. (1992) demonstrate that fraction blends produced by SC and solvent separation, eliminating the lightest and heaviest fractions, show less susceptibility to hardening and higher strength on Marshall stability tests.

# CHAPTER II-3
## ANALYTICAL METHODS

During the course of this work, a new GPC system and a new Rheometer were obtained. The old GPC system was that described in the Study 1155 report (Davison et al., 1991). Some of the data in this study were obtained using a Rheometrics RMS 805 mechanical spectrometer, but most data reported in this section were obtained using the new Carri-Med system.

## Supercritical Separation

Davison, et al. (1991) described the SC apparatus design and operation in detail. This study involves a continuation of the findings of that project. Some modifications in the apparatus and operation of the SC unit were necessary, but the basic process and goals remained the same. A brief description of the process follows.

### Process Description

The SC separation unit separates heavy petroleum products into up to four fractions according to solubility in SC solvents. The unit operates at a constant pressure above the critical pressure of the solvent. The temperatures of the separators determine the density of the solvent and, consequently, its solvent power in each vessel. Heavy components of the feed precipitate when no longer soluble in the solvent, while the lightest constituents remain in solution until removed by decompression during solvent recovery.

Figures II-3-1 and II-3-2 illustrate schematically the operation of the SC separation apparatus. Initially, solvent circulates at operating pressure until each separator reaches the desired operating temperature. A metering pump then introduces feed to mix with the circulating solvent stream in approximately a 12 to 1 solvent to feed ratio. Electric heaters then increase the mixture temperature causing precipitation of the heaviest feed components in the first separator. Further
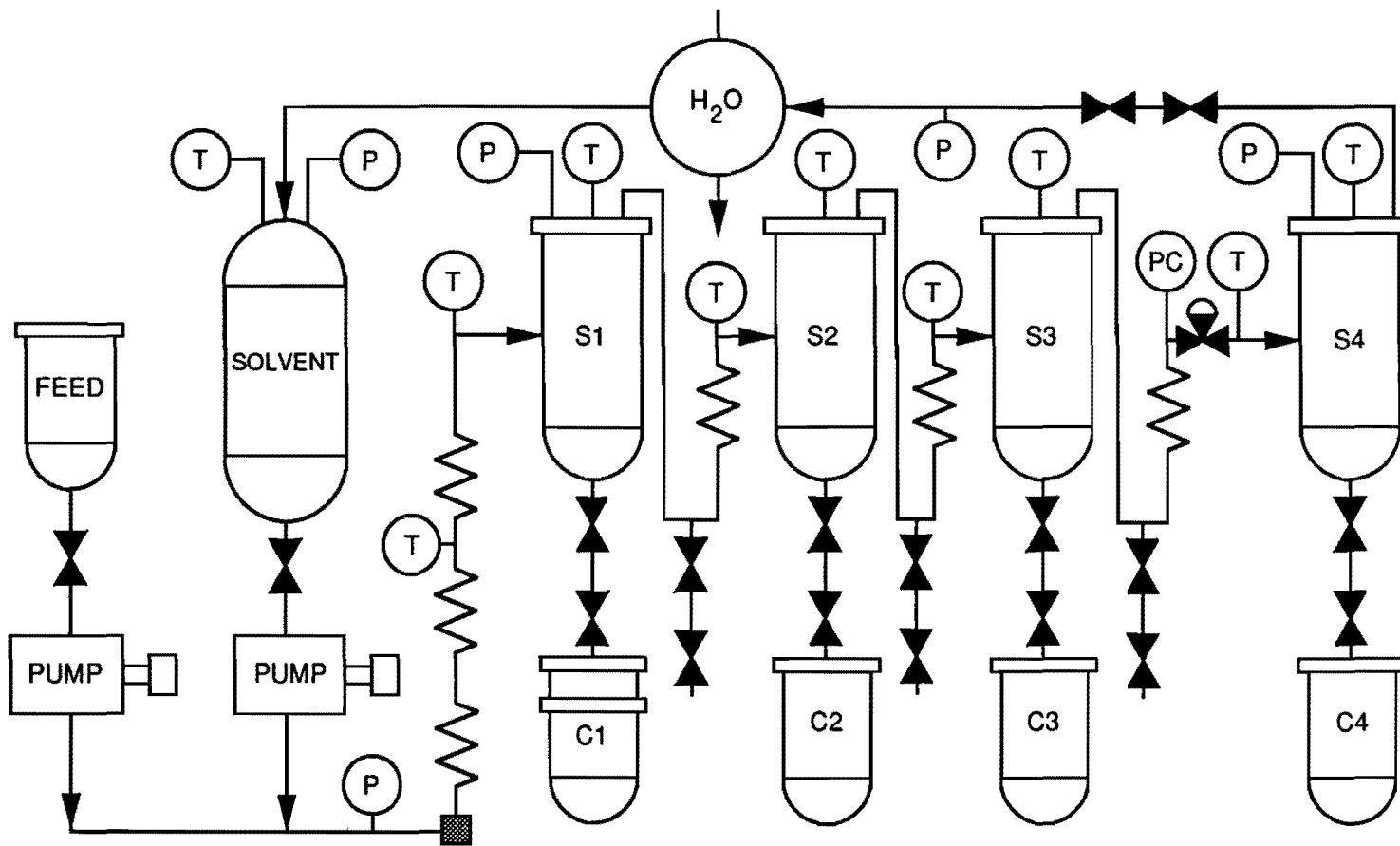
Figure II-3-1.  Schematic Diagram of SC Separation Apparatus

| Symbol | Description |
|--------|-------------|
| (T) | Thermocouple |
| (P) | Pressure Gauge |
| Valve symbol | Valve |
| $H_2O$ (Water Cooled Heat Exchanger symbol) | Water Cooled Heat Exchanger |
| Control Valve symbol | Control Valve |
| (PC) | Pressure Controller |
| Electric Heater symbol | Electric Heater |
| Mixer / Filter symbol | Mixer / Filter |
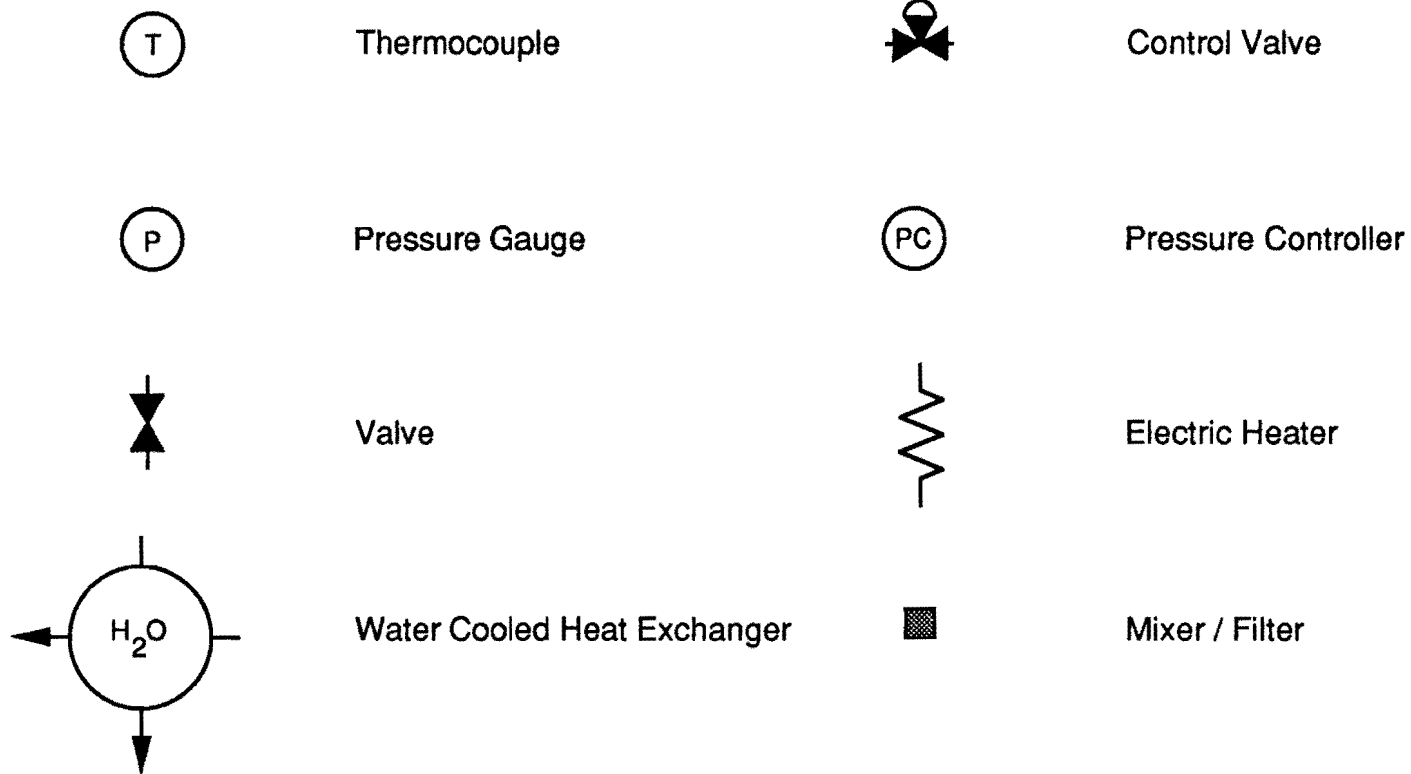
**Figure II-3-2. Legend for Schematic Diagram of SC Separation Apparatus**

heating of the overhead streams causes subsequent fractions to settle in the other separators. Once feeding concludes and mass transfer between the separators subsides, the precipitated fractions are transferred to the collection vessels. After collection, halting the heat input and continual solvent circulation allows the system to cool before stopping the pumps.

Utilizing the properties of SC solvents insures efficient solvent recovery. Expanding the mixture through the control valve before the last separator vaporizes the solvent and precipitates the remaining solute. The overhead contains almost pure solvent and recycles to the solvent tank after further pressure reduction and condensation. Only small amounts of solvent remain in the fractions after the pressure drop during collection.

*Apparatus Modifications*

The modifications to the SC separation apparatus included replacement of the solvent tank, adaptation of the first collection vessel, and placing additional heaters to enable higher operating temperatures.

Metal analyses during the previous work by Stegeman (1991) indicated that the SC separation process deposited large amounts of iron from the carbon steel solvent tank in the asphalt fractions. The rest of the apparatus contained 304 or 316 stainless steel, so a new stainless steel solvent tank replaced the old vessel. Insulation and heating tapes were excluded from the new tank to insure a lower temperature and pressure.

The heaviest fractions obtained from the SC separation process often presented handling problems due to their very high viscosities. These fractions contain solids and tend to cause plugging problems in the lines from the first separator to the collection vessel. Larger valves between the first separator and collector reduced plugging problems during transfer. The pressure reduction during transfer left a very hard fraction that proved difficult to remove from the collection vessel. The addition of a set of flanges near the top of the first collection vessel enabled the removal of the bottom section. This modificaton provided access to the

57

hard material in the container without removing insulation and heating tape or disconnecting valves.

Higher operating temperatures required some slight modifications to the apparatus. Additional heaters were necessary before the first separator to reduce the duty on the present heaters and increase the heat transfer area. Initially, heating tapes often deteriorated due to heat build up, so straight-tubing heaters replaced the previous coiled-heater design. Also, heat transfer cement between the heating tapes and the tubing greatly improved contact and efficiency in the electric heaters.

*Operation Modifications*

The overall operation of the SC apparatus remained unchanged, but a different feed and solvent were implemented, and reduced crudes as well as asphalts were separated. Cyclohexane was added as a solvent for the initial separation of reduced crude and asphalt. The complete solubility of all the feeds in cyclohexane eliminated mixing and settling problems during the initial heating. Cyclohexane also allowed more flexibility than n-pentane in the separation of the asphaltenes fraction.

Analysis of the recycle stream during preliminary runs indicated that some lighter constituents remained in solution. Rough calculations using the temperature and pressure of the last separator verified that expansion through the control valve deviated from isenthalpic and the system remained on the saturated vapor curve for the solvent. Therefore, a liquid phase gradually accumulated in the last vessel and eventually passed overhead into the recycled solvent. After hours of operation, the solute distributed throughout the process and contaminated the fractions during collection. Increasing the heater duty before expansion and on the last separator insured a vapor state well above the saturation curve. Immediate improvement in solvent purity and marked reduction in fraction contamination resulted.

**Infrared Analysis**

Infrared (IR) spectroscopy provides a spectrum that provides information on functional groups present and the structure of the analyzed substance. All IR spectra

were taken using a Nicolet 60SXB spectrometer. The method of attenuated total reflection (ATR) (Davison et al., 1989; Jemison et al., 1992) provided the reflection spectra for the refinery samples, asphalts, blends, and most of the fractions. The solid fractions required a KBr pellet procedure that produces a transmission spectra (Davison et al., 1989, Glover et al., 1989).

## Gel Permeation Chromatography

A Waters chromatography system provided routine analyses of asphalts, fractions, and blends. This system included a Waters 712 sample processor and a 600E controller with quaternary gradient pump. HPLC grade Tetrahydrofuran (THF), the carrier solvent, flowed at 1 ml/min through 30 cm 1000Å and 500Å ultrastyragel columns and a 60 cm 50Å PLgel column to separate the samples. Approximately 500 mg of each sample dissolved in 10 ml of THF provided the sample solution. The sample processor injected 100 $\mu$L of this solution from a dram vial in the sample carousel. A Viscotek H502 differential capillary viscometer and a Waters 410 refractometer provided data for sample analysis.

The refractometer and the viscosity detector allow two methods of calculating the apparent molecular weight of the injected samples. An array of high molecular weight polystyrene standards and low molecular weight IGEPAL standards provide a calibration curve for both detectors. The refractometer uses the elution time and concentration profile of the sample to calculate the molecular weight information by integration and time slicing. The Viscotek detector uses the differential pressure differences in the flow streams to calculate the apparent intrinsic viscosity of the sample and obtain a viscosity distribution. The concentration distribution from the refractometer, viscosity distribution, elution time, and universal calibration enable the calculation of molecular weight data (Haney, 1984; Haney, 1985). The intrinsic viscosity-derived molecular weight data indicate not only the hydrodynamic size of the molecule, but also the amount of branching and shape of the molecules.

**Corbett Analysis**

Corbett analyses (ASTM D 4124) separated the components of the samples according to polarity. Some modifications of the Corbett procedure were implemented to reduce sample size and increase efficiency as suggested by Thenoux et al. (1988).

**Viscosity**

A Carri-Med 500 Controlled Stress Rheometer measured the low shear rate dynamic viscosity ($\eta_0^*$) of the samples. A Peltier heating and cooling system provided rapid and accurate temperature control. The Peltier mechanism resides in the ram which raises and lowers for sample insertion and gap adjustment. Fixtures of different geometries attach to the upper portion of the rheometer. Very low resistance air bearings on the rheometer motor allow input and response signals from the upper portion only. A MS-DOS based computer provides control and data analysis with user-friendly software.

The measuring geometry included a 2.5 cm stainless steel parallel plate fixture with a 0.5 mm sample thickness. Once the sample melted and the ram raised to the preset gap, removing the excess material around the fixture minimized any end effects on the measurements. The low temperature $\eta_0^*$ required a 1 cm stainless steel parallel plate fixture and a 0.5 mm gap. The low temperature data were recorded first and excess material was removed at increasing operating temperatures since the substantial thermal expansion of the samples could cause measurement error.

The reported $\eta_0^*$ represents the shear rate-independent limiting dynamic viscosity determined in a manner similar to that described by Lau (1991). Initial torque sweeps at constant stress and frequencies of 1 and 10 rad/sec indicated the torque values required to provide moduli independent of shear rate. A frequency sweep from 250 to 0.1 rad/sec provided the moduli and viscosity information. Softer samples displayed viscosities that became constant at low frequencies. Some hard samples or low temperature viscosities required moduli information at higher temperatures. Shifting the high temperature storage modulus to that of the low

temperature data, according to the time/temperature superposition described by Ferry (1980), and recalculating the viscosities at the shifted frequencies provided limiting dynamic viscosities for highly viscous samples.

Since only the ram portion of the rheometer provided temperature control, a thermal gradient existed across the sample due to conduction through the sample and fixture. Only at temperatures substantially different than ambient was this gradient significant. A small gap (0.5 mm) minimized this gradient, but calibration provided a satisfactory correction for the gradient during the measurement of the 60°C $\eta_0^*$.

A series of measurements and calculations indicated the correct operating temperature to obtain accurate 60°C measurements. Data were recorded on a sample run at gap thicknesses of 1 mm, 0.75 mm, 0.5 mm, and 0.25 mm at temperatures of 60°C, 61°C, 61.5°C, 62°C, 62.5°C, 63°C, and 63.5°C. Figure II-3-3 shows the linearity of $\eta_0^*$ with gap thickness, and the correct 60°C $\eta_0^*$ was taken as the intercept of the straight line fit through the 60°C points. Lines drawn through similar data taken at different temperatures allow determination of the offset temperature by intersecting the constant $\eta_0^*$ line, determined from the 60°C data, with the desired gap thickness. This method indicates a temperature of about 62°C, as demonstrated by the arrows in Figure II-3-3.

The use of a corrected temperature was verified by controlling the environment around the fixture to eliminate the temperature gradient. A heater gun provided steady heat to maintain the surrounding air and fixture surface at 60°C. A portable Fluke thermocouple located just above the flat portion of the fixture near the sample insured a fairly steady 60°C reading. Without the heater gun, the same arrangement read only slightly above ambient temperature. Measurements recorded with the controlled environment matched those recorded at the offset temperature within a few percent and within the accuracy of the instrument. Repeating the procedure with samples of various viscosities also verified the accuracy of the temperature offset method. Convenience and the noise created by the heater gun recommended avoiding the controlled environment.

61
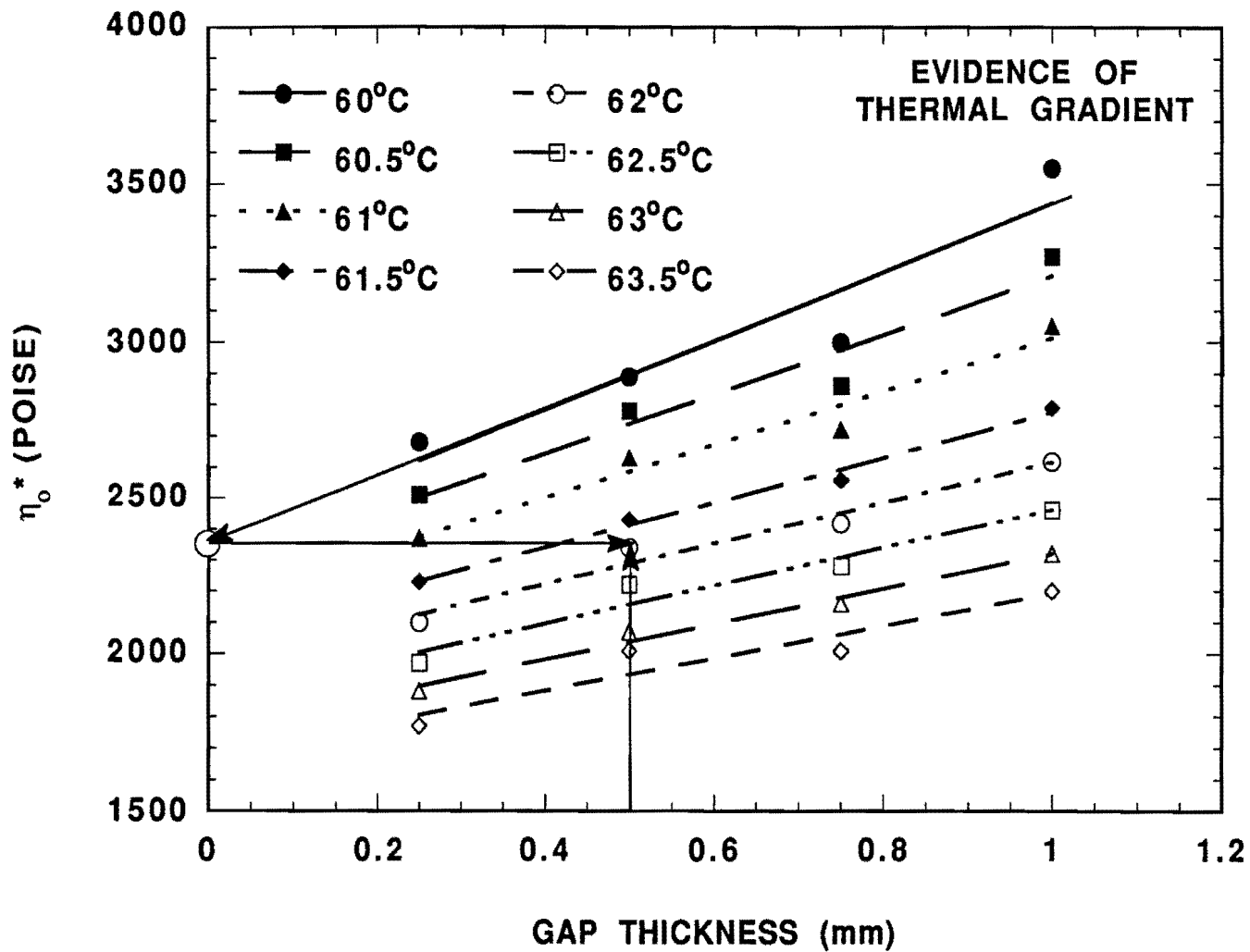
Figure II-3-3. Calibration of Temperature Offset for $60^{\circ}C$ $\eta_0^*$ Measurement

## Atomic Absorption

The iron, nickel, and vanadium analyses were performed in a manner similar to that described by Davison et al. (1989). A modified method allowed smaller samples, reduced the amount of sulfuric acid, and shortened the digestion and ashing times. The modifications provided faster and more efficient sample preparation.

## POV Aging

The POV allowed laboratory aging of asphalt samples to determine the relationship between the chemical and physical property changes during oxidative hardening. Lau (1991) describes the procedures in detail, but a brief summary of the methods follows.

The aging vessels consisted of three vessels made from four inch schedule 80 stainless steel pipe. A constant pressure of 300 psi of pure oxygen was maintained throughout the experiments. The aging vessels operated at 93.3°C (200°F), 82.2°C (180°F) and 71.1°C (160°F) to provide rate data at different temperatures. Table II-3-1 lists the aging times for the different temperatures.

The aluminum trays and racks inside each vessel contained the samples during aging. Each tray held 2.4 g of sample, thus providing enough material to perform IR, viscosity, and GPC analyses on each sample if desired. Rearranging the trays during aging minimized the effects of any possible thermal gradients in the aging vessels.

**Table II-3-1**
**POV Operating Temperatures and Aging Times**

| T (°C) | Aging Time (days) | | | |
|--------|------|------|------|------|
| 93.3 | 2 | 4 | 6 | 8 |
| 82.2 | 4 | 8 | 12 | 16 |
| 71.1 | 4 | 12 | 20 | 28 |

# CHAPTER II-4

## REDUCED CRUDE FRACTIONATION

Reduced crudes (RC) from three different refineries in Texas representing different crude sources and refining methods were used in this study. The Coastal refinery in Corpus Christi, which uses vacuum distillation for asphalt production, provided RC, asphalt, and light and heavy gas oil samples from a Mayan crude. The Fina refinery in Big Spring uses propane deasphalting (PDA) to process West Texas sour crude. Fina supplied samples of the RC, vacuum tower bottoms, and light and heavy vacuum gas oils from their vacuum still; and propane deasphalted oils, zero pen asphalt, and asphalt from the PDA unit. The Texaco asphalt plant in Port Neches refines heavy Saudi Arabian crude using vacuum distillation and provided RC, asphalt and vacuum gas oils.

Obtaining the proper operating parameters for the desired fractionation of the RC required many runs with both cyclohexane and pentane. In an effort to obtain better selectivity and larger temperature subdivisions between the fractions, higher pressures were attempted. However, these high pressures (800-1000 psi) demanded prohibitively high operating temperatures to achieve separation. After establishing a 700 psi operating pressure, the desired weight distribution among the fractions required many attempts to determine separation temperatures.

Initial separations using the equipment modifications noted in Chapter II-3 proved more difficult than expected. The higher temperatures and poor heat transfer in the initial heaters produced thermal decomposition, or coking, of some feed components. Coke deposits on the tubing walls further complicated heat transfer and fluid flow, and eventually caused plugging problems. Coking demanded frequent heater repair and replacement during the early cyclohexane runs. The presence of large amounts of insoluble material in the bottom RC fractions also indicated the coking problems.

Although cyclohexane provided good mixing and solubility for the entire feed, this increase in solubility required much higher temperatures than earlier work with

pentane (Davison et al, 1991; Stegeman, 1991; Stegeman et al., 1992). Cyclohexane also displayed poor selectivity during fractionation, especially during RC fractionation. About half of the RC consists of gas oils, lighter materials that are removed from the asphalt during vacuum distillation. The presence of large amounts of these light constituents acted as an entrainer. The gas oils increased the solubility of the SC solvent enough to require higher fractionation temperatures and to reduce the solvent selectivity.

Complete analyses were not performed on the RC fractions due to the complications in processing and the poor quality of the fractions. Gas oil contamination in the SC fractions cause decreased fraction viscosity relative to their corresponding asphalt SC fractions. The poor selectivity of the cyclohexane solvent during separation exacerbated the situation. Fractions and blends produced from SC separation of RCs appeared inferior to the asphalt produced from vacuum distillation. Due to gas oil contamination, the few blends produced from RC fractions required more asphaltenes to satisfy viscosity specifications. In the interest of time, these incompatible blends were not thoroughly investigated.

Suitable separation of RCs using SC separation techniques instead of vacuum distillation may only be viable if a lighter solvent, such as propane, performed the initial removal of gas oils. Subsequent separation of the asphalt with n-pentane could provide suitable asphalt fractions, a heavy asphaltenes fraction, and additional gas oils. The present SC apparatus is unable to perform separations using butane or lighter solvents due to the modifications necessary for solvent delivery and safety restrictions. Therefore, a series of SC separation processes contain questionable economics, and the resulting asphalt quality is speculative.

**Operating Conditions**

Figure II-4-1 graphically represents the fractionation procedures. Initially, cyclohexane produced four fractions (C1 and 5-7). The bottom fraction (7) contained large amounts of solids and was intentionally kept small in an effort to fractionate the asphaltenes. The larger fractions 5 and 6 were expected to produce prime
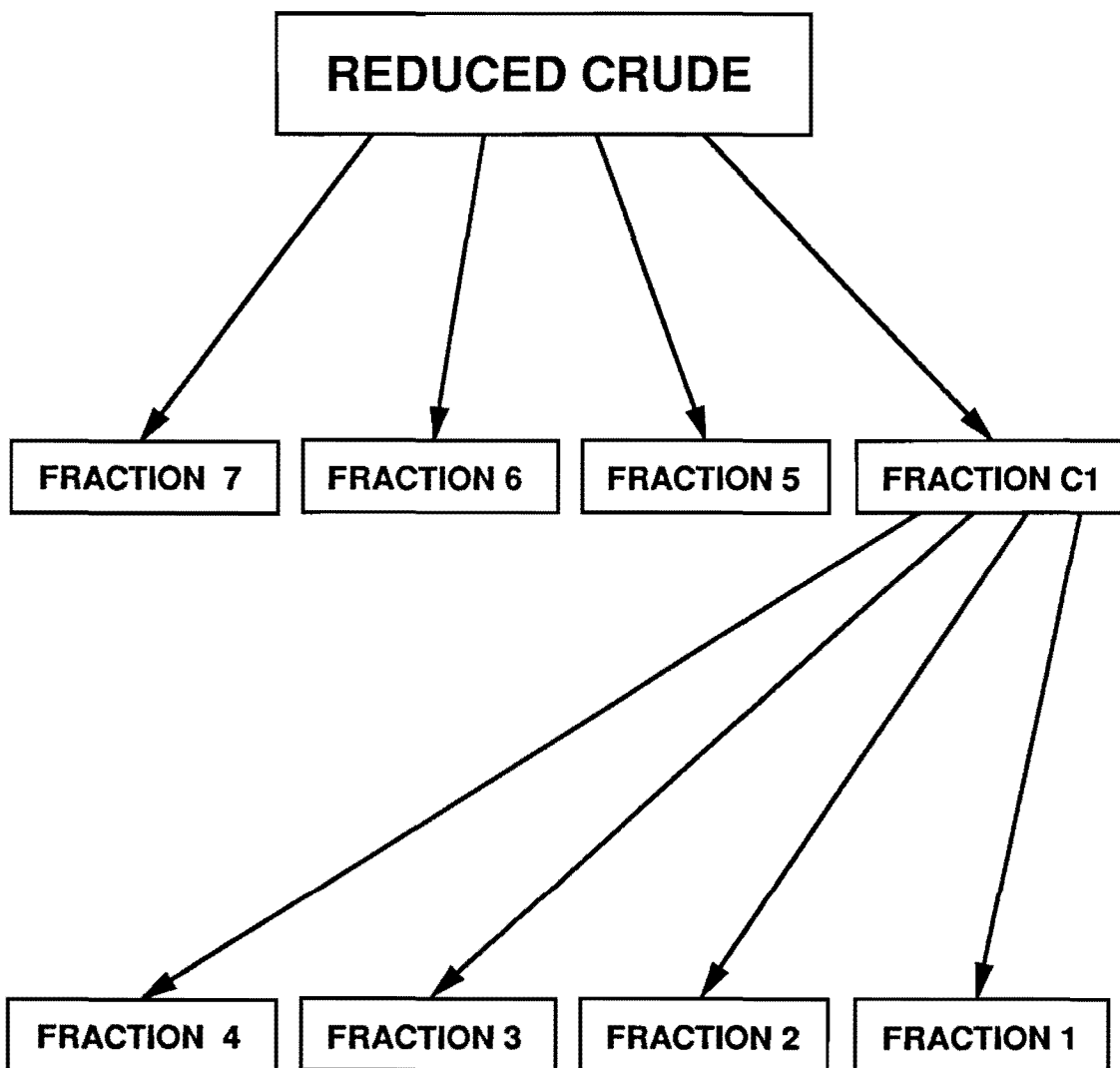
**Figure II-4-1. RC Fractionation**

asphalt blending stock. The top cyclohexane fraction (C1) contained 80-90% of the feed and most of the gas oils.

The pentane separation used fraction C1 as feed to produce fractions 1 through 4. The small amount of asphaltenes present in C1 concentrated in the solid fraction 4, the bottom pentane fraction. Fraction 3 produced a viscous fraction about the same consistency of asphalt. Fractions 1 and 2 contained most of the gas oils and maintained a very low viscosity.

Table II-4-1 gives the operating conditions and mass distributions for the fractionation of the three RCs. The presence of small amounts of solvent in the fractions when weighed causes some error in the mass balance calculations. Figure II-4-2 displays the mass distribution of the three RCs among the seven SC fractions.

**Table II-4-1**
**Operating Conditions for RC SC Fractionation**

| | | | | Fraction Percentages | | |
|---|---|---|---|---|---|---|
| Fraction | Solvent | T($^\circ$C) | P(bar) | Coastal | Fina | Texaco |
| 1 | n-pentane | 149 | 10.1 | 57 | 41 | 44 |
| 2 | n-pentane | 249 | 47.0 | 22 | 38 | 24 |
| 3 | n-pentane | 232 | 47.0 | 4 | 7 | 8 |
| 4 | n-pentane | 204 | 47.0 | 4 | 3 | 6 |
| 5 | cyclohexane | 324 | 47.0 | 11 | 13 | 13 |
| 6 | cyclohexane | 310 | 47.0 | 4 | 3 | 7 |
| 7 | cyclohexane | 299 | 47.0 | 2 | 1 | 3 |
| C1 | cyclohexane | 204 | 10.1 | 88 | 89 | 79 |
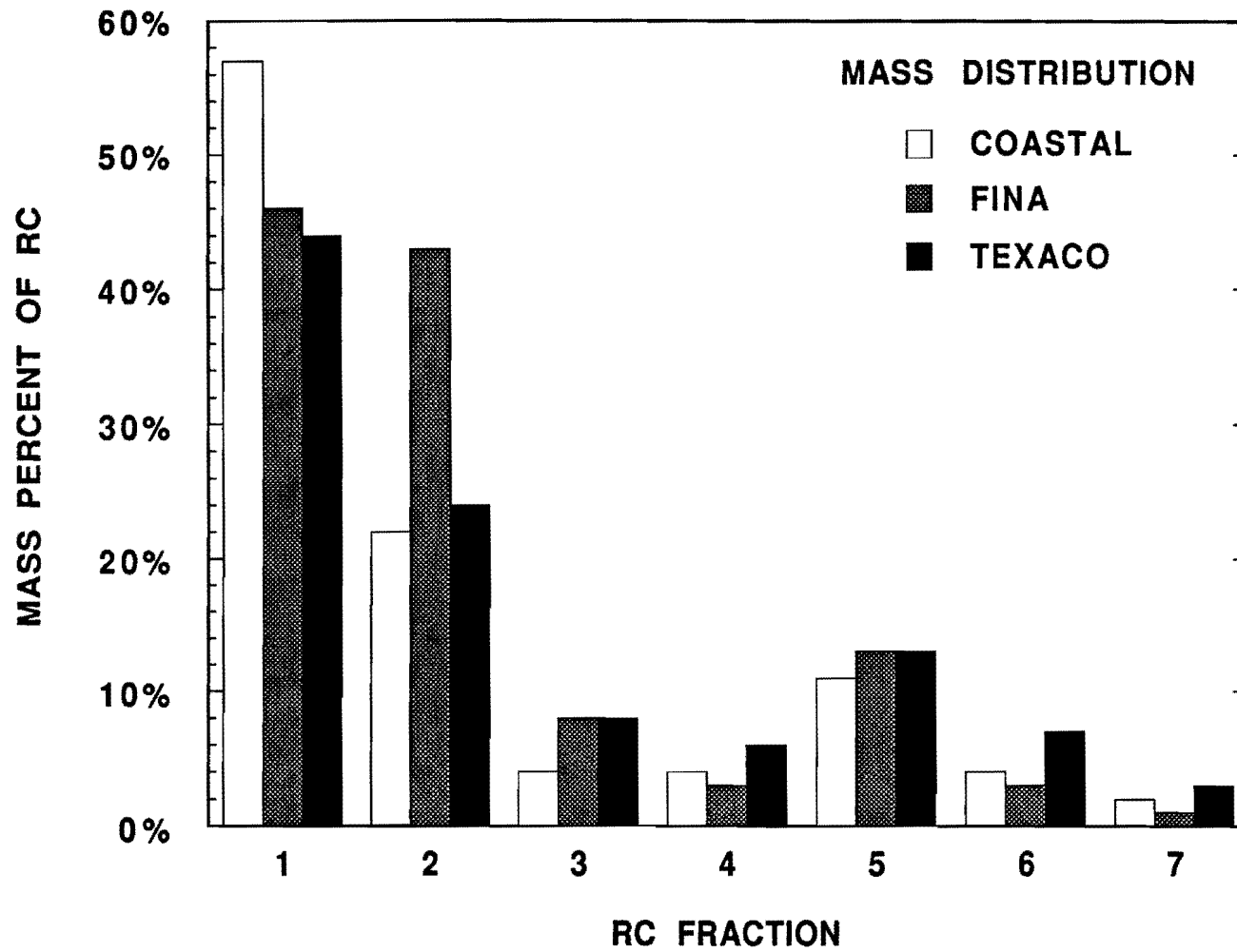
Figure II-4-2. Mass Distribution of RC SC Fractions

## Corbett Analysis

Corbett analyses of the RC SC fractions emphasized the difficulties encountered during separation. Figures II-4-3 through II-4-5 represent the Corbett analyses performed on each fraction of the Coastal, Fina, and Texaco RCs. The Corbett method was designed for separation of asphalts, so the very light and very heavy fractions proved difficult to analyze. The lightest fractions (C1, 1, and 2) and gas oils gave low recoveries due to difficulty of solvent removal from the volatile components. The heaviest fraction (7) contained large amounts of insoluble coke formed during processing and caused difficulty during asphaltene filtration. Highly polar material remained adsorbed on the alumina column after separation. Consequently, the light and heavy fractions proved challenging to analyze and may possess considerable experimental error.

The coking of RC constituents during heating caused inconsistencies in the asphaltene contents. Coking undoubtedly produced substantially larger amounts of asphaltenes than present in the original RC, but some of this coke remained on the tubing walls. The insoluble coke carried from the heaters concentrated in the heaviest fractions. Therefore, the accuracy of the asphaltene content of fraction 7 and possibly fractions 4 and 6 are questionable.

The poor selectivity of cyclohexane causes a discontinuity between the cyclohexane and pentane fractions. Fraction 5 contains substantial amounts of saturates that precipitated from SC cyclohexane. Conversely, fraction 4, the bottom pentane fraction, contains a large concentration of asphaltenes carried overhead into the last separator during the previous cyclohexane run. The pentane more efficiently separated the lighter components, but selectivity remains lower than previous results from asphalt fractionation due to the presence of the gas oils (Davison et al, 1991; Stegeman, 1991; Stegeman et al., 1992).

Calculations using the Corbett fraction distribution in each SC fraction and the mass distributions of the SC fractions produced the amount of the Corbett fractions from the original RC present in each SC fraction. Figures II-4-6 through II-4-8 display the results of these calculations for each RC. The saturates
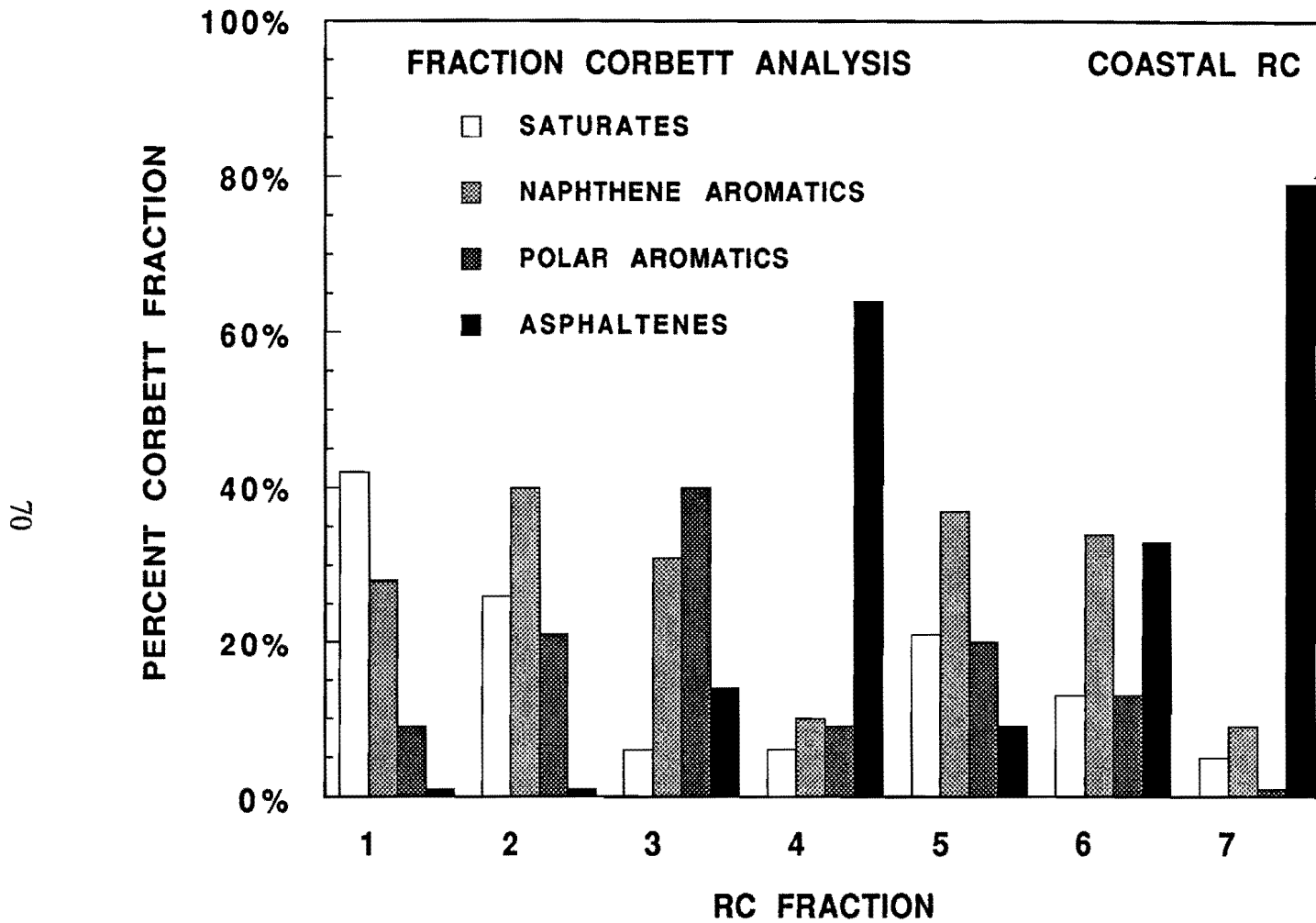
Figure II-4-3.  Corbett Analysis of Coastal RC SC Fractions
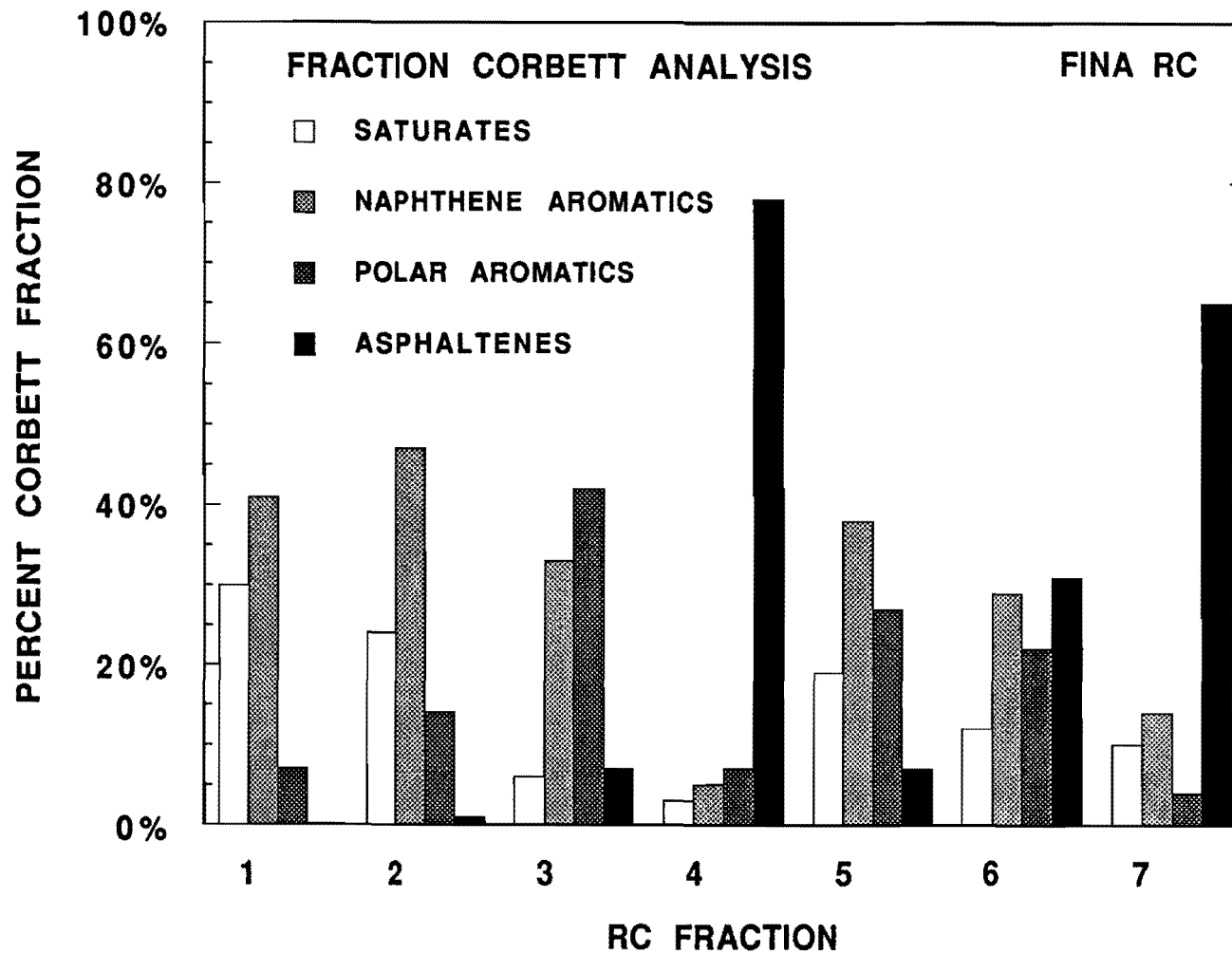
Figure II-4-4.  Corbett Analysis of Fina RC SC Fractions
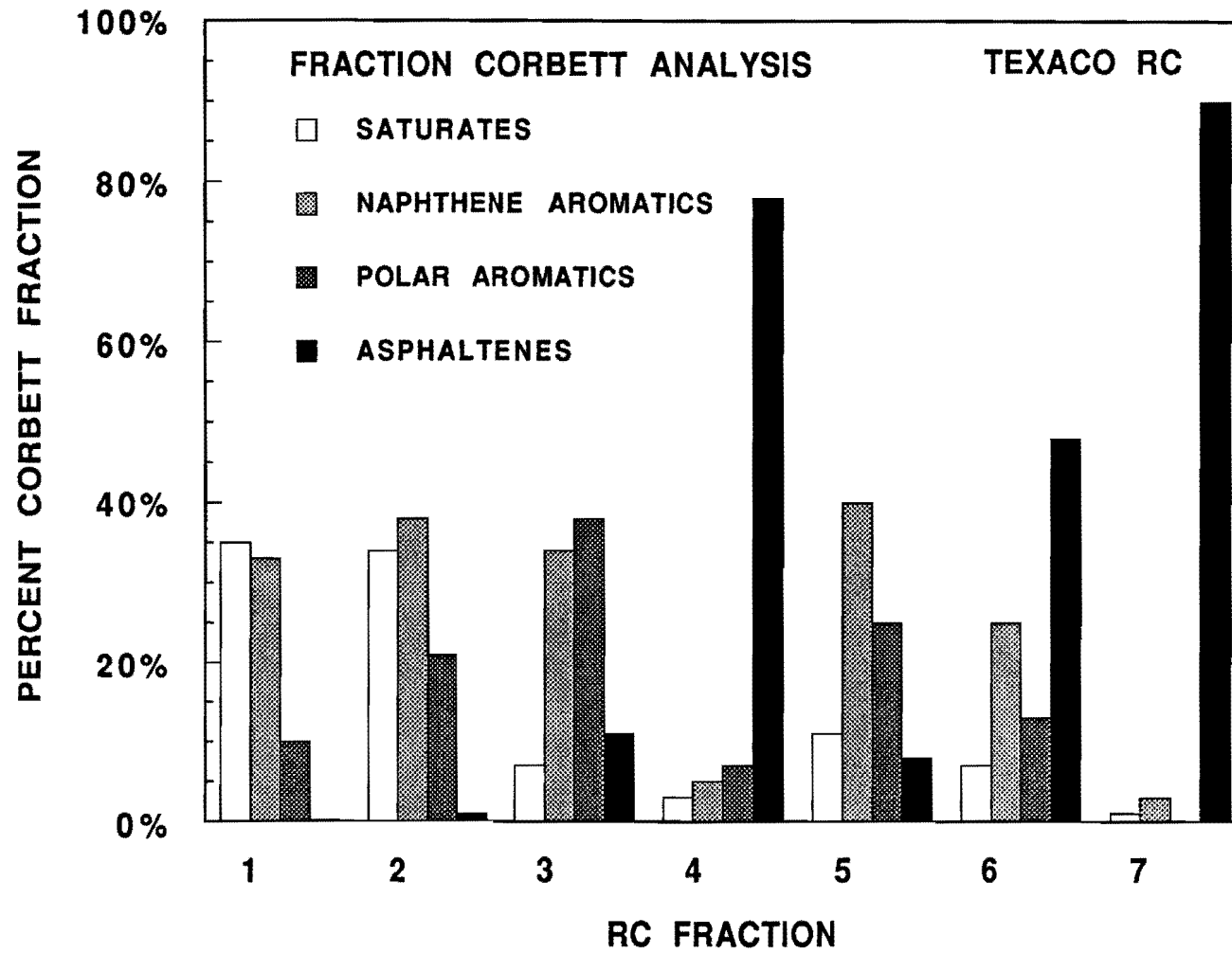
Figure II-4-5. Corbett Analysis of Texaco RC SC Fractions
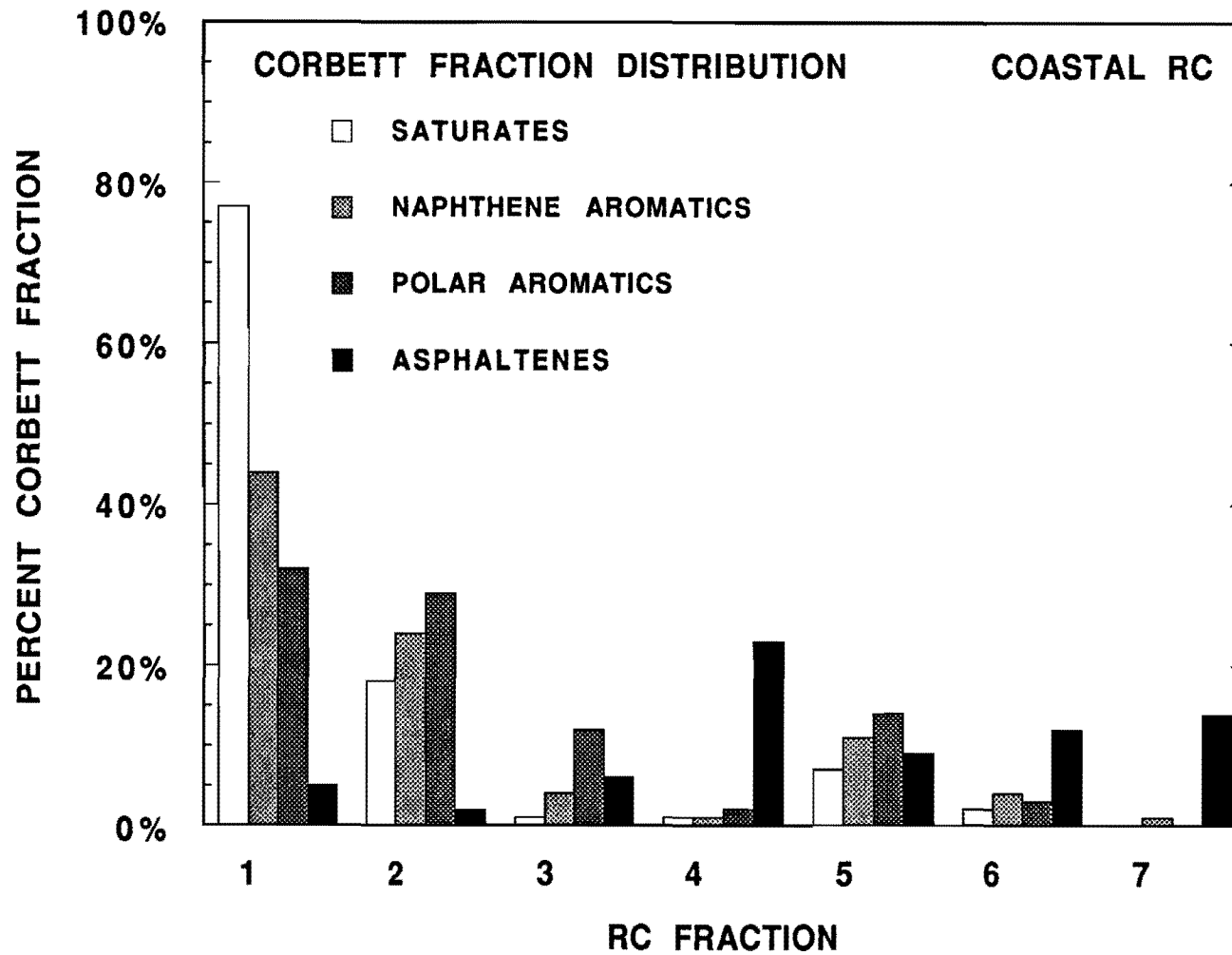
Figure II-4-6. Distribution of the Coastal RC's Corbett Fractions Among the SC Fractions
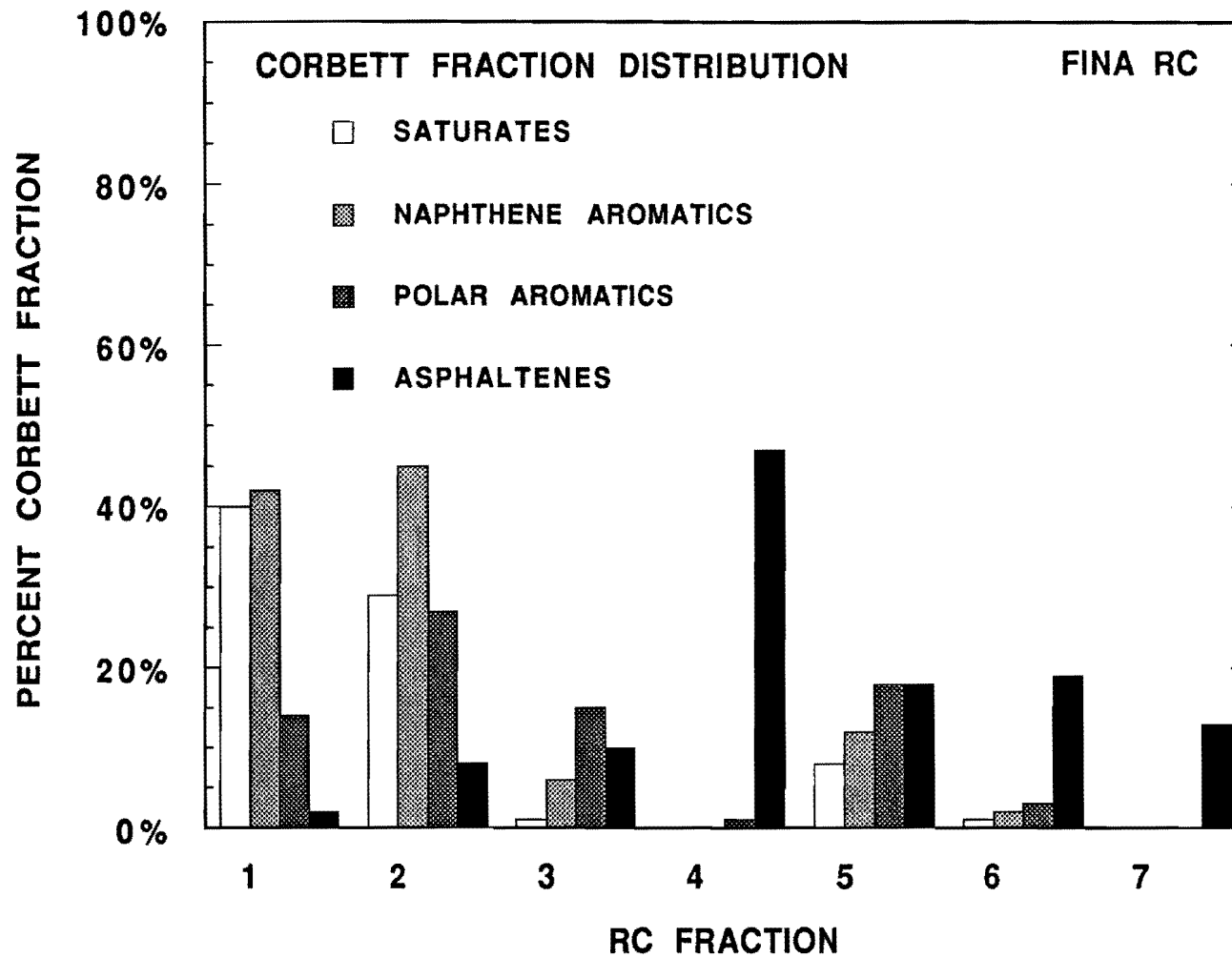
Figure II-4-7. Distribution of the Fina RC's Corbett Fractions Among the SC Fractions
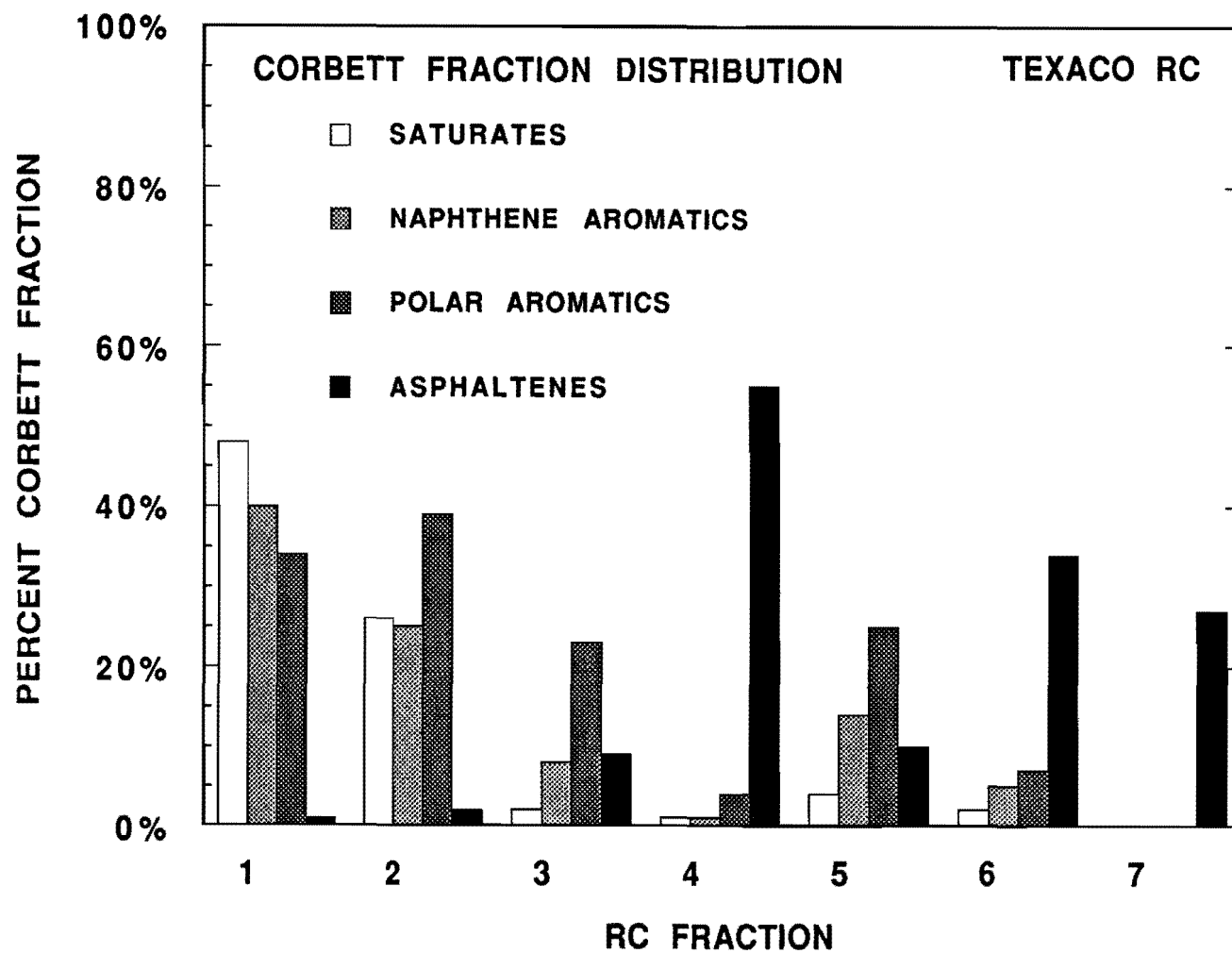
Figure II-4-8. Distribution of the Texaco RC's Corbett Fractions Among the SC Fractions

concentrated well in the top fractions, but surprisingly large amounts of naphthene and polar aromatics also resided in these light fractions. The large size of fractions 1 and 2 contribute to their high aromatic content, but the presence of significant amounts of asphaltenes in these fractions indicates the decrease in selectivity of the SC solvent during RC separation.

## Infrared Analysis

The IR spectra taken of the reduced SC fractions demonstrated the increasing aromaticity of the heavier fractions, as indicated by the Corbett analyses. As in previous work, the fraction IR spectra show general similarity in the chemical nature of the fractions (Davison et al, 1991; Stegeman, 1991; Stegeman et al., 1992). Figure II-4-9 illustrates the differences in aromaticity of Fina fractions 1 through 3.

The IR spectra of the RCs and most of the fractions were obtained using the ATR method. Fractions 4 and 7 required the use of KBr pellets due to their solid state and low solubility in a suitable casting solvent. The fraction IR spectra show surprisingly little difference in character, but indicate an increase in aromaticity with fraction number by an increase in absorbance, especially at 1600 wavenumbers.

## Metal Analysis

Iron, nickel, and vanadium contents were measured using atomic absorption on the Texaco RC SC fractions to indicate the distribution of the metals. The measured values of the metals in the RC and SC fractions are shown in Table II-4-2. Figure II-4-10 displays graphically the concentration of the metals in the heavy fractions. The discontinuities shown in the Corbett data are also apparent in the metal distributions.

Davison et al. (1991) demonstrated a strong linear relationship between nickel, vanadium, and asphaltene content in SC and solvent extracted fractions. Figure II-4-11 shows a similar relationship obtained for the nickel and vanadium contents from the RC SC fractions. Figure II-4-12 demonstrates a deviation from linearity for the asphaltene and nickel content data of the heaviest fractions. This

76
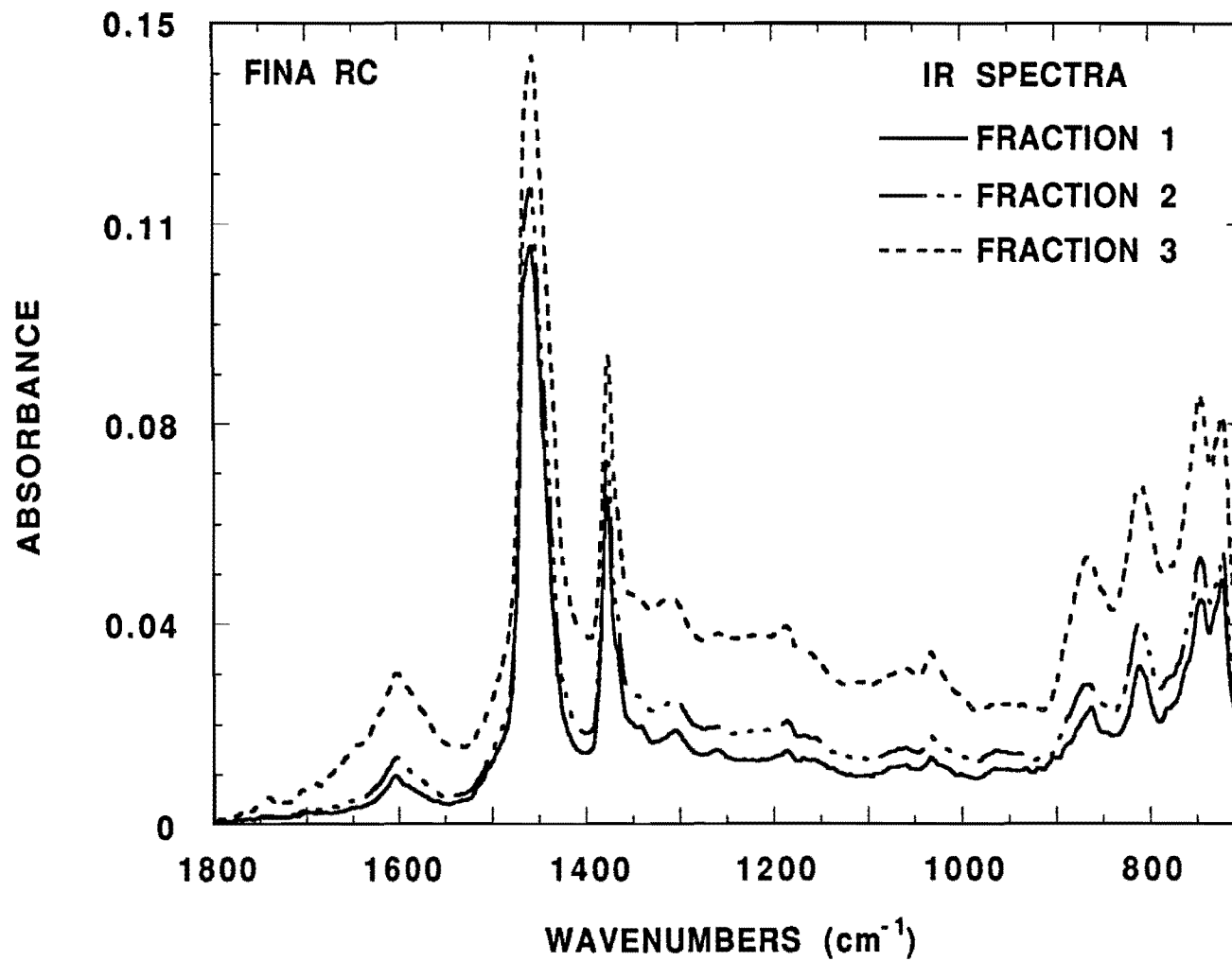
Figure II-4-9. IR Spectra of Fina RC SC Fractions 1-3
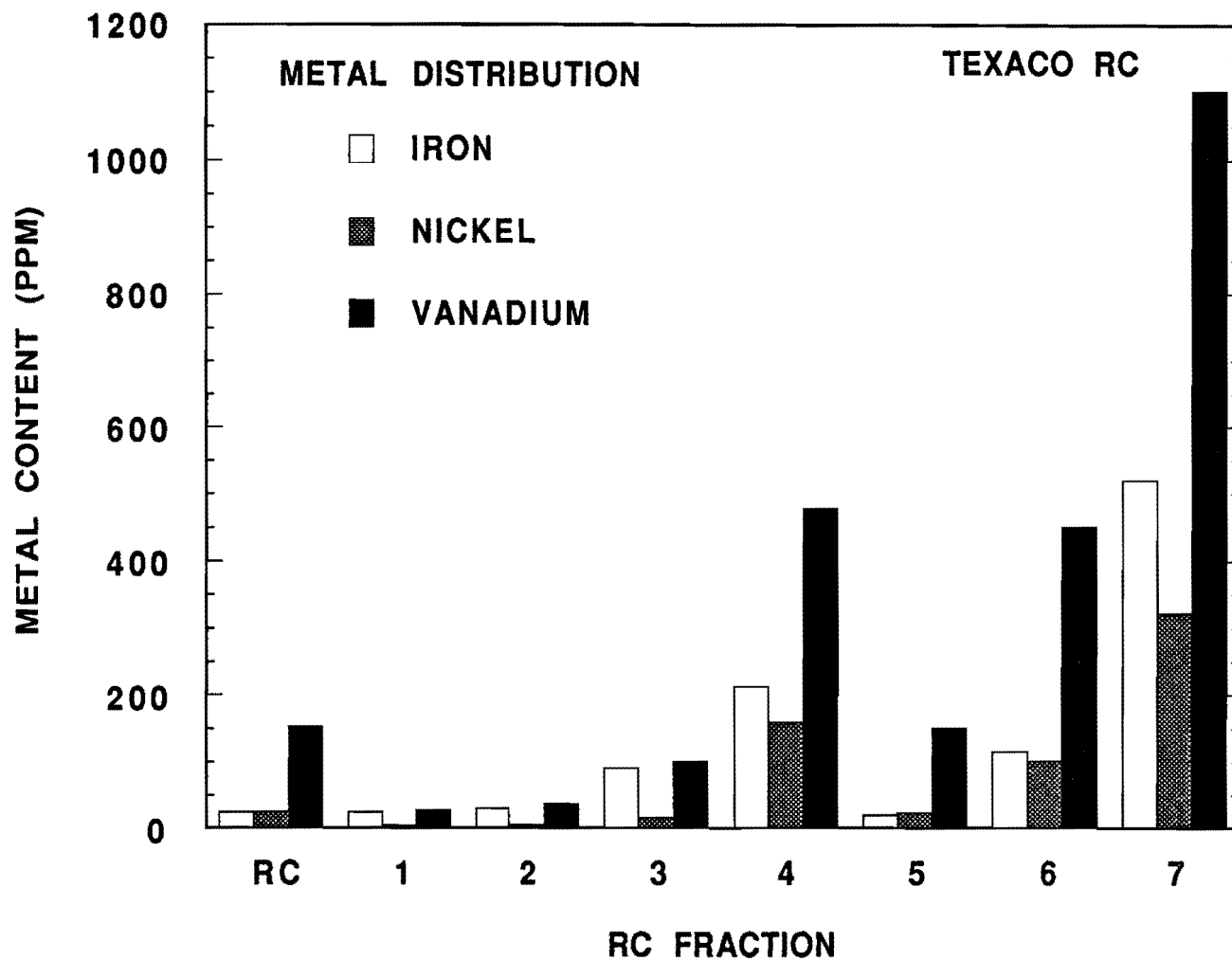
Figure II-4-10. Metal Distribution in Texaco RC SC Fractions
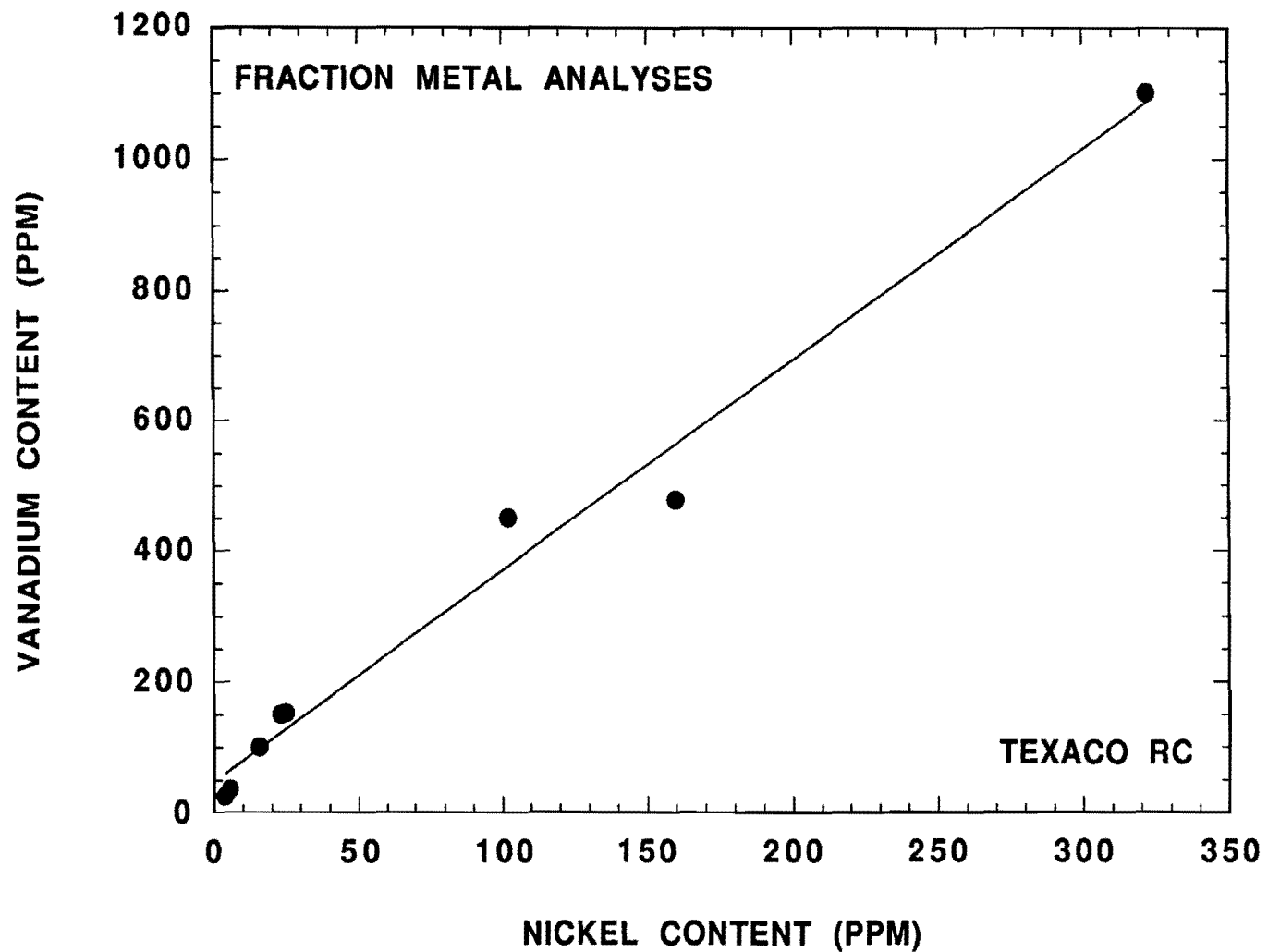
Figure II-4-11. Vanadium Versus Nickel for Texaco RC SC Fractions
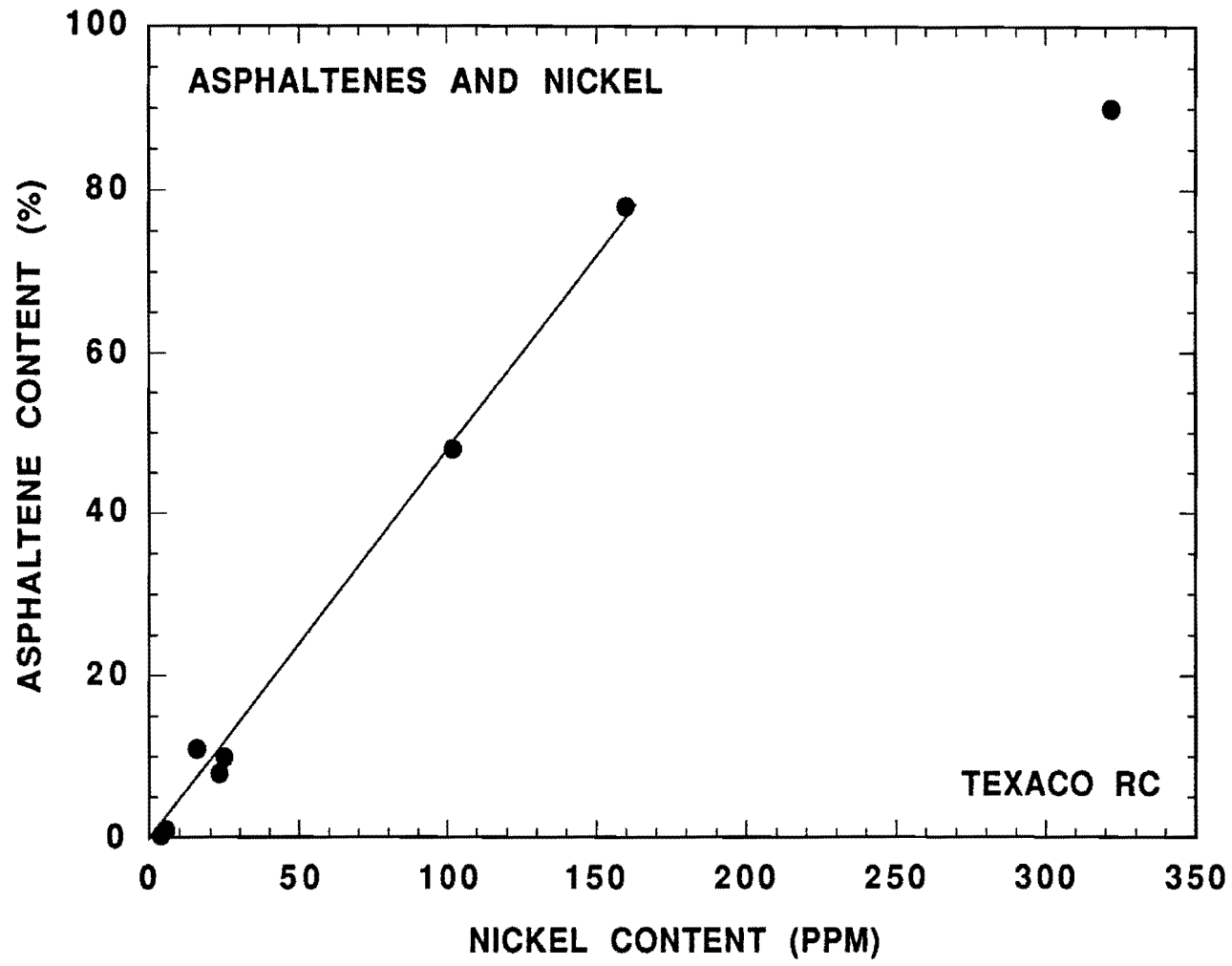
Figure II-4-12. Asphaltenes Versus Nickel for Texaco RC SC Fractions

**Table II-4-2**
**Metal Distribution in Texaco RC SC Fractions**

| Sample | Concentration (ppm) | | |
|--------|------|--------|----------|
| | Iron | Nickel | Vanadium |
| RC | 23.8 | 24.8 | 153 |
| Fraction 1 | 24.2 | 3.85 | 27.0 |
| Fraction 2 | 29.7 | 5.38 | 37.4 |
| Fraction 3 | 90.5 | 15.8 | 102 |
| Fraction 4 | 213 | 160 | 479 |
| Fraction 5 | 19.8 | 23.1 | 152 |
| Fraction 6 | 116 | 102 | 451 |
| Fraction 7 | 520 | 322 | 1100 |
| Fraction C1 | 12.7 | 15.3 | 100 |

deviation evidently results from the suspicious values for the asphaltene content of fraction 7 mentioned previously.

A material balance using the metal concentrations and the fraction sizes yields interesting results. The calculated vanadium content of the RC is 7.2% lower than the measured value. A slightly lower value is expected due to solvent contamination in the lightest fractions during weighing. The derived nickel data showed 36% more nickel than the feed, and the iron showed a 169% increase. Figure II-4-10 verifies that even the light SC fractions contain more iron than the feed. Since the carbon steel solvent tank had been replaced with a stainless vessel, the iron contamination indicated in previous research was eliminated (Davison et al, 1991; Stegeman et al., 1992). The extra iron and nickel originated from the deterioration of the stainless steel tubing under the severe operating conditions necessary for the separation of RCs with cyclohexane. High operating temperatures and poor heat transfer in the initial heaters generated areas of intense heat that produced thermal decomposition of feed components and disintegration of some tubing. Inspection of replaced tubing walls from the heaters verified deterioration of the stainless steel.

## GPC Analysis

The chromatograms obtained from GPC analysis confirm, as do the other analytical methods, the poor selectivity during SC separation of RCs. Figure II-4-13 shows the RI chromatograms of the Coastal fractions 1 through 4. The small shoulders on the tailing end of the chromatograms at about 40 minutes indicates the presence of gas oils.
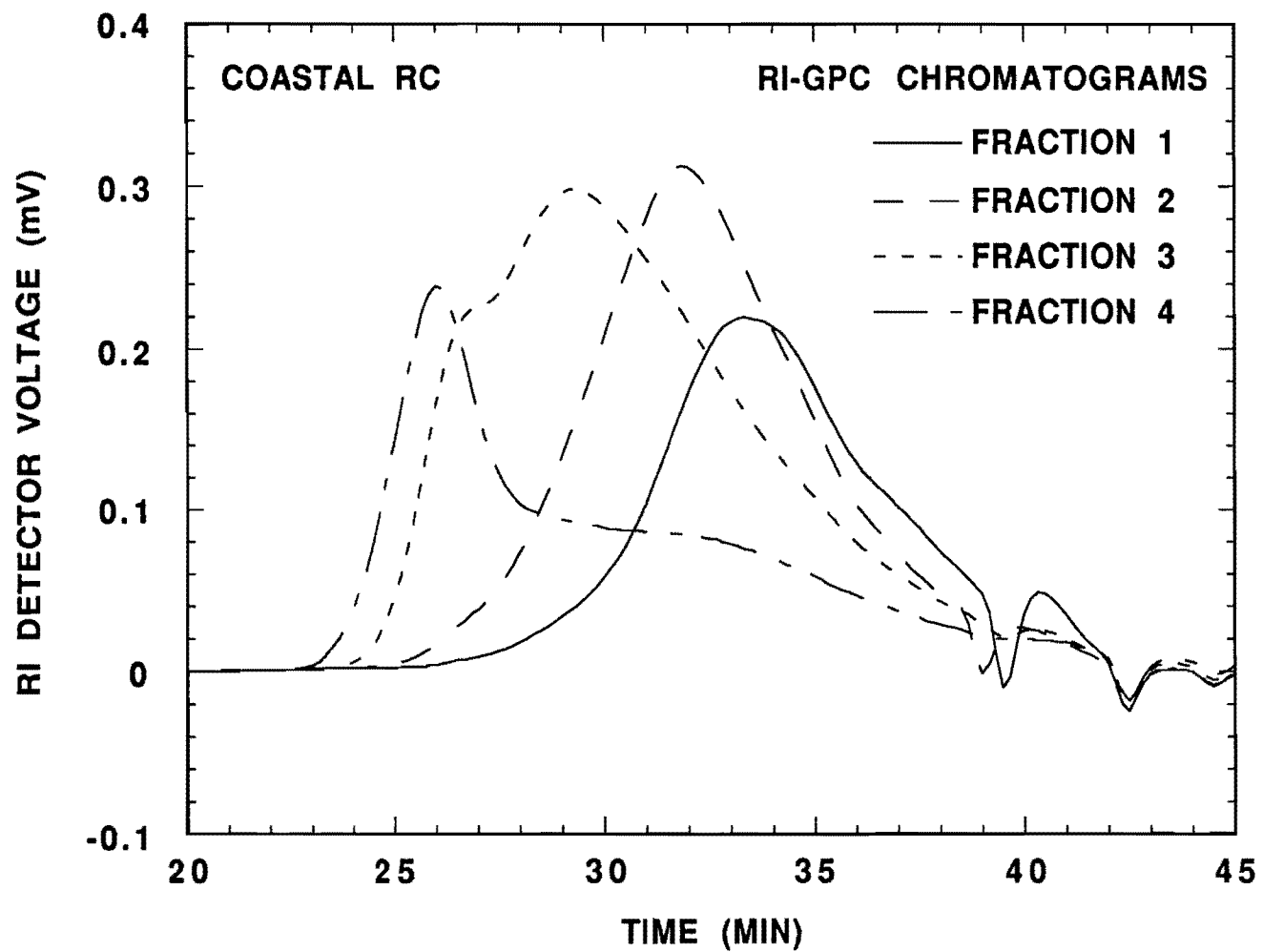
Figure II-4-13.  RI-GPC Chromatograms of Coastal RC SC Fractions 1-4

# CHAPTER II-5

## ASPHALT FRACTIONATION

The Coastal, Fina, and Texaco refineries that supplied the RC samples also provided asphalt for analysis and fractionation. The SC apparatus separated the asphalts with less difficulty than the RCs. The experience gained from the RC separation allowed fewer asphalt runs to achieve the desired fraction size distribution. The absence of the gas oils during processing reduced the operating temperatures for asphalt fractionation and improved the selectivity of both cyclohexane and pentane solvents. The asphalt separation employed the same operating pressure as previously reported by Stegeman (1991) for both the cyclohexane and pentane runs.

The use of cyclohexane as the initial solvent for asphalt separation eliminated some of the problems encountered by Stegeman (1991). The asphaltenes often precipitated in the mixers and heaters using pentane as the only SC extracting solvent. The complete solubility of the asphalt in cyclohexane allowed thorough mixing and eliminated asphaltene precipitations in the initial runs. However, the high operating temperatures required during the cyclohexane runs still produced coke formation in the heaters before the first separator. The heaviest cyclohexane fractions contained insoluble material not present in the original asphalt.

### Operating Conditions

Asphalts were separated into ten SC fractions using conditions similar to that of the RCs, but at temperatures 10-30°C (20-50°F) lower. Initial separation using cyclohexane produced four fractions (C1 and 8-10). After cleaning the system with toluene and recharging with pentane, fraction C1 was further separated into four pentane fractions (P1 and 5-7). The operating parameters of Stegeman (1991) were used to estimate the conditions for the pentane fractionation of asphalt, but produced a larger than expected top fraction (P1). Therefore, four more SC fractions were produced using pentane to further separate fraction P1. Interestingly, the top four

84

fractions (1-4) required only 3°C (5°F) intervals for separation. Figure II-5-1 shows the asphalt fractionation procedures schematically, and Table II-5-1 gives the operating conditions for the SC separation and the mass distributions of the three asphalts. Figure II-5-2 compares the mass distributions of the asphalt SC fractions.

The asphalt SC fractions varied widely in consistency, and the irregularity between the cyclohexane and pentane fractions noted in the RC fractionation also existed for the asphalt fractions. Fractions 9 and 10 contained large amounts of solids. Fraction 10 accumulated significant amounts of coke, as did the heaviest RC fraction. Fraction 8 maintained a consistency similar to asphalt. Fraction 7, the heaviest pentane fraction, also contained large amounts of solids, but lacked the insoluble coke of the heavy cyclohexane fraction. Fraction 6 proved more viscous than fraction 8, underscoring the discontinuity between cyclohexane and pentane

**Table II-5-1**
**Operating Conditions for Asphalt Fractionation**

| | | | | Fraction Percentages | | |
|---|---|---|---|---|---|---|
| Fraction | Solvent | T(°C) | P(bar) | Coastal | Fina | Texaco |
| 1 | n-pentane | 149 | 10.1 | 16 | 15 | 14 |
| 2 | n-pentane | 229 | 47.0 | 13 | 10 | 11 |
| 3 | n-pentane | 227 | 47.0 | 9 | 9 | 8 |
| 4 | n-pentane | 224 | 47.0 | 3 | 9 | 3 |
| 5 | n-pentane | 221 | 47.0 | 10 | 13 | 11 |
| 6 | n-pentane | 213 | 47.0 | 3 | 5 | 4 |
| 7 | n-pentane | 204 | 47.0 | 12 | 19 | 14 |
| 8 | cyclohexane | 307 | 47.0 | 19 | 17 | 17 |
| 9 | cyclohexane | 299 | 47.0 | 9 | 3 | 17 |
| 10 | cyclohexane | 288 | 47.0 | 6 | 2 | 3 |
| | | | | | | |
| P1 | n-pentane | 149 | 10.1 | 42 | 45 | 33 |
| C1 | cyclohexane | 204 | 10.1 | 67 | 80 | 58 |
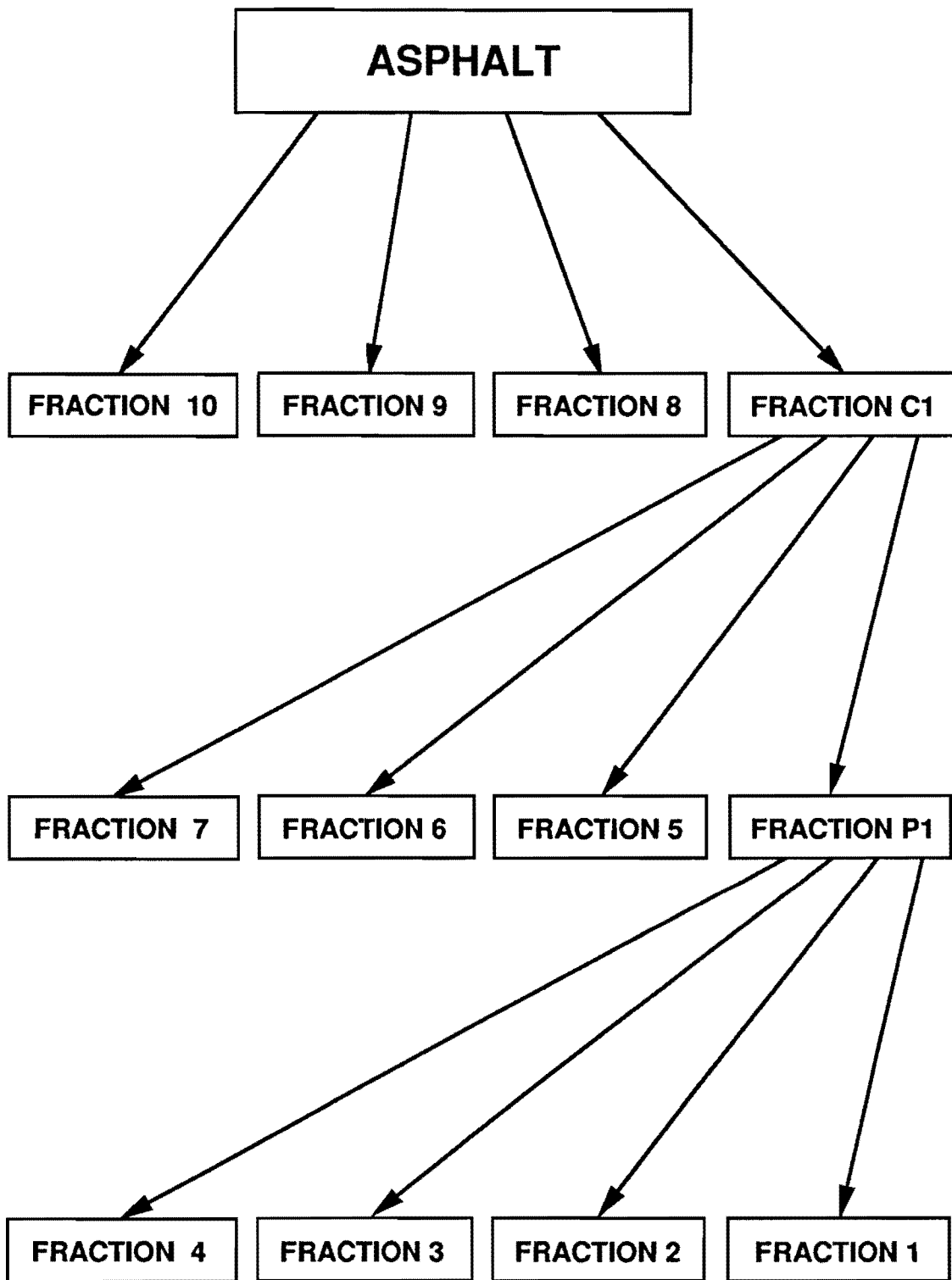
Figure II-5-1.  Asphalt Fractionation
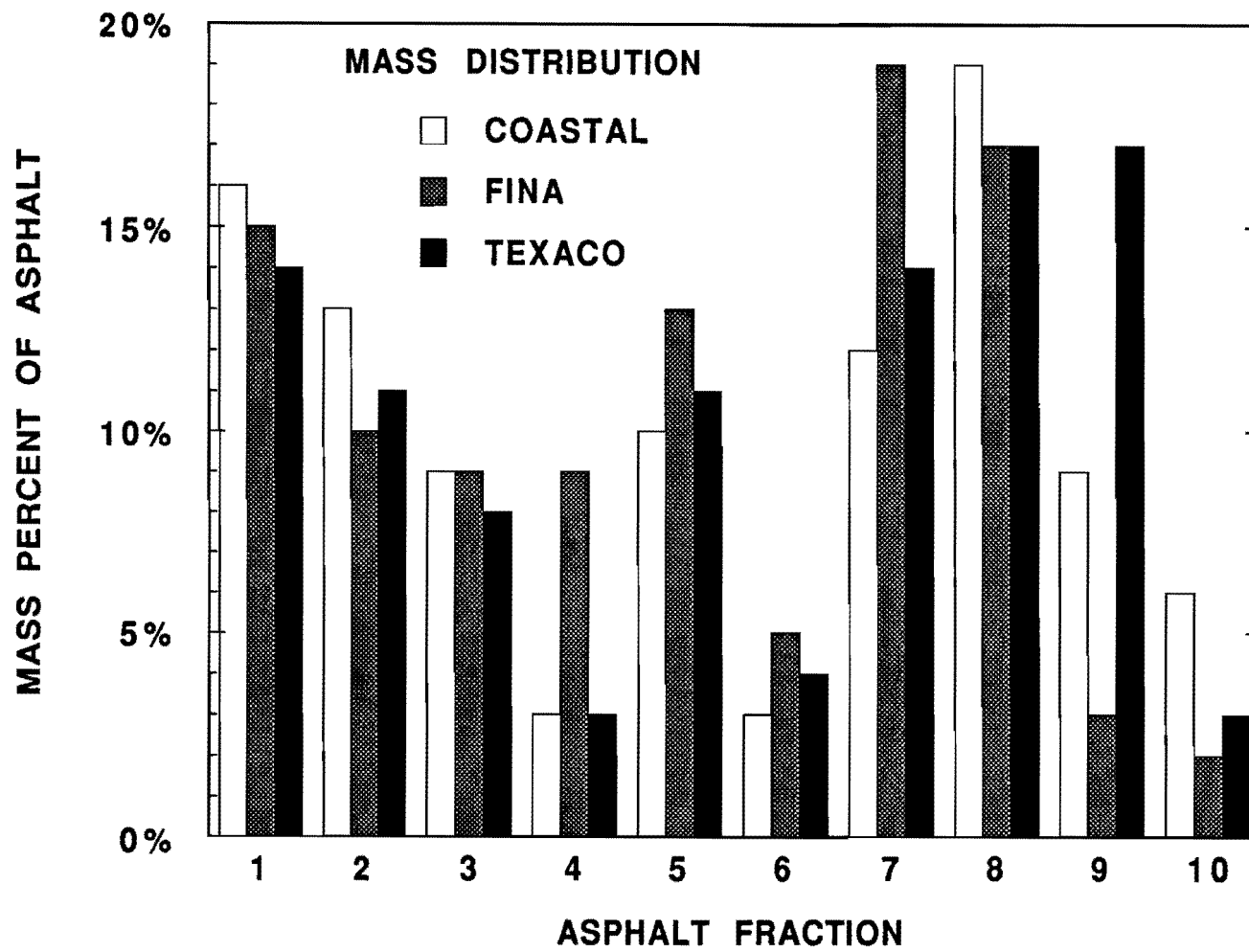
Figure II-5-2. Mass Distribution of Asphalt SC Fractions

fractions and the poor selectivity of cyclohexane. Fraction 5 was slightly less viscous than the asphalt, but approximately the same consistency as fraction 4. The last pentane separation produced fraction 4 as the bottom fraction. Fraction 4 probably contains small amounts of residual asphaltenes that accumulated in the apparatus from previous runs. Fractions 1 through 3 have very low viscosities and are a more brown or red color, rather than the black of the original asphalt or heavier fractions. Fraction 1 has a low enough viscosity that it can be poured, but only after agitation. This shear rate dependent behavior indicates that the wax concentrates in fraction 1. Removal of the waxy constituents of the asphalt should improve performance and will provide increased gas oil yields.

**Corbett Analysis**

The Corbett analysis results demonstrate a better separation of chemical functionalities among asphalt fractions than RC fractions. Figures II-5-3 through II-5-5 display the results of the Corbett analysis performed on each fraction. The inconsistency between the cyclohexane and pentane fractions are magnified in the distributions of the Corbett fractions. Although fractionating the asphaltenes as desired, cyclohexane remains a poor solvent for the fractionation of heptane soluble material, or maltenes.

Pentane proves much more selective in supercritically separating the asphalts. The asphaltenes concentrate well in the heavy fractions, and the lightest fractions are virtually asphaltene free. Fractions 5 through 8 contain the largest amounts of polar aromatics, while fractions 2 through 5 acquired the most naphthene aromatics. The saturates, as expected, concentrated in the top fractions.

The distribution of the original asphalt's Corbett fractions among the SC fractions provided additional information about the efficiency of the SC separation. These Corbett fraction distributions were calculated in the manner described in Chapter II-4 for the RC data. Figures II-5-6 through II-5-8 portray the distributions for each asphalt and emphasize the mass of the fractions and the improvement in separation with the absence of the gas oils. All of the asphalts show excellent
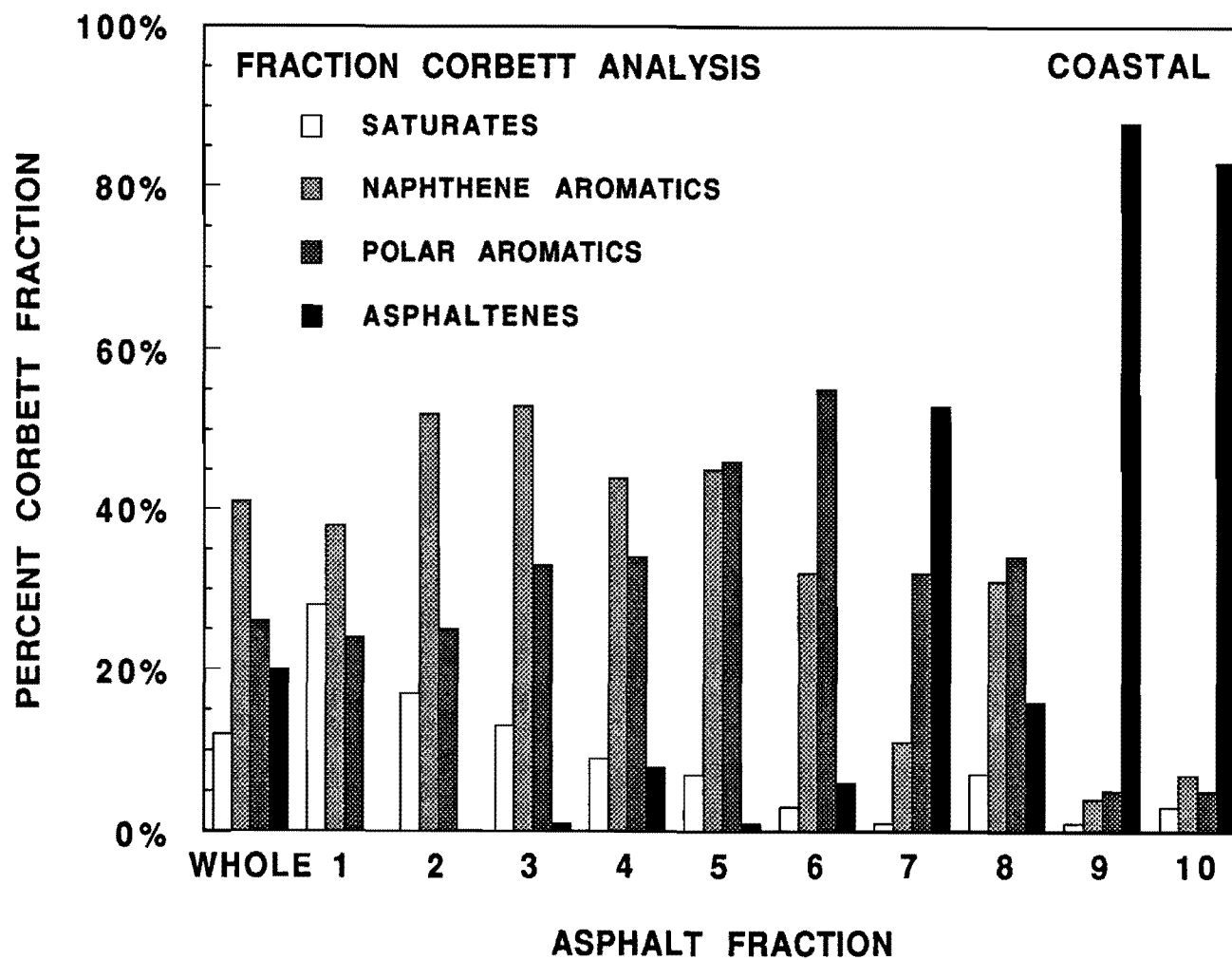
Figure II-5-3.  Corbett Analysis of Coastal Asphalt SC Fractions
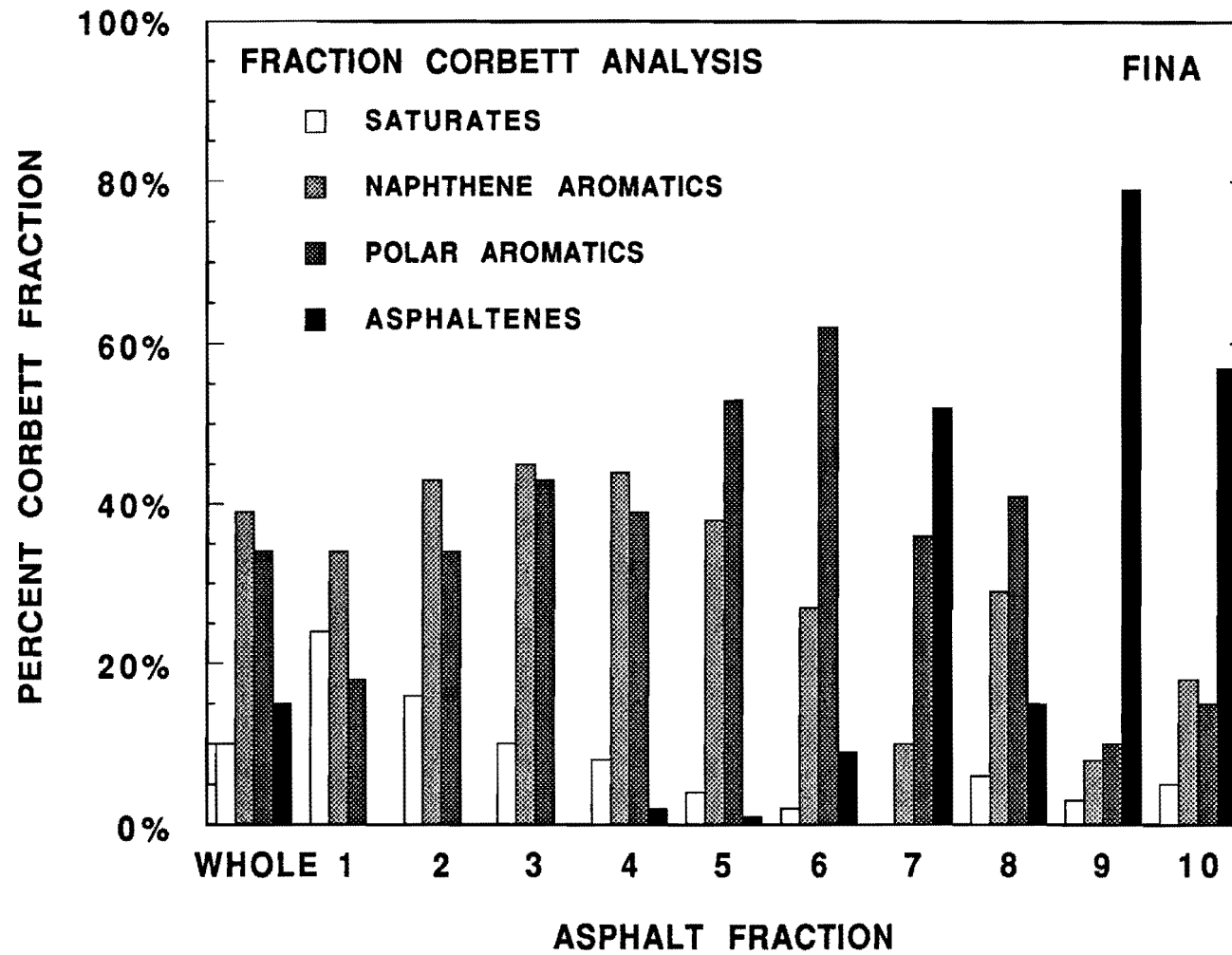
Figure II-5-4. Corbett Analysis of Fina Asphalt SC Fractions
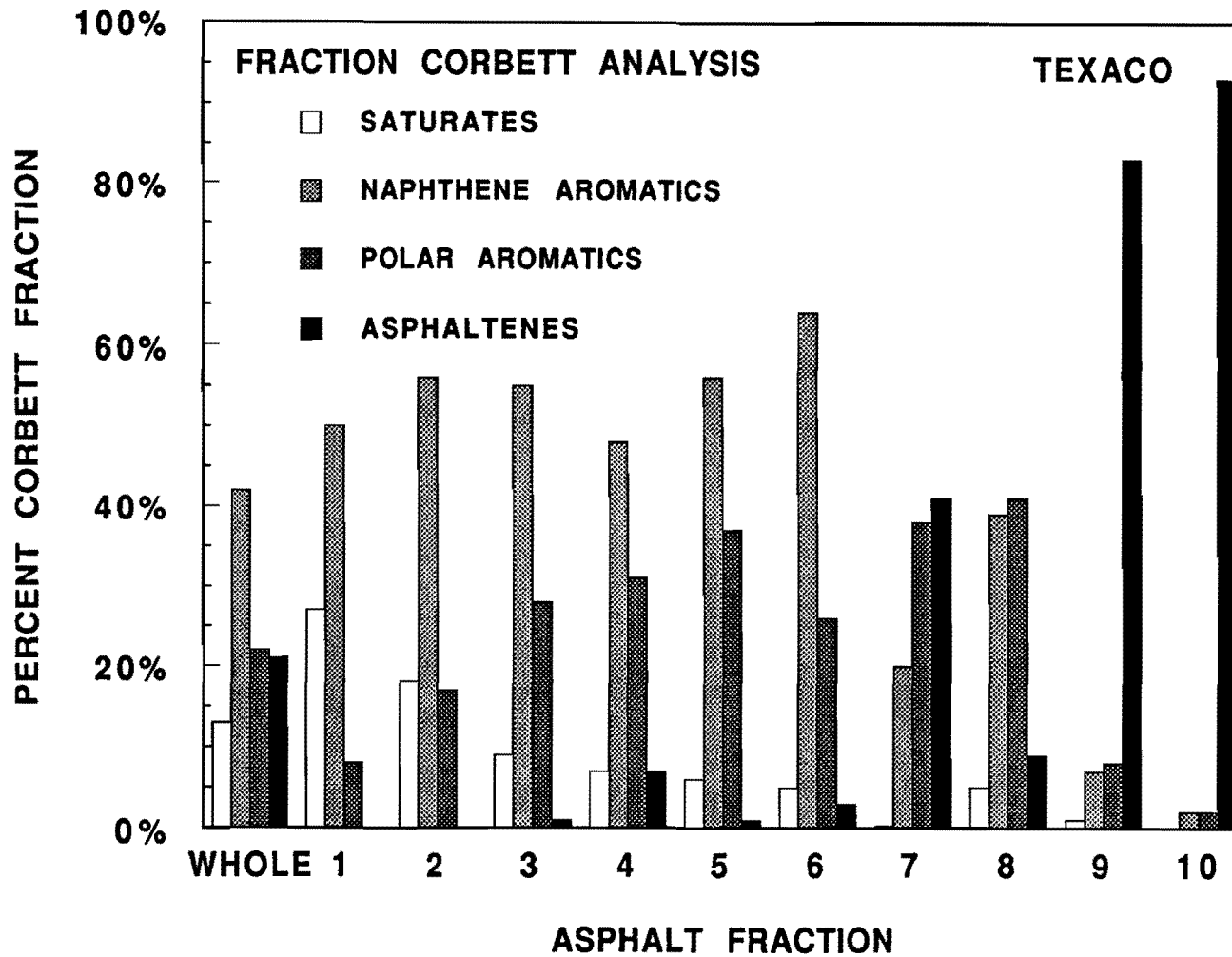
Figure II-5-5.  Corbett Analysis of Texaco Asphalt SC Fractions
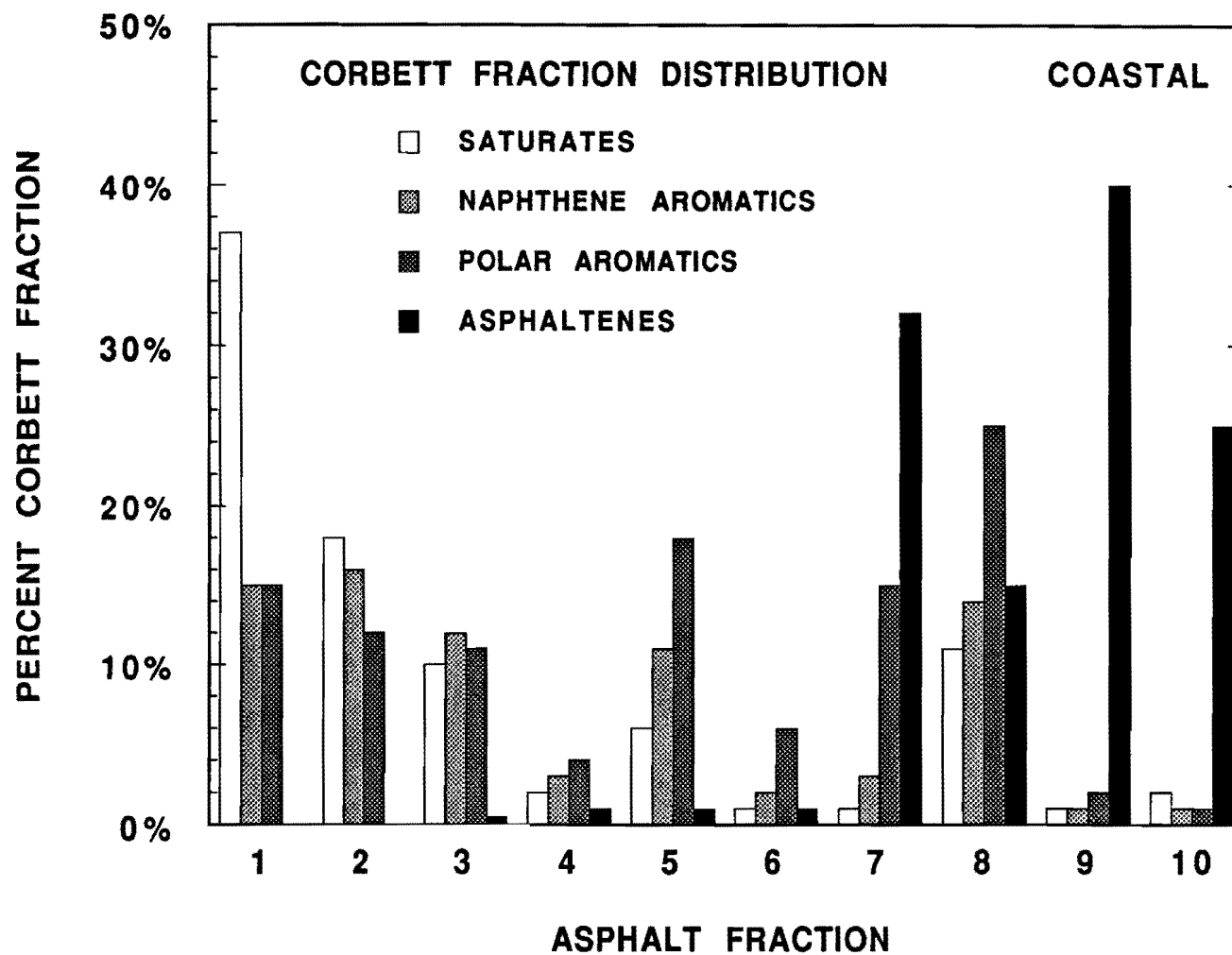
Figure II-5-6.  Distribution of the Coastal Asphalt's
Corbett Fractions Among the SC Fractions
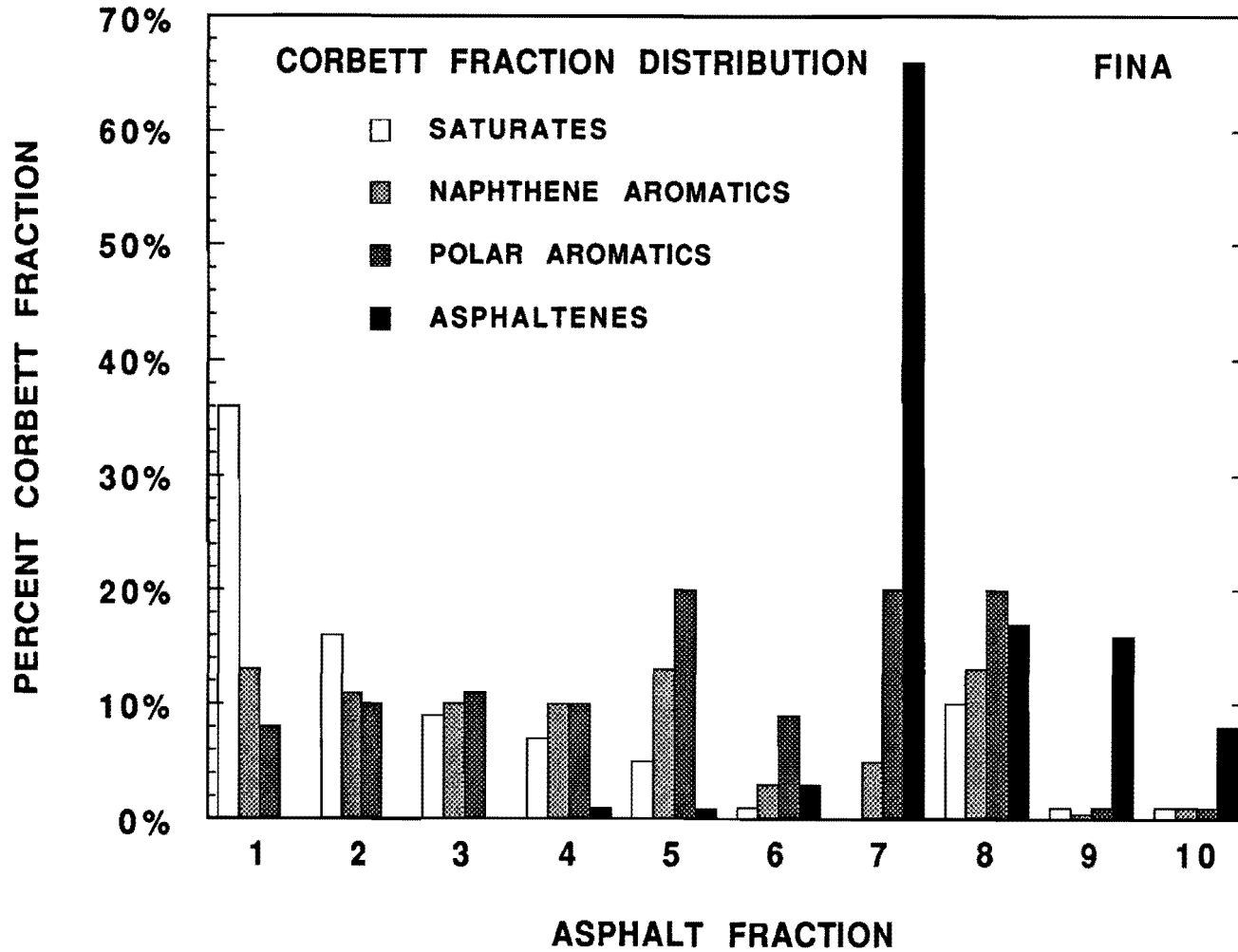
Figure II-5-7. Distribution of the Fina Asphalt's
Corbett Fractions Among the SC Fractions

93
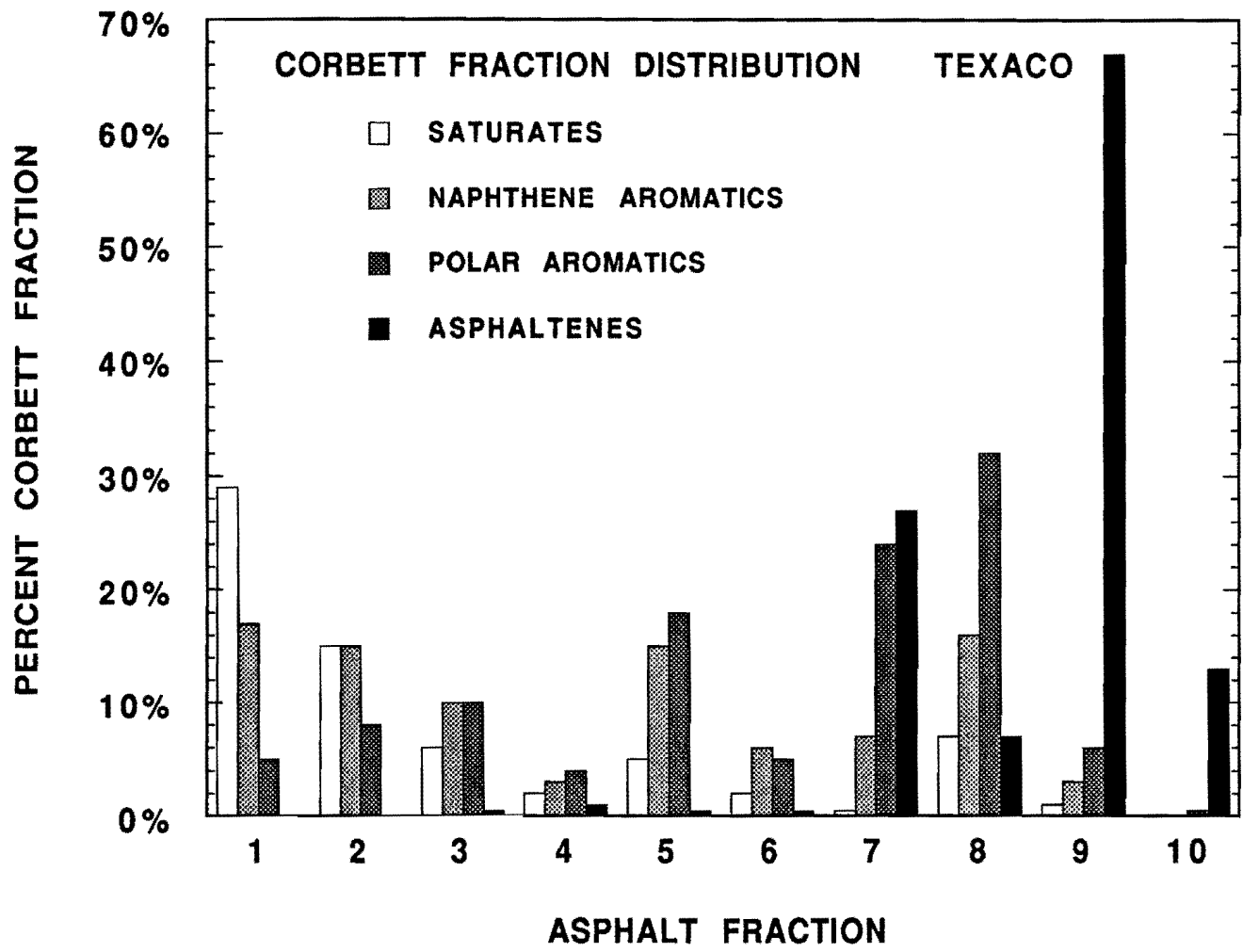
Figure II-5-8. Distribution of the Texaco Asphalt's
Corbett Fractions Among the SC Fractions

isolation of the asphaltenes from the saturates. Virtually all of the asphaltenes reside in the bottom four fractions, while the top two fractions contain at least half of all the saturates.

A mass balance calculated from the Corbett fraction distribution data provides insight into some of the processing difficulties. Table II-5-2 presents the totals of the individual Corbett fraction distributions among the SC fractions. Ideally, each fraction should total to 100%. The saturate and naphthene aromatic totals were low for all asphalts, while the polar aromatic and asphaltene values were high. These mass balance data and the existence of coke in the bottom fraction indicate significant thermal degradation during processing.

**Table II-5-2**
**Mass Balance from Corbett Fraction Distribution Data**

| Asphalt | Saturates | Naphthenes | Polars | Asphaltenes |
|---------|-----------|------------|--------|-------------|
| Coastal | 89 | 78 | 109 | 116 |
| Fina | 86 | 84 | 110 | 112 |
| Texaco | 68 | 92 | 113 | 117 |

**Infrared Analysis**

The IR spectra for the SC asphalt fractions showed the same trends seen in the RC fractions and in previous work (Davison et al., 1991; Stegeman, 1991; Stegeman et al., 1992). Figure II-5-9 displays the increasing aromaticity with fraction number for the four lightest Coastal asphalt SC fractions. All fractions except 7, 9 and 10 were analyzed using the ATR method. These solid fractions required the use of KBr pellets.

**Metal Analysis**

Atomic Absorption provided the iron, nickel, and vanadium concentrations for the asphalts and SC fractions presented in Table II-5-3. Figures II-5-10 through II-5-

95
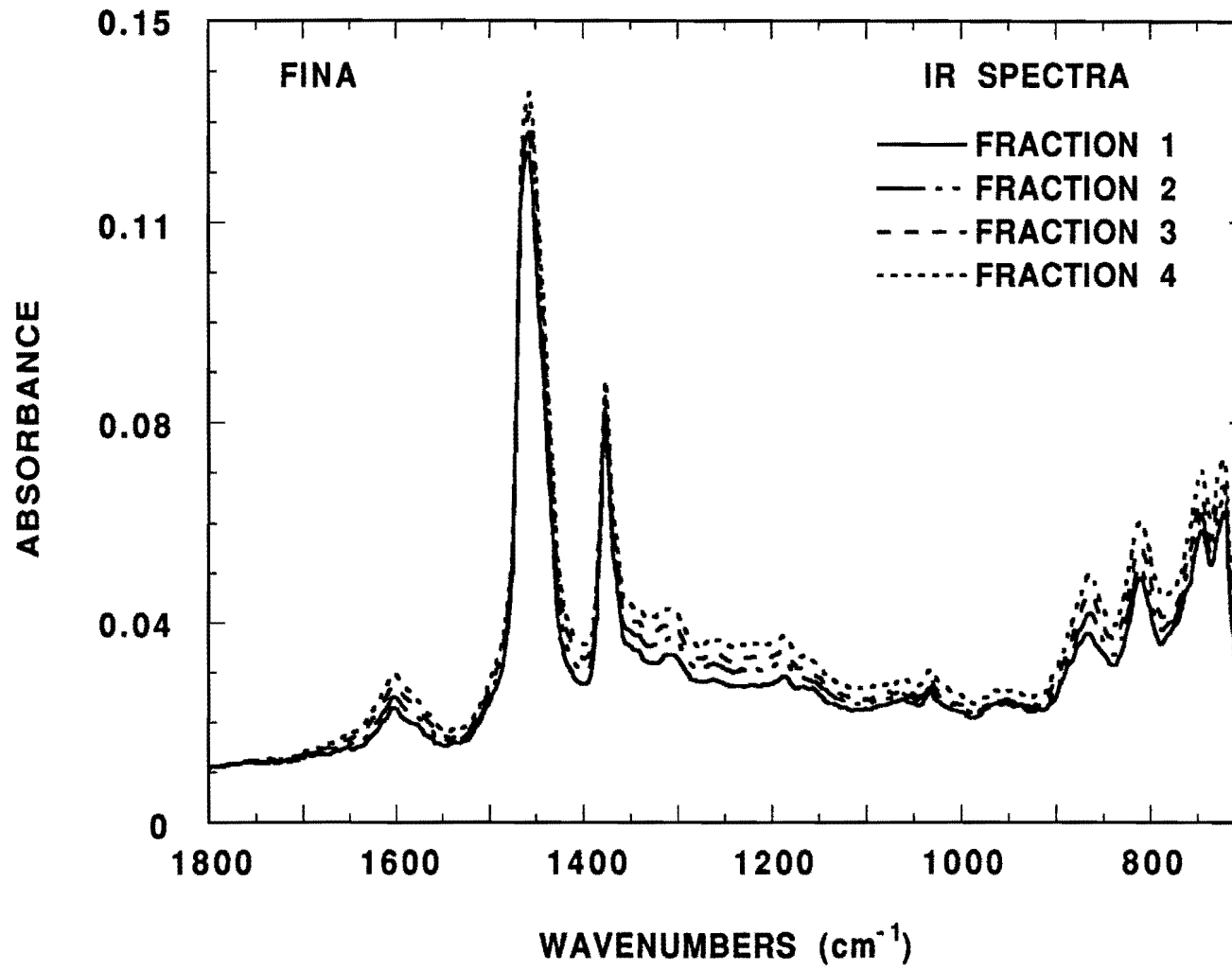
Figure II-5-9. IR Spectra of Fina Asphalt SC Fractions 1-4
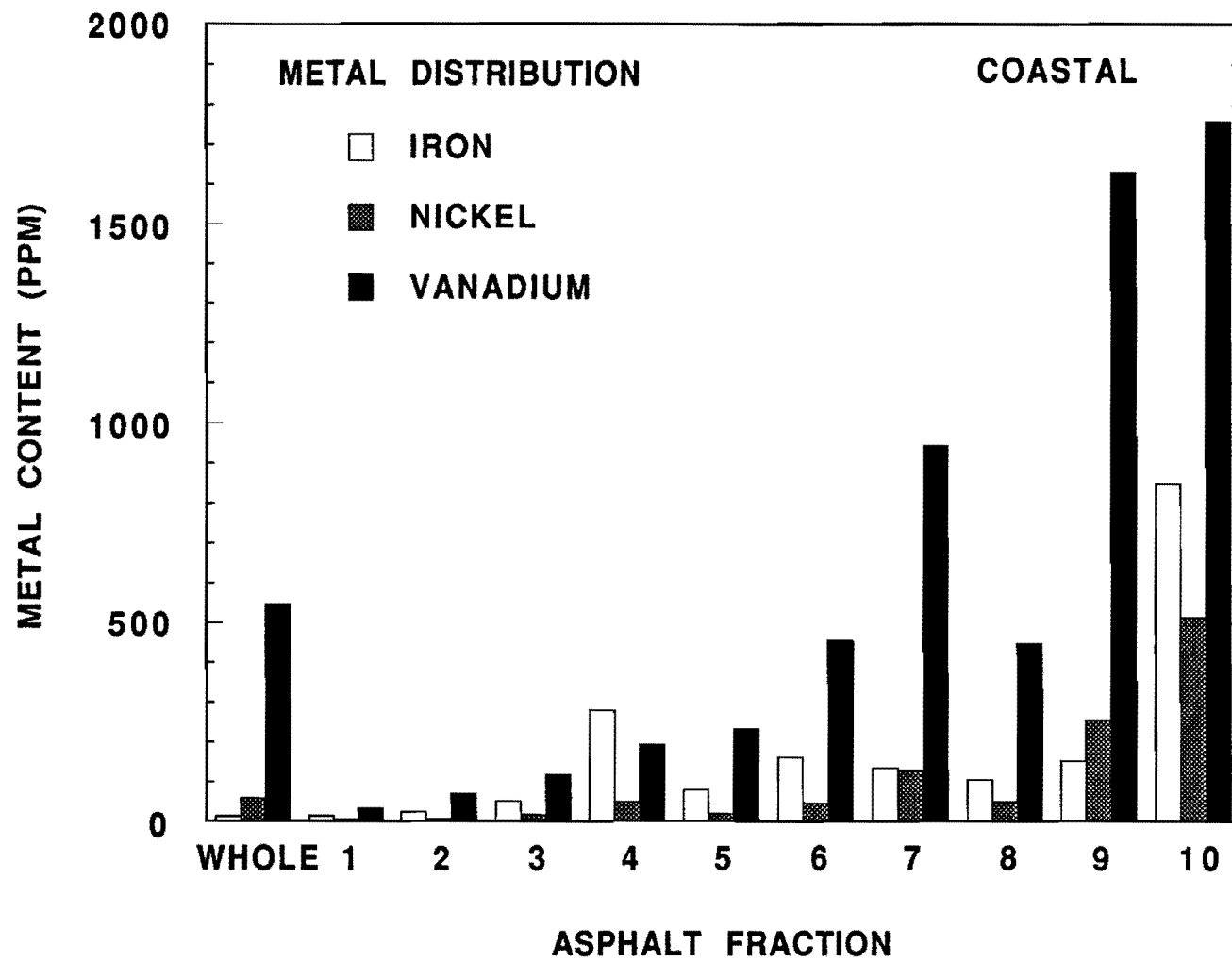
Figure II-5-10. Metal Distribution in Coastal Asphalt SC Fractions
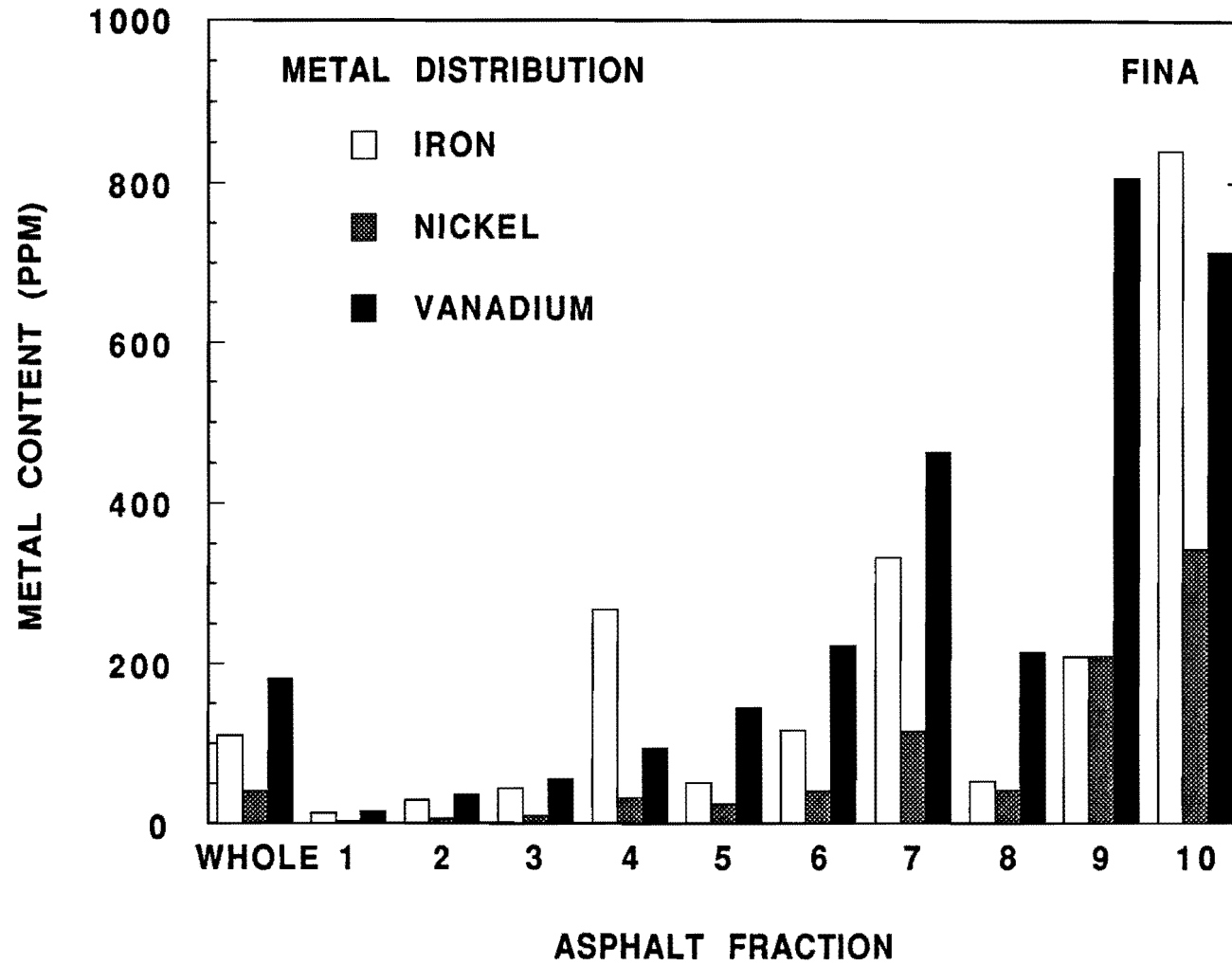
Figure II-5-11. Metal Distribution in Fina Asphalt SC Fractions
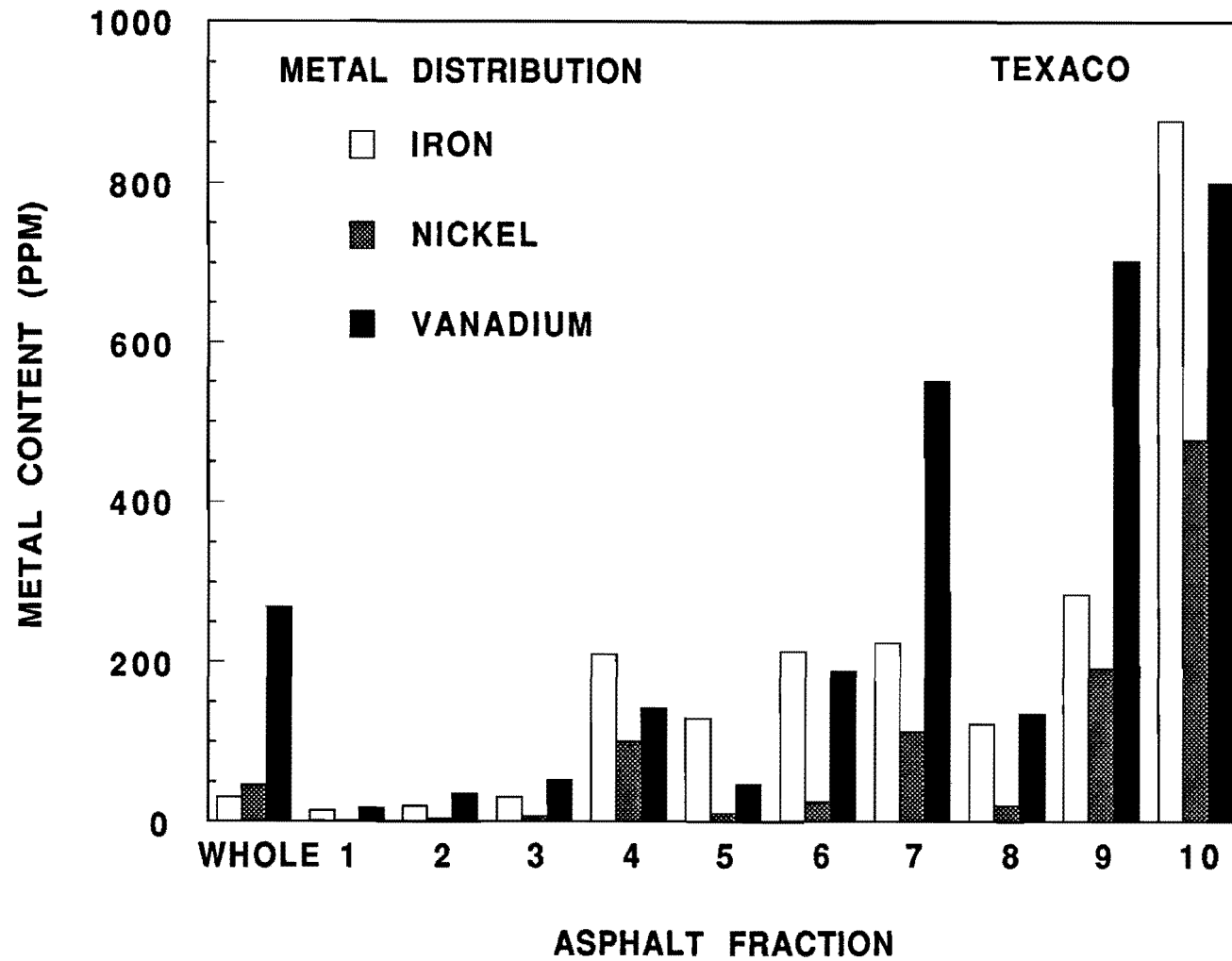
Figure II-5-12. Metal Distribution in Texaco Asphalt SC Fractions

12 illustrate how well the metals concentrate in the heavier fractions and exclude from the lighter fractions. The irregularity in the trend of metal content in fraction 7 and 8 once again demonstrates the poor selectivity of the cyclohexane. As with the RC fractions, the linear relationship between nickel, vanadium, and asphaltene contents shown by Davison et al. (1991) exists for all but the heaviest fractions. Figures II-5-13 through II-5-15 display these relationships for all three asphalts.

Table II-5-3 also gives the results of mass balance calculations using the metals analysis data. As reported for the Texaco RC fractions, the deviations indicate deterioration of the stainless steel in the heaters during the cyclohexane runs. Only the vanadium content and possibly the nickel concentrations of the lighter fractions can be considered indicative of the actual values obtained from the separation of the original asphalt. The calculated iron contents of the whole asphalt indicate varying amount of contamination in the asphalt fractions.

**GPC Analysis**

Inspection of the refractive index (RI) chromatograms of the asphalt SC fractions shows an increase with fraction number of hydrodynamic volume, which indicates molecular size and weight. Figure II-5-16 displays the RI-GPC chromatograms of fractions 1 through 4 from the Texaco asphalt. The molecular size distributions for these light fractions resemble Gaussian distributions and progress in size as previously reported by Davison et al. (1991). The light asphalt fractions lack the gas oils of the light RC fractions; therefore, they lack the detector response at about 40 minutes shown in Figure II-4-13.

The large molecular size (LMS) regions of the chromatograms of the heavier fractions become more pronounced due to the increase in asphaltene content. The RI-GPC chromatograms of Texaco fractions 5, 6, and 8 are similarly presented in Figures II-5-17. Figure II-5-18 shows the chromatograms for Texaco fractions 7, 9, and 10. Due to the inferior cyclohexane selectivity, fraction 8 from Figure II-5-17 displays a much smaller LMS region than fraction 7. The substantially smaller LMS region of fraction 7 relative to fraction 9 indicates that cyclohexane successfully

100

divided the asphaltenes roughly according to hydrodynamic volume. Fraction 10 displays a surprisingly small LMS region (smaller than fraction 9). Fraction 10 contains a large amount of coke that will not dissolve in the THF carrier solvent, and sample preparation requires filtration of insoluble material. Therefore, the resulting

**Table II-5-3**
**Metal Distribution in Asphalt SC Fractions (ppm)**

| Fraction | Coastal | | | Fina | | | Texaco | | |
|---|---|---|---|---|---|---|---|---|---|
| | Fe | Ni | V | Fe | Ni | V | Fe | Ni | V |
| Whole | 13.8 | 59.3 | 547 | 111 | 40.6 | 182 | 30.8 | 46.1 | 269 |
| 1 | 14.6 | 4.67 | 34.2 | 12.9 | 3.21 | 15.8 | 13.8 | 2.12 | 16.7 |
| 2 | 25.4 | 7.12 | 70 | 29.2 | 6.58 | 36.2 | 19.6 | 4.21 | 35.8 |
| 3 | 51.7 | 17.5 | 118 | 43.7 | 10.5 | 56.7 | 30.8 | 7.38 | 53.8 |
| 4 | 280 | 51.2 | 196 | 269 | 32.9 | 94.6 | 210 | 101 | 143 |
| 5 | 80.8 | 20.6 | 234 | 52.1 | 24.8 | 145 | 130 | 10.7 | 48.1 |
| 6 | 162 | 45.8 | 458 | 117 | 41.1 | 224 | 214 | 25.4 | 190 |
| 7 | 134 | 129 | 945 | 333 | 116 | 464 | 225 | 113 | 551 |
| 8 | 106 | 49.7 | 450 | 53.7 | 42 | 216 | 122 | 20.4 | 136 |
| 9 | 152 | 257 | 1630 | 209 | 211 | 807 | 286 | 194 | 704 |
| 10 | 851 | 516 | 1760 | 840 | 344 | 714 | 878 | 478 | 802 |
| P1 | 21.2 | 8.92 | 101 | 15 | 8.72 | 62.8 | 19.9 | 5.24 | 132 |
| C1 | 65.3 | 33.2 | 314 | 39.2 | 32.8 | 168 | 134 | 18.4 | 112 |
| Total* | 864% | 47% | -5.1% | 28% | 30% | 17% | 429% | 59% | 1.1% |

*Deviation of the fraction total from the whole asphalt

101
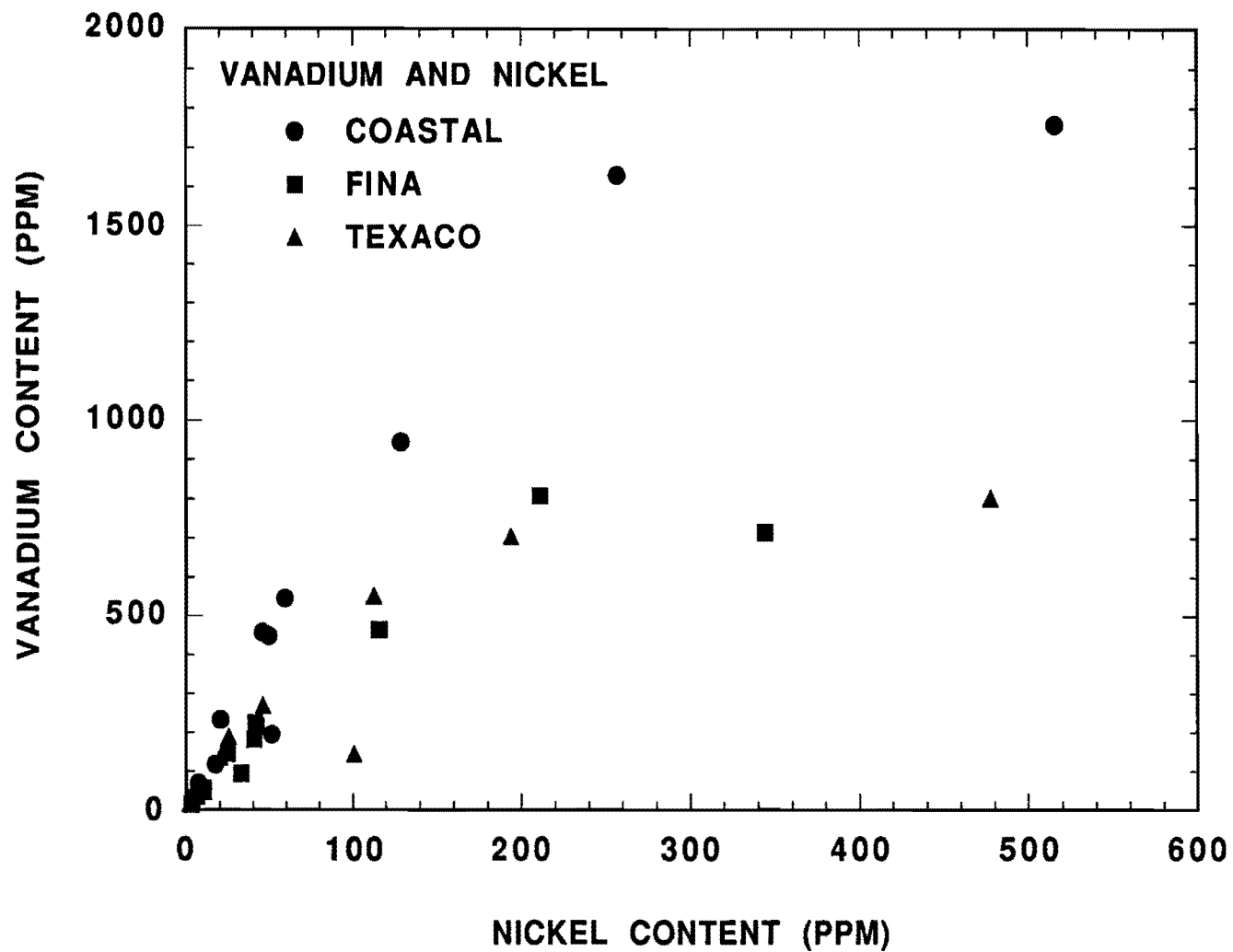
Figure II-5-13. Vanadium Versus Nickel for Asphalt SC Fractions
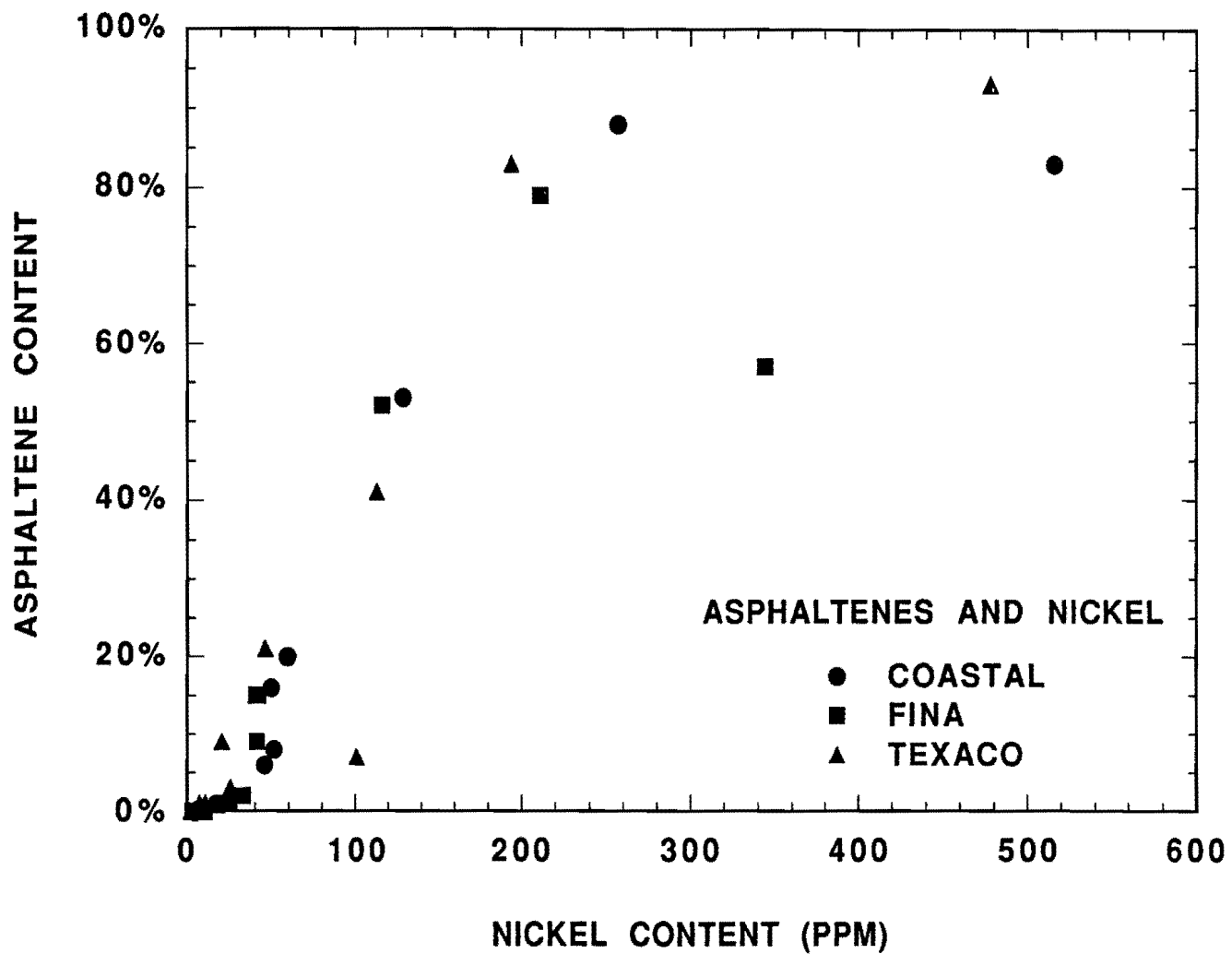
Figure II-5-14. Asphaltenes Versus Nickel for Asphalt SC Fractions
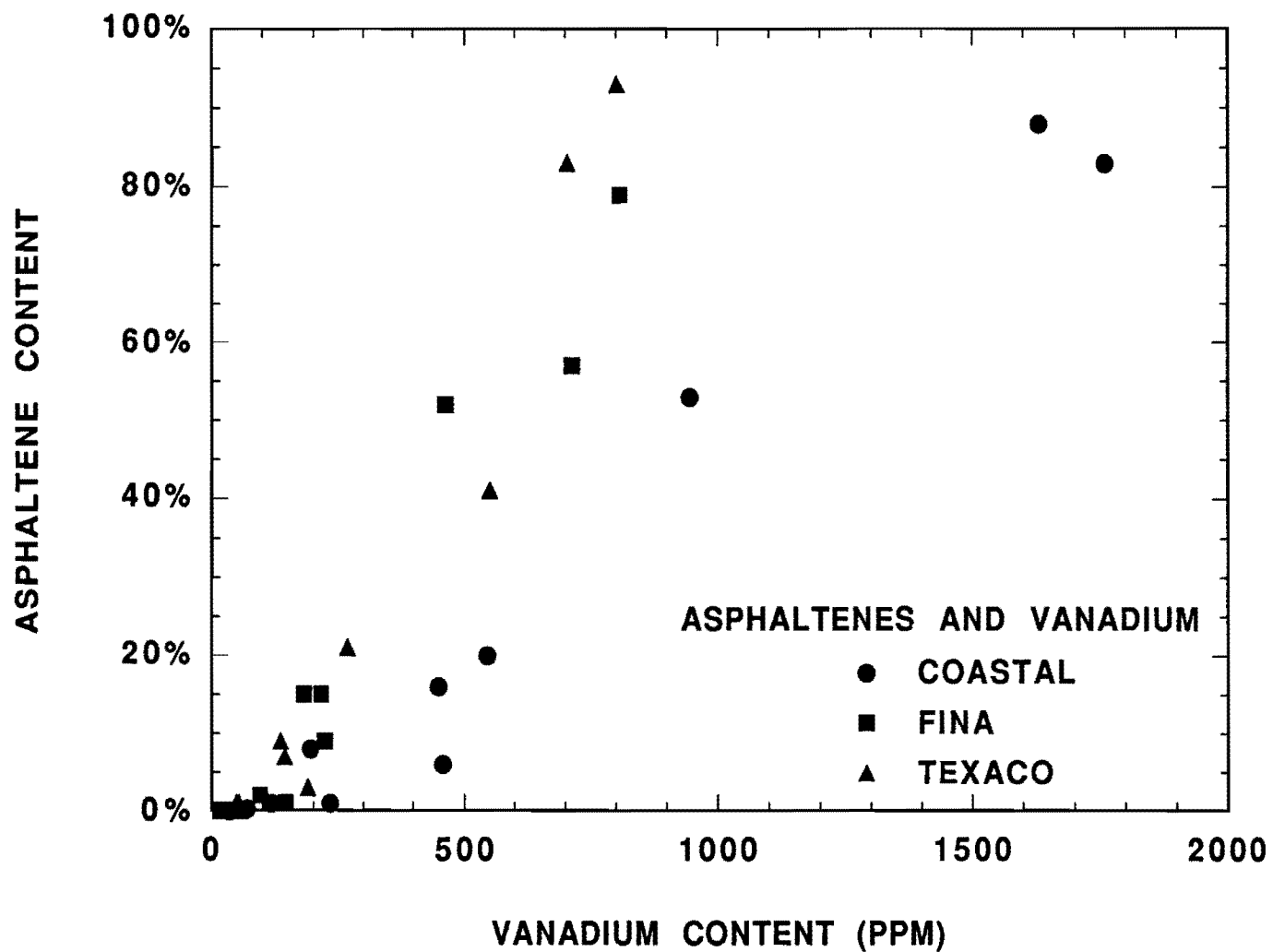
Figure II-5-15. Asphaltenes Versus Vanadium for Asphalt SC Fractions
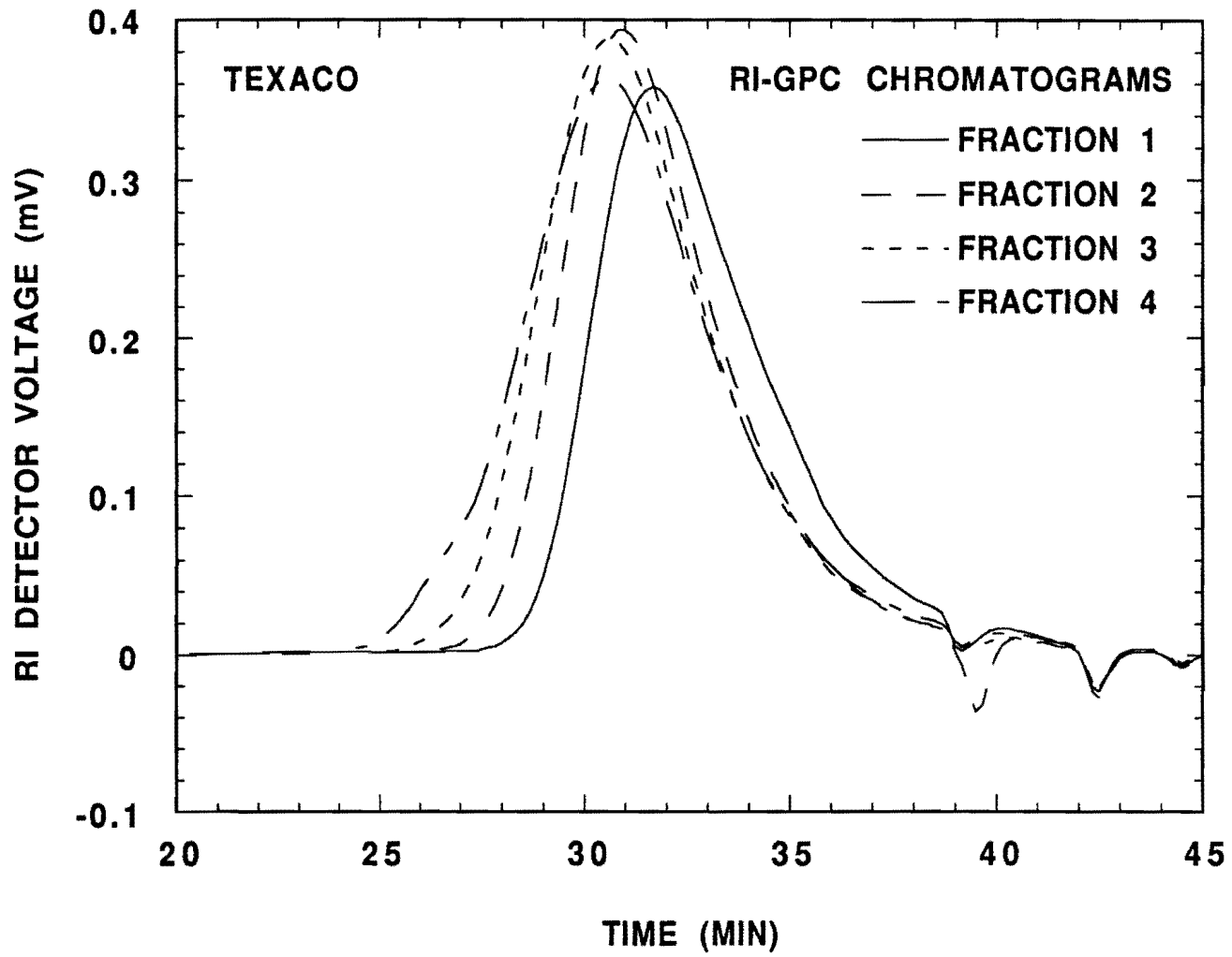
Figure II-5-16. RI-GPC Chromatograms of Texaco Asphalt SC Fractions 1-4
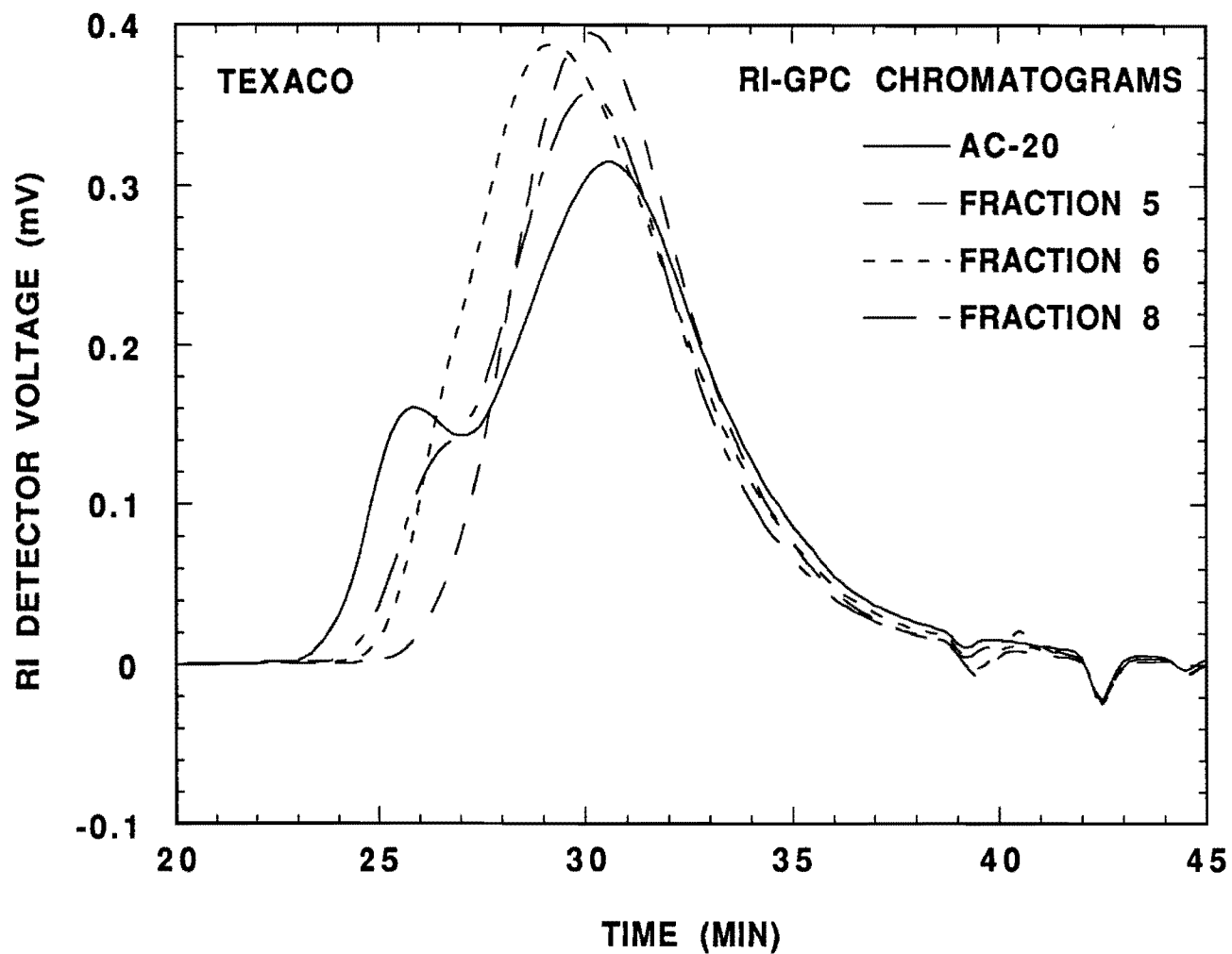
Figure II-5-17. RI-GPC Chromatograms of Texaco Asphalt and SC Fractions 5, 6, and 8
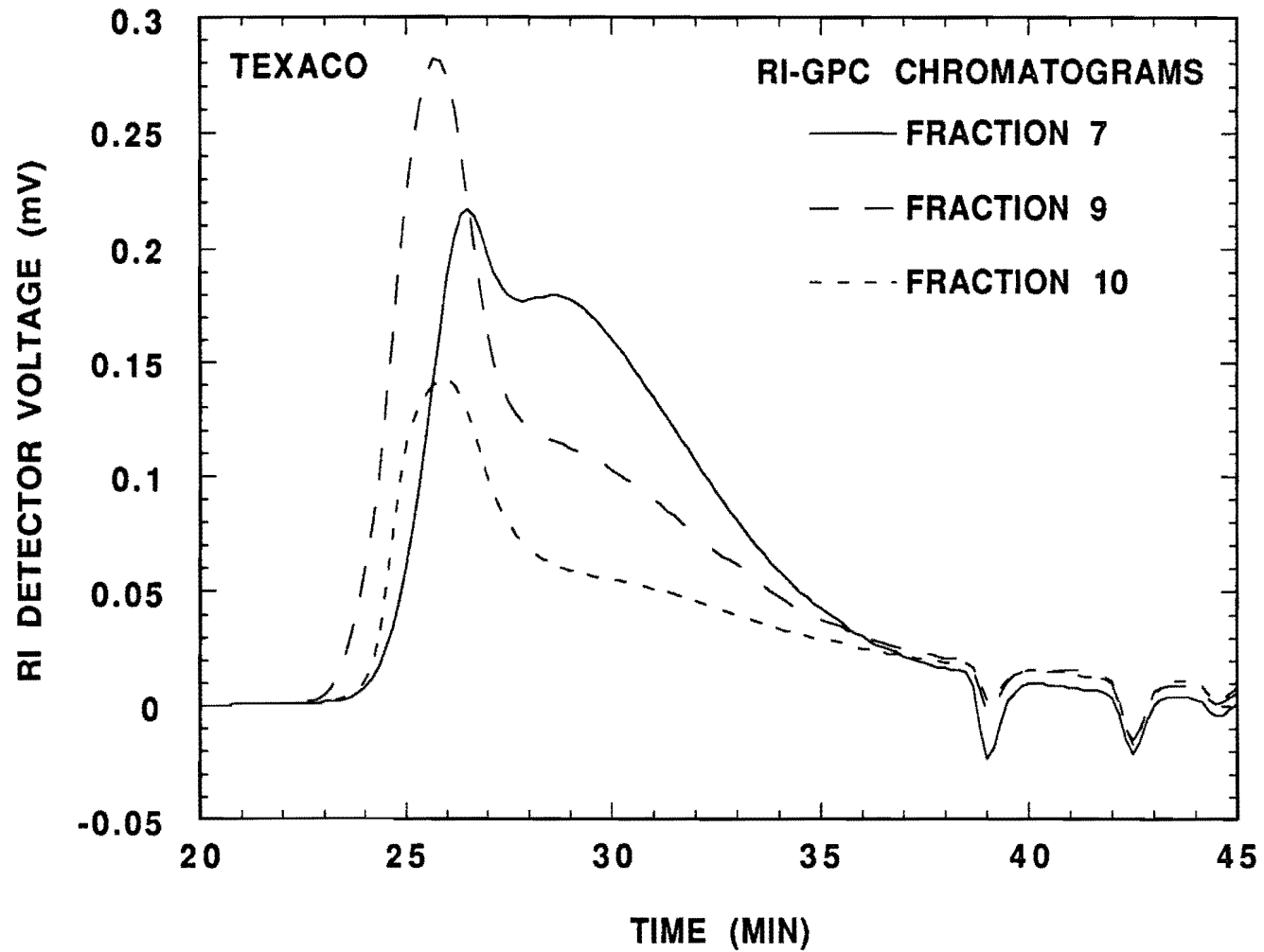
Figure II-5-18. RI-GPC Chromatograms of Texaco Asphalt SC Fractions 7, 9, and 10

chromatograms of fraction 10 do not adequately represent the actual distribution in molecular size or weight.

Chromatograms for the asphaltene fractions of the Coastal SC fractions 6 through 10 are shown in Figure II-5-19. The concentration of the fraction 6 chromatogram is lower due to the small sample size available. Fraction 10 appears small. As before, much of the sample weight included insoluble coke that was excluded by filtering during sample preparation. The cyclohexane soluble fraction 6 and 7 asphaltenes show lower molecular sizes than the heavier fractions. The cyclohexane apparently separated the asphaltenes somewhat according to molecular size.

Molecular weights were calculated using both the RI-GPC chromatogram only, and the intrinsic viscosity, RI, and universal calibration information for each of the SC fractions. Weight-, number-, and z-average molecular weights were calculated for each sample, but the weight-average molecular weights ($M_w$) were the least sensitive to sample and measurement. Table II-5-4 lists the $M_w$ data for the asphalt and SC fractions. Figure II-5-20 shows that $M_w$ calculated using the RI detector response ($M_w^{RI}$) and with the addition of the intrinsic viscosity measurements ($M_w^{IV}$) agree for the light fractions, but the $M_w^{IV}$ becomes relatively higher as the asphaltene content and viscosity increase. Figure II-5-20 omits the solid fractions (7, 9, and 10) due to the presence of insoluble materials and/or excessive tailing from column adsorption, which produces erroneous results. Since the calibration curves used polystyrene standards for the high $M_w$, the asphaltene molecules appear more branched and/or more compact than polystyrene molecules with the same hydrodynamic volume. The $M_w^{RI}$ and $M_w^{IV}$ values are not independent as shown in Figure II-5-20. Therefore, only the $M_w^{IV}$ values are shown in other correlations due to the increased sensitivity for the more viscous fractions.

Inconsistencies in the $M_w$ trends in Table II-5-4 are attributed to processing difficulties. Coastal and Texaco fraction 4 contain asphaltenes either accumulated from previous runs or formed during the final pentane runs. Asphaltenes in fraction 4 for all asphalts account for the slightly larger $M_w$ values than shown by fraction 5.

108
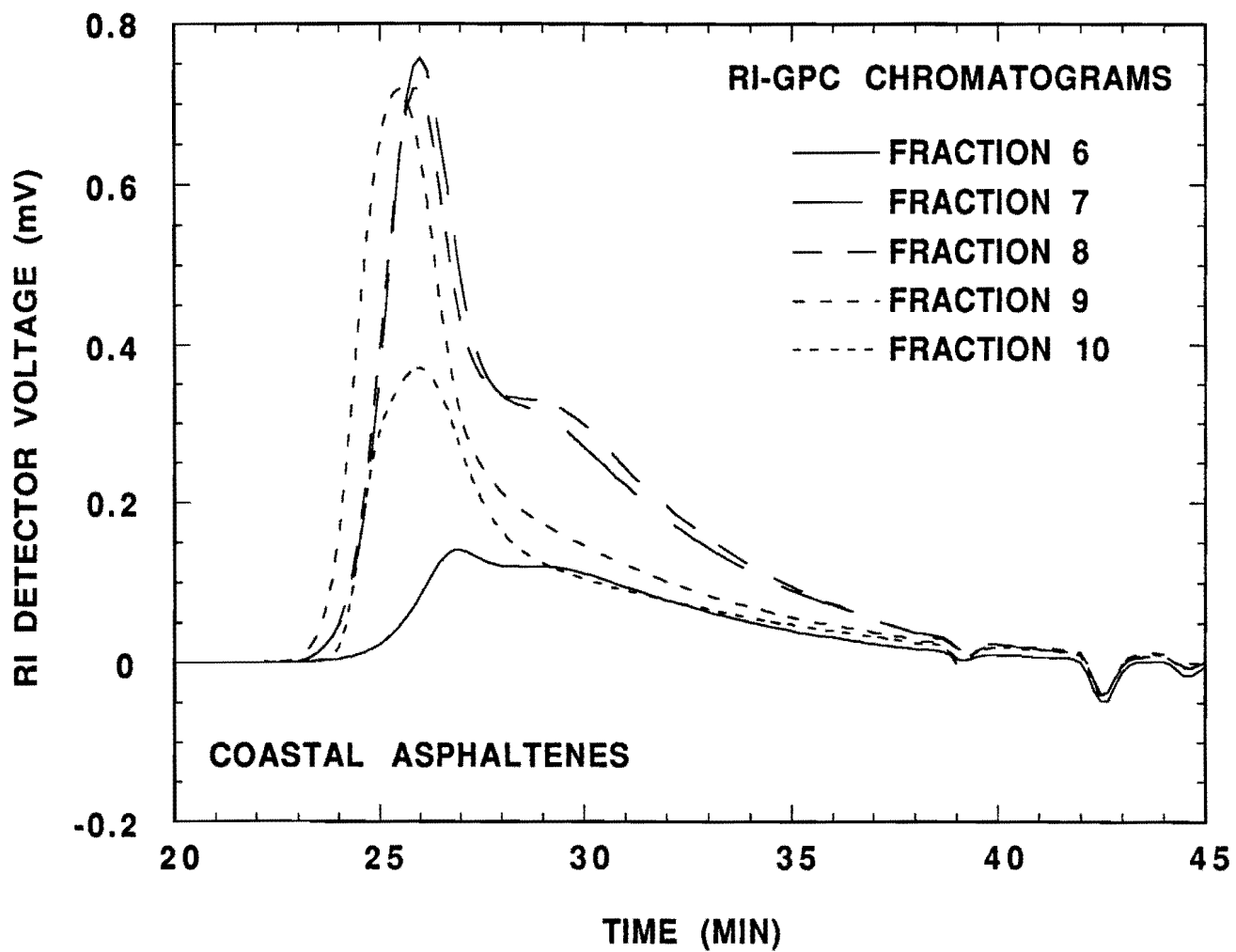
Figure II-5-19. RI-GPC Chromatograms of the Asphaltenes of Coastal Asphalt SC Fractions 6-10
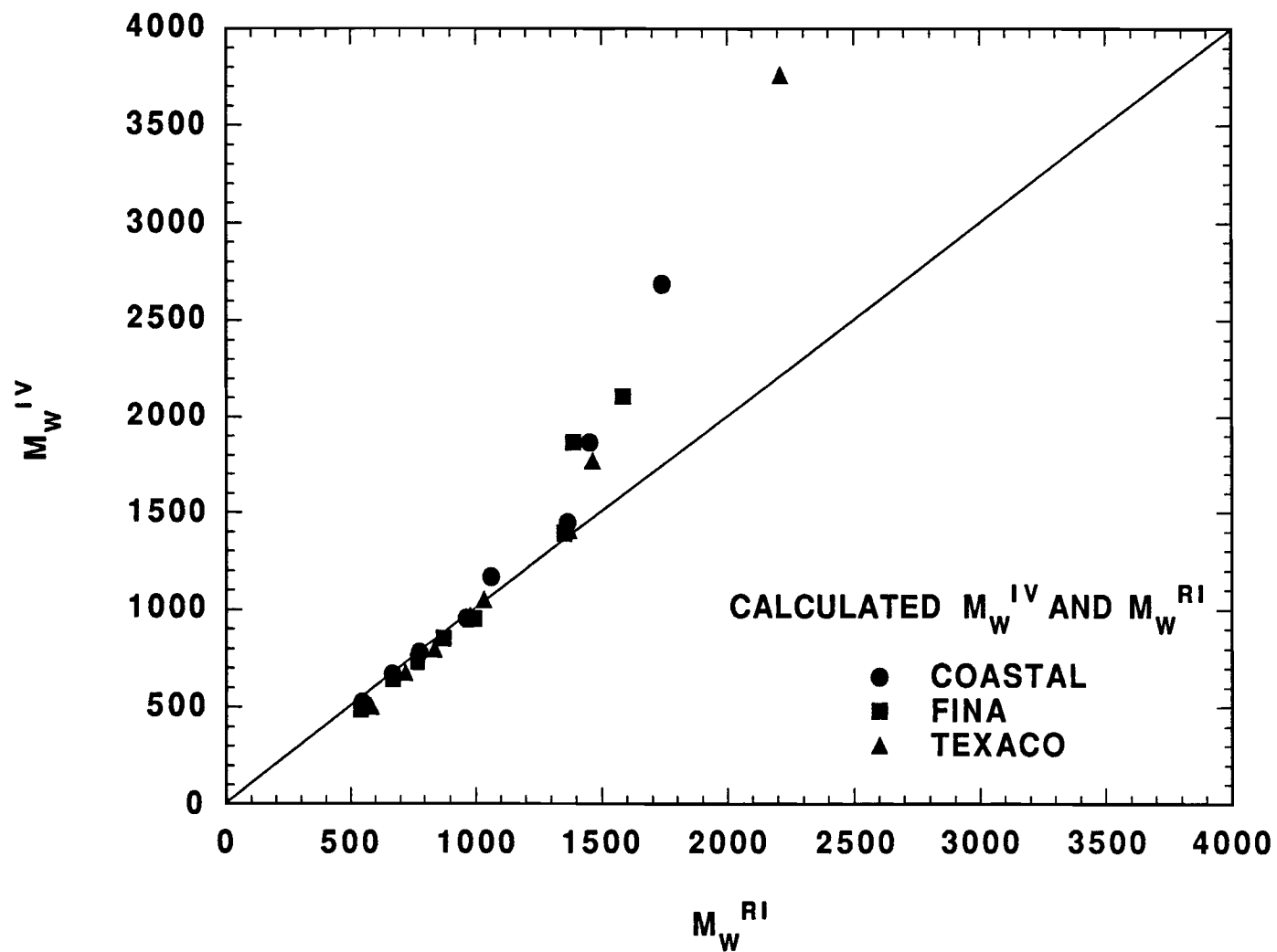
Figure II-5-20. $M_w^{IV}$ Versus $M_w^{IV}$ for Asphalts and SC Fractions

**Table II-5-4**
**GPC Molecular Weight Data for Asphalts and SC Fractions**

| Fraction | Coastal $M_w^{RI}$ | Coastal $M_w^{IV}$ | Fina $M_w^{RI}$ | Fina $M_w^{IV}$ | Texaco $M_w^{RI}$ | Texaco $M_w^{IV}$ |
|---|---|---|---|---|---|---|
| Whole | 1740 | 2690 | 1388 | 1867 | 2212 | 3762 |
| 1 | 546 | 527 | 542 | 488 | 584 | 505 |
| 2 | 669 | 670 | 671 | 645 | 722 | 676 |
| 3 | 780 | 783 | 771 | 732 | 839 | 797 |
| 4 | 1062 | 1171 | 874 | 853 | 1034 | 1050 |
| 5 | 966 | 958 | 993 | 954 | 981 | 967 |
| 6 | 1366 | 1449 | 1354 | 1391 | 1373 | 1406 |
| 7 | 2255 | 2809 | 2609 | 3260 | 2284 | 2813 |
| 8 | 1453 | 1867 | 1585 | 2107 | 1465 | 1771 |
| 9 | 3574 | 9418 | 4404 | 11200 | 3601 | 9521 |
| 10 | 2031 | 16420 | 1865 | 2258 | 2290 | 11010 |

The poor separation during cyclohexane runs generates lower $M_w$ species in fraction 8 than fraction 7. The apparently low $M_w^{RI}$ of fraction 10 results from the large amounts of insoluble coke produced during the cyclohexane runs that were necessarily excluded during sample GPC preparation. The high $M_w^{IV}$ results indicate that the molecules remaining are viscous and very dense.

**Viscosity**

The Carri-Med rheometer provided limiting dynamic viscosities ($\eta_o^*$) as described by Lau (1991) for the asphalts and viscous SC fractions. The irregularities due to processing noted in the Corbett and GPC analyses are also present in the $\eta_o^*$ results. Table II-5-5 gives the 60°C $\eta_o^*$ data obtained.

111

In a manner similar to that described by Davison et al. (1991), viscosities were plotted versus fraction mean. The fraction mean represents the mean of the fraction composition. For example, a hypothetical lightest fraction containing 10% of the whole asphalt would have a fraction mean of 95%. The fraction mean of a whole asphalt will always be 50%. Figure II-5-21 shows the fraction mean and $\eta_o^*$ data. A relatively smooth curve exists through the pentane fractions and the whole asphalts. The cyclohexane fractions (fraction 8) produce a curve very different from that of the pentane fractions. The large separation between the fraction 8 values and the pentane data again demonstrate the significant differences in solvent properties.

### Table II-5-5
### Asphalt and SC Fraction Viscosities

| Fraction | 60°C $\eta_o^*$ (poise) | | |
| --- | --- | --- | --- |
| | Coastal | Fina | Texaco |
| Whole | 2350 | 2570 | 2780 |
| 1 | 1.5 | 2 | 3.1 |
| 2 | 3.9 | 7.2 | 4.6 |
| 3 | 31.5 | 52 | 31 |
| 4 | 201 | 167 | 109 |
| 5 | 203 | 1390 | 220 |
| 6 | 19300 | 394000 | 2700 |
| 7 | solid | solid | solid |
| 8 | 3300 | 39000 | 1290 |
| 9 | solid | solid | solid |
| 10 | solid | solid | solid |
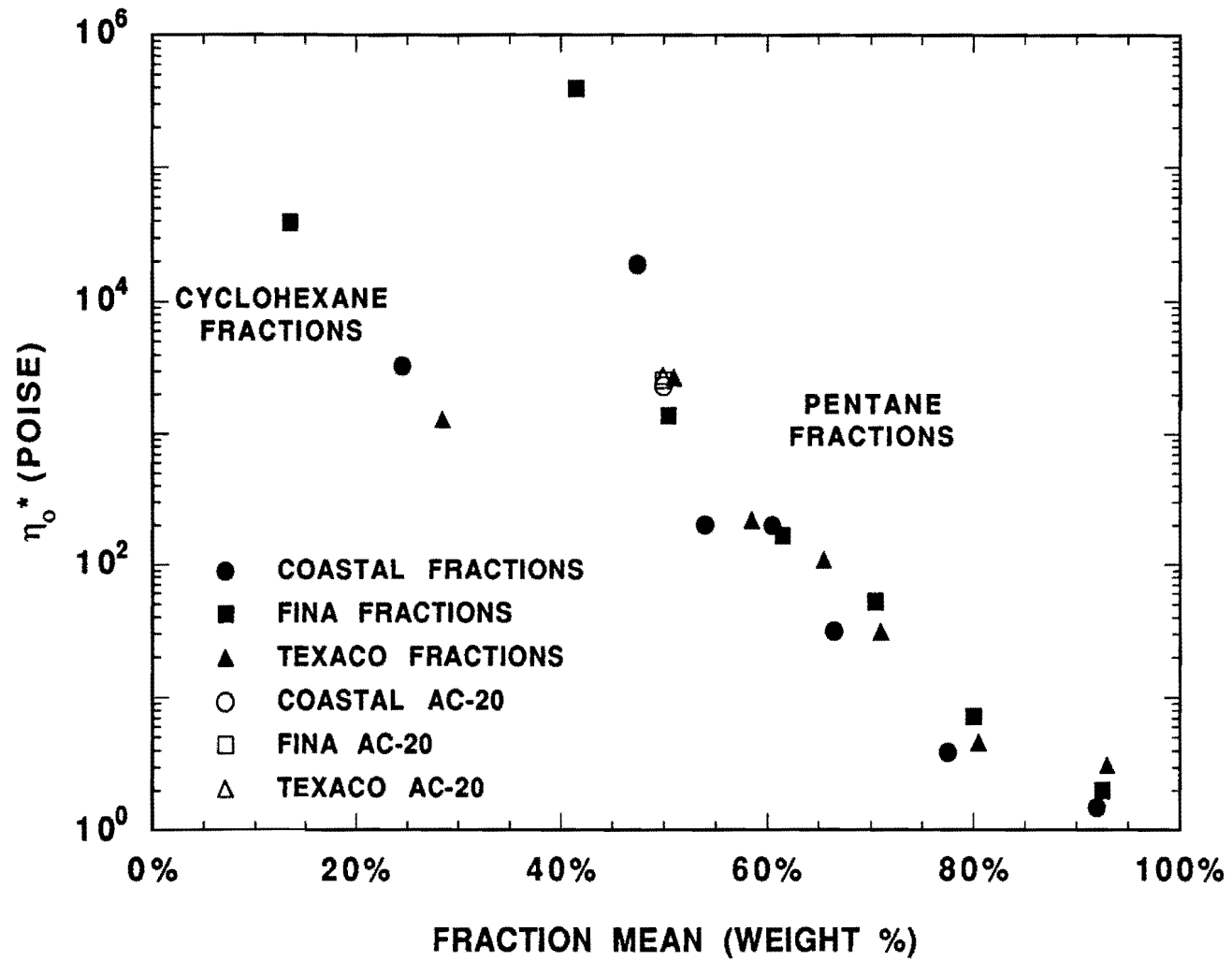
Figure II-5-21. Viscosity of Asphalts and SC Fractions

**POV Aging**

The three asphalts and selected SC fractions were aged under high oxygen pressure at three different temperatures. The aged fractions include fractions 2, 3, 5, and 8 for each asphalt with fraction 6 also included for the Texaco asphalt. Samples were removed at four different aging times at each temperature as listed in Table II-3-1. IR spectra and $\eta_0^*$ data provided hardening susceptibility (HS) information as described by Lau (1991). The HS is calculated from the aging data as the slope of the exponential fit through the $\eta_0^*$ versus the carbonyl area calculated from the IR spectra (Jemison, et al., 1991). Previous work has demonstrated that a very strong relationship exists between $\eta_0^*$ increase and carbonyl formation during the aging of asphalts, but this relationship is very asphalt dependent (Davison et al., 1989; Harnsberger et al., 1991; Jemison et al., 1991; Jemison et al., 1992; Lau, 1991; Lau et al., in press).

Figures II-5-22 through II-5-24 show the aging data from all three temperatures for the asphalts and selected SC fractions. The slope of the line through each data set represents the HS. All of the fractions analyzed, except Fina fraction 8, show an improved HS over the original asphalt. Although the HS represents the sensitivity of an asphalt's $\eta_0^*$ to carbonyl formation, it does not indicates the rate of carbonyl formation or of hardening.

The POV aging data allows the calculation of carbonyl and $\eta_0^*$ growth rates at each temperature for the asphalts and fractions. Using the Fina asphalt and fractions as examples, Figures II-5-25 through II-5-27 represent the carbonyl growth rates for aging at 93.3°C (200°F), 82.2°C (180°F), and 71.1°C (160°F), respectively. Similarly, Figures II-5-28 through II-5-30 show the $\eta_0^*$ growth rates for the aged Fina samples at the three temperatures.

The $\eta_0^*$ values of the whole asphalt are higher than those of the fractions. However, the asphalt produces carbonyl areas which are about the same as those for fraction 5, which maintained a much lower $\eta_0^*$. Partial thermal degradation of some components in the SC fractions may produce reactive sights that readily oxidize but do not contribute significantly to the $\eta_0^*$. Increased concentrations of iron relative

114
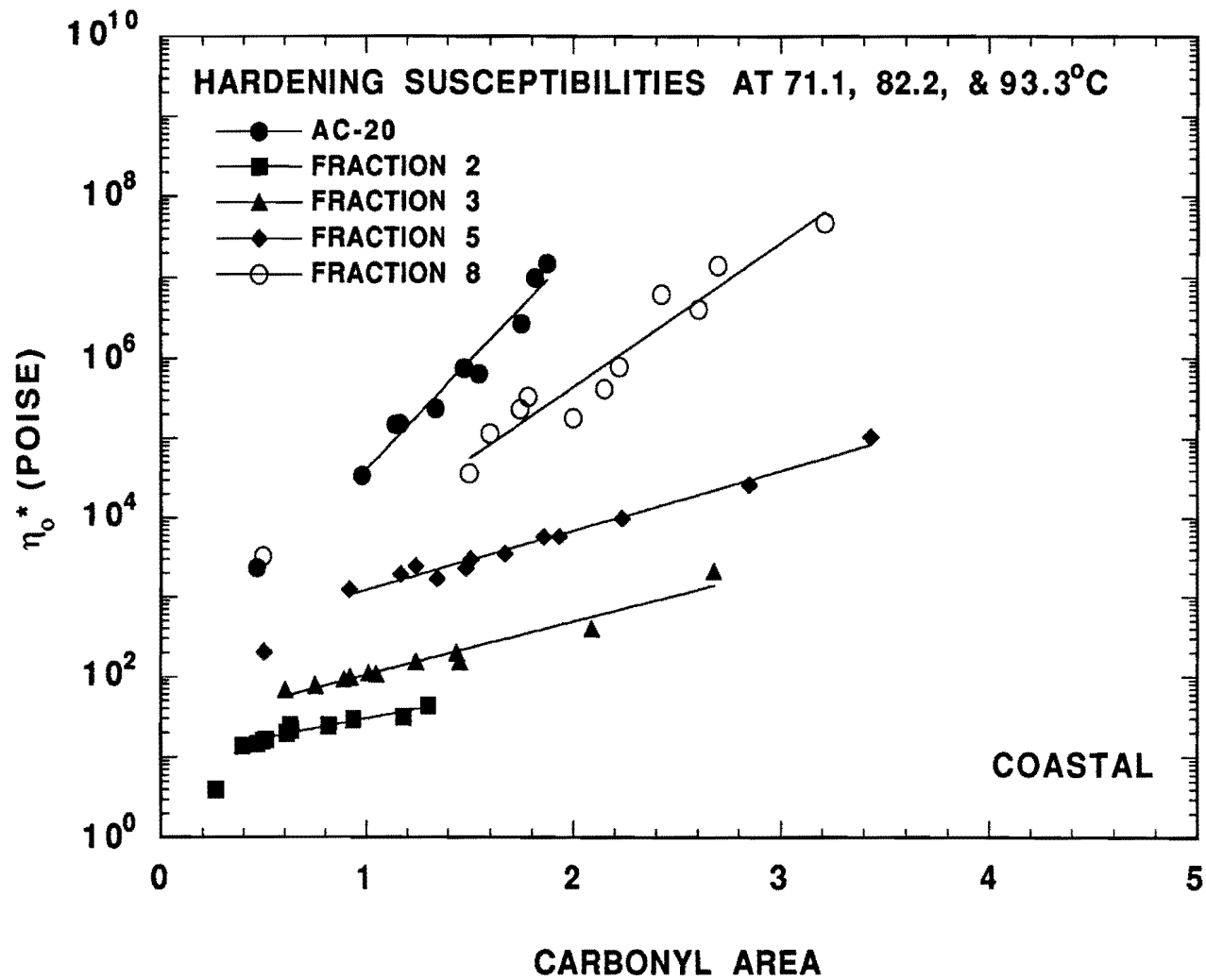
Figure II-5-22. HS of Coastal Asphalt and Selected SC Fractions
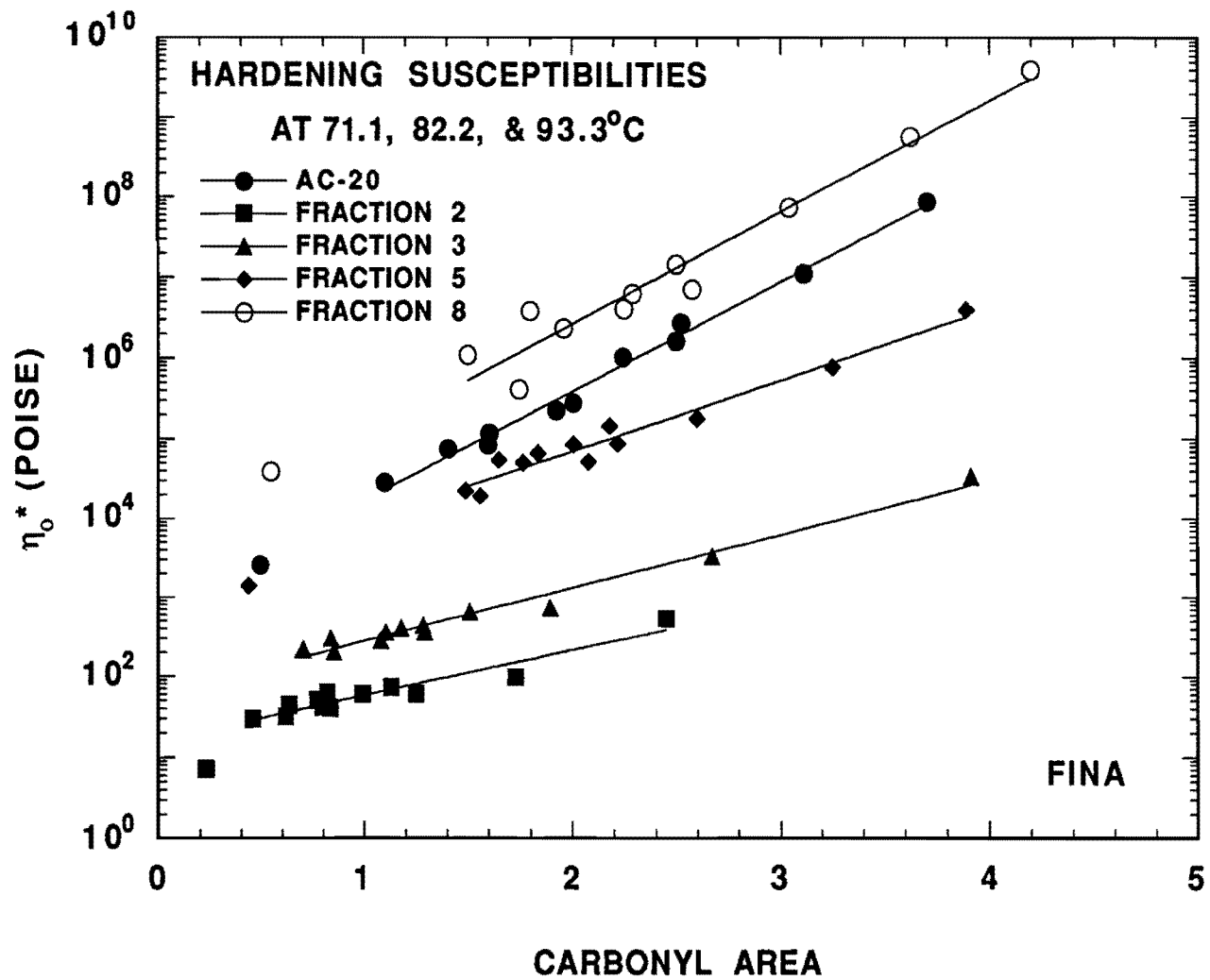
Figure II-5-23.  HS of Fina Asphalt and Selected SC Fractions
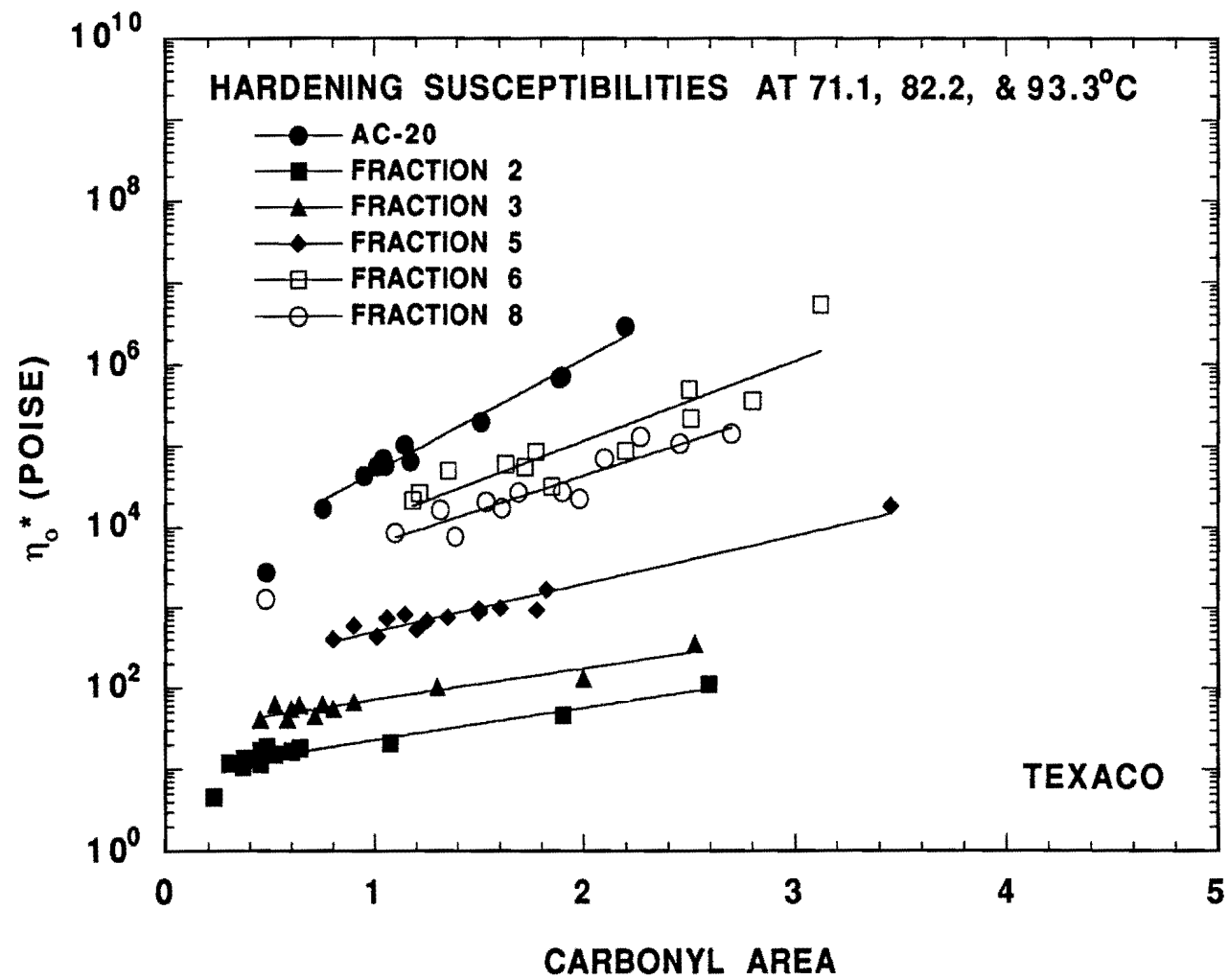
Figure II-5-24. HS of Texaco Asphalt and Selected SC Fractions
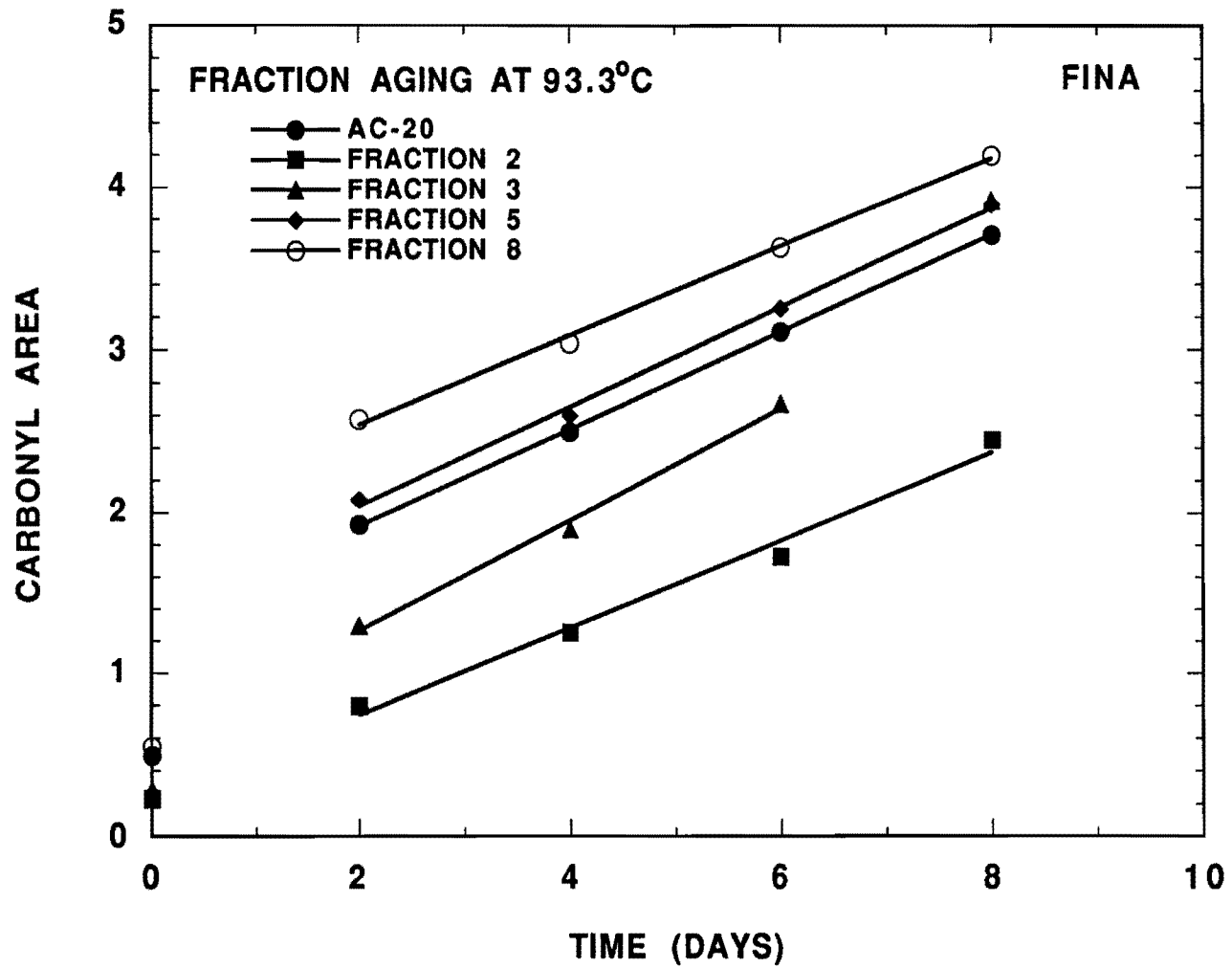
Figure II-5-25. Carbonyl Growth with Time of Fina Asphalt and SC Fraction at 93.3°C
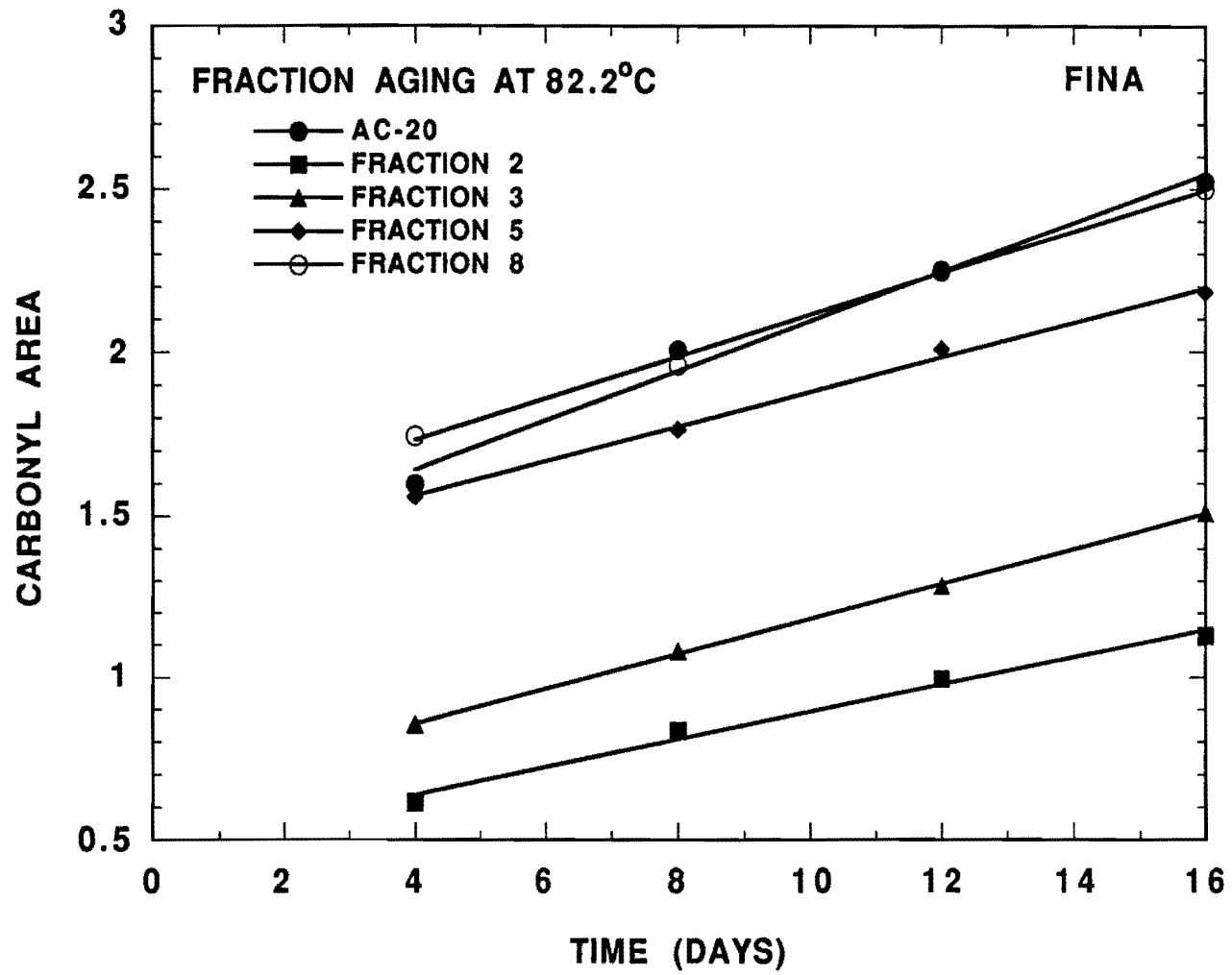
Figure II-5-26. Carbonyl Growth with Time of Fina Asphalt and SC Fraction at 82.2°C
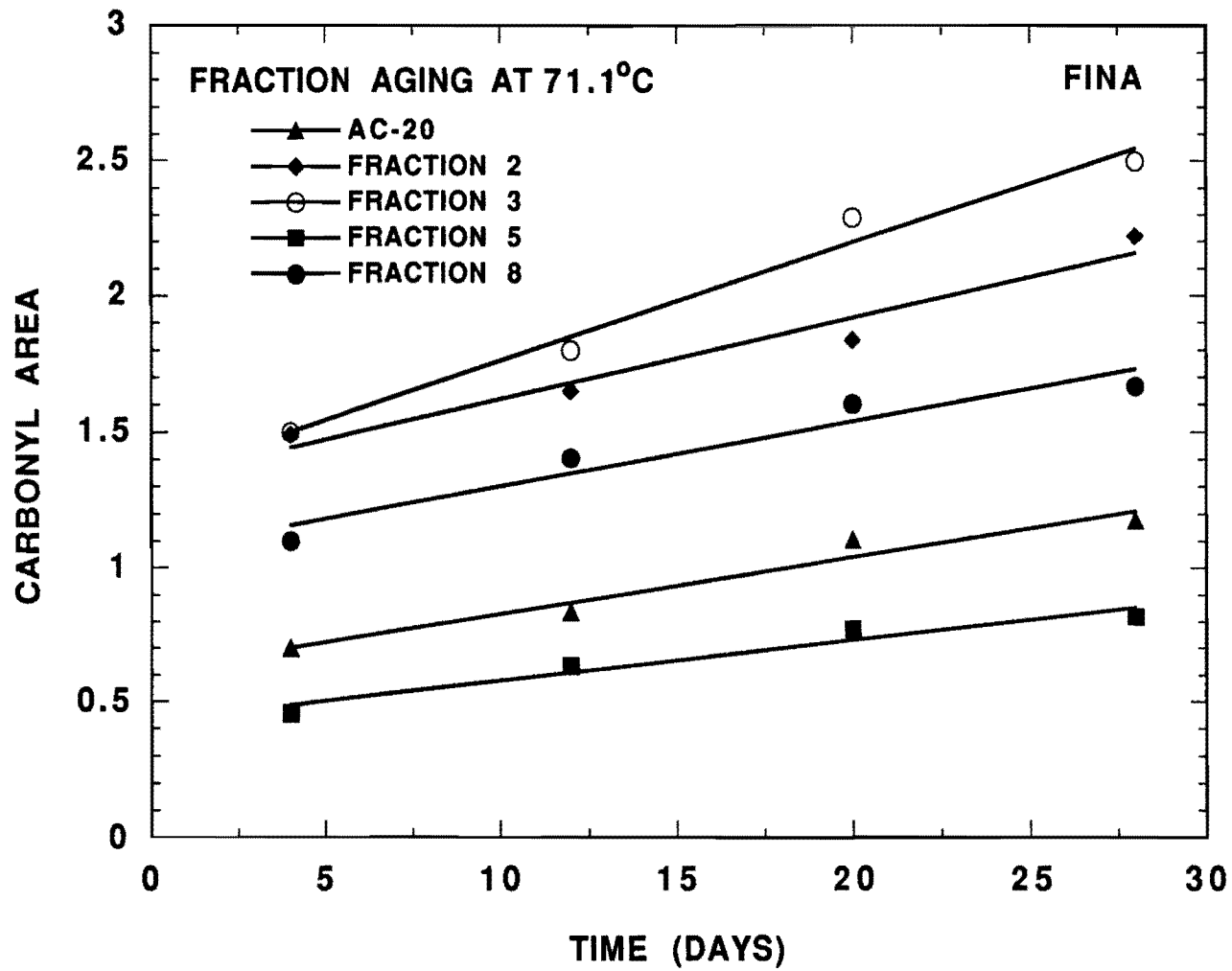
Figure II-5-27.  Carbonyl Growth with Time of Fina Asphalt and SC Fractions at 71.1°C
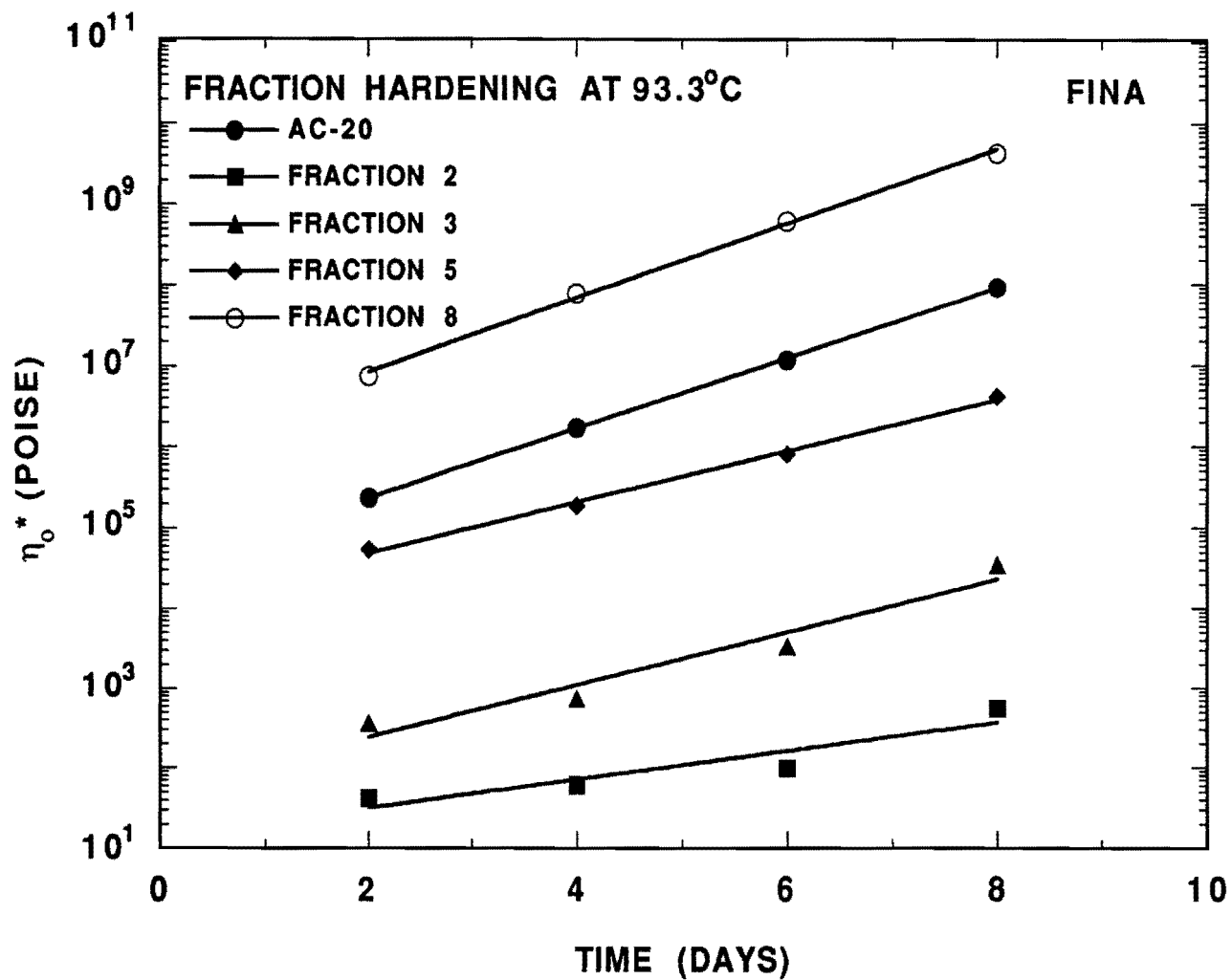
Figure II-5-28. Hardening with Time of Fina Asphalt and SC Fractions at 93.3°C
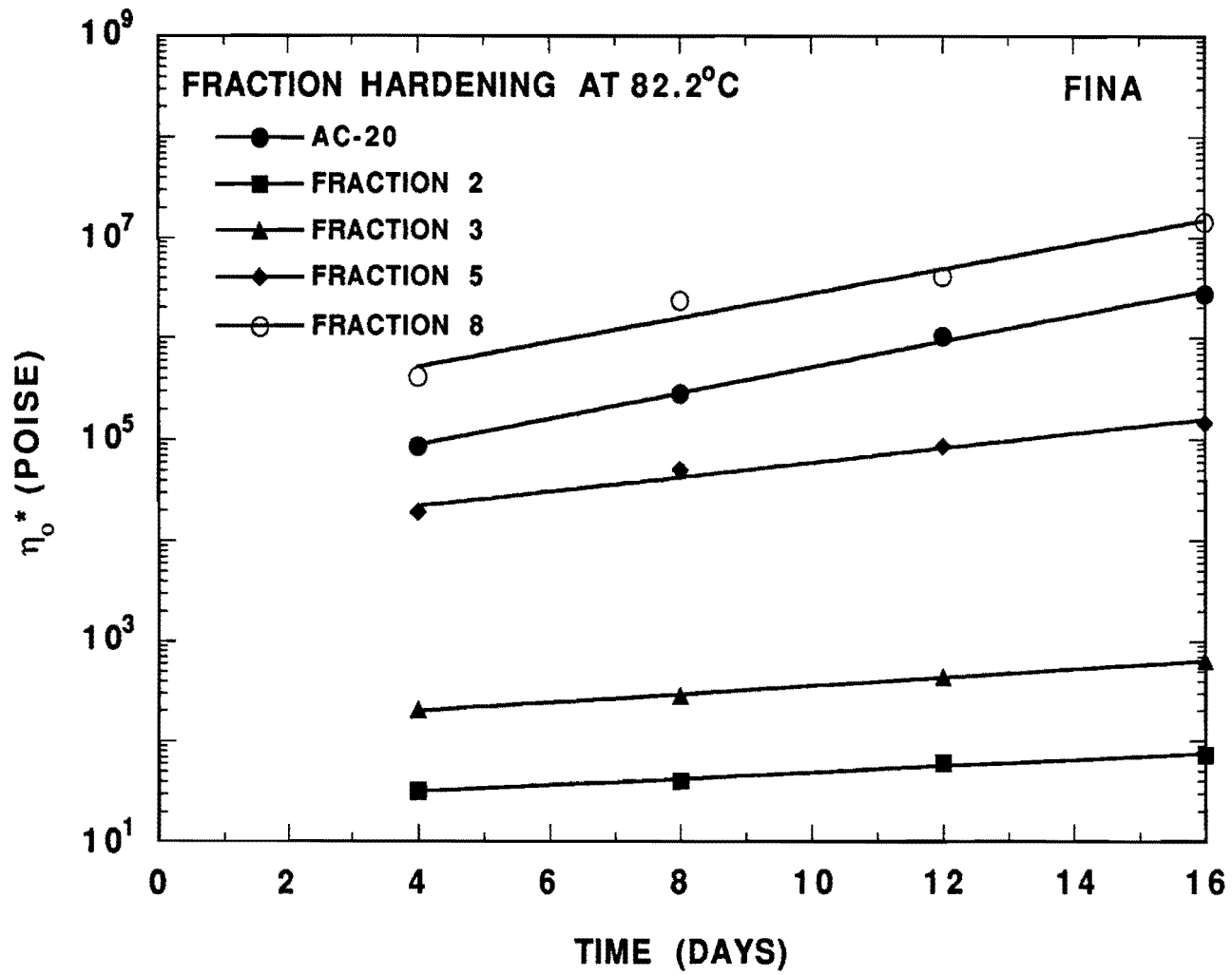
Figure II-5-29. Hardening with Time of Fina Asphalt and SC Fractions at 82.2°C
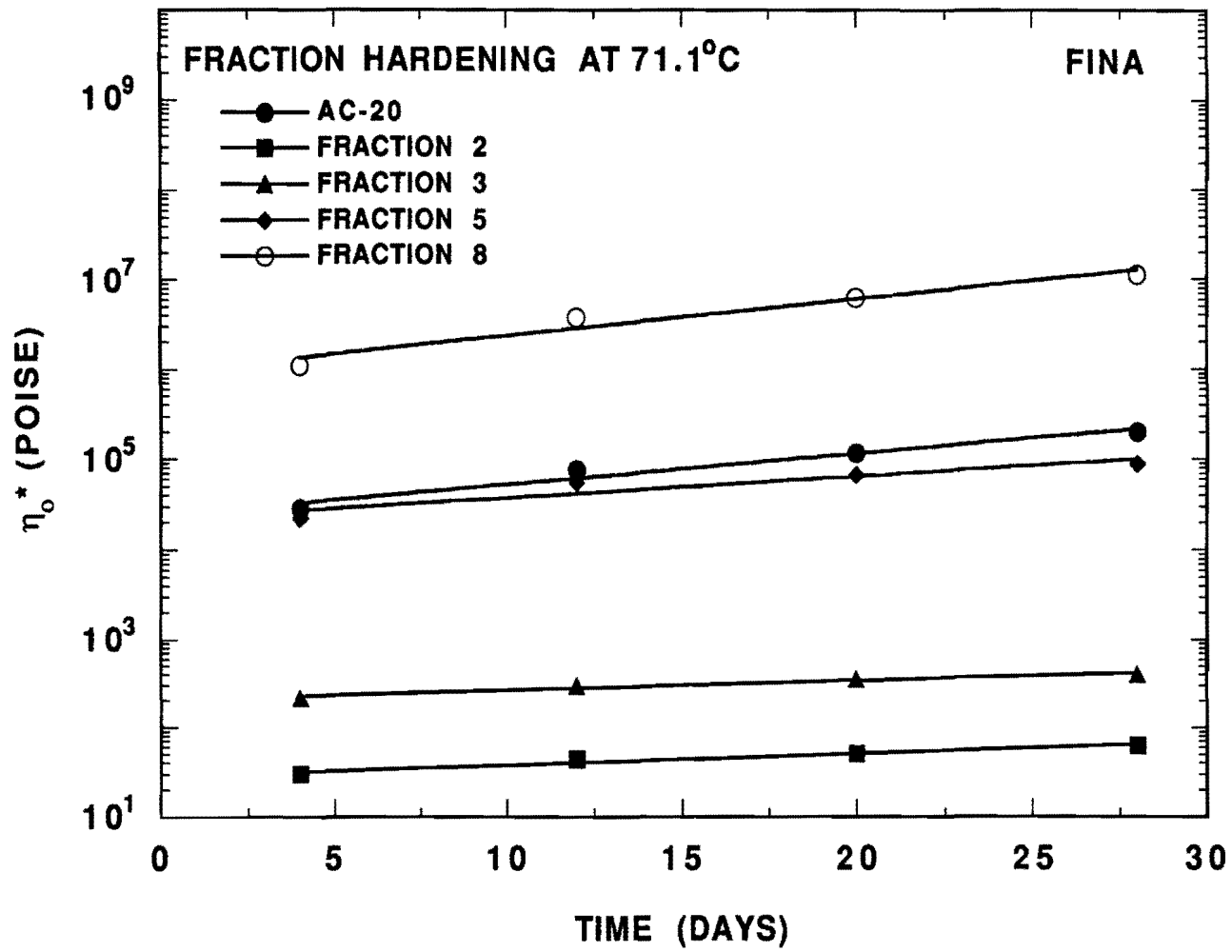
Figure II-5-30. Hardening with Time of Fina Asphalt and SC Fractions at 71.1°C

to the whole asphalt may also influence the initial carbonyl formations. The large fraction carbonyl areas relative to the whole asphalt indicate that although carbonyl formation may predict hardening, it is not necessarily the cause.

Figure II-5-31 and II-5-32 display the carbonyl growth and $\eta_o^*$ rates, respectively, at the three aging temperatures for the Coastal asphalt. Using the procedure described by Lau (1991), an activation energy for carbonyl and hardening rates may be calculated by applying an Arrhenius relationship. Figures II-5-33 and II-5-34 show the plot of the log carbonyl and log hardening rates versus $1/T$, as in the Arrhenius equation, for the whole asphalts.

Although the Arrhenius plots for the whole asphalt produce straight lines, similar plots for many of the aged SC fractions are not as linear. The 93.3°C (200°F) aging data had to be repeated for some Texaco samples due to initially unrealistic results. The reacquired data seemed more reasonable but cast doubt on the reliability of the rest of the 93.3°C (200°F) data. Figure II-5-35 illustrates that the aging at 93.3°C (200°F) appears too severe for some of the Fina fractions. Omitting the data acquired at 93.3°C (200°F) leaves only two points with which to calculate the Arrhenius constants. Therefore, the values obtained from this method should be considered only qualitative.

**Chemical and Physical Property Correlations**

The production of improved asphalts requires an understanding of the influence of chemical composition on the rheological behavior. This section gives the results of the relationships found between various chemical analyses and physical charactersitics. Most correlations found in this work and others, such as HS, are very asphalt dependent. However, some important relationships that are asphalt independent have been discovered that will dramatically enhance the understanding of the influence of chemical composition on physical properties.

*Viscosity*

Initially, simple correlations of $\eta_o^*$ with characteristics of the IR spectra
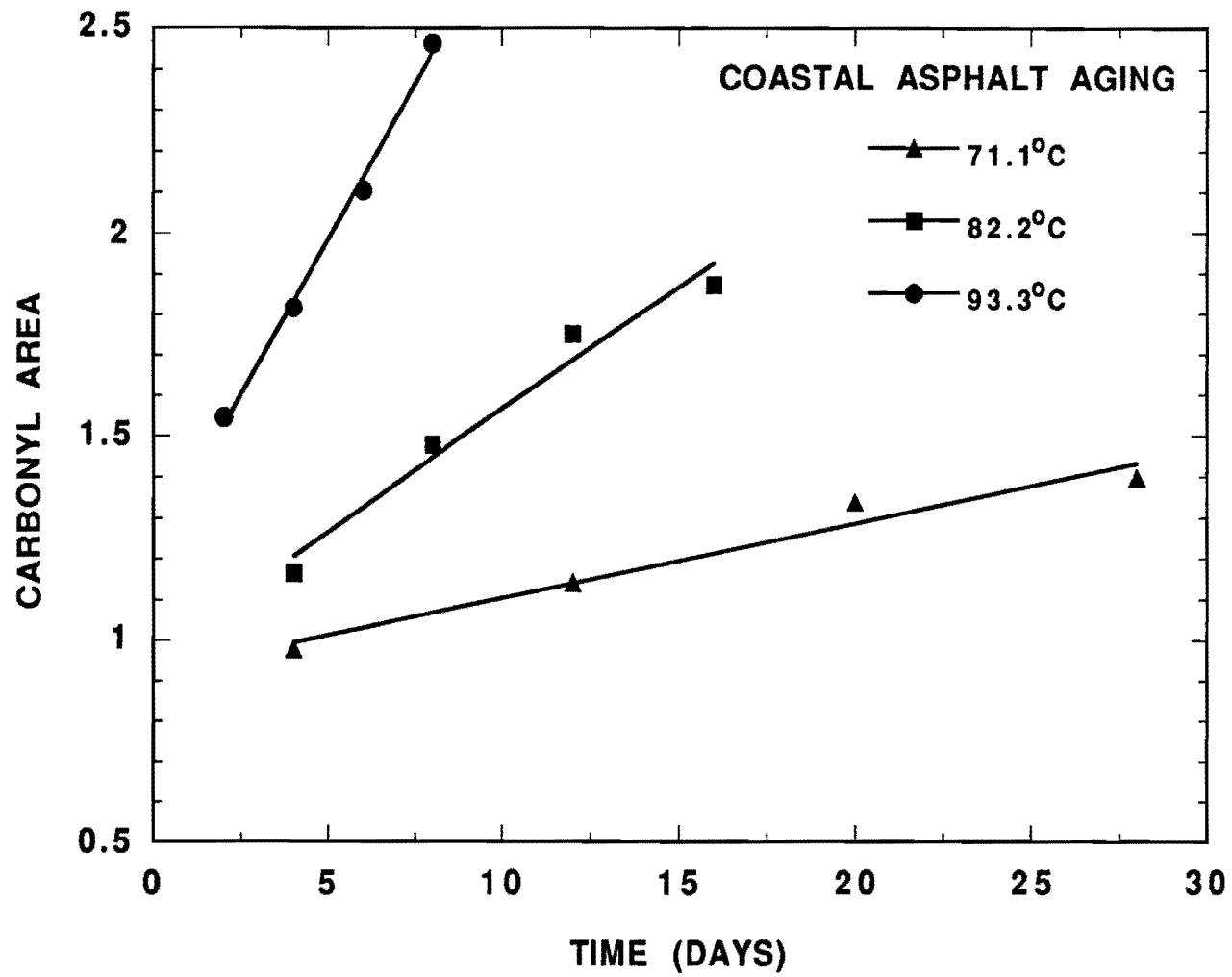
Figure II-5-31. Carbonyl Growth with Time of Coastal Asphalt at 93.3°C, 82.2°C, and 71.1°C
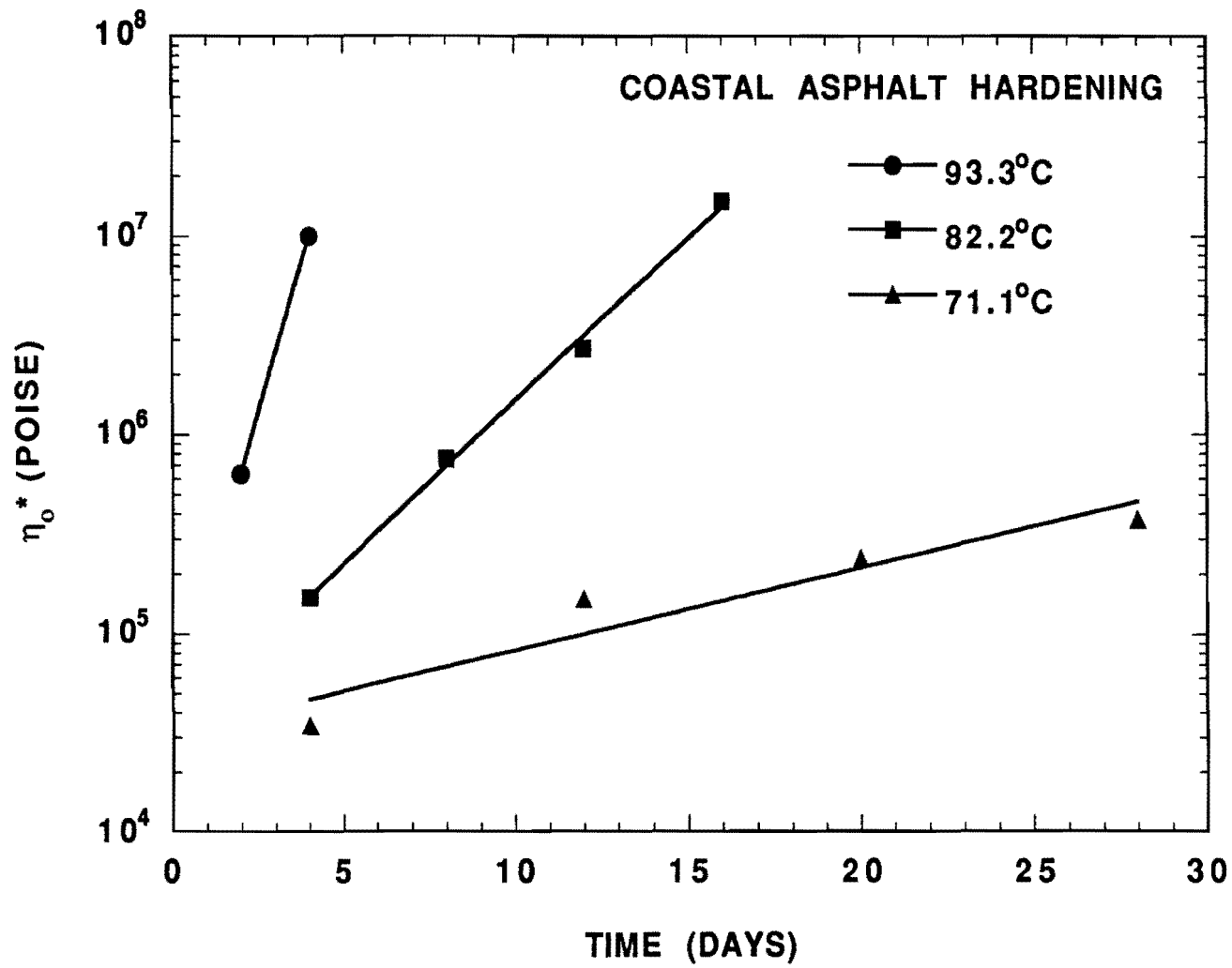
Figure II-5-32. Hardening with Time of Coastal Asphalt at 93.3°C, 82.2°C, and 71.1°C
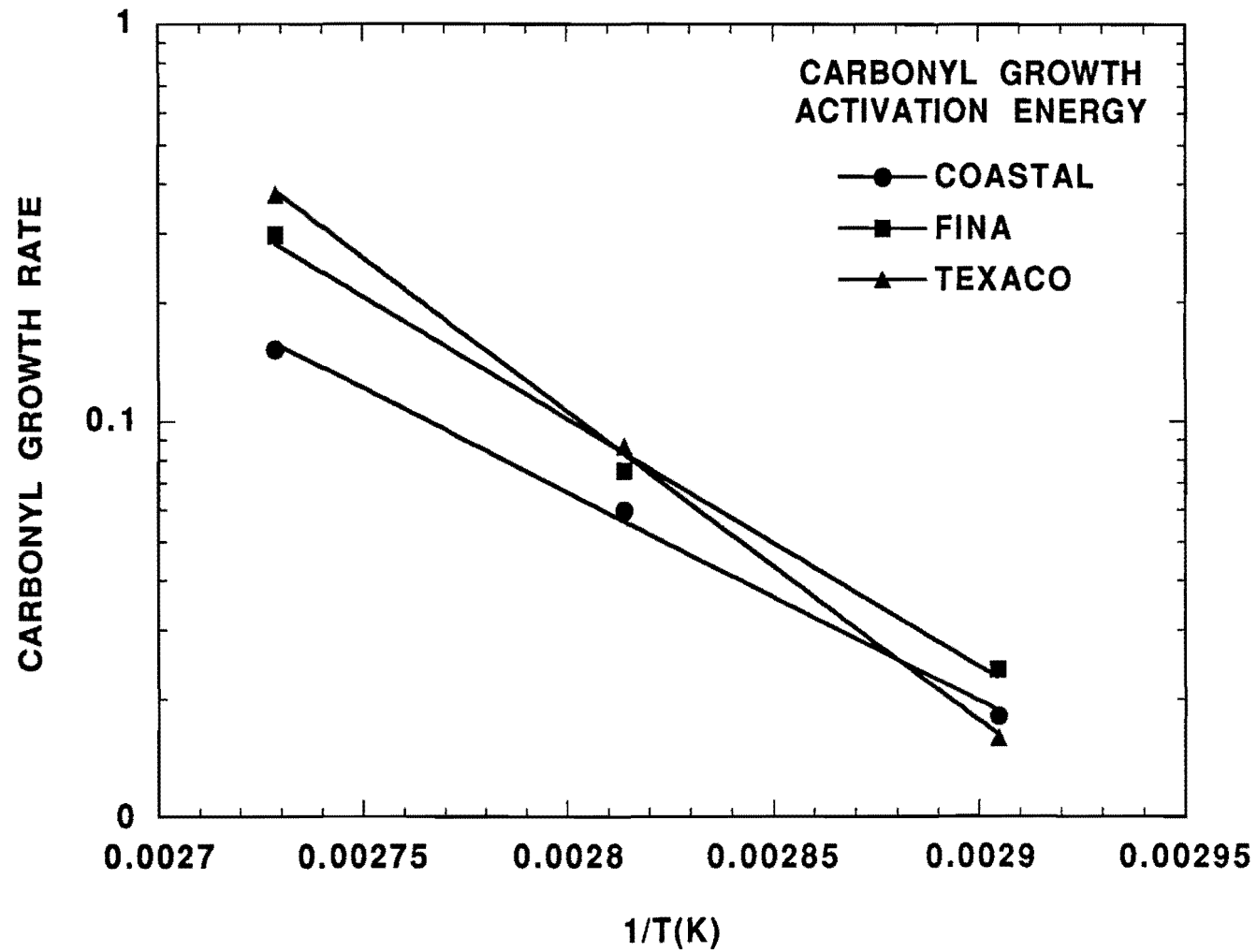
Figure II-5-33. Arrhenius Plots of Carbonyl Growth of Whole Asphalts
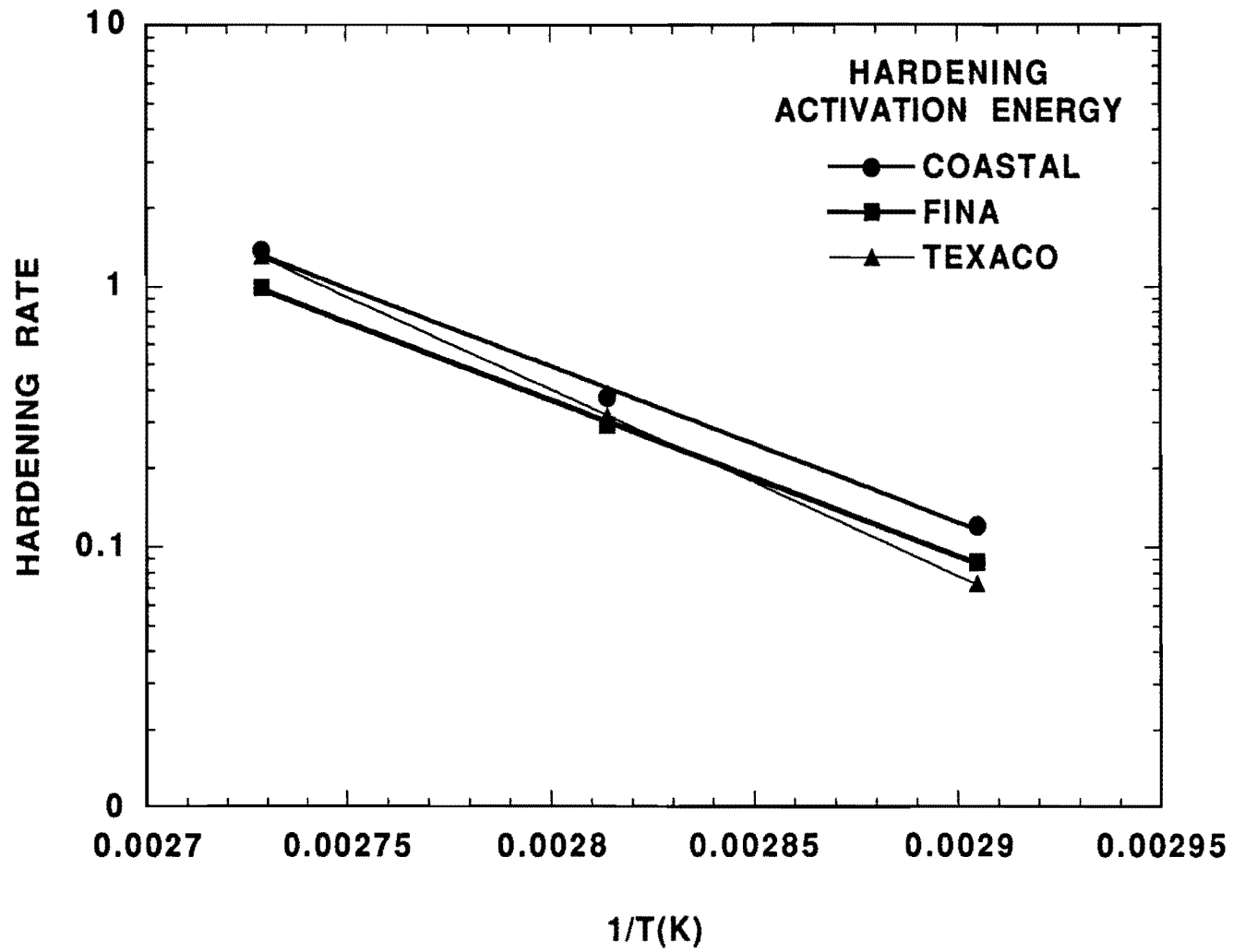
Figure II-5-34. Arrhenius Plots of Hardening of Whole Asphalts
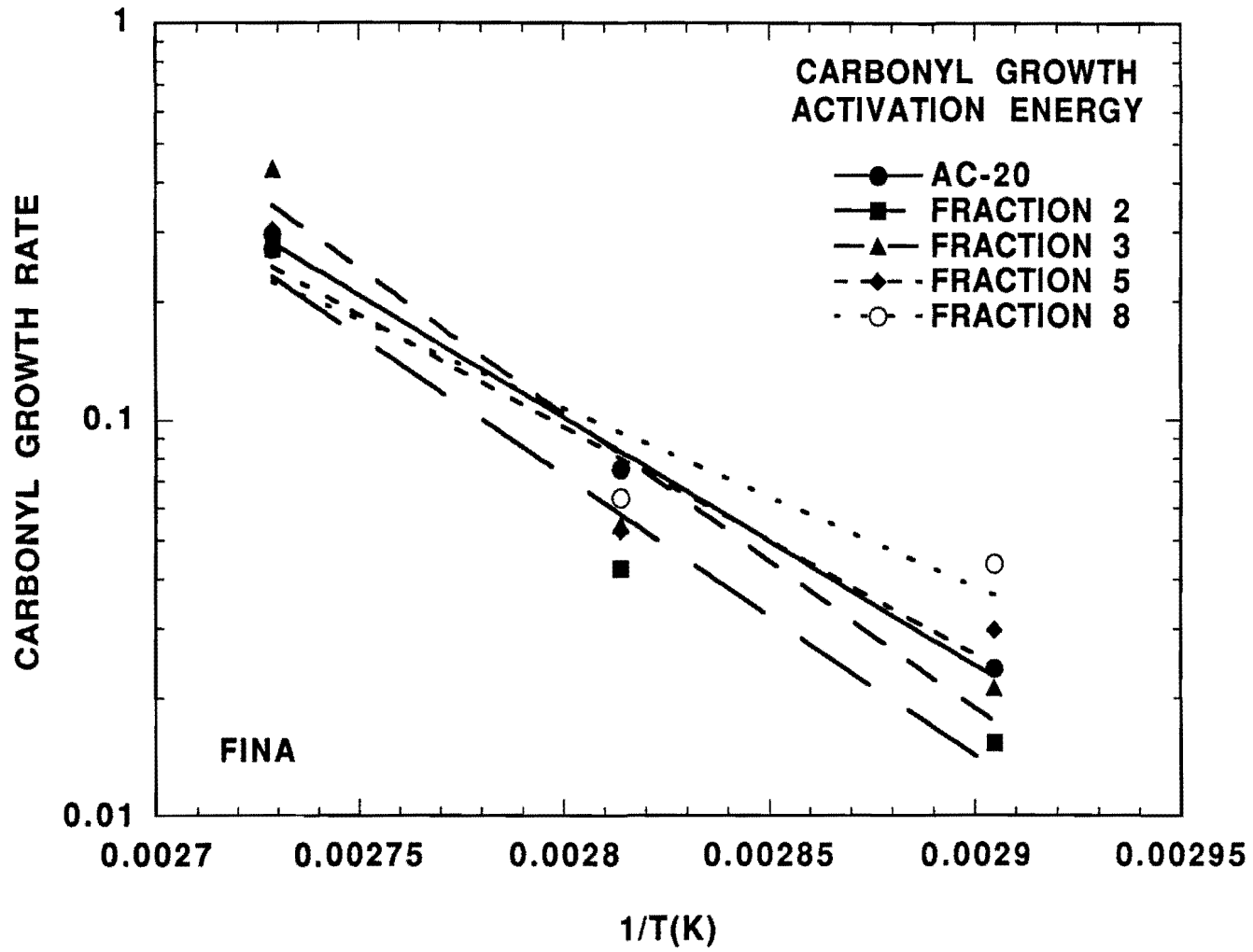
Figure II-5-35. Arrhenius Plots of Carbonyl Growth of Fina Asphalt and SC Fractions

provided interesting results. The relationship of carbonyl formation to hardening has been well documented (Davison et al., 1991; Jemison et al., 1991; Jemison et al., 1992; Jemison et al., in press; Lau et al., in press). However, correlations also exist between chemical functionalities and the viscosity of the unaged asphalts and fractions. Figure II-5-36 illustrates the relationship between $\eta_0^*$ and the IR absorbance at 720 cm$^{-1}$ for the asphalts and SC fractions. Similarly, the relationship at 1310 cm$^{-1}$ is given in Figure II-5-37. These relationships indicate a lack of strong asphalt source dependencies. Figure II-5-38 shows that the 1600 absorbance also indicates $\eta_0^*$ independent of asphalt for the three sources investigated. The IR absorbance at 1600 cm$^{-1}$ indicates the amount of aromatic carbon-carbon double bonds present in the samples. An increase in $\eta_0^*$ with increasing aromaticity is not surprising, but the ability to quantify the relationship for all asphalts and fractions is an important finding that requires further study.

Figure II-5-39 exhibits $\eta_0^*$ plotted versus $M_w$ obtained from the GPC analysis for the unaged asphalts and viscous SC fractions. The $\eta_0^*$ of the light fractions for all asphalts seem to relate well with the $M_w$ data, but the correlation disintegrates above about 1000 poise. The presence of asphaltenes and increased aromaticity among the heavier fractions probably produces molecular associations that complicate the calculation of $M_w$. The calculated molecular weights of asphalt and especially asphaltenes are very dependent on concentration, temperature, and solvent. However, the relationships between $\eta_0^*$ and calculated $M_w$ values may be useful in determining the presence of molecular associations and their effect on the performance of asphalt from different sources.

*Molecular Weight*

A rough relationship exists between asphaltene content and $M_w$ for the asphalts and SC fractions, as shown in Figure II-5-40. The asphalt fractions 7, 9, and 10 data were not reported in this figure due to the presence of insoluble coke in the samples and excessive tailing in the chromatograms. For the fractions containing asphaltenes, a relationship exists that is fairly independent of source. The

130
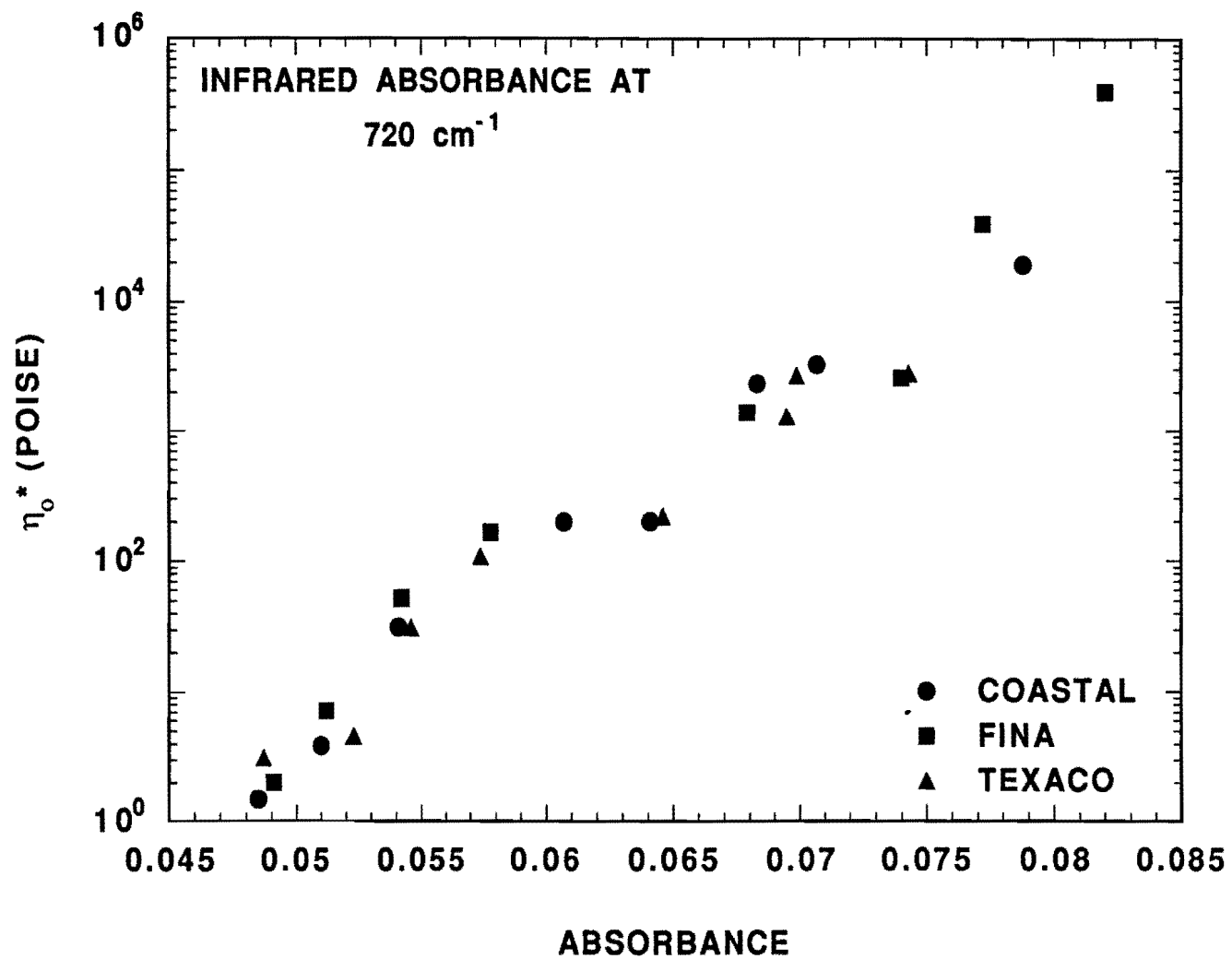
Figure II-5-36. Viscosity Versus Absorbance at 720 cm$^{-1}$ for Asphalts and SC Fractions
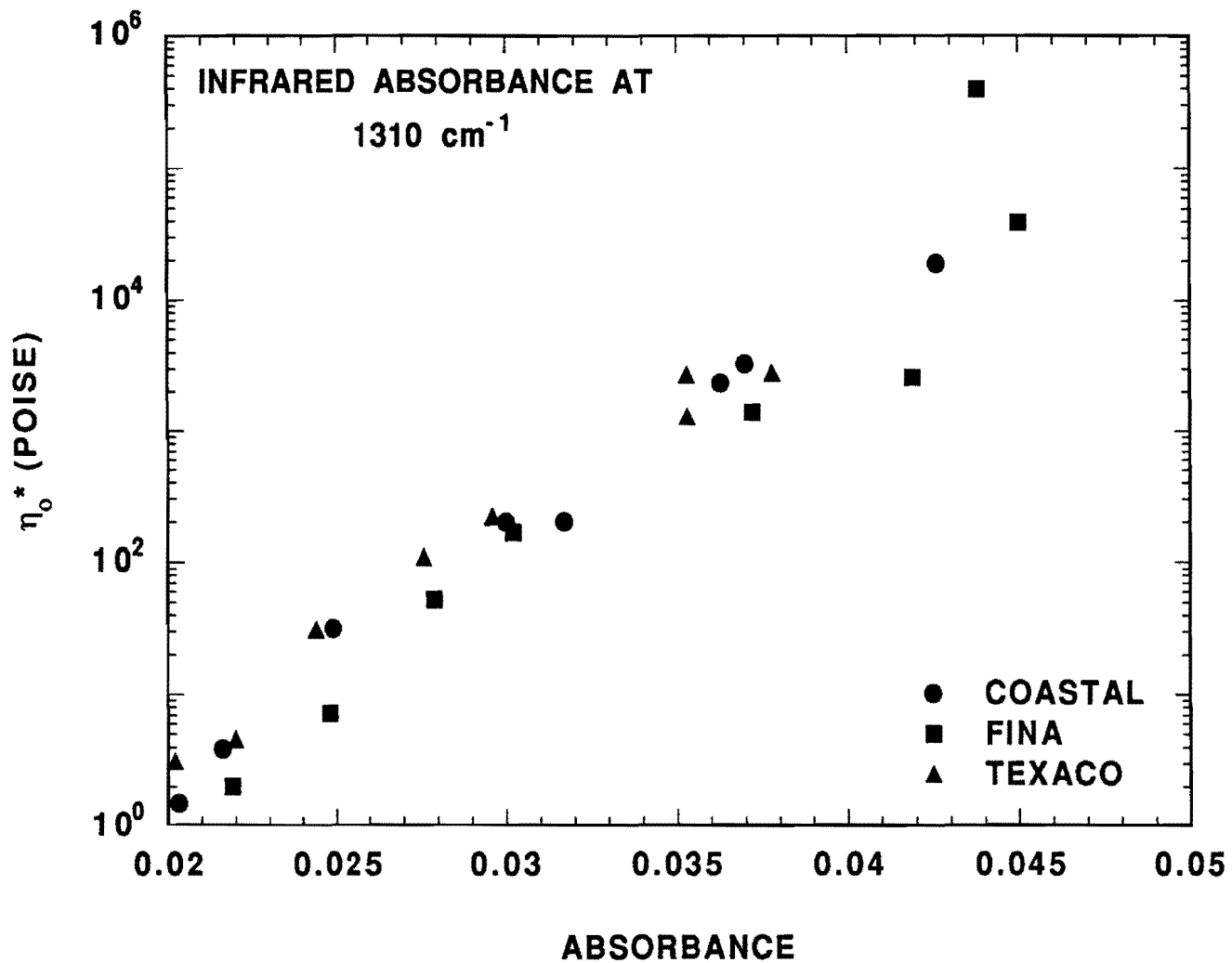
Figure II-5-37. Viscosity Versus Absorbance at 1310 cm$^{-1}$ for Asphalts and SC Fractions
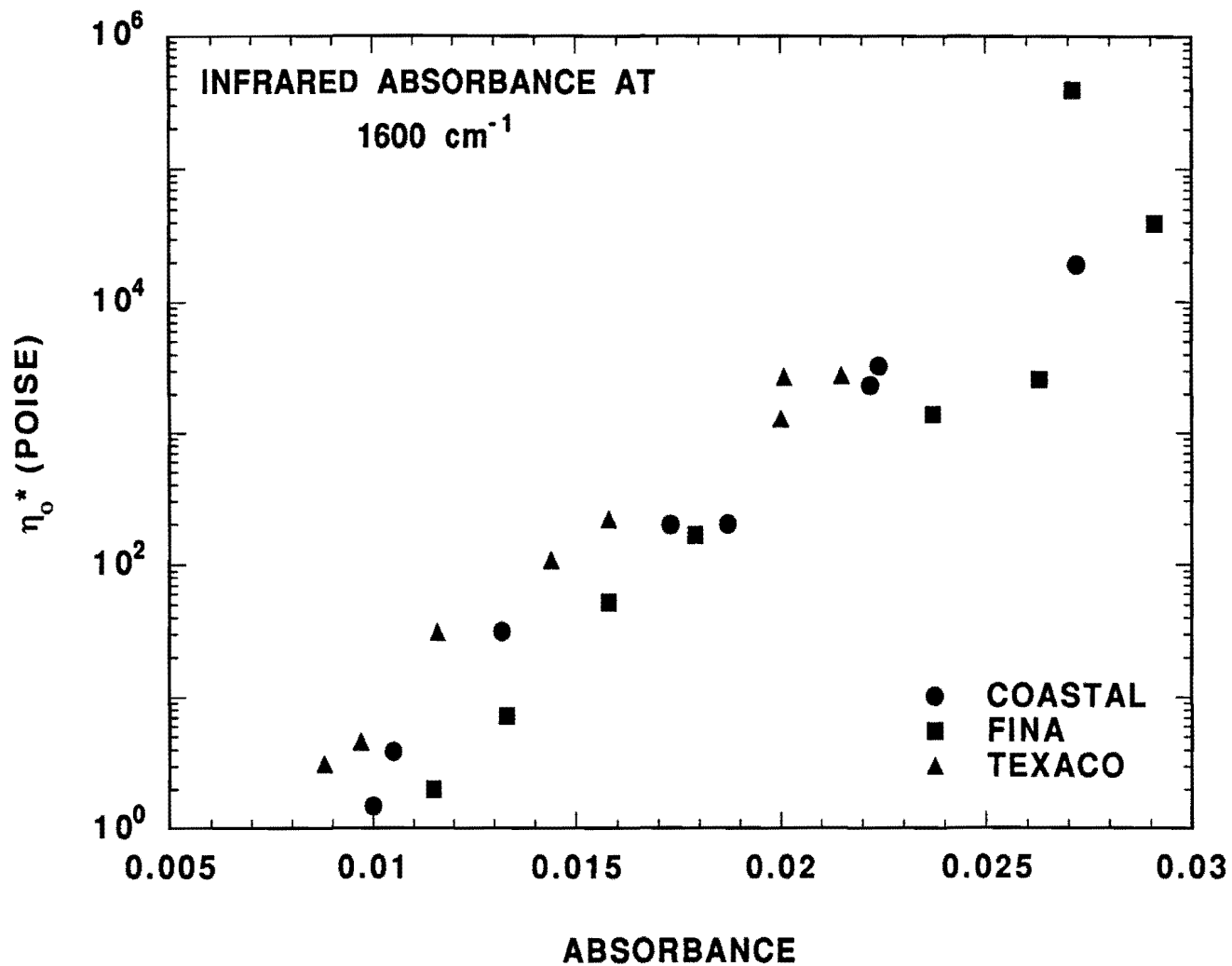
Figure II-5-38. Viscosity Versus Absorbance at 1600 cm$^{-1}$ for Asphalts and SC Fractions
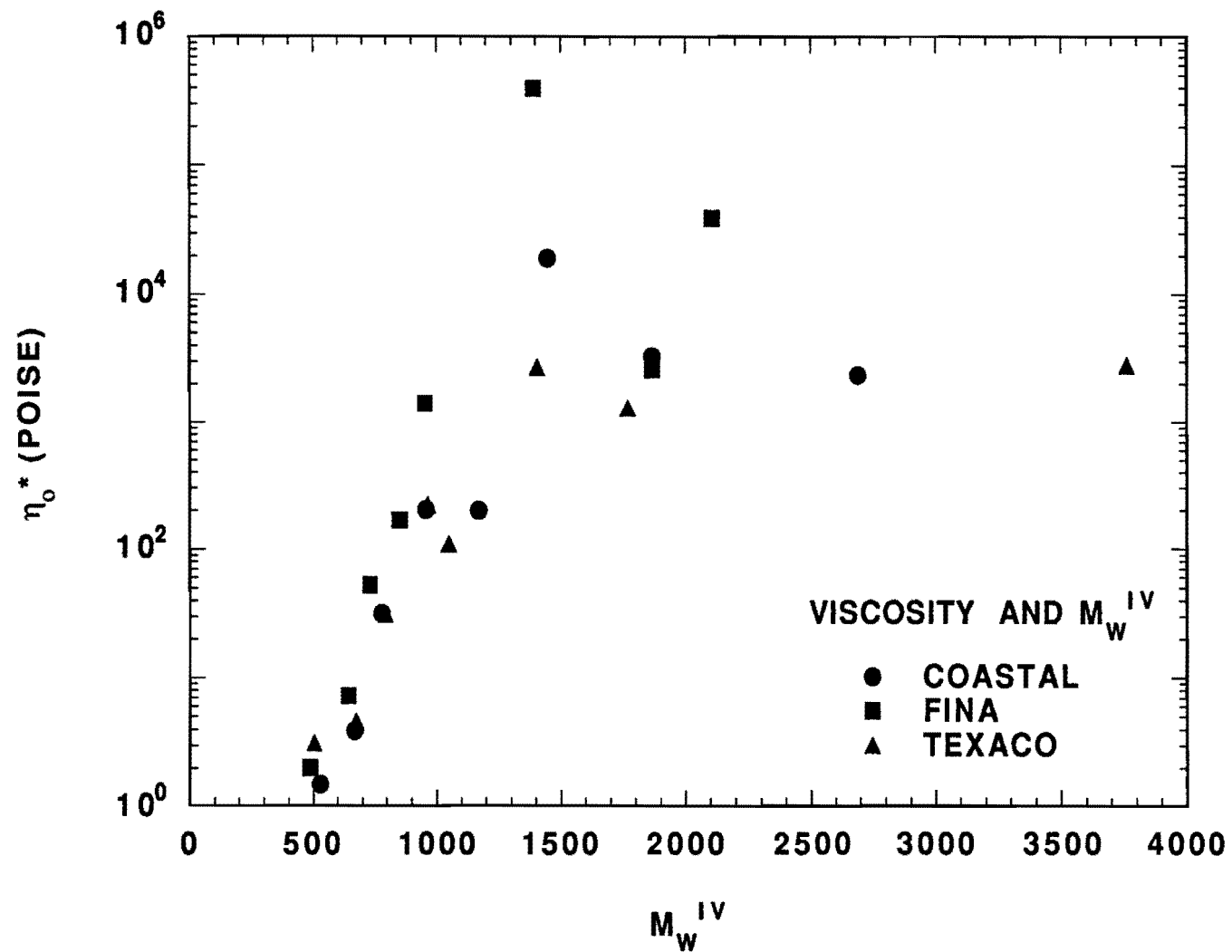
Figure II-5-39. Viscosity Versus $M_W^{IV}$ for Asphalts and SC Fractions
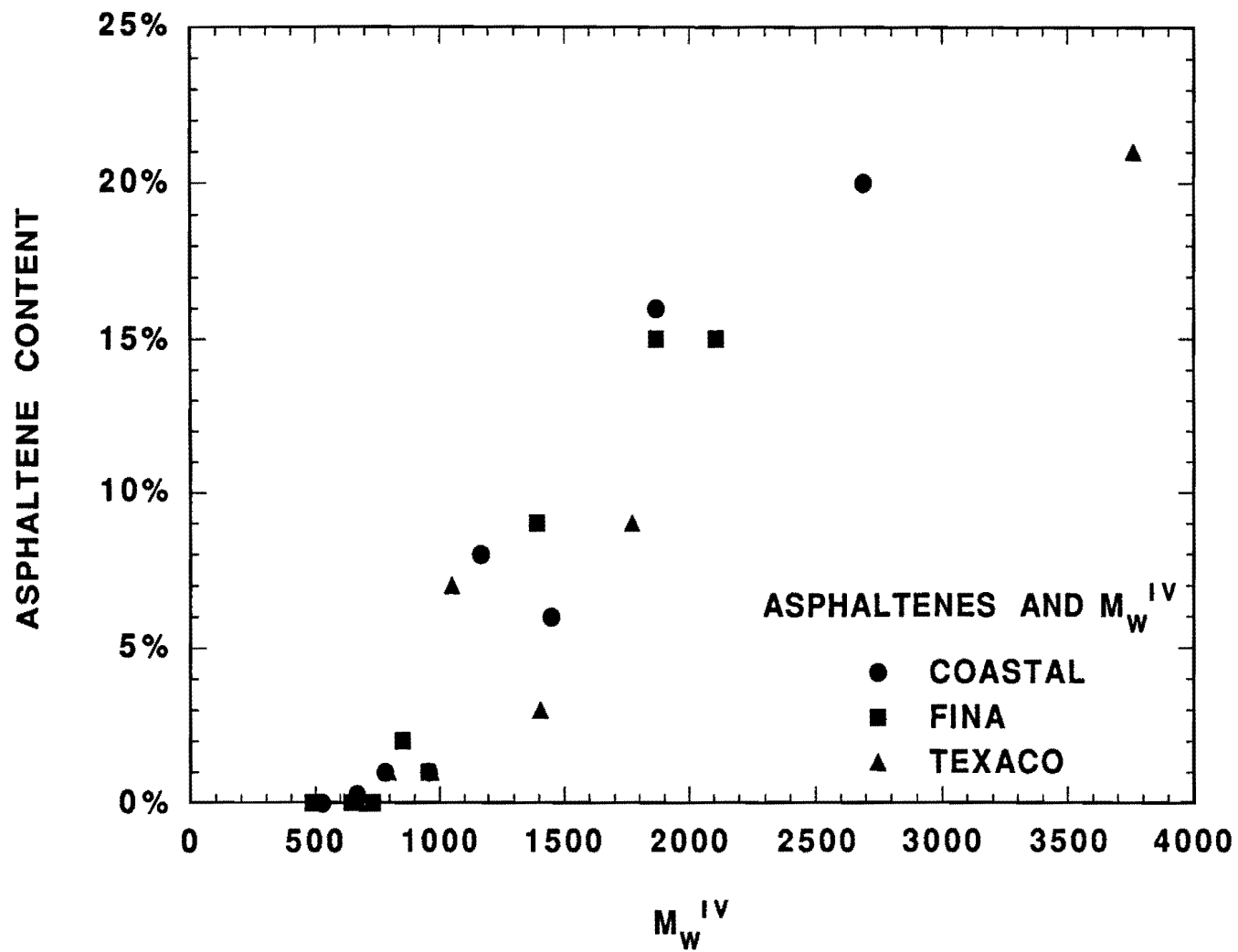
Figure II-5-40. Asphaltenes Versus $M_w^{IV}$ for Asphalts and SC Fractions

relationship between asphaltenes and $M_w{}^{IV}$ indicates that the asphaltenes greatly influence the viscosity of the asphalt in dilute solution and increase the calculated molecular weight. Asphaltenes must have an even greater impact on the viscosity and other rheological properties of neat asphalt.

The correlation of the HS with other more easily obtained properties would be very advantageous since calculation of the HS requires so much time and effort. Figure II-5-41 shows the weak influence of asphaltenes on HS for the asphalts and SC fractions. $M_w$ values provided a better correlation with HS as illustrated in Figure II-5-42, but the relationships are obviously crude source dependent.
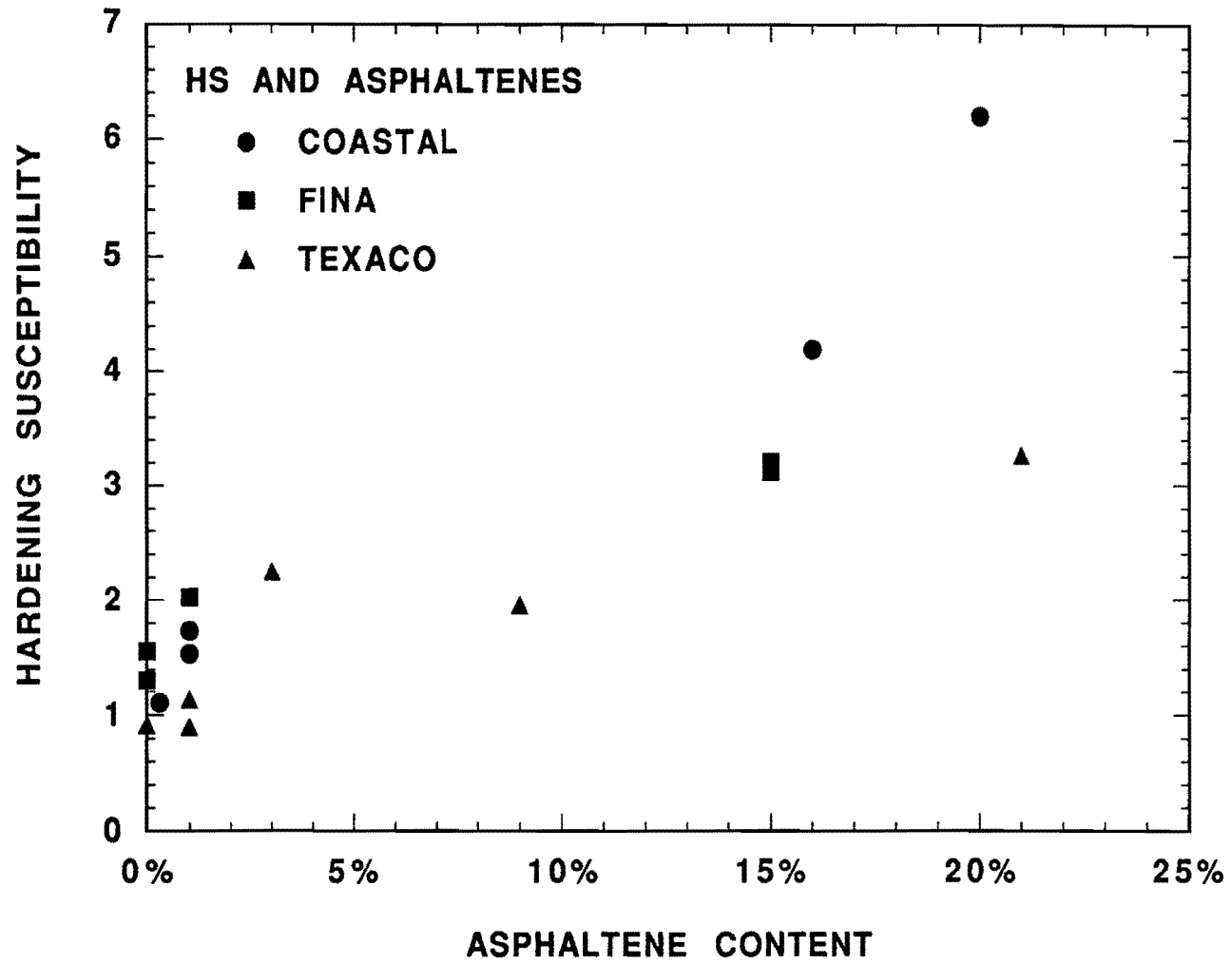
Figure II-5-41. HS Versus Asphaltene Content for Asphalts and Supercritical Fractions
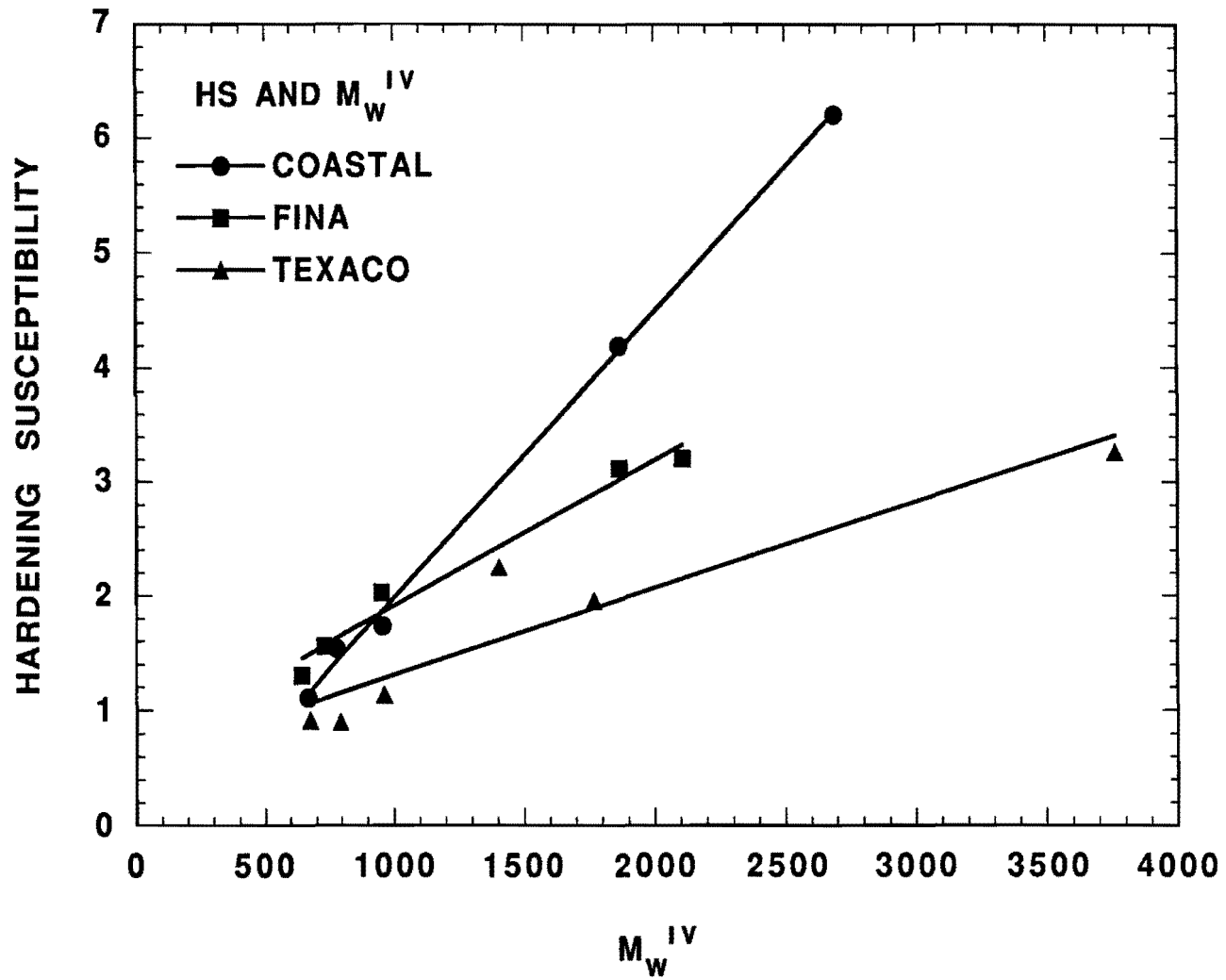
Figure II-5-42. HS Versus Viscosity $M_w$ for Asphalts and Supercritical Fractions

138

# CHAPTER II-6
## ASPHALT BLENDS

The SC fractions obtained from the Coastal, Fina, and Texaco asphalts were used to produce blends suitable as paving asphalts. The blends were composed of adjacent fractions mixed together using weights proportional to their weight distributions in the whole asphalt. The intent was to make blends representing a middle asphalt cut capable of being produced by an industrial SC process, such as a ROSE unit. Blending all of the fractions to reconstruct the original asphalt was not attempted due to the mild thermal degradation and metal contamination during processing.

The blending process required the use of solvent in order to insure homogeneity. Fifty grams of each blend were produced by first weighing the appropriate amount of each fraction into a sample tin. The tin is then attached to a recovery apparatus designed by Burr (unpublished), which fits onto a rotary evaporator. About 200-300 mL of toluene or TCE was added to the recovery apparatus which was maintained above the oil bath and rotated for about 30 minutes; thus, all of the fractions dissolved producing a uniform solution. The solvent was then removed using the procedure described by Burr et al. (1990). GPC analysis verified complete solvent removal.

Fractions 1, 9, and 10 were omitted from all blends. Fraction 1 maintained a very low viscosity, but would not flow at room temperature unless stirred; this indicated a large amount of wax in fraction 1. Fraction 10 contained insoluble coke not present in the original asphalt. Fraction 9 had difficulty dissolving during blending probably due to coke and was consequently eliminated from further blends. Table II-6-1 gives the fractional composition of each of the asphalt blends.

The blends were intended to have $\eta_0^*$ values of about 2000 poise. The actual $\eta_0^*$ recorded ranged from 800 to 3400 poise. A great deal of effort was not spent trying to refine these viscosities, because a change of a few percent of a fraction contribution could dramatically effect the blend viscosity. The aging properties are

## Table II-6-1
### Asphalt Blend Compositions

| Blend | Fraction Percentages | | | | | | |
|---|---|---|---|---|---|---|---|
| | 2 | 3 | 4 | 5 | 6 | 7 | 8 |
| Coastal A | - | - | - | - | - | - | 100 |
| Coastal B | - | - | - | 50 | 50 | - | - |
| Coastal C | - | - | - | 73 | 22 | 5 | - |
| Coastal D | - | - | 17 | 56 | 17 | 10 | - |
| Coastal E | 19 | 13 | 4 | 14 | 4 | 17 | 28 |
| Fina A | - | - | - | 100 | - | - | - |
| Fina B | - | - | 40 | 50 | 10 | - | - |
| Fina C | - | 25 | 25 | 36 | 14 | - | - |
| Fina D | 20 | 18 | 18 | 26 | 10 | 8 | - |
| Texaco A | - | - | - | - | 100 | - | - |
| Texaco B | - | - | - | - | - | - | 100 |
| Texaco C | - | - | - | 60 | 30 | 10 | - |
| Texaco D | - | - | 14 | 52 | 19 | 15 | - |
| Texaco E | - | 25 | 9 | 34 | 12 | 20 | - |
| Texaco F | 16 | 12 | 4 | 16 | 6 | 20 | 25 |

negligibly different from a similar blend made to slightly different proportions. The measured $\eta_o^*$ data for the blends are listed in Table II-6-2.

The viscosities of the fractions determined the composition necessary to obtain the desired consistency. The high viscosity Fina fractions limited the amount of heavier fractions possible in the blends. Significant amounts of asphaltenes were required in some Coastal and Texaco blends in order to include some of the low viscosity fractions. However, all of the blends maintain far better compatibilities than the original asphalts.

140

## Table II-6-2
## Asphalt Blend Viscosities

| | 60°C $\eta_0^*$ (poise) | | |
| --- | --- | --- | --- |
| Blend | Coastal | Fina | Texaco |
| A | 3300 | 1390 | 2700 |
| B | 3400 | 1800 | 1290 |
| C | 1800 | 1200 | 1200 |
| D | 2200 | 800 | 1200 |
| E | 1750 | - | 850 |
| F | - | - | 1060 |

### Corbett and Metal Calculations

The Corbett fractions and metal contents of the blends were calculated using the values for the individual fractions included in each blend. Table II-6-3 presents the calculated Corbett fraction and metal data for each blend. The data show that the SC process reduces the amount of saturates and asphaltenes from the whole asphalt in each of the blends. The Coastal and Fina blends show increased amounts of polar aromatics with little change in the naphthene aromatic content, but some Texaco blends have a larger increase in naphthene than polar aromatics.

### GPC Analysis

Comparing the chromatograms of the asphalts with those of the blends confirms the superior compatibility of the blends. Figures II-6-1 through II-6-3 show that the blends contain far less large and small molecular size regions than the original asphalts. The trends in the chromatograms are reflected in the $M_w$ values given in Table II-6-4. The removal of the heaviest asphaltenes greatly reduces the $M_w$ for the blends. The $M_w^{RI}$ values are slightly lower than the $M_w^{IV}$ measurements for the samples with little or no asphaltenes, but the $M_w^{IV}$ values become

141

**Table II-6-3**
**Calculated Corbett Fraction and Metal Data for Asphalt Blends**

| Blend | Corbett Fractions (%) | | | | Metal content (ppm) | | |
|---|---|---|---|---|---|---|---|
| | Sat. | N. A. | P. A. | Aspn. | Fe | Ni | V |
| Coastal | | | | | | | |
| Whole | 12 | 41 | 26 | 20 | 13.8 | 59.3 | 547 |
| A | 7 | 31 | 34 | 16 | 106 | 49.7 | 450 |
| B | 5 | 38 | 50 | 3 | 121 | 33.2 | 346 |
| C | 6 | 40 | 47 | 1 | 101 | 31.6 | 319 |
| D | 6 | 39 | 44 | 0.1 | 134 | 40.9 | 337 |
| E | 8 | 37 | 34 | 14 | 93 | 46.2 | 374 |
| Fina | | | | | | | |
| Whole | 10 | 39 | 34 | 15 | 111 | 40.6 | 182 |
| A | 4 | 38 | 53 | 1 | 52.1 | 24.8 | 145 |
| B | 4 | 39 | 48 | 0.2 | 145 | 29.7 | 133 |
| C | 6 | 40 | 48 | 2 | 113 | 25.5 | 122 |
| D | 8 | 38 | 44 | 6 | 114 | 29 | 132 |
| Texaco | | | | | | | |
| Whole | 13 | 42 | 22 | 21 | 30.8 | 46.1 | 269 |
| A | 5 | 64 | 26 | 3 | 214 | 25.4 | 190 |
| B | 5 | 39 | 41 | 9 | 122 | 20.4 | 136 |
| C | 5 | 55 | 34 | 6 | 165 | 25.3 | 141 |
| D | 5 | 51 | 34 | 8 | 171 | 41.5 | 164 |
| E | 6 | 49 | 33 | 10 | 142 | 40.4 | 176 |
| F | 7 | 44 | 33 | 11 | 124 | 36.5 | 181 |
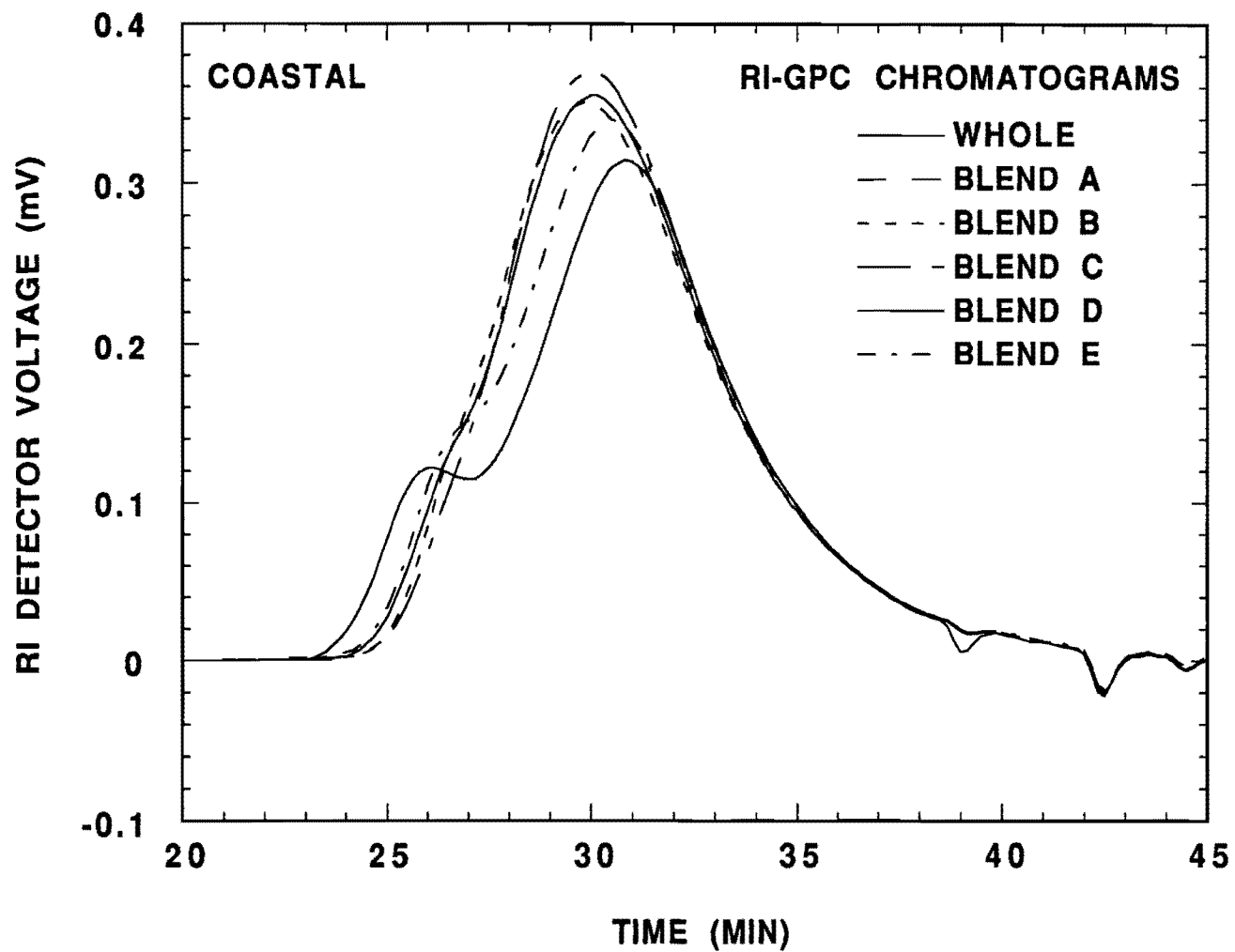
Figure II-6-1. RI-GPC Chromatograms of Coastal Asphalt and Blends
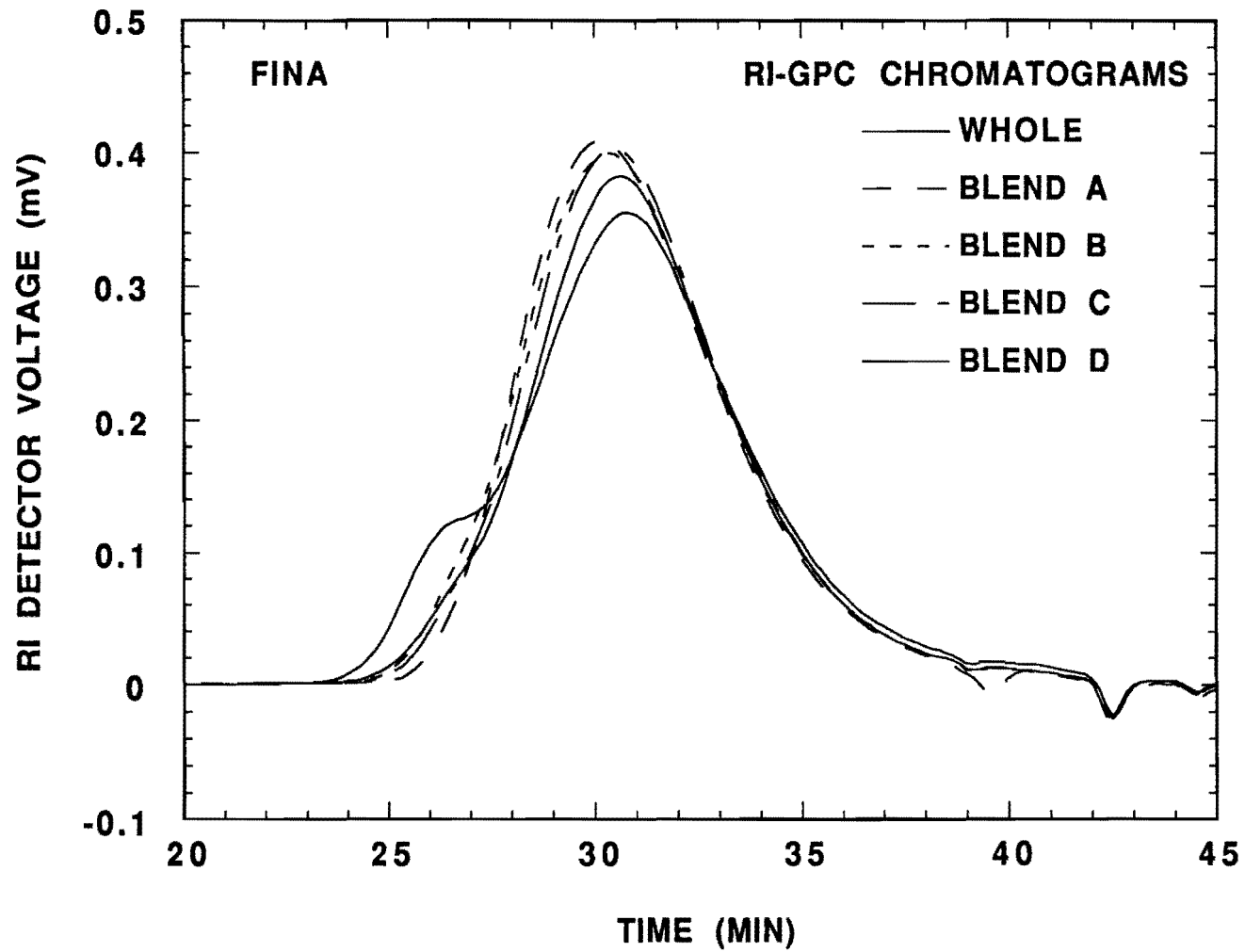
Figure II-6-2. RI-GPC Chromatograms of Fina Asphalt and Blends
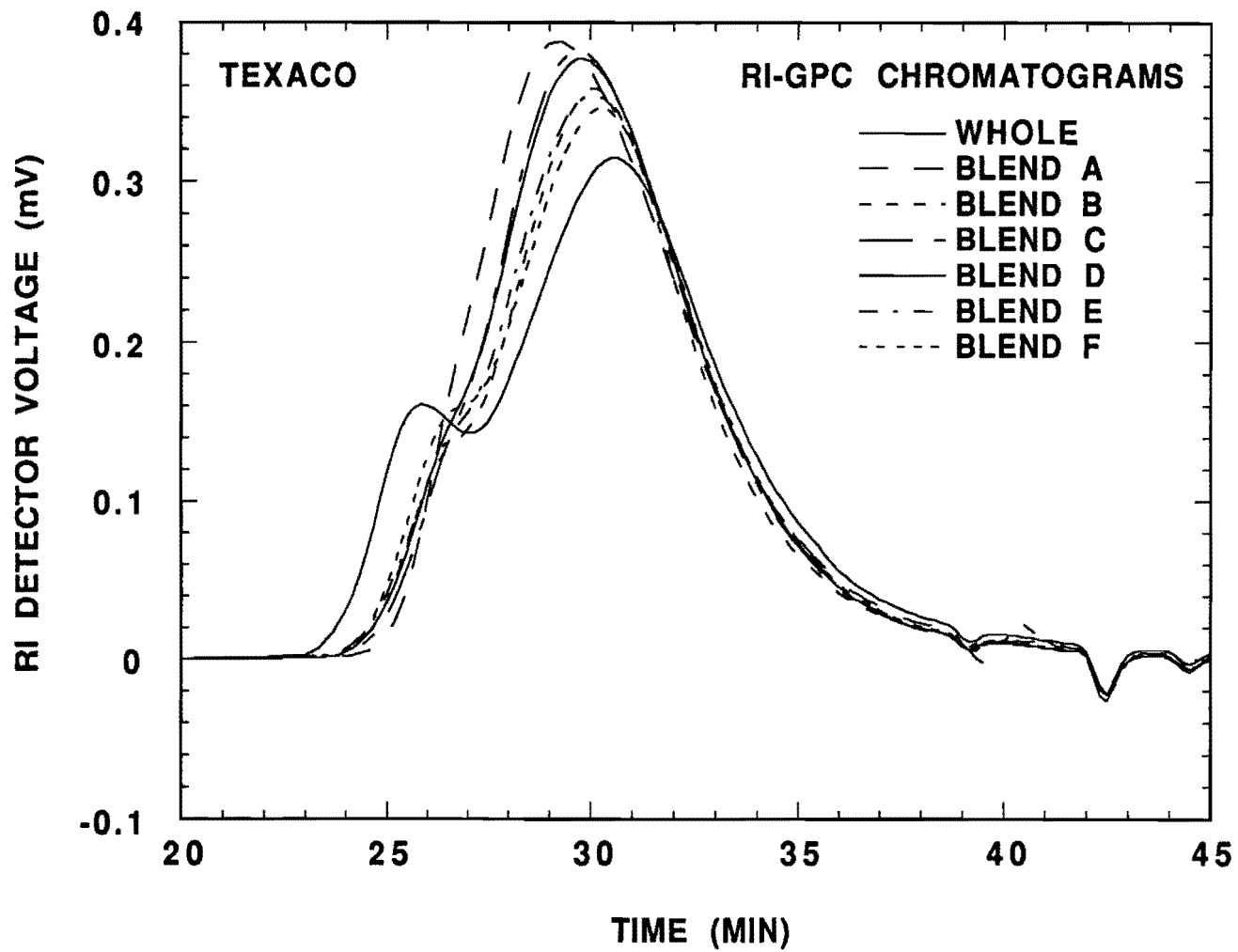
Figure II-6-3. RI-GPC Chromatograms of Texaco Asphalt and Blends

## Table II-6-4
## GPC Molecular Weight Data for Whole Asphalts and Blends

| Blend | Coastal $M_w^{RI}$ | Coastal $M_w^{IV}$ | Fina $M_w^{RI}$ | Fina $M_w^{IV}$ | Texaco $M_w^{RI}$ | Texaco $M_w^{IV}$ |
|---|---|---|---|---|---|---|
| Whole | 1740 | 2690 | 1388 | 1867 | 2212 | 3762 |
| A | 1453 | 1867 | 993 | 954 | 1373 | 1406 |
| B | 1249 | 1224 | 1056 | 1034 | 1465 | 1771 |
| C | 1172 | 1150 | 1000 | 963 | 1407 | 1393 |
| D | 1314 | 1345 | 1041 | 1014 | 1467 | 1535 |
| E | 1378 | 1594 | - | - | 1513 | 1724 |
| F | - | - | - | - | 1543 | 1844 |

considerably larger with higher asphaltene content.

## POV Aging

All of the blends listed in Table II-6-1 were aged in the POV for the same times and at the temperatures as the SC fractions. The data recorded at 93.3°C (200°F) in the POV were not reproducible for most blends. Suspecting minute amounts of TCE contamination, the blends were recovered again using toluene; but the results were equally unpredictable. Therefore, as noted with some of the fractions, the 93.3°C (200°F) data can not be considered reliable and were not included in subsequent calculations for carbonyl growth rates or $\eta_o^*$ rates. Interestingly, even though the high temperature data were not reproducible in terms of kinetics, each aging condition still fell on the HS curve. Apparently, asphalts aged with high pressure oxygen will not deviate from the relationship between $\eta_o^*$ and carbonyl area represented by the HS.

POV aging of the blends allowed the computation of the HS for each blend.

146

Figures II-6-4 through II-6-6 compare the HS curves for the whole asphalt and blends of the Coastal, Fina, and Texaco sources, respectively. As expected from trends in the fraction data, the blends show significantly improved HS values but increased carbonyl formation over the original asphalt. Surprisingly, the most compatible blends (consisting of only one fraction), although better than the tank asphalts, possessed the worst HS values of all the blends. Figure II-6-7 presents the HS curves for the tank asphalts and the blends exhibiting the best HS values from each source. All of the blends are better in this respect than all of the original asphalts. Additionally, the close grouping of the blends relative to the whole asphalts indicates that the refining of asphalts using an SC process has indeed reduced the crude source dependency of this asphalt property.

The measured $\eta_0^*$ data for the blends after aging were considerably lower than the corresponding values of the whole asphalt, but the initial carbonyl areas of the blends were very high. Figure II-6-8 illustrates the dramatic improvement in blend viscosity growth rates over those of the original asphalt. The carbonyl growth rates of these same Fina samples are shown in Figure II-6-9. The large carbonyl areas and low viscosities of the blends proves that the carbonyl formation alone does not cause hardening. The definite relationship between $\eta_0^*$ and carbonyl area of the HS indicates that carbonyl formation relates to viscosity increase for a particular asphalt, but the carbonyl formed may only be a by-product or competing reaction of those that cause hardening.

GPC analyses of the aged asphalts and selected blends at 82.2°C (180°F) show much lower LMS formation and $M_w^{IV}$ increase for the blends relative to the original asphalt. Figure II-6-10 displays the RI-GPC chromatograms of the Texaco asphalt after 0, 4, 8, 12, and 16 days of aging at 82.2°C (180°F). The RI-GPC chromatograms of Texaco blend C aged under identical conditions are shown in Figure II-6-11. The enormous differences in LMS for the samples is reflected in the $M_w^{IV}$ values shown in Table II-6-5.

The irreproducible data obtained at 93.3°C (200°F) allowed the use of only two data points for the calculation of the oxidation and hardening activation energies.

147
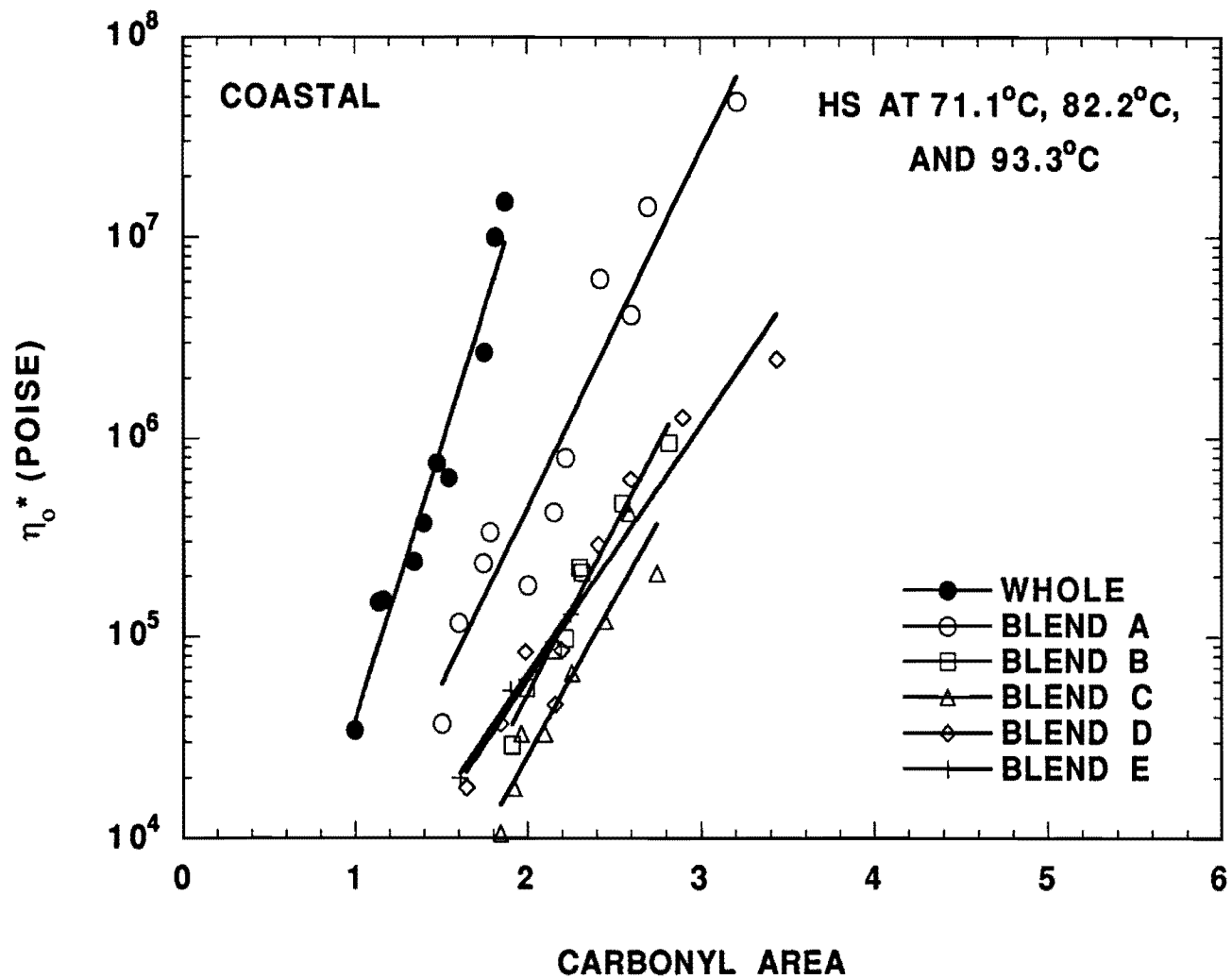
Figure II-6-4. HS of Coastal Asphalt and Blends
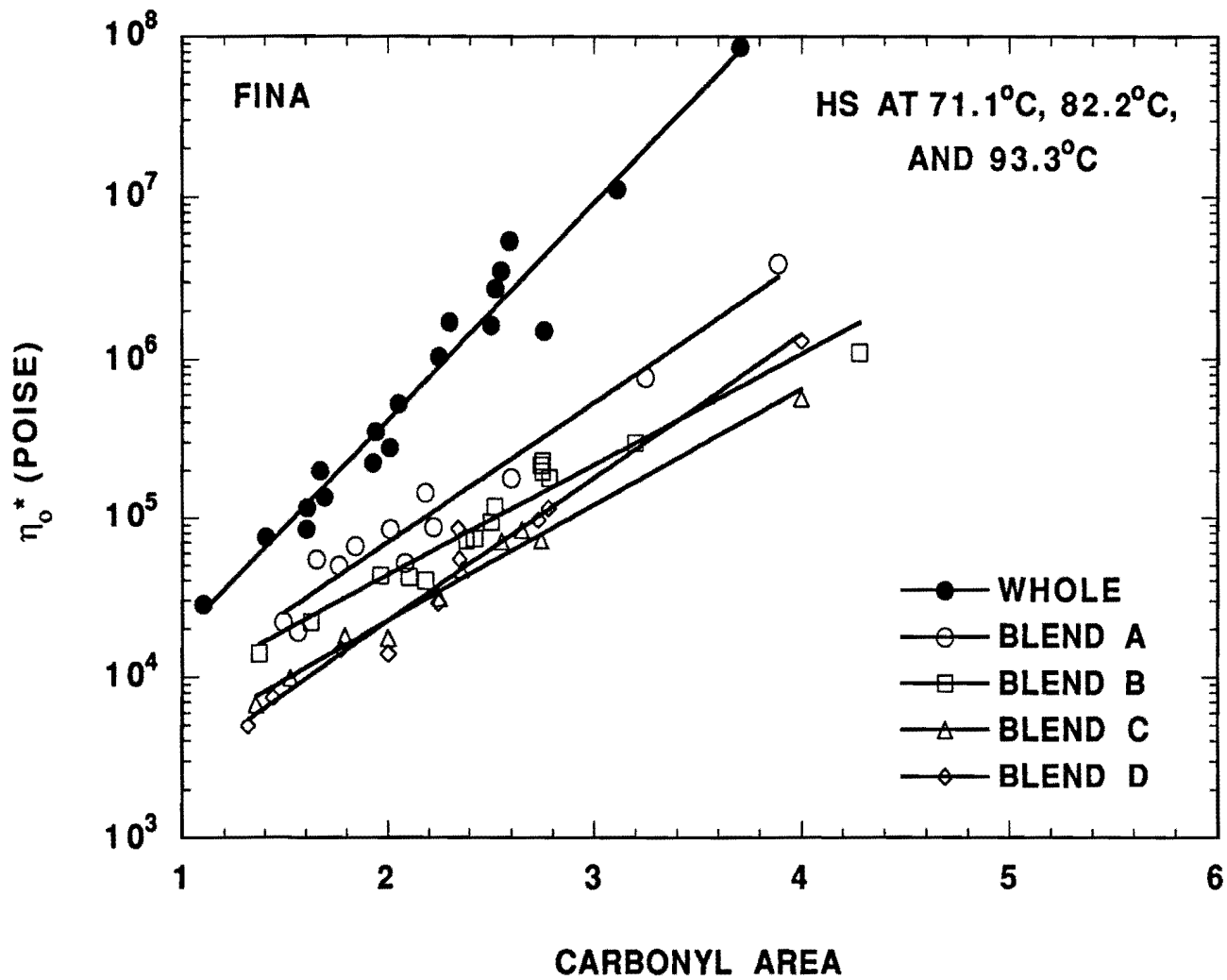
Figure II-6-5. HS of Fina Asphalt and Blends
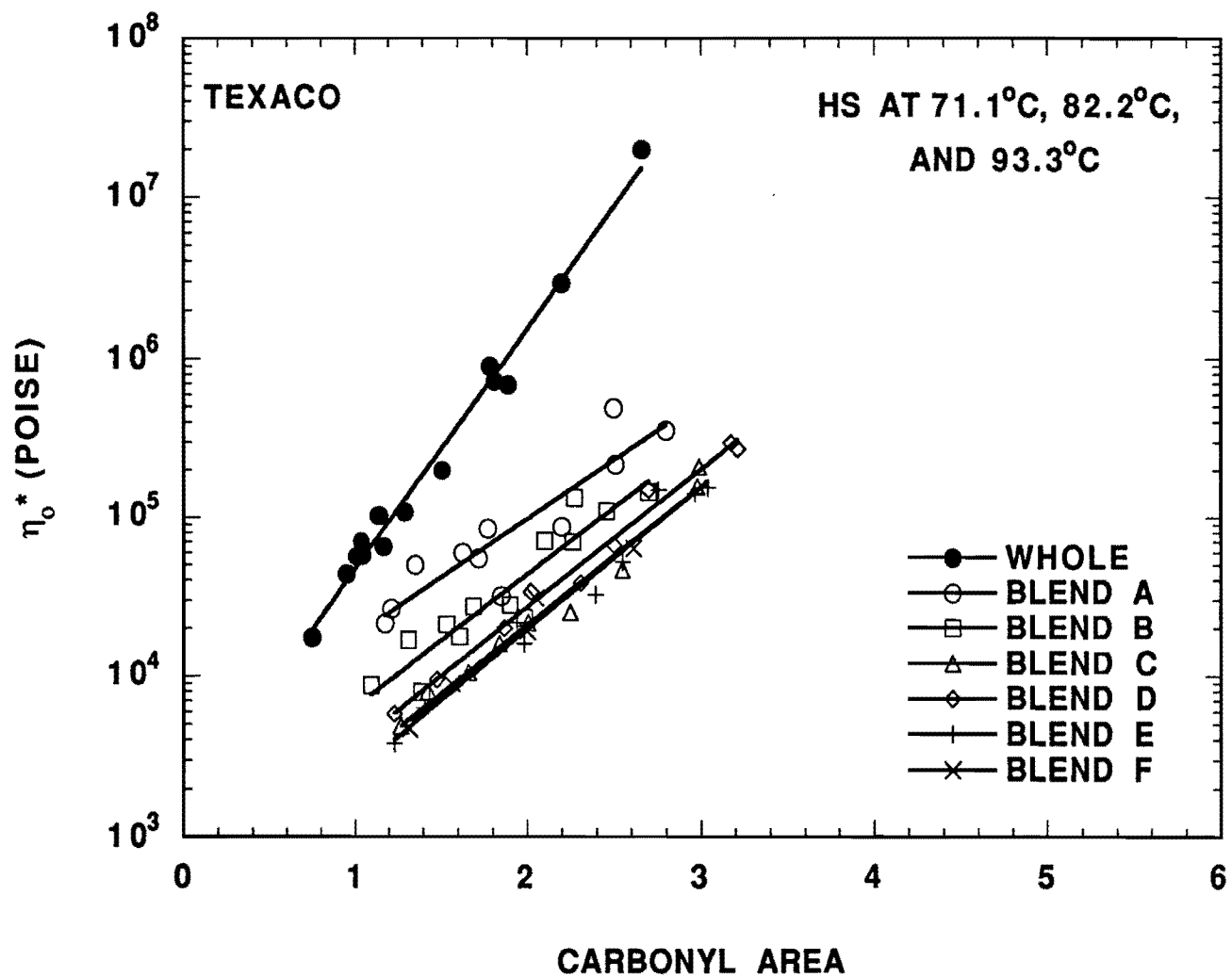
Figure II-6-6.  HS of Texaco Asphalt and Blends
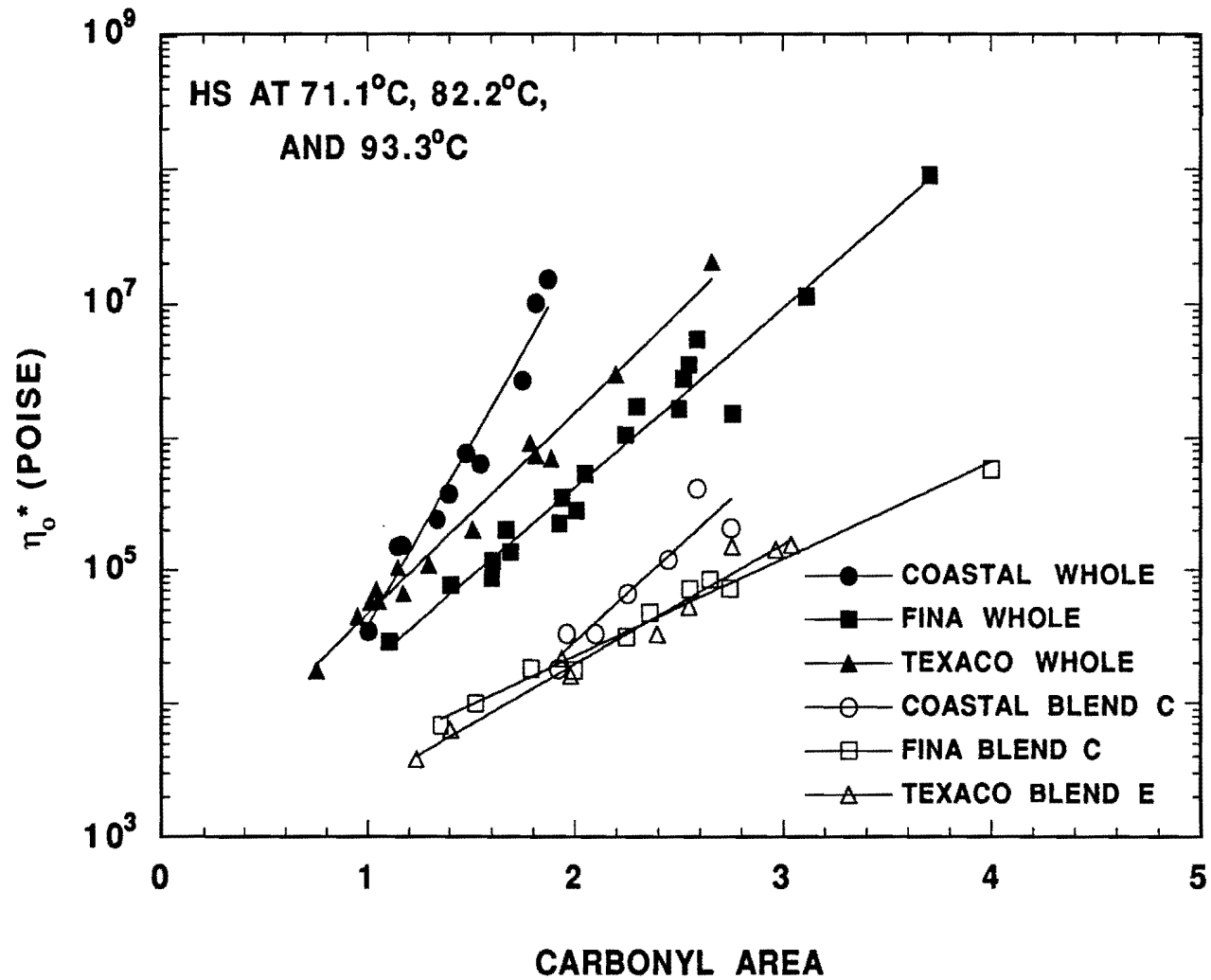
Figure II-6-7. HS of Asphalts and Most Improved Blends
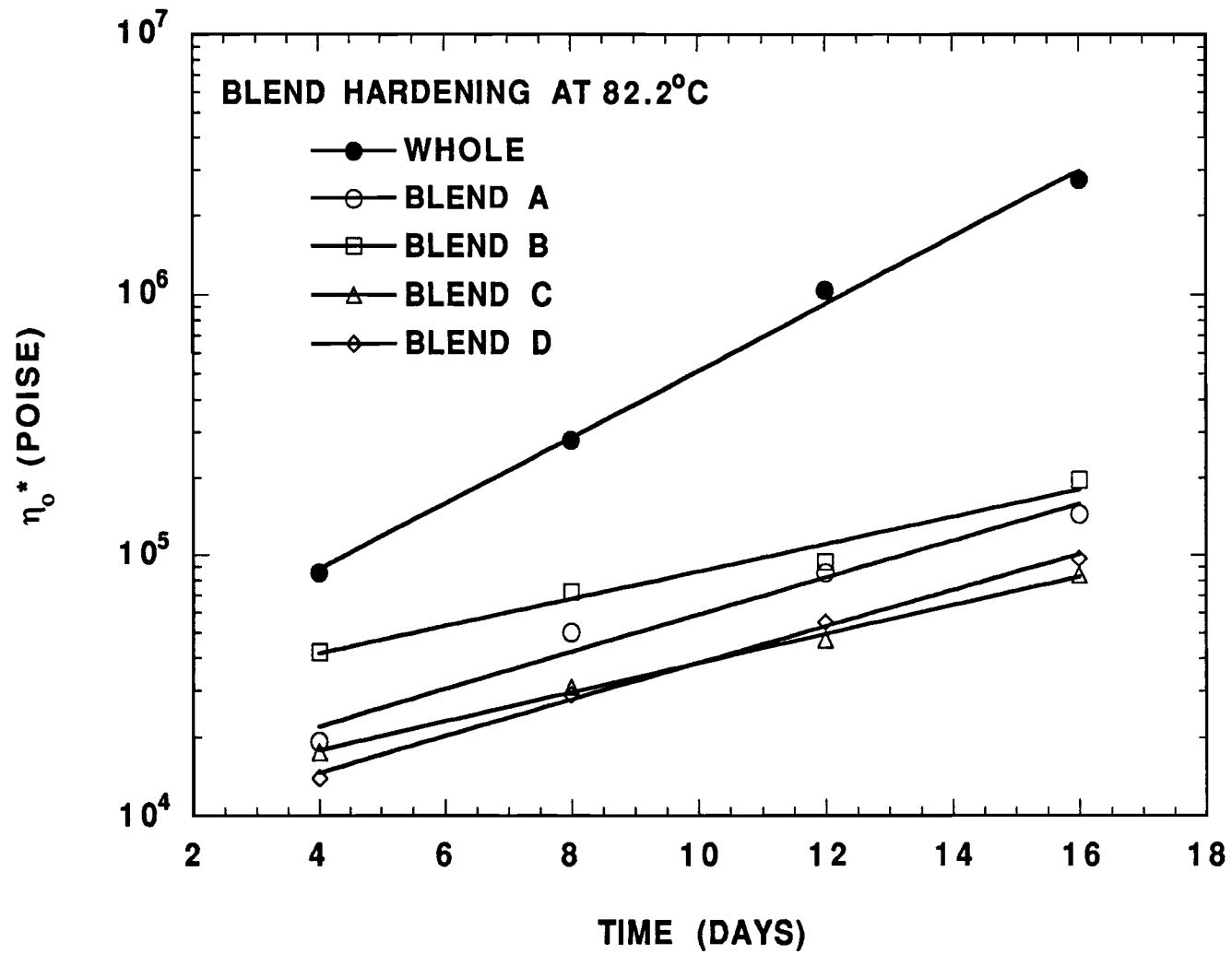
Figure II-6-8. Hardening Rates at 82.2°C for Fina Asphalt and Blends
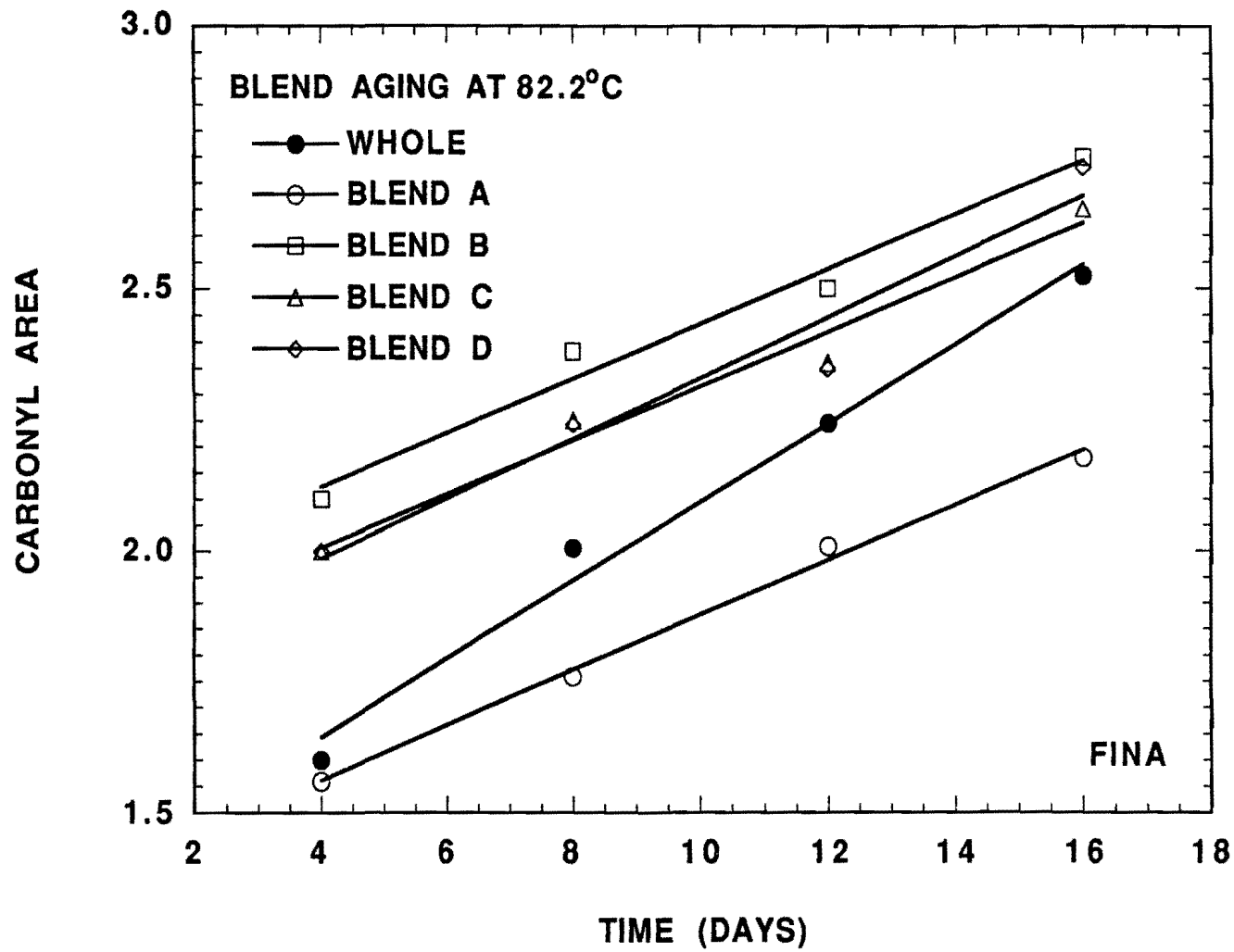
Figure II-6-9. Carbonyl Growth Rates at 82.2°C for Fina Asphalt and Blends

153
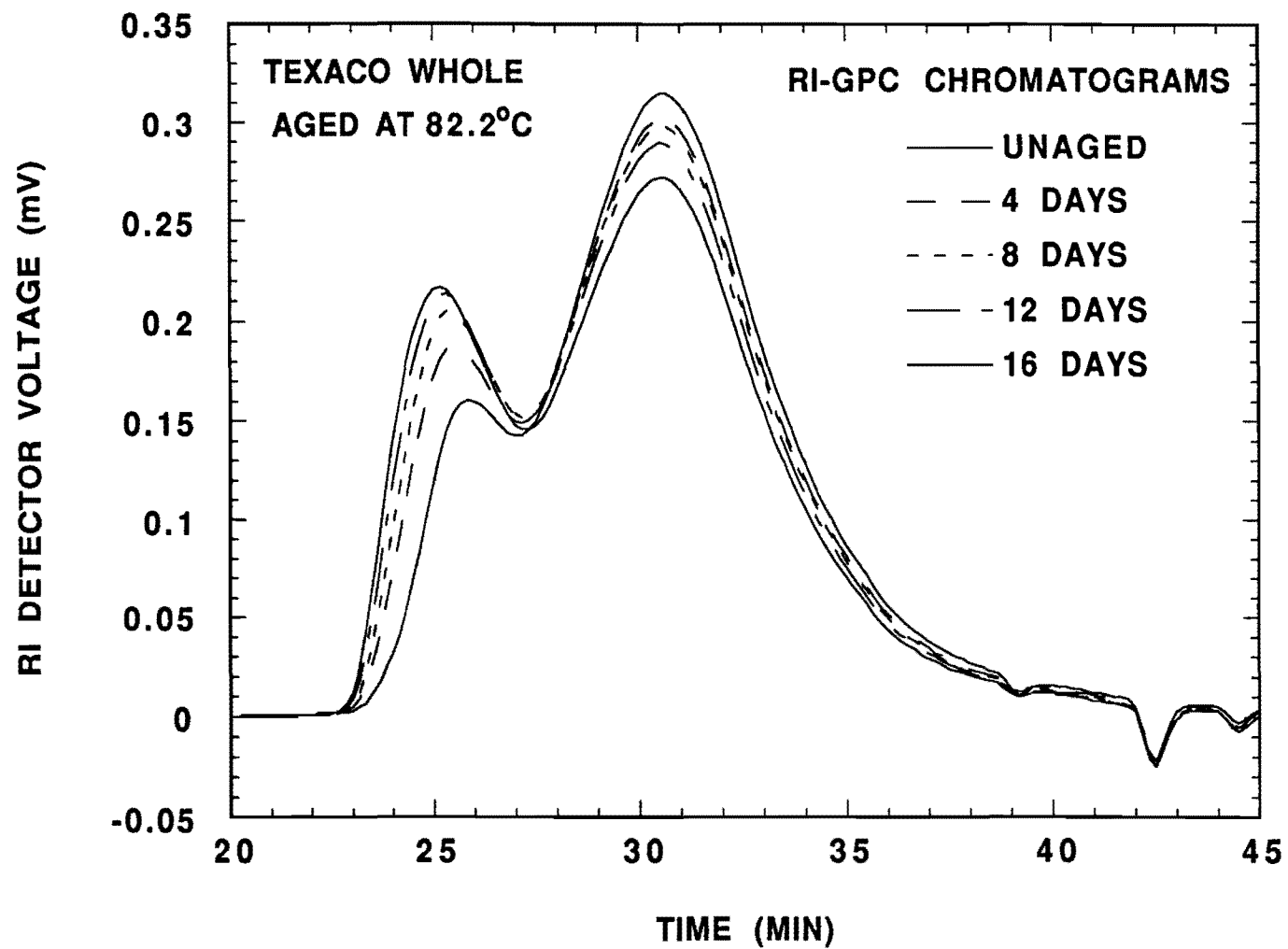
Figure II-6-10. RI-GPC Chromatograms of Texaco Asphalt Aged at 82.2°C
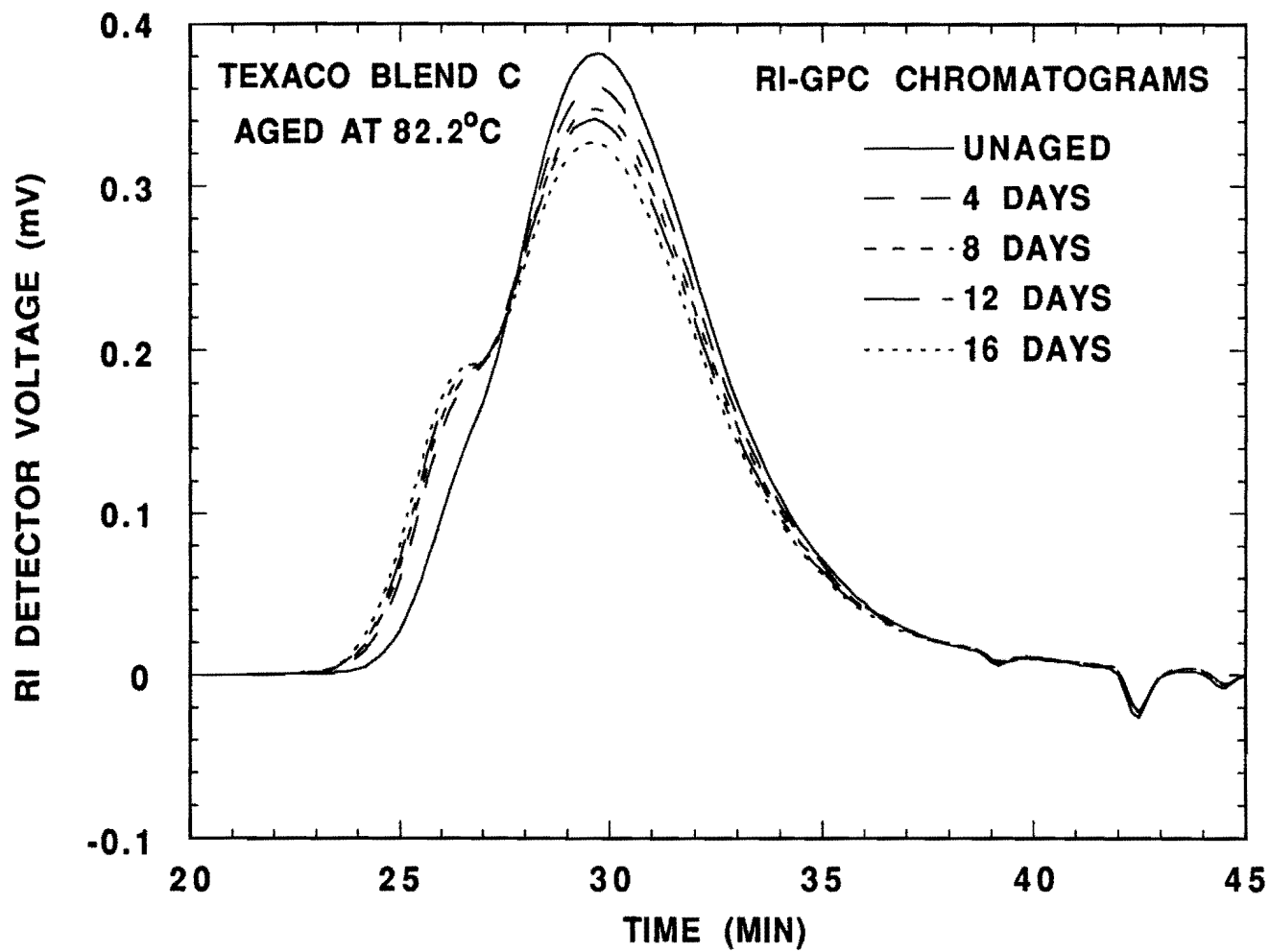
Figure II-6-11. RI-GPC Chromatograms of Texaco Blend C Aged at 82.2°C

**Table II-6-5**

**GPC $M_w^{IV}$ for Asphalts and Selected Blends Aged at 82.2°C**

| Time | Coastal | | | Fina | | | Texaco | | |
|------|------|------|------|------|------|------|------|------|------|
| (days) | Tank | C | D | Tank | B | D | Tank | C | E |
| 0 | 2690 | 1150 | 1345 | 1867 | 1034 | 1014 | 3762 | 1393 | 1724 |
| 4 | 3705 | 1706 | 2420 | 2686 | 1437 | 1558 | 5700 | 2072 | 3378 |
| 12 | 5267 | 2049 | 3077 | 3317 | 1648 | 1811 | 7853 | 2365 | 4111 |
| 16 | 5853 | 2114 | 3323 | 3880 | 1746 | 1952 | 8950 | 2584 | 4796 |

Figure II-6-12 displays the activation energies of the Fina asphalt and blends; the activation energy is the slope of each line. The blends do not appear to possess significantly different activation energies than the original asphalt.

In Section I-2, we suggested the estimation of asphalt service life by using the activation energies calculated with POV aging data. By assuming a road aging temperature, oxidation or hardening rates may be extrapolated using the activation energies. Assuming a failure viscosity allows the approximation of the amount of POV time required to reach a specified viscosity at road temperature. Table II-6-6 lists the calculated aging times for the asphalts and blends to reach 500,000 poise with a POV temperature of 35°C (95°F).

The results of the aging time estimates show considerable scatter due to insufficient data and other considerations. The blend aging data were obtained at only two temperatures, and the asphalts at only three, for a substantial extrapolation to the road temperature. Also, since the calculations use only the oxidation rates, the large initial jumps in the viscosities of the asphalts are not considered. The net effect is that the aging time estimates of the asphalts and blends, good or bad, cannot be considered reliable.

156
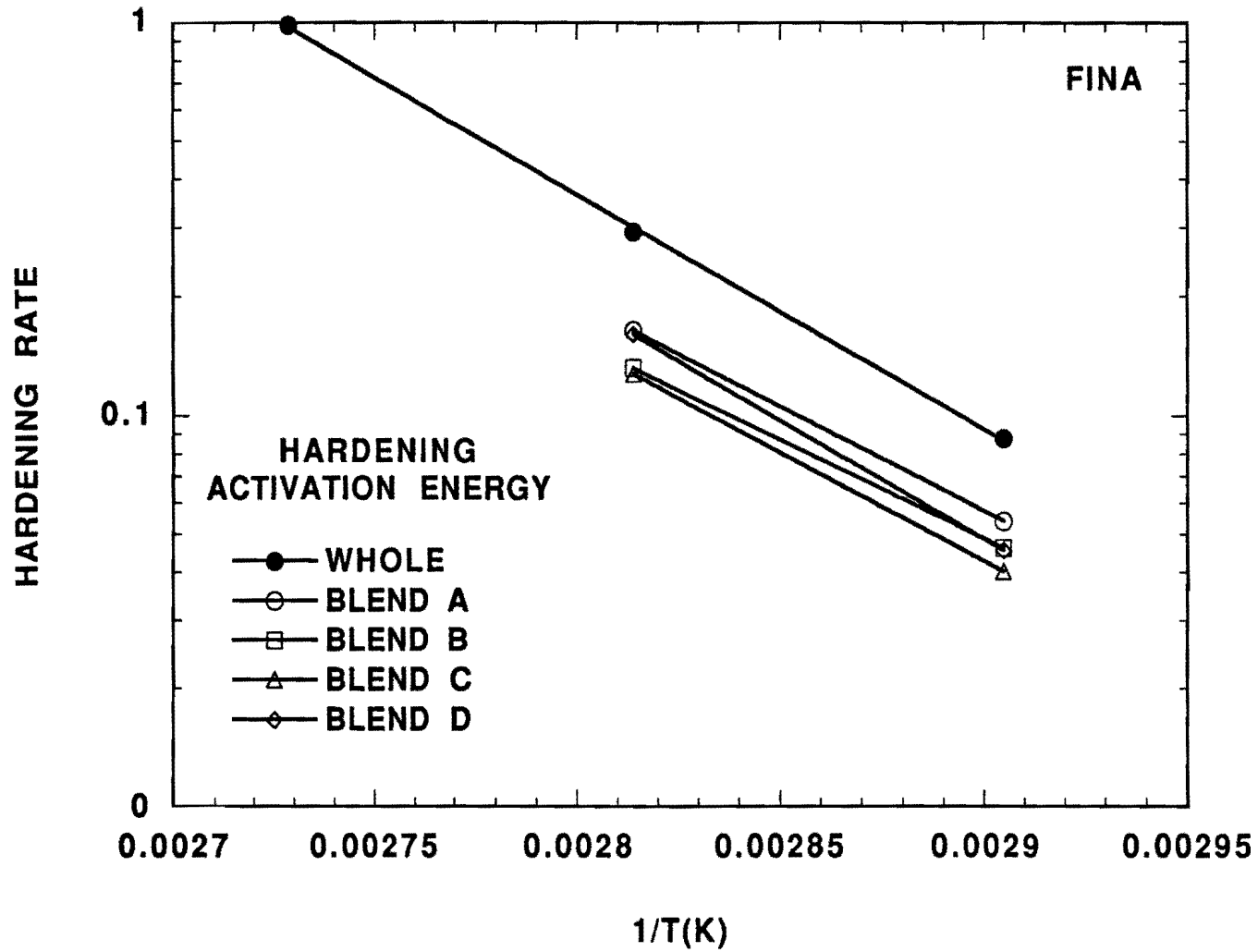
Figure II-6-12. Arrhenius Plot of Hardening for Fina Asphalt and Blends

## Table II-6-6
## Aging Times for Asphalts and Blends

| | Time (days) | | |
|---|---|---|---|
| Blend | Coastal | Fina | Texaco |
| Whole | 1940 | 7110 | 23200 |
| A | 31250 | 616 | 10300 |
| B | 89500 | 1500 | 1870 |
| C | 204000 | 8680 | 7130 |
| D | 32000 | 8410 | 1140 |
| E | - | - | 1390 |
| F | - | - | 39500 |

**Chemical and Physical Property Correlation**

The correlations discussed in Chapter II-5 for the asphalts and SC fractions are reinforced by the blend data.

*Viscosity*

The $\eta_0^*$ versus $M_w^{IV}$ plot in Figure II-6-13 for the asphalts and blends aged at 82.2°C (180°F), as well as the unaged SC fractions, shows that a source-dependent relationship exists for all but the lighter fractions. Above 1000 poise the relationship becomes not only source dependent, but each blend possesses its own relationship with aging. The Texaco asphalt and blends maintain the highest molecular weight for a given viscosity. The Texaco asphalt exhibits the highest asphaltene content, but not proportionally as large as the increase in molecular weight. Figure II-6-14 isolates the Texaco asphalt and blends C and E from Figure II-6-13 to highlights the differences between the aging characteristics of each sample. Texaco AC-20

158
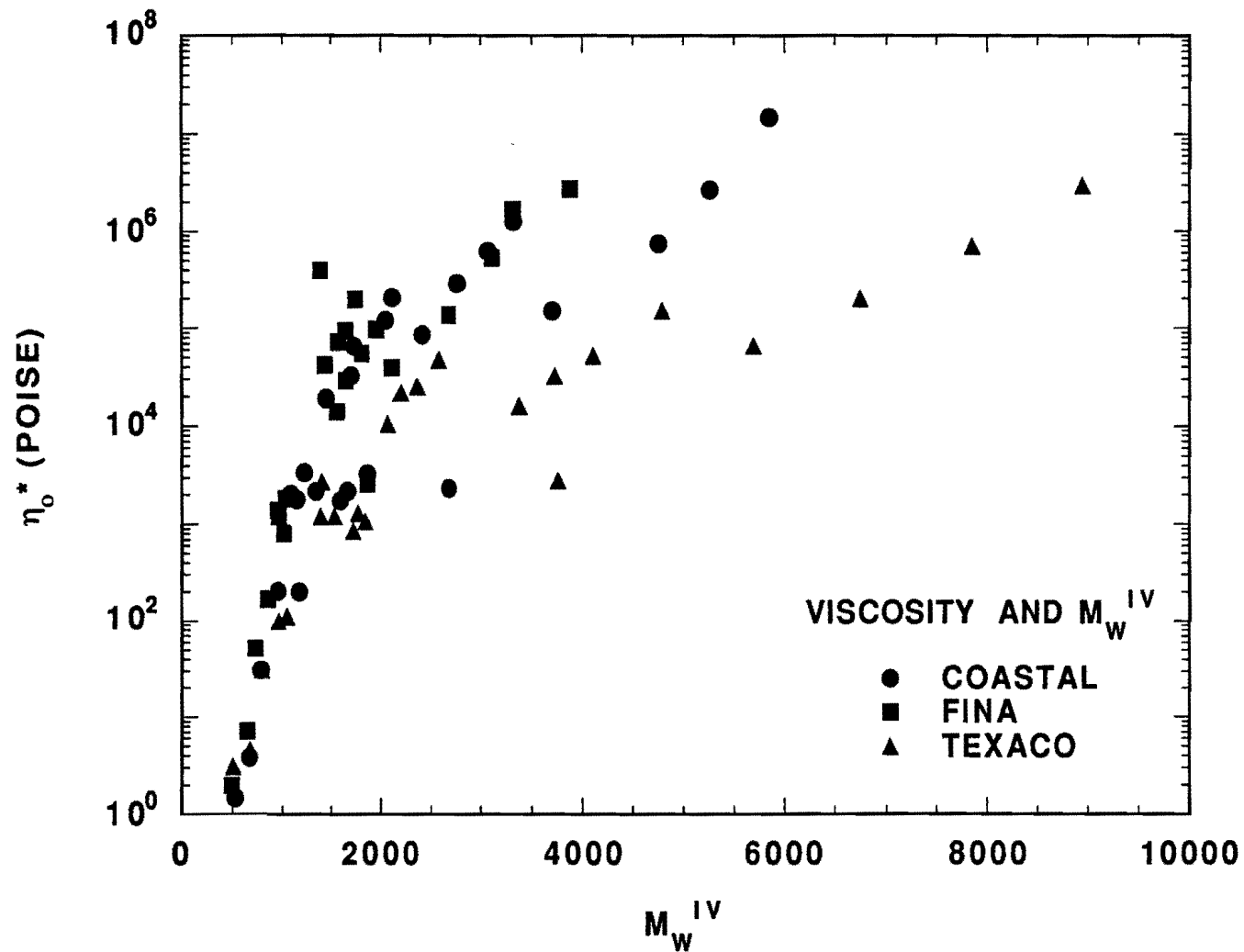
Figure II-6-13. Viscosity Versus $M_w^{IV}$ for Asphalts and Selected Blends Aged at 82.2°C and SC Fractions
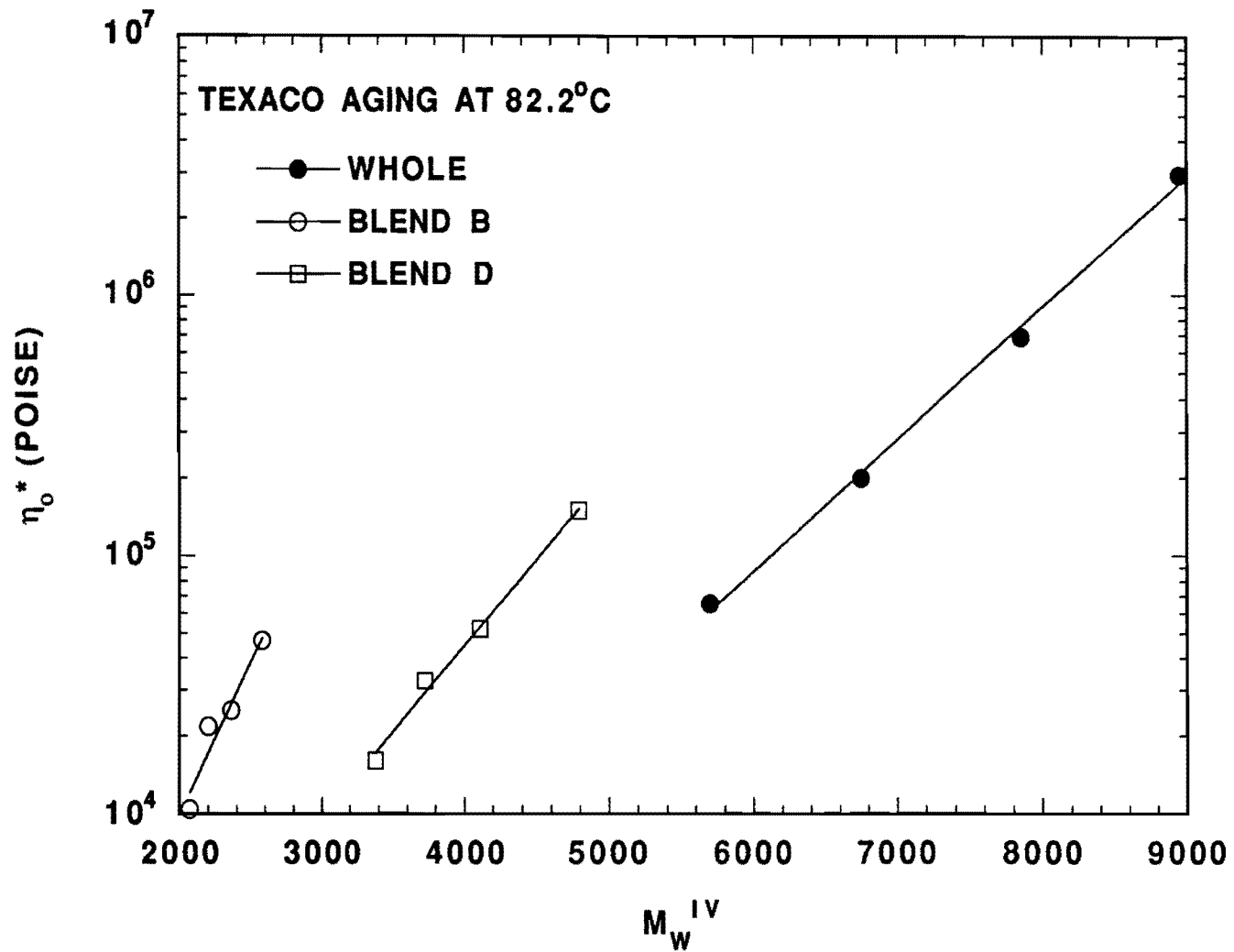
Figure II-6-14. Viscosity Versus $M_W{}^{IV}$ for Texaco Asphalt, Blend B, and Blend D Aged at 82.2°C

produces large increases in $\eta_0^*$ and $M_w^{IV}$ for each aging time. The relatively small increases in $\eta_0^*$ and $M_w^{IV}$ for the blends indicates that fewer asphaltenes are being formed during blend aging.

*Carbonyl Formation*

The carbonyl growth during aging correlates with the $M_w$ values as well. Figure II-6-15 demonstrates that blends B and D, which have lower viscosities than the whole asphalt, display larger carbonyl areas than the whole asphalt aged under the same conditions. The rate of molecular weight increase varies with asphaltene content, but the carbonyl formation does not appear affected by the asphaltene content or the $M_w^{IV}$.

Results from blend aging reinforce the relationships determined for the HS and $\eta_0^*$ growth rates. Adding the blend data to the plot of HS versus $M_w^{IV}$ shown in Figure II-6-16 adds scatter to the correlations but generally agrees with the fraction trends. The blends, especially Fina and Texaco, produce very similar HS values; but the varying amounts of asphaltenes in the blends affect the $M_w^{IV}$ values.

## Viscosity Temperature Susceptibility

The low temperature rheological properties were obtained for the whole asphalts and selected blends. At temperatures of 0°C, 10°C, 25°C, 40°C, and 60°C, $\eta_0^*$ values were calculated using the time/temperature superposition principle suggested by Ferry (1980). Viscosities were also calculated at 95°C using the Carri-Med rheometer, but the large temperature gradient across the gap experienced at this high temperature produced unreliable data, unless only used for time/temperature superposition calculations. By calculating the viscosity temperature susceptibility (VTS) of the asphalts and blends, the influence of the compositional changes incurred by refining the asphalts using a SC process may be determined. There was some concern that the removal of most of the asphaltenes would adversely affect the VTS. This is possible, but the removal of most of the wax as well would undoubtedly improve the VTS.

161
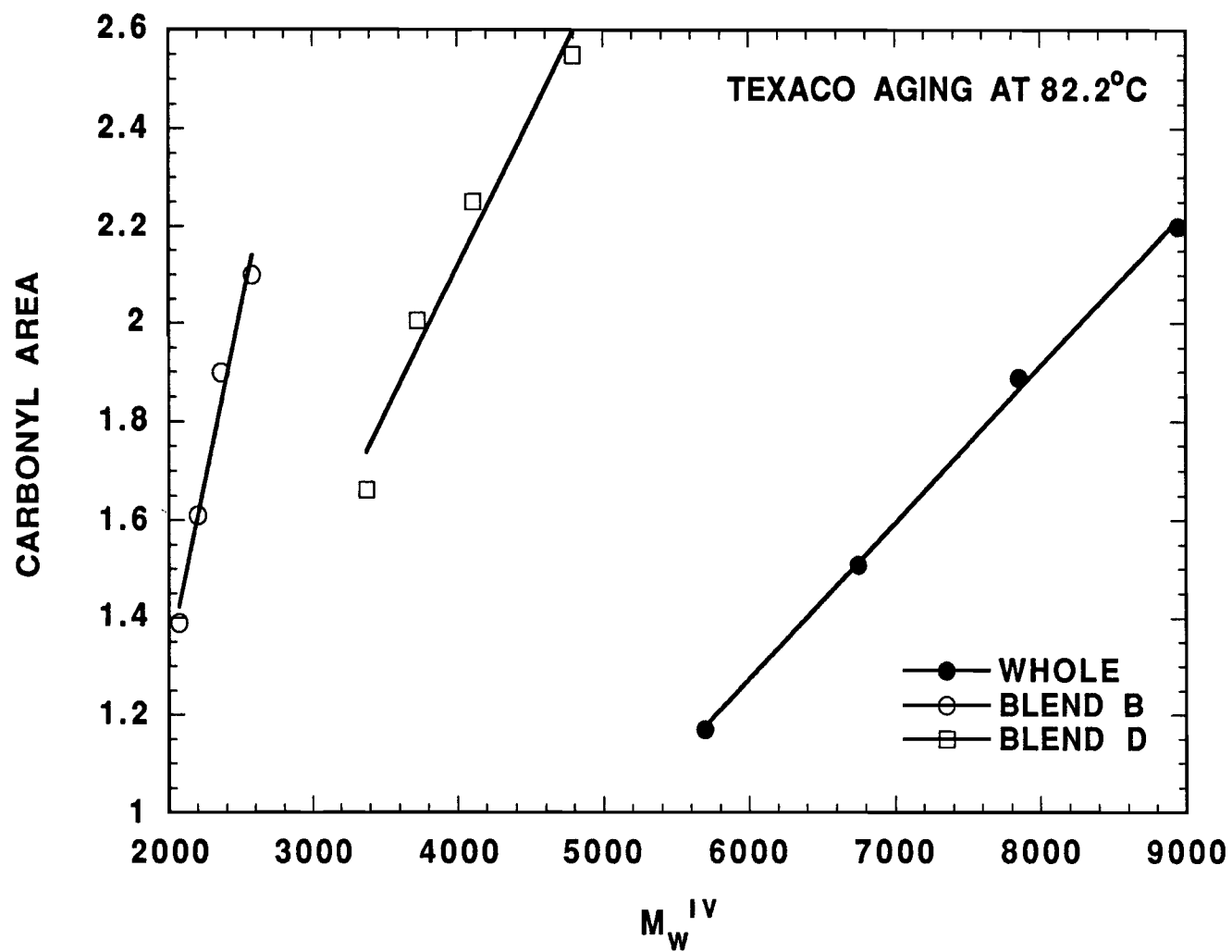
Figure II-6-15. Carbonyl Area Versus $M_W^{IV}$ for Texaco Asphalt, Blend B, and Blend D Aged at 82.2°C
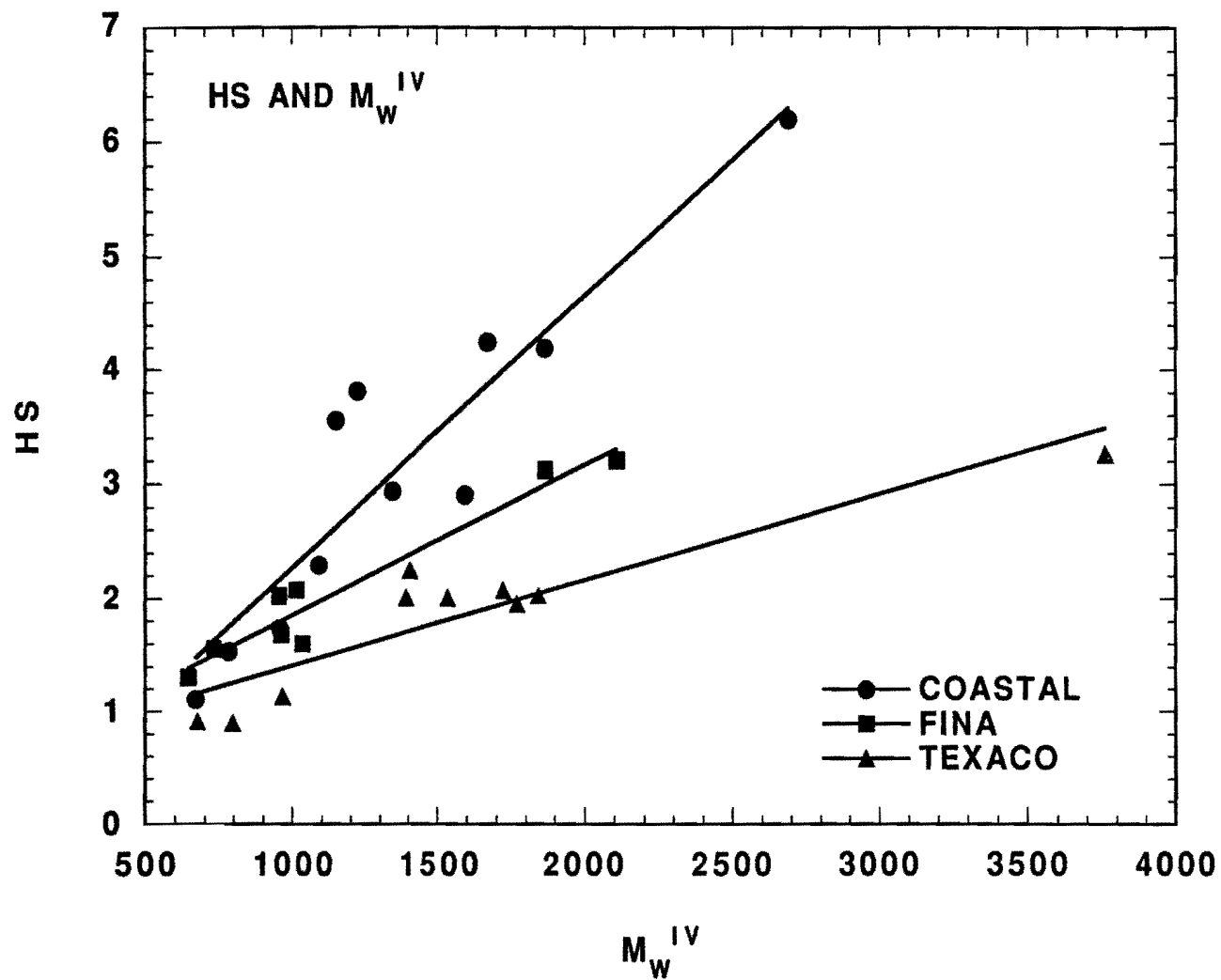
Figure II-6-16. HS Versus $M_w^{IV}$ for Asphalts, Blends, and SC Fractions

Figure II-6-17 displays the data representing the $\eta_0^*$ values from each of the whole asphalts plotted using the VTS form suggested by Puzinauskas (1979). Obviously, a considerable amount of curvature exists in the trend of the data and a fit using different equations was attempted. By using the form of the Boltzmann distribution or Arrhenius equation, where the viscosity of a liquid is proportional to $\exp(E_a/RT)$, a much better and scientifically reasonable correlation is obtained (Atkins, 1982). Figure II-6-18 shows the marked improvement in the linearity of the data for the three tank asphalts. Obviously, the Boltzmann distribution is the correct form to describe the affect of temperature on viscosity at least in the measured temperature range.

Figures II-6-19 through II-6-21 presents the Boltzmann distributions for the asphalts and selected blends. Surprisingly, the vast differences in processing and properties of the asphalts and blends, as well as contamination and degradation in the blends, did not affect the VTS of the asphalt. The VTS seems only dependent upon the source of the asphalt. The differences between sources may provide information on the contribution of molecular structures to rheological properties. The activation energies, or VTS, associated with the Boltzmann distribution may provide some structural information. Better understanding of the VTS relationships require further study but are beyond the scope of this research project.
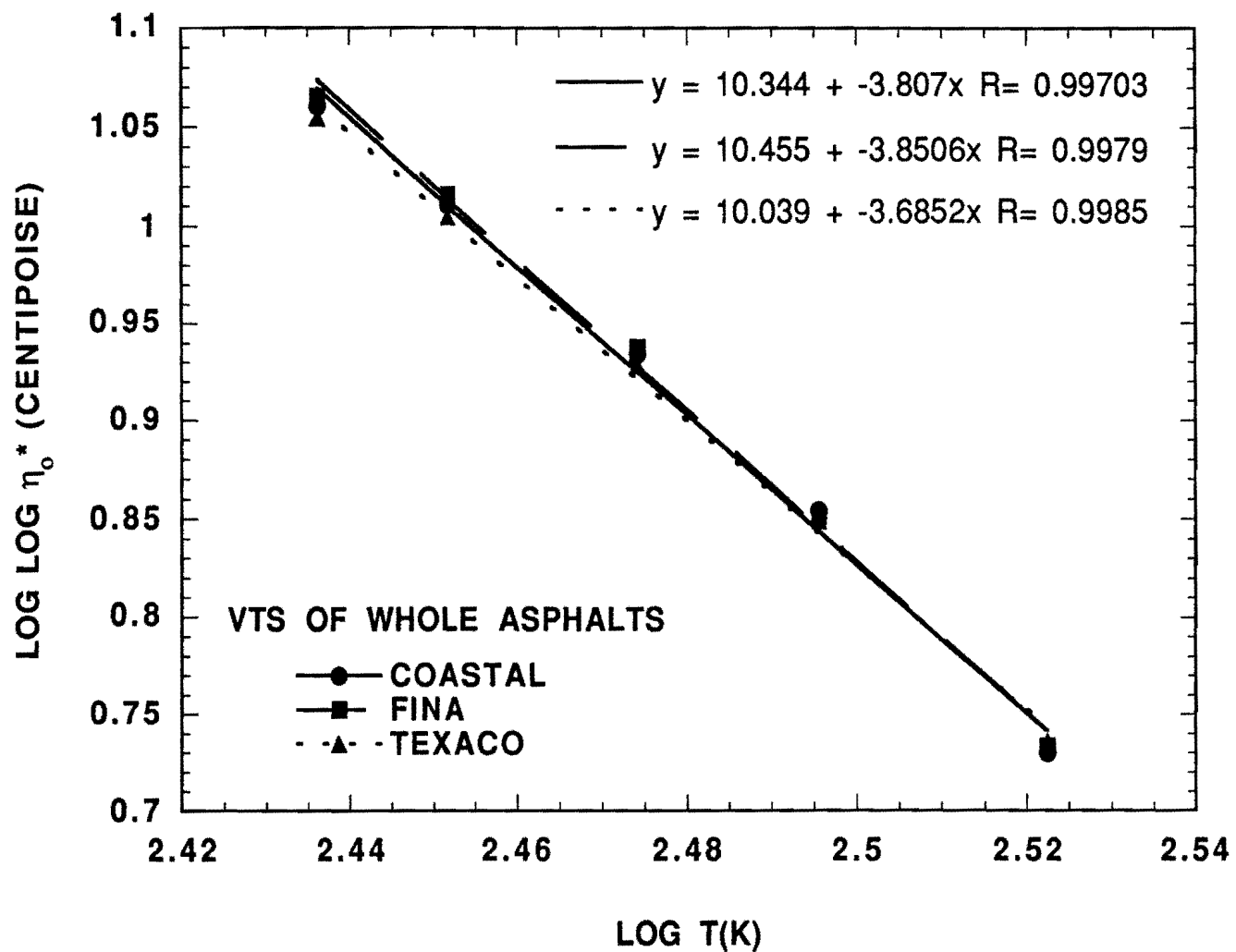
Figure II-6-17. VTS of Whole Asphalts
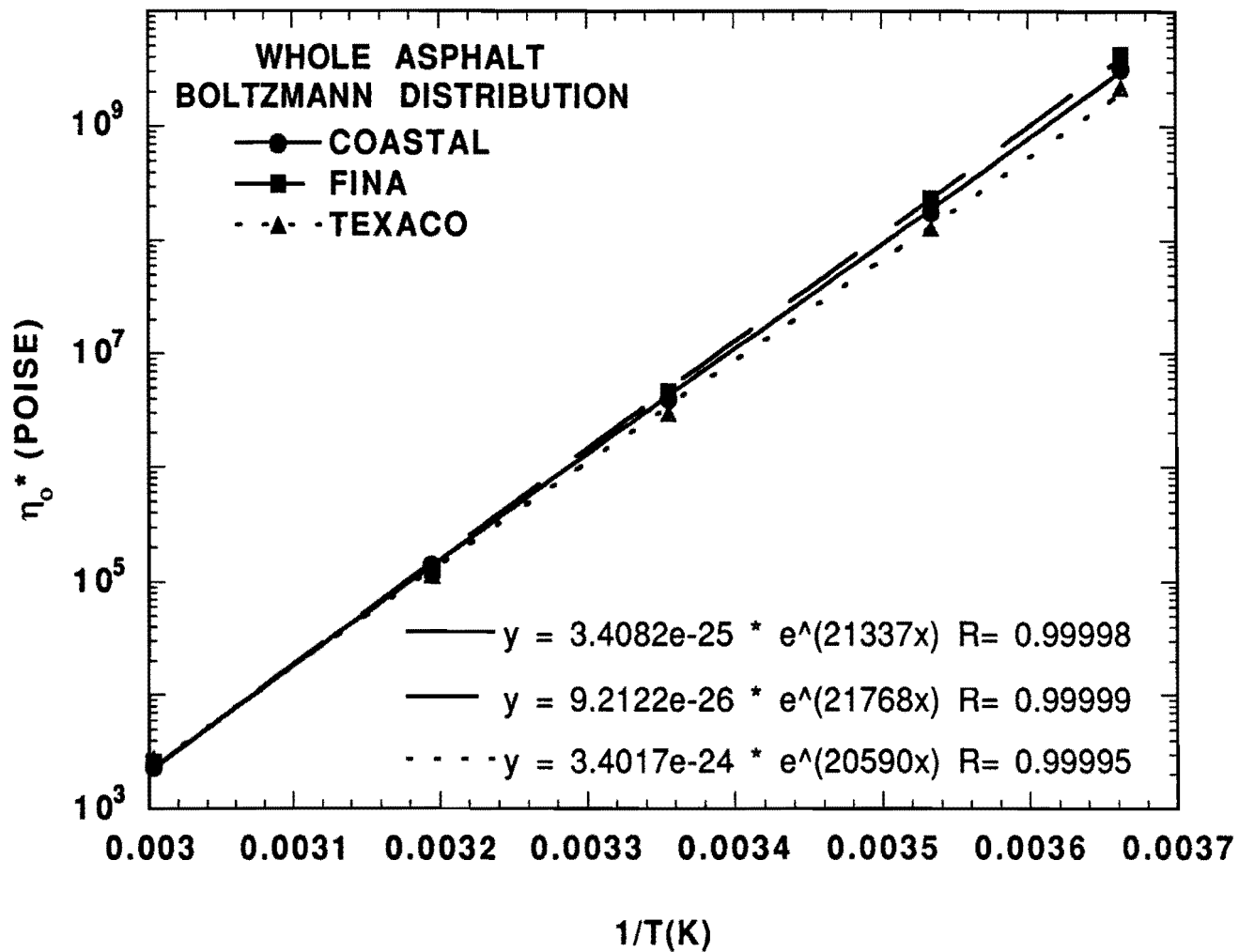
Figure II-6-18. Boltzmann Distribution of Viscosities of Whole Asphalts
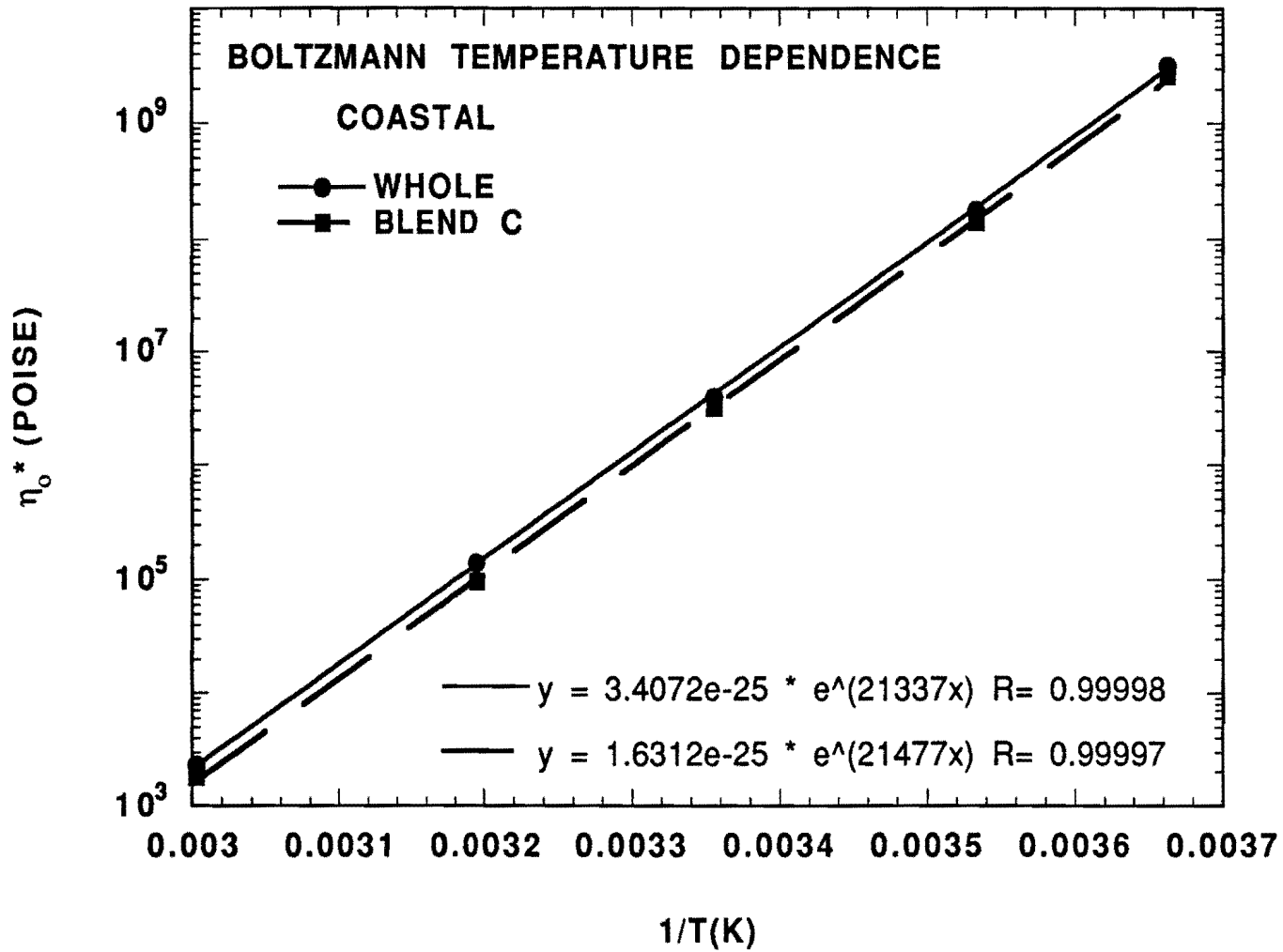
Figure II-6-19. Boltzmann Distribution of Viscosities of Coastal Asphalt and Blend C
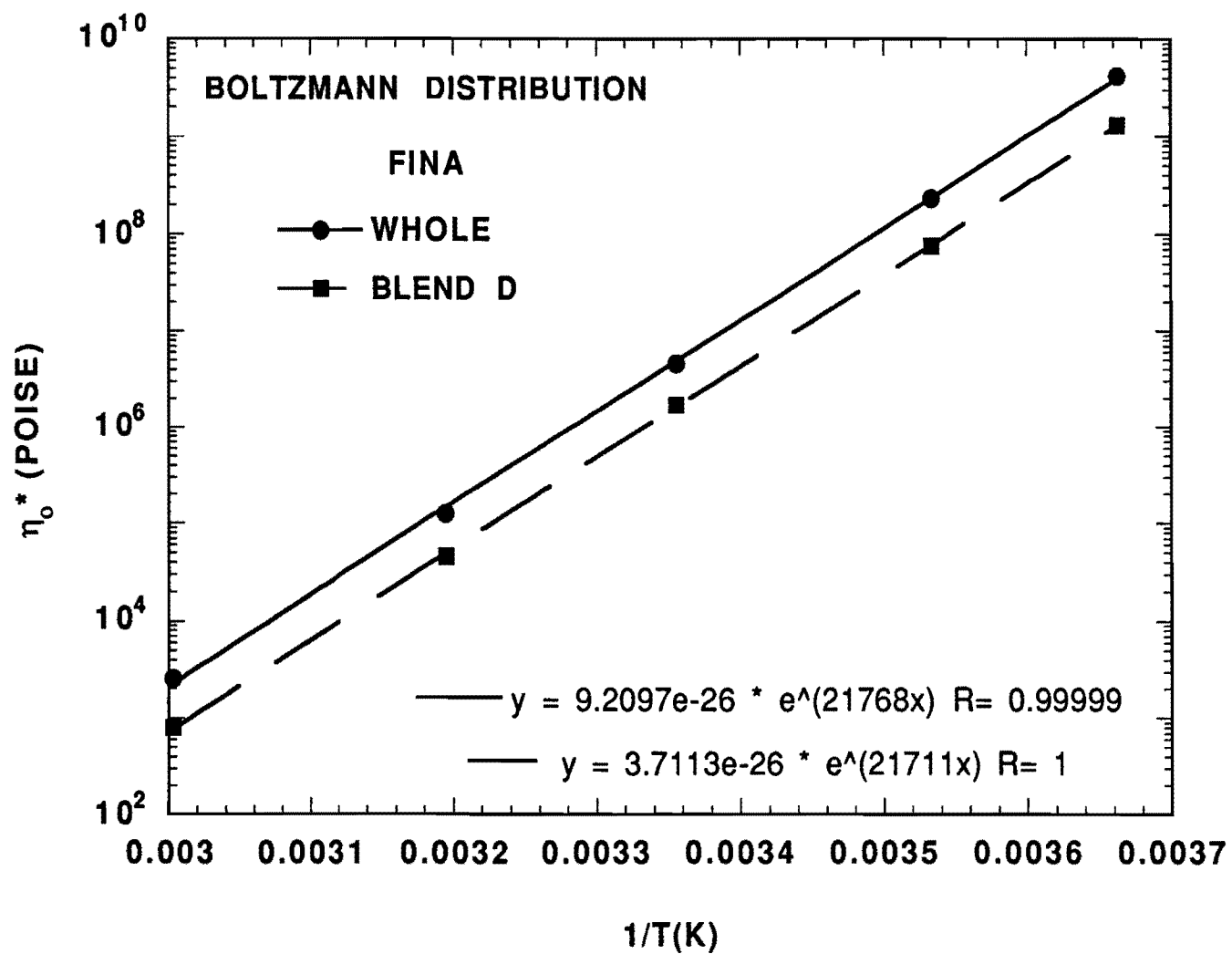
Figure II-6-20. Boltzmann Distribution of Viscosities of Fina Asphalt and Blend D
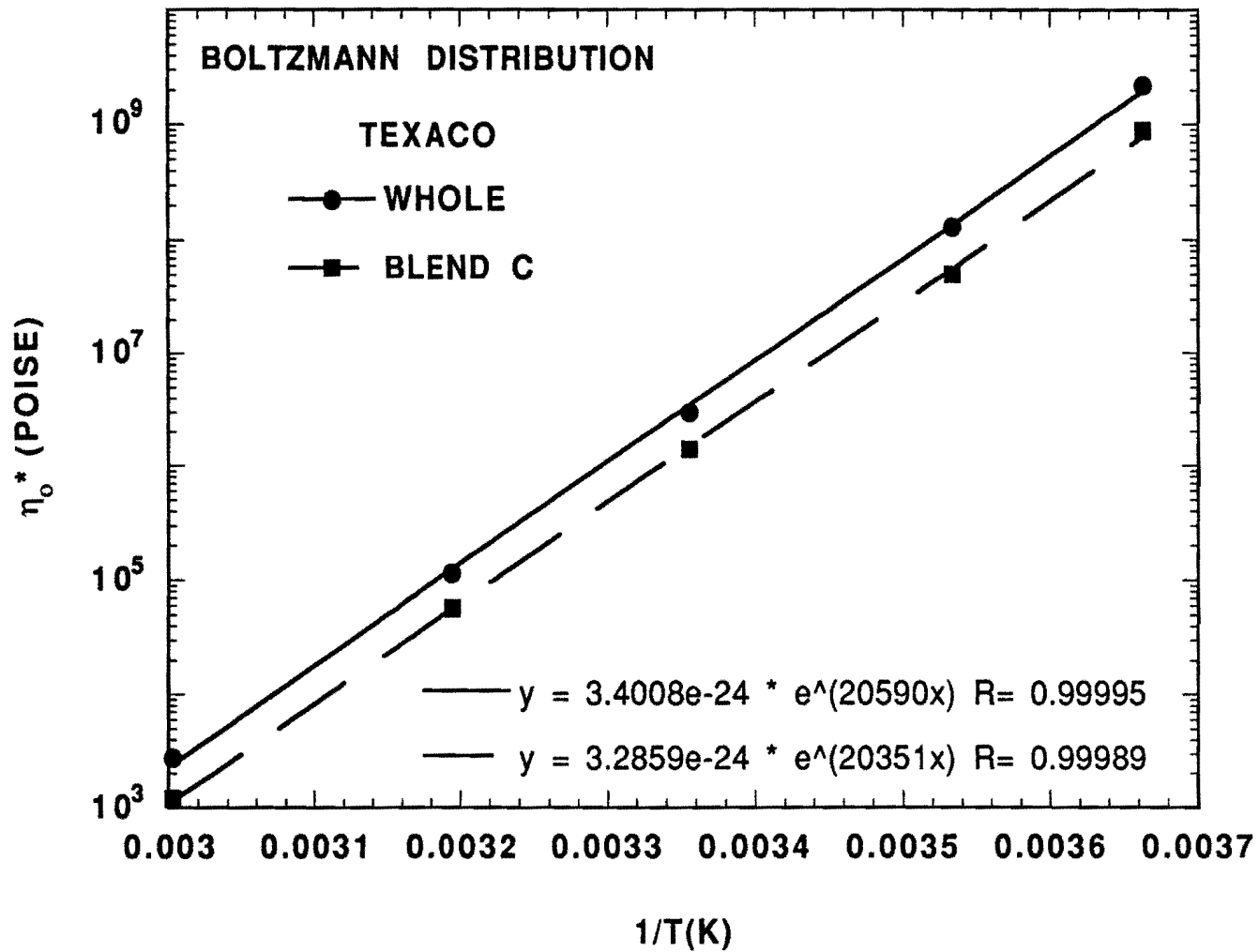
Figure II-6-21. Boltzmann Distribution of Viscosities of Texaco Asphalt and Blend C

# SECTION III

## Conclusions and Recommendations

# CHAPTER III-1

## CONCLUSIONS

The aging work described in this report is highlighted by the following conclusions:

1. The response of an asphalt's physical properties to aging for a period of time is extremely important in determining its long term performance. Asphalts with good properties when the pavement is first placed do not necessarily maintain those properties over extended periods of time.

2. The rate of change of the physical properties of an asphalt over time as the result of exposure to oxygen and high temperatures can be divided into chemical aging (as manifested for example by carbonyl growth in the infrared spectrum) and a physical response to those chemical changes (the hardening susceptibility of the asphalt to these chemical changes).

3. The hardening susceptibility of an asphalt is a very important parameter in understanding the physical changes an asphalt undergoes as a result of aging and may be capable of modification by proper asphalt design.

4. The chemical aging of asphalts obeys an Arrhenius activation energy relationship. As a result the relative aging rates of asphalts measured at elevated oven temperatures are not necessarily comparable to the relative aging rates at pavement temperatures. This introduces the possibility of considerable error in estimating an asphalt's pavement durability based upon elevated oven aging tests.

5. As a result of this Arrhenius relationship, however, oven tests conducted at more than one elevated temperature can be extrapolated to lower temperatures and used to obtain more accurate predictions of roadway aging performance.

6.  Based upon the separate characteristics of aging rate and hardening susceptibility, an aging test can be developed which, for example, would estimate the length of time in service for a road to reach a given physical condition. Such a test could be of considerable value in planning pavement maintenance as well as in designing new pavements.

7.  Studies on the aging of asphalt by sunlight indicate extensive chemical changes to the asphalt material can occur and that water leachable materials are formed. The role of this process in the bulk aging of the asphalt binder is not yet established.

The following conclusions derive from the supercritical fractionation effort:

1.  The modification of the collection vessels for collecting the heavy, solids fractions was successful. Additionally, the use of higher temperatures with the cyclohexane solvent enabled it to be used as an effective supercritical fluid. As such it was capable of solubilizing all of the asphalt components thereby preventing precipitation problems upstream of the separators.

2.  The use of a reduced crude feed to the supercritical unit was not as successful as hoped. This was largely the result of the lighter components of the reduced crude acting as entrainers in the separation thereby making the supercritical cyclohexane a better solvent for the asphalt materials and preventing complete separation in the last stage and poor selectivity throughout the process. Nevertheless, a trend of increasing aromaticity with fraction number is achieved by supercritical cyclohexane, followed by pentane, fractionation of reduced crudes.

3.  The use of cyclohexane to supercritically fractionate asphalt materials worked very well except that the high temperatures required caused considerable stress to the heaters of the unit.

4.  The combined cyclohexane-pentane fractionation achieved a better separation of the functionalities of the asphalt material than was achieved in the reduced crude separations. In particular, an excellent separation of the asphaltenes from the saturates was achieved with the asphaltenes appearing almost exclusively in the heavier fractions and the saturates in the light fractions. Metals also concentrated in the heavy fractions.

5.  Metal contamination of the asphalt occurred as a result of excessive temperatures in the heaters when using cyclohexane solvent.

The next items are conclusions concerning the aging of fractions and the composition and physical property relationships of asphalts and their fractions:

1.  The aging of the supercritical fractions showed the same relationship between the log of the viscosity and carbonyl growth. This hardening susceptibility relationship seems to be universal among the asphalts and their fractions.

2.  The hardening susceptibility of the fractions varied from one fraction to the next. The heavier fractions generally had higher hardening susceptibilities than the lighter fractions.

3.  Definitive conclusions on the aging kinetics of the asphalt fractions are not possible because of discrepancies in aging measurements at the highest temperature. These discrepancies could be the result of a different aging mechanism occurring at these higher temperatures and requires further studies to evaluate.

4.  Besides the hardening susceptibility relation between viscosity and aging there appears to be an underlying dependence of an asphalt or fraction viscosities and infrared absorption at three frequencies. Absorption at $1600 cm^{-1}$ suggests that aromaticity plays a role in the viscosity of the material and that this role is not strongly source dependent. Additionally, the viscosity correlates quite well with an

intrinsic viscosity molecular weight, at least for low molecular weight materials. For higher molecular weight materials the relationship diverges, indicating source dependency.

5.  The hardening susceptibility appears to be weakly related to asphaltene content and also to the intrinsic viscosity molecular weight.

The final set of conclusions relates to blends produced from the asphalt supercritical fractions:

1.  The purpose of this work was to produce midcut asphalt-grade blends that would be inherently more compatible than the original asphalt.

2.  GPC chromatograms of the blends showed much less LMS than the parent asphalt which is consistent with a more compatible material.

3.  The aging of the blends qualitatively followed the same hardening susceptibility relationship between viscosity and carbonyl growth as do the whole asphalts and their fractions.

4.  The hardening susceptibility of an asphalt is a critically important property which strongly influences the life expectancy of the pavement. The hardening susceptibilities of the blend materials are universally lower than the hardening susceptibilities of the parent whole asphalts; the blends are more tolerant of aging, thereby hardening less, than the whole asphalts. This provides strong support for the concept of designing asphalts to have superior aging properties. Additionally, GPC chromatograms of the blends show much less LMS formation on aging than do those for the parent whole asphalt.

5.  Viscosity temperature susceptibilities of the asphalt materials are essentially unaffected by supercritical fractionation and reblending.

6.  Consideration of viscosity activation energies for asphalt, fractions, and their blends may provide useful insight into molecular structure.

# CHAPTER III-2
## RECOMMENDATIONS

The chemical aging of asphalt binders and the response to this aging as manifested in physical properties is critically important to both the short term and long term performance of the pavement. Accordingly, we provide the following recommendations:

1. The effort to understand both the chemistry and physical events associated with asphalt binder aging is crucial and we recommend that it continue.

2. We recommend the development of a pavement aging model and an aging test for the purposes of predicting asphalt performance. The use of existing test sections from Study 287 and the adhoc test sections of Study 458 will be of great value in such developments. The development of such a model will be of great value to planning, maintenance, and replacement projects.

3. We recommend that the effort to understand how to make meaningful comparisons of asphalts and blends with respect to aging continue. The separation of the chemical kinetics from the physical response by the use of the hardening susceptibility is a tremendously important first step in making these comparisons

4. We recommend that the effort to understand how to design asphalt binders to have good aging properties continue. As a result of the other items mentioned which are related to aging, this step will occur naturally.

The supercritical fractionation process shows considerable promise in producing improved asphalts and should continue. Specifically:

1. We recommend that the supercritical process for producing asphalt binders with superior mechanical and aging characteristics be

175

continued.

2. We recommend that the supercritical process be used to investigate the use of recycling agents with highly aged asphalt binders and specifically that it be used to produce superior recycling agents.

3. We recommend that the supercritical process be used to further develop and understand recycled tire rubber applications in asphalt pavements.

# REFERENCES

"1984 Refining Process Handbook," *Hydrocarbon Processing*, **62**, 9 (1984).

"Refining Handbook '90," *Hydrocarbon Processing*, **69**, 11, p. 85 (1990).

Atkins, P., *Physical Chemistry*, Second Ed., W. H. Freeman Co., San Francisco, CA (1982).

Audeh, C., and Yan, T., "Supercritical Selective Extraction of Hydrocarbons from Asphaltic Petroleum Oils," U.S. Patent No. 4,341,619 (27 July 1982).

Bakshi, A., and Lutz, I., "Combination of Visbreaking and Solvent Deasphalting Boosts Gas Oil Yields for FCCU Feed," *Oil and Gas Journal*, **85**, Feb. 17, p. 52 (1986).

Barbour, A.F., Barbour, R.V., and Petersen, J.C., "A Study of Asphalt-Aggregate Interactions Using Inverse Gas-Liquid Chromatography," *Journal of Applied Chemical Biotechnology*, **24**, 645-654 (1974).

Beitchman, B.D., "Infrared Spectra of Asphalts," *J. Res. Nat. Bur. Std.* Sect. A, **63**, 189 (1959).

Billon, A., Peries, J., Fehr, E., and Lorenz, E., "SDA Key to Upgrading Heavy Crudes," *Oil and Gas Journal*, **76**, Jan. 24, p. 43 (1977).

Bousquet, J., and Laboural, T., "Deasphalted Oils Acceptable FCC Feed in Europe," *Oil and Gas Journal*, **86**, Apr. 20, p. 62 (1987).

Burr, B.L., Davison, R.R., Jemison, H.B., Glover, C.J., and Bullin, J.A.,"Asphalt Hardening in Extraction Solvents," *Trans. Res. Rec.*, in press.

Burr, B.L., Davison, R.R., Glover, C.J., and Bullin, J.A., "Solvent Removal from Asphalt," *Trans. Res. Rec.*, **1269**, 1-8 (1990).

Campbell, P.G., and Wright, J.R., "Determination of Oxidation Rates of Air-Blown Asphalts by Infra-red Spectroscopy," *J. Appl. Chem.*, **12**, 256 (1962).

Campbell, P.G., and Wright, J.R., "Infrared Spectra of Asphalts: Aspects of The Changes Caused by Photooxidation," *J. of Research of the National Bureau of Standards*, **68C**, 115 (1964a).

Campbell, P.G., and Wright, J.R., "Oxidation Products in An Oxygen-Blown Kuwait Asphalt," *Ind. Eng. Chem. Product Research and Development*, **5**, 319 (1966).

Campbell, P.G., and Wright, J.R., "Ozonation of Asphalt Flux," *Ind. Eng. Chem. Product Research and Development*, **3**, 186 (1964b).

Cipione, C.A., Davison, R.R., Burr, B.L., Glover, C.J., and Bullin, J.A., "Evaluation of Solvents for Extraction of Residual Asphalt from Aggregates," *Trans. Res. Rec.*, **1323**, 47-52 (1991).

Conaway, J., Graham, J., and Rogers, L., "Effects of Pressure, Temperature, Adsorbent Surface, and Mobile Phase Composition on the Supercritical Fluid Chromatographic Fractionation of Monodisperse Polystyrene," *Journal of Chromatographic Science*, **16**, 102 (1978).

Corbett, L.W., "Refinery Processing of Asphalt Cement," *Trans. Res. Rec.*, **999**, 1 (1984).

Corbett, L., "Relationship Between Composition and Physical Properties of Asphalt," *Association of Asphalt Paving Technologists*, **39**, 342 (1970).

Davison, R.R., Bullin, J.A., Glover, C.J., Burr, B.L., Jemison, H.B., Kyle, A.L.G., and Cipione, C.A., *Development of Gel Permeation Chromatography, Infrared and Other Tests to Characterize Asphalt Cements and Correlate with Field Performance*, FHWA/TX-90/458-1F (1989).

Davison, R.R., Bullin, J.A., Glover, C.J., Stegeman, J.R., Jemison, H.B., Burr, B.L., Kyle, A.L, and Cipione, C.A., *Design and Manufacture of Superior Asphalt Binders*, FHWA/TX-91/1155-1F (1991).

Ditman, J., "Deasphalt to Get Feed for Lubes," *Hydrocarbon Processing*, **52**, 5 (1973).

Dorrence, S.M., Barbour, F.A., and Petersen, J.C., "Direct Evidence of Ketones in Oxidized Asphalts," *Analytical Chemistry*, **46**, 2242 (1974).

Edler, A.C., Hattingh, M.M., Servas, V.P., and Marais, C.P., "Use of Aging Tests to Determine the Efficacy of Hydrated Lime Additions in Retarding Oxidative Hardening," *Proc. AAPT*, **54**, 118-139 (1985).

Eisenbach, W., Niemann, K., and Gottsch, P., "Supercritical Fluid Extraction of Oil Sands and Residues from Oil and Coal Hydrocarbons," Chapter 20 of *Chemical Engineering at Supercritical Conditions*, Paulitis, M., Penninger, J., Gray, R., and Davidson, P., ed., Ann Arbor Science, New York, NY, p. 419 (1983).

Ely, J., and Baker, J., "A Review of Supercritical Fluid Extraction," *National Bureau of Standards Technical Note 1070* (1983).

Ensley, E.K., Petersen, J.C., and Robertson, R.E., "Asphalt-Aggregate Bonding Energy Measurements by Microcalorimetric Methods," *Thermochimica Acta*, **77**, 95-107 (1984).

Ferry, J., *Viscoelastic Properties of Polymers*, 3rd Edition, John Wiley and Sons, New York, NY (1980).

Fink, D.F., "Research Studies and Procedures," *Proc. AAPT*, **27**, 176 (1958).

Gearhart, J., "Solvent Treat Resids," *Hydrocarbon Processing*, **59**, 5 (1980).

Gearhart, J., and Garwin, L., "Resid-Extraction Process Offers Flexibility," *Oil and Gas Journal*, **75**, Jun 14, p. 63 (1976a).

Gearhart, J., and Garwin, L., "ROSE Process Improves Resid Feed," *Hydrocarbon Processing*, **55**, 5 (1976b).

Glover, C.J., Davison, R.R., Ghoereishi, S.M., Jemison, H.B., and Bullin, J.A., "Evaluation of Oven Simulation of Hot-Mix Aging by an FT-IR Pellet Procedure and Other Methods," *Trans. Res. Rec.*, **1228**, 177 (1989).

Griffin, R.L., Miles, R.K., and Penther, C.J., "Microfilm Durability Test for Asphalt," *Proc. AAPT*, **24**, 31 (1955).

Haney, M., "A New Differential Viscometer -- Part 1 and 2," *American Laboratory*, March and April (1985).

Haney, M., U. S. Patent No. 4,463,598 (7 Aug. 1984).

Harnsberger, P., Wolf, J., and Petersen, J., "Oxidation of SHRP Asphalts at Different Temperatures Using the TFAAT Method," *Proceedings of the International Symposium on the Chemistry of Bitumens*, Vol. II, p. 706, Giavarini, C. and Speight, J., ed., Rome, Italy, June 5-8 (1991) (private collection, R. Davison).

Hattingh, M., "The Fractionation of Asphalt," *Association of Asphalt Paving Technologists*, **53**, 197 (1984).

Heithaus, J.J., Johnson, R.W., "A Microviscometer Study of Road Aspphalt Hardening in the Field and Laboratory," *Proc. AAPT*, **27**, 17 (1958).

Holbrook, K., "Refinery Economics," *Trans. Res. Rec.*, **999**, 6 (1984).

Irani, C., and Funk, E., "Separations Using Supercritical Gases," *Recent Developments in Separation Science,* Vol. III, Part A, CRC Press, West Palm Beach, FL, 171 (1977).

Jamieson, I.L., and Hattingh, M.M., "The Correlation of Chemical and Physical Properties of Bitumens with Their Road Performance," *Australian Road Research Conf. Proc.,* 5, 293-324 (1970).

Jemison, H.B., Burr, B.L., Davison, R.R., Bullin, J.A., and Glover, C.J., "Application and Use of the ATR FT-IR Method to Asphalt Aging Studies," *Fuel Science and Technology International,* 10(4-6), 195-808 (1992).

Jemison, H. B., Davison, R. R., Glover, C. J., and Bullin, J. A., "Evaluation of Standard Oven Tests for Hot-Mix Plant Aging," *Trans. Res. Rec.,* 1323, 77-84 (1991).

Jemison, H.B., Lunsford, K.M., Davison, R.R., Glover, C.J., and Bullin, J.A., "Properties of Asphalt Fractions Obtained by Supercritical Extraction with Pentane and Cyclohexane," *Preprints, Division of Petroleum Chemistry, ACS* (in press).

Jennings, P.W., *Uses of High Pressure Liquid Chromatography to Determine the Effects of Various Additives and Fillers on Characteristics of Asphalt,* Montana Department of Highways, Report No. FHWA/MT-82/001, June 1982.

Katz, D., and Whaley, T., "High Pressure Separation", U.S. Patent No. 2,391,576 (25 Dec. 1945).

Kemp, G.R., "Asphalt Durability Tests and Their Relationship to Field Hardening," *ASTM STP,* 532, 100-122 (1973).

Kim, O., Bell, C.A., Wilson, J.E. and Boyle, G., "Development of Laboratory Oxidative Aging Procedures for Asphalt Cements and Asphalt Mixtures," *Trans. Res. Rec.,* 1115, 101-112 (1987).

King, M., and Bott, T., "Problems Associated with the Development of Gas Extraction and Similar Processes," *Separation Science and Technology,* 17, 1, pp. 119-150 (1982).

Kleinschmidt, L.R., and Snoke, H.R., "Effect of Light and Water on The Degradation of Asphalt," *J. Res. Nat. Bur. Stand.,* 63C, 31 (1959).

Klesper, E., "Chromatography with Supercritical Fluids," *Extraction with Supercritical Gases*, Schneider, G., Stahl, E., and Wilke, G., ed., Verlag Chemie, Deerfield, FL, p. 115 (1980).

Lau, C.K., *Oxidative Reactions and Their Impact on the Properties of Asphalt as a Pavement Binder*, Thesis, Texas A&M University, College Station, TX (1991).

Lee, D.Y., "Asphalt Durability Test Correlations in Iowa," *Hwy. Res. Rec.*, **468**, 43-60 (1973).

Lee, D.Y., "Development of a Laboratory Durability Test for Asphalt," *HRB Report*, **231**, 34 (1968).

Lee, D.Y., and Huang, R.J., "Weathering of Asphalts as Characterized by Infrared Multiple Internal Reflection Spectra," *Applied Spectroscopy*, **27**, 435 (1973).

Martin, K.L., Davison, R.R., Glover, C.J., and Bullin, J.A., "Asphalt Aging in Texas Roads and Test Sections," *Trans. Res. Rec.*, **1269**, 9-19 (1990).

McHugh, M., and Krukonis, V., *Supercritical Fluid Extraction: Principles and Practice*, Butterworths, Boston, MA (1986).

Messmore, H., "Process for Producing Asphaltic Materials," U.S. Patent No. 2,420,185 (6 May 1947).

Monge, A., and Prausnitz, J., "An Experimental Method for Measuring Solubilities of Heavy Fossil-Fuel Fractions in Compressed Gases to 100 bar and 300°C," Chapter 7 of *Chemical Engineering at Supercritical Conditions*, Paulitis, M., Penninger, J., Gray, R., and Davidson, P., ed., Ann Arbor Science, New York, NY, p. 159 (1983).

Oliver, J.W.H., and Gibson, H., "Source of Water-Soluble Photooxidation Products in Asphalt," *Ind. Eng. Chem. Product Research and Development*, **11**, 66 (1972).

Peter, S., and Brunner, G., "The Separation of Nonvolatile Substances by Means of Compressed Gases in Countercurrent Processes," *Extraction with Supercritical Gases*, Schneider, G., Stahl, E., and Wilke, G., ed., Verlag Chemie, Deerfield, FL, p. 141 (1980).

Petersen, J.C., *A Thin Film Accelerated Aging Test for Evaluating Asphalt Oxidative Aging*, AAPT preprint volume; Session II, February 1989.

Petersen, J.C., "Chemical Composition of Asphalt Durability: State of the Art," *Transportation Research Record*, No. 999, 13 (1984).

Petersen, J.C., Barbour, F.A., and Dorrence, S.M., "Catalysis of Asphalt Oxidation by Mineral Aggregate Surfaces and Asphalt Components," *Proc. AAPT*, **43**, 162-177 (1974a).

Petersen, J.C., Ensley, E.K., and Barbour, F.A., "Molecular Interactions of Asphalt in the Asphalt-Aggregate Interface Region," *Trans. Res. Rec.*, **515**, 1974b.

Pilat, S., and Godlewicz, M. (Shell Development Co.), "Method of Separating High Molecular Mixtures," U.S. Patent No. 2,188,012 (23 Jan. 1940).

Plancher, H., Dorrence, S.M., and Petersen, J.C., "Identification of Chemical Types in Asphalts Strongly Adsorbed at the Asphalt-Aggregate Interface and Their Relative Displacement by Water," *Proc. AAPT*, **46**, 151-175 (1977).

Puzinauskas, V.P., "Properties of Asphalt Cements," *Proc. AAPT*, **48**, 646-710 (1979).

Que, G., Liang, W., Chen, Y., Liu, C., and Zhang, Y., "Relationship Between Chemical Composition and Performance of Paving Asphalt," *Proceedings of the International Symposium on the Chemistry of Bitumens*, Vol. II, p. 517, Giavarini, C. and Speight, J., ed., Rome, Italy, June 5-8 (1991) (private collection, R. Davison).

Randall, L., "Analysis of Dense (Supercritical) Gas Systems," Chapter 24 of *Chemical Engineering at Supercritical Conditions*, Paulitis, M., Penninger, J., Gray, R., and Davidson, P., ed., Ann Arbor Science, New York, NY, p. 477 (1983).

Randall, L., "The Present Status of Dense (Supercritical) Gas Extraction and Dense Gas Chromatography: Impetus for DGC/MS Development," *Separation Science and Technology*, **17**, 1, p. 1-118 (1982).

Roach, J., "Process for Separating Bituminous Materials," U.S. Patent No. 4,279,739 (21 July 1981).

Rostler, F., "Fractional Composition: Analytical and Functional Significance," in Bituminous Materials, Vol. II - Asphalts, Hoiberg, A., ed., R. E. Krieger Pub. Co., New York, NY, 151 (1979).

Rostler, F., and White, R., "Fractional Components of Asphalts-Modification of the Asphaltenes Fraction," *Association of Asphalt Paving Technologists*, **30**, 532 (1970).

Schmidt, R.J., "Laboratory Measurement of the Durability of Paving Asphalts," *ASTM STP*, **532**, 79 (1973a).

Schmidt, R.J., "The Rolling Thin-Film Circulating Oven - An Improved Rolling Thin-Film Oven Test," *ASTM STP*, **532**, 52 (1973b).

Schmidt, R.J., and Santucci, L.E., "The Effect of Asphalt Properties on the Fatigue and Cracking of Asphalt Concrete on the Zaca-Wigmore Test Project," *Proc. AAPT*, **38**, 39 (1969).

Simpson, W.C., Griffin, R.L., and Miles, T.K., "Correlation of the Microfilm Durability Test with Field Hardening Observed in the Zaca-Wigmore Experimental Project," *ASTM STP*, **277**, 52 (1959).

Simpson, W.C., Griffin, R.L., and Miles, T.K., "Relationship of Asphalt Properties to Chemical Composition," *Journal of Chemical Engineering Data*, **6**, 426 (1961).

Speight, J., *The Desulfurization of Heavy Oils and Residua*, Marcel Dekker, Inc., New York, NY (1981).

Stahl, E., Quirin, K., and Gerard, D., *Dense Gases for Extraction and Refining*, Springer-Verlag, New York, NY (1988).

Stegeman, J.R., *Improved Asphalts with Supercritical Extraction*, Thesis, Texas A&M University, College Station, TX (1991).

Stegeman, J.R., Kyle, A.L., Burr, B.L., Jemison, H.B., Davison, R.R., Glover, C.J., and Bullin, J.A., "Compositional and Physical Properties of Asphalt Fractions Obtained by Supercritical Extraction," *Fuel Science and Technology International*, **10**(4-6), 767-794 (1992).

Streett, W., "Phase Equilibria in Fluid and Solid Mixtures at High Pressures," Chapter 1 of *Chemical Engineering at Supercritical Conditions*, Paulitis, M., Penninger, J., Gray, R., and Davidson, P., ed., Ann Arbor Science, New York, NY, p. 3 (1983).

Streiter, O.G., and Snoke, H.R., "Modified Accelerated Weathering Test for Asphalts and Other Materials," *J. of Research of the National Bureau of Standards*, **16**, 481 (1936).

Thenoux, G., Bell, C.A., Wilson, J.E., Eakin, D., and Shroeder, M., "Experiences with the Corbett-Swarbrick Procedure for Separation of Asphalt into Four Generic Fractions," *Trans. Res. Rec.*, **1171**, 66-70 (1988).

Traxler, R.N., "Changes in Asphalt Cements During Preparation, Laying, and Service of Bituminous Pavements," *Proc. AAPT*, **36**, 541 (1967).

Traxler, R.N., and Schweyer, H., "Separating Asphalt Materials... n-Butanol-Acetone Method," *Oil and Gas Journal*, **52**, Aug. 31, p. 133 (1953).

Vallerga, B.A., Monismith, C.L., and Granthem, K., "A Study of Some Factors Influencing the Weathering of Paving Asphalts," *Proc. AAPT.* **26**, 126 (1957).

Vermillion, W., and Gearhart, J., "Cut Resid Make", *Hydrocarbon Processing*, **62**, 9, (1983).

Welborn, J.Y., "Physical Properties as Related to Asphalt Durability: State of the Art," *Trans. Res. Rec.*, **999**, 31 (1984).

White, R.M., Mitten, W.R., and Skog, J.B., "Fractional Components of Asphalts - Compatibility and Interchangeability of Fractions Produced from Different Asphalts," *Proc. AAPT,* **39**, 492-531 (1970).

Williams, D., "Extraction with Supercritical Gases," *Chemical Engineering Science*, **36**, 11 (1981).

Wilson, R., Keith, P., and Haylett, R., "Liquid Propane -- Use in Dewaxing, Deasphalting, and Refining Heavy Ends," *Industrial and Engineering Chemistry*, **28**, 1065 (1936).

Yilgor, I., and McGrath, J., "Novel Supercritical Fluid Techniques for Polymer Fractionation and Purification," *Polymer Bulletin*, **12**, 491 (1984).

Zarchy, A. "Process for Producing High Yield of Gas Turbine Fuel from Residual Oil," U.S. Patent No. 4,528,100 (9 July 1985).

Zhuze, T., "Compressed Hydrocarbon Gases as a Solvent," *Petroleum*, **23**, 298 (1960).

Zosel, K. "Separation with Supercritical Gases: Practical Applications," *Extraction with Supercritical Gases*, Schneider, G., Stahl, E., and Wilke, G., ed., Verlag Chemie, Deerfield, FL, p. 1 (1980).